1245437
[0069095 H]

GJO-99-101-TAR
GJO-HAN-27

Hanford Tank Farms Vadose Zone

T Tank Farm Report

September 1999

RECEIVED
AUG 09 2017
EDMC

U.S. Department of Energy

GRAND JUNCTION OFFICE

Work Performed Under DOE Contract No. DE–AC13–96GJ87335 for the U.S. Department of Energy

Approved for public release; distribution is unlimited.

This report was prepared as an account of work sponsored by an agency of the United States Government. Neither the United States Government nor any agency thereof, nor any of their employees, makes any warranty, express or implied, or assumes any legal liability or responsibility for the accuracy, completeness, or usefulness of any information, apparatus, product, or process disclosed in this report, or represents that its use would not infringe privately owned rights. Reference herein to any specific commercial product, process, or service by trade name, trademark, manufacturer, or otherwise, does not necessarily constitute or imply its endorsement, recommendation, or favoring by the United States Government or any agency thereof. The views and opinions of authors expressed herein do not necessarily state or reflect those of the United States Government or any agency thereof.

MACTEC ENVIRONMENTAL RESTORATION SERVICES, LLC

CONTRACT NO.: DE-AC13-96GJ87335
TASK ORDER NO.: MAC-99-09
CONTROL NO.: 3100-T99-1219

MEMO TO: Distribution

FROM: Jim Bertsch, Project Manager

DATE: September 20, 1999

SUBJECT: T Tank Farm Report (Final)

Please find enclosed a copy of the subject report. The official letter will be coming from DOE-GJO Project Manager, Mr. Joel Berwick.

Should you have any questions or comments, please contact me at (509) 946-3635.

JFB:jmm
Enclosure

cc: Contract File (C. Spor)
VZCP 1.1.1.2
JFB LB

Distribution:

C. Abraham, GAO
S. Agnew, LANL
D. Barnes, LMHC ✓
R. Bassett, Expert Panelist
E. Berkey, Expert Panelist
J. Berwick, DOE-GJO
C. Brevick, LMHC
J. Brodeur, Energy Sciences & Engineering
R. Bryce, PNNL
M. Butherus, MACTEC-ERS
T. Carpenter, GAP
Central Files, LMHC
J. Conaway, Expert Panelist
G. deBruler, Columbia River United
M. Dexter, LMHC
D. Dunning, Oregon Office of Energy
M. Gossett, MACTEC-ERS (3)
M. Graham, BHI
Hanford File (2)
M. Harmon, DOE-HQ
J. Karr, Expert Panelist
M. Kavanaugh, Expert Panelist
A. Knepp, LMHC
S. Leja, WDOE
J. Matuszek, Expert Panelist
M. McCarthy, LMHC (2)
S. McKinney, WDOE
R. Patt, Expert Panelist
PNNL Technical Library
W. Riggsbee, Yakama Indian Nation
P. Rogers, Jacobs Engineering Group
C. Ruud, WDOE
D. Sherwood, EPA
J. Silko, DOE-ORP (2)
S. Sobczyk, Nez Perce Indian Nation
W. Steele, MACTEC-ERS
S. Stokes, DNFSB (2)
M. Thompson, DOE-RL
P. Wierenga, Expert Panelist
J. Wilkinson, Umatilla Indian Nation
J. Williams, FDH
R. Yasek, DOE-ORP/RL

C:\MyFiles\Letterbook\FY99\99-095

639 CULLUM AVENUE
RICHLAND, WASHINGTON 99352
(PHONE) 509/946-0882 (FAX) 509/946-0920

Printed on recycled paper

GJO–99–101–TAR
GJO–HAN–27

Hanford Tank Farms Vadose Zone

T Tank Farm Report

September 1999

Prepared for
U.S. Department of Energy
Richland Operations Office
Richland, Washington

Prepared by
U.S. Department of Energy
Albuquerque Operations Office
Grand Junction Office
Grand Junction, Colorado

Work performed under DOE Contract No. DE–AC13–96GJ87335.

Contents

Page

Signature Page xi

Executive Summary xiii

1.0 Introduction 1

2.0 Purpose and Scope 2
- 2.1 Purpose of the Project 2
- 2.2 Scope of the Project 2
- 2.3 Regulatory Basis 3
- 2.4 Purpose of the Report 4

3.0 Radionuclides of Interest 5
- 3.1 Cesium-137 (^{137}Cs) 6
- 3.2 Cobalt-60 (^{60}Co) 6
- 3.3 Europium 7
- 3.4 Strontium-90 (^{90}Sr) 8
- 3.5 Antimony-125 (^{125}Sb) 9
- 3.6 Technetium-99 (^{99}Tc) 10
- 3.7 Uranium 11
- 3.8 Niobium-94 (^{94}Nb) 12
- 3.9 Tin-126 (^{126}Sn) 12
- 3.10 Plutonium, Americium-241 (^{241}Am), Neptunium-237 (^{237}Np), Iodine (^{129}I), Ruthenium-106 (^{106}Ru) 12

4.0 Geology and Hydrology 14
- 4.1 Regional Geology 14
- 4.2 Structural Geology of the Pasco Basin 14
- 4.3 General Stratigraphy of the Hanford Site 14
  - 4.3.1 Basement Basalt and Sedimentary Units 15
  - 4.3.2 Suprabasalt Sediments 15
    - 4.3.2.1 Ringold Formation 15
    - 4.3.2.2 Plio-Pleistocene Sediments 16
    - 4.3.2.3 Pre-Missoula Gravels 16
    - 4.3.2.4 Early Palouse Soil 16
    - 4.3.2.5 Hanford Formation 17
    - 4.3.2.6 Holocene Surficial Sediments 18
- 4.4 Geology of the 200 West Area 18
- 4.5 T Tank Farm Geology 19

Contents (continued)

Page

4.6 T Tank Farm Hydrology 21
4.7 Groundwater Monitoring 23
4.8 Groundwater Contamination in the Area of the T Tank Farm 24

5.0 Review of Tank Farm History 26
5.1 Tank Construction 26
5.2 Tank Waste Constituents 28
5.3 Current Status 32
5.4 Unplanned Releases 33
5.4.1 UPR-200-W-7 34
5.4.2 UPR-200-W-147 34
5.4.3 UPR-200-W-148 34
5.5 Leak-Detection Monitoring 34
5.6 Vadose Zone Monitoring Boreholes 35
5.7 Gross Gamma Logging 38

6.0 Adjacent Waste Site Information 39
6.1 216-T-3 Reverse Well 40
6.2 216-T-4-1 Ditch 41
6.3 216-T-4-2 Ditch 41
6.4 216-T-4-A Pond 42
6.5 216-T-4-B Pond 42
6.6 216-T-5 Trench 43
6.7 216-T-6 Cribs 43
6.8 216-T-7 Crib and Tile Field 44
6.9 216-T-14 through 216-T-17 Trenches 45
6.10 216-T-32 Crib 45
6.11 216-T-36 Crib 46
6.12 TX and TY Tank Farms 46

7.0 Spectral Gamma Log Measurements 47
7.1 Equipment 47
7.2 Calibration 48
7.3 Logging Process and Procedures 51
7.4 Data Management 52
7.5 Data Analysis 53

8.0 Log Data Results 54
8.1 Instrumentation Performance 54

Contents (continued)

Page

8.2 Direct Gamma Radiation and Gamma-Ray Attenuation 55
8.3 Radionuclides Detected 56
8.4 Log Plots 56
8.5 Tank Summary Data Reports 57
8.6 Spectral Shape Factor Analysis 57
8.7 Interpreted Data Sets 58
8.7.1 Boreholes Associated With Tank T-101 59
8.7.2 Boreholes Associated With Tank T-102 61
8.7.3 Boreholes Associated With Tank T-103 62
8.7.4 Boreholes Associated With Tank T-104 63
8.7.5 Boreholes Associated With Tank T-105 64
8.7.6 Boreholes Associated With Tank T-106 65
8.7.7 Boreholes Associated With Tank T-107 69
8.7.8 Boreholes Associated With Tank T-108 70
8.7.9 Boreholes Associated With Tank T-109 71
8.7.10 Boreholes Associated With Tank T-110 72
8.7.11 Boreholes Associated With Tank T-111 73
8.7.12 Boreholes Associated With Tank T-112 74

9.0 Development of the Visualizations 75
9.1 Introduction 75
9.2 Geostatistical Structural Model 76
9.3 Three-Dimensional Plume Calculation and Visualizations 76
9.4 Potential Uncertainties and Inaccuracies 77

10.0 Discussion of Results 79
10.1 Radionuclide Contaminant Distribution 79
10.2 Tank-by-Tank Discussion 81
10.2.1 Tank T-101 83
10.2.2 Tank T-102 85
10.2.3 Tank T-103 87
10.2.4 Tank T-104 89
10.2.5 Tank T-105 90
10.2.6 Tank T-106 91
10.2.7 Tank T-107 95
10.2.8 Tank T-108 97
10.2.9 Tank T-109 98
10.2.10 Tank T-110 99
10.2.11 Tank T-111 100
10.2.12 Tank T-112 101

Contents (continued)

Page

11.0 Summary of Results 102

12.0 Conclusions 106

13.0 Recommendations 108
13.1 Data Uses 108
13.2 Tank and Tank Farm Characterization Data 108
13.3 Future Vadose Zone Characterizations 109
13.4 Specific Recommendations for Vadose Zone Investigation and Monitoring 110

14.0 Figures 113
14-1. Map of the Northwest Portion of the Hanford Site 200 West Area Showing the Location of the T Tank Farm 114
14-2. Columbia Plateau and Surrounding Structural Provinces 115
14-3. Structural Subprovinces of the Columbia Plateau 116
14-4. Geologic Structure of the Pasco Basin in the Vicinity of the Hanford Site 117
14-5. Conceptual Hydrogeologic Column for the Hanford Site 118
14-6. Late Neogene Stratigraphy of the Pasco Basin Emphasizing the Ringold Formation 119
14-7. Geomorphological Map of the 200 East and 200 West Areas at the Hanford Site 120
14-8. Pasco Basin Surface Geology and Structural Features 121
14-9. Cross Section AA' Across the T Tank Farm 122
14-10. Cross Section BB' Across the T Tank Farm 123
14-11. Conceptual Geohydrological Setting of the T-TX-TY Tank Farms 124
14-12. Lithological Features Identified from SGLS (KUT) Data from Borehole 50-00-03 125
14-13. Lithological Features Identified from SGLS (KUT) Data from Borehole 50-00-10 126
14-14. Plan Map of WMA-T Showing the Locations of the Groundwater Monitoring Wells 127
14-15. 1997 Water Table Elevation Map for a Portion of the 200 West Area 128
14-16. Estimated Annual Recharge of Precipitation and Irrigation 129
14-17. Plan Map of the T Tank Farm Showing the Locations of the Tank Monitoring Boreholes 130
14-18. Cutaway Section of a Typical Single-Shell Tank Showing Tank Risers and Various Instrument Ports 131

Contents (continued)

Page

Figure 14-19. Plan Map of the 200 West Area in the Vicinity of the T Tank Farm Showing Adjacent Tank Farms, Waste Disposal Facilities, Unplanned Release Locations, and Monitoring Sites 132
14-20. View of a Spectral Gamma Logging System Rigged for Logging 133
14-21. Probe with High-Purity Germanium Detector Suspended Over a Borehole . . . 133
14-22. SGLS Base Calibration Efficiency Function 134
14-23. Hanford Tank Farm Vadose Zone Data Analysis Process 135
14-24. Visualization of ^{137}Cs SGLS Data Acquired at the T Tank Farm 136
14-25. Visualization of ^{60}Co SGLS Data Acquired at the T Tank Farm 137
14-26. Visualization of ^{154}Eu SGLS Data Acquired at the T Tank Farm 138
14-27. Visualization of ^{152}Eu SGLS Data Acquired at the T Tank Farm 139
14-28. Visualization of ^{238}U SGLS Data Acquired at the T Tank Farm 140
14-29. Visualization of ^{235}U SGLS Data Acquired at the T Tank Farm 141
14-30. Visualization of ^{126}Sn SGLS Data Acquired at the T Tank Farm 142
14-31. Visualization of ^{94}Nb SGLS Data Acquired at the T Tank Farm 143
14-32. Visualization of ^{125}Sb SGLS Data Acquired at the T Tank Farm 144
14-33. Visualization of ^{137}Cs Contamination at the T Tank Farm at a Depth of 5 Ft Below Ground Surface Viewed From Above the Tanks 145
14-34. Visualization of ^{137}Cs Contamination at the T Tank Farm at a Depth of 10 Ft Below Ground Surface Viewed From Above the Tanks 146
14-35. Visualization of ^{137}Cs Contamination at the T Tank Farm at a Depth of 18 Ft Below Ground Surface Viewed From Above the Tanks 147
14-36. Visualization of ^{137}Cs, ^{60}Co, and ^{154}Eu Contamination at the T Tank Farm at a Depth of 26 Ft Below Ground Surface Viewed From Above the Tanks . . 148
14-37. Visualization of ^{137}Cs, ^{60}Co, and ^{154}Eu Contamination at the T Tank Farm at a Depth of 43 Ft Below Ground Surface (Base of Tanks) Viewed From Above the Tanks 149
14-38. Visualization of ^{137}Cs, ^{60}Co, and ^{154}Eu Contamination at the T Tank Farm at a Depth of 53 Ft Below Ground Surface Viewed From Above the Tanks . . 150
14-39. Visualization of ^{137}Cs, ^{60}Co, and ^{154}Eu Contamination at the T Tank Farm at a Depth of 72 Ft Below Ground Surface Viewed From Above the Tanks . . 151
14-40. Visualization of ^{137}Cs and ^{60}Co Contamination at the T Tank Farm at a Depth of 72 Ft Below Ground Surface Viewed From Above the Tanks 152
14-41. Visualization of ^{137}Cs Contamination Plumes at the T Tank Farm Superimposed Over the ^{137}Cs SGLS Data, Viewed From Below the Tanks From the Southeast 153
14-42. Visualization of ^{137}Cs Contamination Plumes at the T Tank Farm Superimposed Over the ^{137}Cs SGLS Data, Viewed From Above the Tanks From the Northwest 154

Contents (continued)

Page

Figure 14-43. Visualization of ^{60}Co Contamination Plumes at the T Tank Farm Superimposed Over the ^{60}Co SGLS Data, Viewed From Below the Tanks From the Southeast 155
14-44. Visualization of ^{154}Eu Contamination Plumes at the T Tank Farm Superimposed Over the ^{154}Eu SGLS Data, Viewed From Below the Tanks From the Southeast 156
14-45. Visualization of ^{137}Cs and ^{60}Co Contamination at the T Tank Farm Viewed from Below the Tanks from the Southeast 157
14-46. Visualization of ^{137}Cs and ^{60}Co Contamination at the T Tank Farm Viewed from Above the Tanks from the Northwest 158
14-47. Visualization of ^{137}Cs and ^{154}Eu Contamination at the T Tank Farm Viewed from Below the Tanks from the Southeast 159
14-48. Visualization of ^{137}Cs and ^{154}Eu Contamination at the T Tank Farm Viewed from Above the Tanks from the Northwest 160
14-49. Visualization of ^{137}Cs Contamination in the Vicinity of Tanks T-101, T-102, and T-103, Superimposed Over the ^{137}Cs SGLS Data, Viewed From Below the Tanks From the South-Southwest 161
14-50. Visualization of ^{137}Cs and ^{60}Co Contamination in the Vicinity of Tanks T-101, T-102, and T-103, with the ^{60}Co Contamination Superimposed Over the ^{60}Co SGLS Data, Viewed From Below the Tanks From the South-Southwest 162
14-51. Visualization of ^{137}Cs and ^{154}Eu Contamination in the Vicinity of Tanks T-101, T-102, and T-103, with the ^{154}Eu Contamination Superimposed Over the ^{154}Eu SGLS Data, Viewed From Below the Tanks From the South-Southwest 163
14-52. Visualization of ^{137}Cs Contamination in the Vicinity of Tanks T-103, T-106, and T-109, Superimposed Over the ^{137}Cs SGLS Data, Viewed From Below the Tanks From the Southeast 164
14-53. Visualization of ^{137}Cs and ^{60}Co Contamination in the Vicinity of Tanks T-103, T-106, and T-109, with the ^{60}Co Contamination Superimposed Over the ^{60}Co SGLS Data, Viewed From Above the Tanks From the Southeast 165
14-54. Visualization of ^{137}Cs and ^{154}Eu Contamination in the Vicinity of Tanks T-103, T-106, and T-109, with the ^{154}Eu Contamination Superimposed Over the ^{154}Eu SGLS Data, Viewed From Above the Tanks From the Southeast ... 166
14-55. Visualization of ^{137}Cs and ^{60}Co Contamination in the Vicinity of Tanks T-103 and T-106, Viewed From Above the Tanks From the Southeast 167
14-56. Visualization of ^{137}Cs and ^{154}Eu Contamination in the Vicinity of Tanks T-103 and T-106, Viewed From Above the Tanks From the Southeast 168

Contents (continued)

Page

15.0 References 169

Appendix A. Groundwater Monitoring Data A-1
Appendix B. T Tank Farm Correlation Plots B-1

Tables

Table 1. General Waste Information, T Tank Farm 28
2. General T Tank Farm Information 33

This page intentionally left blank.

Hanford Tank Farms Vadose Zone

T Tank Farm Report

Prepared by:

Eric Larsen — Date: 9/8/99
MACTEC-ERS, Hanford

Concurrence:

R.G. McCain, Technical Lead — Date: 9/8/99
MACTEC-ERS, Hanford

C.J. Koizumi, Technical Lead — Date: 9/10/99
MACTEC-ERS, Grand Junction Office

Approved by:

J.F. Bertsch, Project Manager — Date: 9/8/99
MACTEC-ERS, Hanford

M.C. Butherus, Task Order Manager — Date: 9/10/99
MACTEC-ERS, Grand Junction Office

J. Berwick, Project Manager — Date: 9-13-99
U.S. Department of Energy
Grand Junction Office

J.M. Silko, Project Manager — Date: 09.14.99
U.S. Department of Energy
Richland Operations Office

This page intentionally left blank.

Executive Summary

The U.S. Department of Energy Grand Junction Office (DOE-GJO) was tasked by the DOE Richland Operations Office (DOE-RL) to perform a baseline characterization of the gamma-ray-emitting radionuclides that are distributed in the vadose zone sediments beneath and around the single-shell tanks (SSTs) at the Hanford Site. The intent of this characterization is to determine the nature and extent of the contamination, to identify contamination sources when possible, and to develop a baseline of the contamination distribution that will permit future data comparisons. The results of this initial baseline provide the information necessary to plan and prioritize more comprehensive characterization projects. This characterization work also allows an initial assessment of the impacts of the vadose zone contamination as required by the Resource Conservation and Recovery Act (RCRA). This characterization is limited to the depths and areal distribution of existing boreholes; no new boreholes were constructed for this project.

The scope of this project involves acquiring information regarding vadose zone contamination utilizing borehole geophysical logging methods, assessing and interpreting that information and documenting it in a series of reports for each SST (Tank Summary Data Reports) and for each tank farm (Tank Farm Reports). The methods utilized are presently limited to detection of gamma-emitting radionuclides from both man-made and natural sources.

Logging operations utilized high-purity germanium detection systems to assess the distribution of the gamma-emitting radionuclides in the sediments surrounding and below the T Tank Farm tanks. Log data were acquired in 67 existing vadose zone monitoring boreholes with two spectral gamma logging systems. Logging of all the boreholes was completed by December 1998, and the last Tank Summary Data Report was issued in July 1999. Twelve Tank Summary Data Reports were prepared for the tanks in the T Tank Farm (DOE 1995d, 1995e, 1998c, 1998d, 1998e, 1998f, 1999b, 1999c, 1999d, 1999e, 1999f, and 1999g).

Cesium-137 (^{137}Cs), cobalt-60 (^{60}Co), europium-154 (^{154}Eu), and, to a lesser degree, europium-152 (^{152}Eu), were the major gamma-emitting contaminants detected in the T Tank Farm vadose zone. Limited and relatively isolated occurrences of niobium-94 (^{94}Nb), antimony-125 (^{125}Sb), tin-126 (^{126}Sn), uranium-235 (^{235}U), and uranium-238 (^{238}U) were also detected around several boreholes.

The spectral gamma log data were utilized to prepare visualizations showing the apparent distributions of ^{137}Cs, ^{60}Co, and ^{154}Eu in the vadose zone at the T Tank Farm. The visualizations depict the distributions of these radionuclides as three-dimensional plumes of contamination. Unfortunately, the precision of portions of the visualizations is limited due to inaccuracies in the assays resulting from double-cased and grouted boreholes and due to a lack of data with which to perform good geostatistical structural analyses.

Near-surface and shallow subsurface ^{137}Cs contamination was detected primarily in the central and eastern portions of the T Tank Farm. This contamination most likely resulted from surface spills or leaks from piping systems related to routine tank farm operations. The highest ^{137}Cs

concentrations were detected within the near-surface backfill material in the east-central portion of the tank farm between tanks T-104 and T-107. The thickest distributions of ^{137}Cs (27 feet [ft]) contamination were also detected in this region, suggesting a larger spill or several spills or leaks may have occurred in this area.

A vertically continuous, elongated ^{137}Cs plume was detected around one borehole near the southeast side of tank T-101, which is an assumed leaker. The plume extends to a depth of more than 100 ft and appears to be the result of a large volume leak from spare fill lines on the southeast side of the tank that probably resulted from overfilling the tank. A large ^{60}Co and ^{154}Eu plume identified near the south side of tank T-101 may also have originated from the same leak source. Visualization data show that the ^{60}Co component of the plume trends in a southwesterly direction, passing under the southern portion of tank T-101 and portions of tanks T-104 and T-105.

A ^{137}Cs and ^{60}Co plume was identified in one borehole near the south side of tank T-102. Although tank T-102 is classified as sound, the data indicate that the plume probably originated from a leak from the spare fill lines connected to this tank in a manner similar to spare fill-line leaks originating from adjacent tanks within the cascade series. The ^{137}Cs component of the plume appears to have spread laterally from the suspected leak source to the south and west along the base of the tank farm excavation.

A distinct plume of ^{60}Co, ^{154}Eu, and ^{152}Eu contamination was intercepted by boreholes located near the southeast and south sides of tank T-103. The contamination is believed to have originated from a leak in the seal of a spare fill line on the southeast side of the tank. Some of the ^{60}Co and ^{154}Eu contamination within the plume has migrated laterally to the south and has apparently intermingled with contamination resulting from a large leak from tank T-106.

The very extensive plume of ^{137}Cs, ^{60}Co, ^{154}Eu, and ^{152}Eu contamination identified around and below the base of the tank T-106 originated from large leak from the tank in 1973. The leak source is located on the southeast side of the tank, and the resulting plume extends laterally as much as 100 ft and vertically beyond the depth of most of the boreholes.

Man-made radionuclide contamination was detected at the bottoms of several of the deepest T Tank Farm monitoring boreholes, indicating that the contamination has penetrated to a depth of at least 120 ft. Because the boreholes were not deep enough to intercept the bottommost portions of the contaminant plumes, the vertical extent of these contaminants into the deeper regions of the vadose zone could not be determined.

In 1995 and 1996, groundwater samples collected from monitoring well 299-W11-27, which is located downgradient from the T Tank Farm, showed large increases in several parameters, including specific conductance, chromium, nitrate, tritium, technetium-99 (^{99}Tc), and ^{60}Co. A Phase I Groundwater Quality Assessment concluded that these contaminants are most likely the result of sources within T Tank Farm (Hodges 1998). Brief summaries of groundwater data and previously published interpretations of groundwater contaminants are included in this report to

allow the reader to understand the relation between vadose zone contamination and groundwater contamination.

Several waste disposal facilities adjacent to the T Tank Farm were investigated during the preparation of this report to evaluate the potential influence that wastes disposed of at these facilities may have had on the distribution of contamination at the T Tank Farm. There is no indication that wastes discharged to these facilities are related to contamination detected in the vadose zone beneath the tanks.

The initial characterization of the T Tank Farm vadose zone is limited to the areal distribution and depths of the existing monitoring boreholes within the tank farm. Because most of the boreholes are 120 ft deep or less and the local groundwater level is approximately 220 ft deep, only the upper portion of the vadose zone beneath the T Tank Farm has been characterized. Although this characterization project is limited to detecting only gamma-emitting radionuclides, several plumes have been identified that define targets for additional, more comprehensive chemical and radiological characterization.

This page intentionally left blank.

1.0 Introduction

The T Tank Farm is located in the northern portion of the 200 West Area of the Hanford Site (Figure 14-1). This tank farm consists of twelve 530,000 gallon (gal) and four 55,000-gal single-shell tanks (SSTs) that were constructed to store high-level radioactive waste generated during chemical processing of irradiated uranium reactor fuel. This waste was generated primarily at T plant, which is located about 2,000 feet (ft) east of the T Tank Farm. These tanks presently contain a total of 1.87 million gal of high-level radioactive waste. Seven of the 530,000 gal tanks in the T Tank Farm are designated assumed leakers. These seven tanks are estimated to have leaked a total volume of 134,500 gal liquid waste into the vadose zone sediments. The remainder of the 530,000 gal tanks and the four 55,000 gal tanks are classified as sound (Hanlon 1999).

In 1994, the Department of Energy Richland Office (DOE-RL) requested the DOE Grand Junction Office (DOE-GJO), Grand Junction, Colorado, to conduct a baseline characterization of gamma-emitting contamination in the vadose zone at all the Hanford Site SST farms by conducting spectral gamma-ray logging of boreholes that surround the tanks. Existing monitoring boreholes in the T Tank Farm were logged with high-purity intrinsic germanium (HPGe) spectral gamma-ray logging systems (SGLSs) to produce assays of the gamma-emitting radionuclides in the sediments surrounding the boreholes. Monitoring boreholes were installed only around the twelve 530,000-gal tanks. Radionuclide concentration logs depicting concentrations in picocuries per gram (pCi/g) (of soil material) versus depth for individual boreholes were compiled and presented in twelve individual Tank Summary Data Reports (DOE 1995d, 1995e, 1998c, 1998d, 1998e, 1998f, 1999b, 1999c, 1999d, 1999e, 1999f, and 1999g), one for each of the T Tank Farm tanks. The log data were correlated to assess the vadose zone across the T Tank Farm. A rudimentary geostatistical analysis of the data was performed and was used to help perform correlation of contamination intervals between boreholes and ultimately to develop three-dimensional visualizations of the contaminant distributions.

The T Tank Farm Report presents the results of the farm-wide assessment of the vadose zone and reports what has been learned about the distribution of contaminants at the T Tank Farm.

Data acquired during this characterization work establish a baseline of the current distribution of gamma-emitting radionuclides, and a limited assessment of the impacts of this contamination is presented in this report. This work may be used to define a tank monitoring program, to help focus future more comprehensive characterizations, and to determine the implications or impacts of the vadose zone contamination.

2.0 Purpose and Scope

2.1 Purpose of the Project

The purpose of this baseline characterization is to quantify gamma-emitting radionuclides to determine the nature and extent of subsurface contamination. The gamma-ray photons from the decay of the radionuclides in the subsurface can be detected through existing steel-cased boreholes that surround the tanks. An integral objective of this characterization project is to identify sources of contamination when possible. Although only gamma-emitting radionuclides can be directly detected, the distribution of these contaminants can be viewed as an indication of the distribution and migration pathways of other contaminants.

Compiling the acquired data into a baseline is an objective of the characterization project. Acquired borehole log data are baseline measurements of the gamma-emitting contamination concentrations around the individual boreholes and constitute a baseline of the distribution of these contaminants within the T Tank Farm. This baseline consists not only of the individual borehole logs or the log database, but also of the contamination distribution models used to create the visualizations. These data can be used for future comparisons of radionuclide migration studies that may aid in identifying and/or quantifying new tank leaks.

Additionally, an objective of this project is to provide more site-specific geologic information by generating logs of the naturally occurring potassium-40 (^{40}K), uranium-238 (^{238}U), and thorium-232 (^{232}Th) (KUT) concentrations, which can be used to identify changes in the lithology that may influence contaminant migration. These KUT data are correlated with geologic information from nearby groundwater monitoring wells, as well as with historical geologic data that were recorded during monitoring borehole construction.

2.2 Scope of the Project

The primary scope of this project involves spectral gamma logging of existing vadose zone monitoring boreholes. No new boreholes were drilled in the T Tank Farm during the course of this project, and none of the existing boreholes were deepened; therefore, the assessments of the vadose zone contamination are based on the limited depth and areal distribution of the existing boreholes. Most of these boreholes extend to depths between 80 and 125 ft into the vadose zone, while the groundwater is approximately 220 ft below the ground surface.

A major portion of this project involves assessment and correlation of historical or existing data, such as the gross gamma logs, drilling logs, groundwater monitoring information, geology and hydrogeology information, tank-leak documentation, and tank operations information. Much of this information has not been comprehensively compiled, reviewed, and analyzed to understand its significance in relation to the T Tank Farm vadose zone contamination. The historical information helps to identify potential sources of contamination and to explain the nature and extent of the contamination identified by the new spectral gamma log data.

This project is limited in scope to passive spectral gamma-ray logging data acquisition methods. As a result, radionuclides that do not decay with the emission of gamma-ray photons are not assayed, nor are other regulated chemical constituents that may have been present in the tank waste and leaked into the vadose zone.

The scope of the project also includes preparation of reports that provide the results to current and future Hanford Site personnel and identification of the quality of the data in terms of precision and accuracy as well as quality assurance. Documentation of procedures, instrument calibration, quality assurance, and data analysis methods has been prepared (DOE 1995a, 1995b, 1995c, 1996c, 1996d, 1997a, 1997b, 1997c, 1997d, 1997e, 1997f, and 1997g). All reports are available from Hanford document control centers and from the project files. Currently, log data are only available in the MACTEC-ERS project databases; upon completion of the project the log data will be stored by current and future Hanford contractors.

2.3 Regulatory Basis

The operation and eventual closure of the SST farms are regulated by both Federal and State laws. The mixed waste in the SSTs is regulated through the Resource Conservation and Recovery Act of 1976 (RCRA) and the Washington Hazardous Waste Management Act of 1976 (HWMA) for the hazardous waste component and through the Atomic Energy Act of 1954 (AEA) as amended for the radioactive waste component (DOE 1996b). For purposes of this vadose zone characterization project, RCRA and the HWMA are the environmental laws of primary importance.

Under RCRA and the HWMA, the Washington State Department of Ecology (Ecology) regulates the SSTs as hazardous waste storage-tank systems under Washington Administrative Code (WAC) 173-303 (DOE 1996b). The SSTs are a treatment, storage, and/or disposal (TSD) unit, and, therefore, part of the larger Hanford Facility that consists of all TSD units at the Hanford Site.

TSD units of the Hanford Facility are regulated as either interim status or final status units. A final status permit, *Dangerous Waste Portion of the Resource Conservation and Recovery Act Permit for the Treatment, Storage, and Disposal of Dangerous Waste* (Ecology 1994), was issued for the Hanford Facility in 1994. Under a negotiated permitting approach, additional TSD units will be added to this permit as the units are evaluated through the RCRA permitting process. Eventually all TSD units of the Hanford Facility, which will continue dangerous waste management, will be converted from interim status to final status and be included in the permit (Ecology 1994). TSD units that will not be used for continued dangerous waste management, such as the SSTs, will be closed under interim status rather than converted to final status.

In addition to providing necessary information to support closure of the SSTs, the vadose zone characterization will provide a baseline of gamma-ray activity in boreholes near the SSTs. Newly acquired spectral gamma-ray data can be compared to this baseline to help identify any new or continuing leaks. Monitoring of the SSTs is required under a number of regulations,

including DOE orders and interim status requirements of RCRA. By developing a baseline characterization, future monitoring activities will be more effective.

According to the *Hanford Federal Facility Agreement and Consent Order* (Ecology et al. 1996), also known as the Tri-Party Agreement or TPA, closure of the SSTs will be pursuant to WAC 173-303-610. DOE is required to remove or decontaminate all waste residues, contaminated containment system components, contaminated soils, and contaminated equipment at the time of closure; closure of the SSTs as landfills is allowed if all the contaminated soil cannot be practicably decontaminated or removed (DOE 1996a). In either case, characterization of the nature and extent of the leaked waste is needed to evaluate remedial action alternatives for closure of the soils contaminated by waste leaked from the SSTs. Without appropriate data on the nature and extent of contamination, it will not be possible to develop or assess the risk associated with various closure options for the SSTs.

2.4 Purpose of the Report

This report presents a compilation of the results of the spectral gamma logging characterization at the T Tank Farm that were originally reported in individual Tank Summary Data Reports. Visualizations of the distributions of ^{137}Cs, ^{60}Co, and ^{154}Eu contamination (based on the empirical model) that correlate the individual borehole logs in three dimensions are presented. The visualizations help identify contamination plumes and show relationships between the plumes, as well as help determine the sources of the contamination.

A significant portion of this report presents background information regarding the logging equipment and spectral gamma log data, geologic information, and historical information regarding tank farm operations. Sections 4.0, "Geology and Hydrology," and 5.0, "Review of Tank Farm History," present brief descriptions of the geology and hydrology in the vicinity of the T Tank Farm, tank construction, waste constituents, and operational histories for each tank in the T Tank Farm. Section 6.0, "Adjacent Waste Site Information," describes facilities and their associated waste discharges at several sites adjacent to the T Tank Farm. Sections 7.0, "Spectral Gamma Logging Measurements," and 8.0, "Log Data Results," describe the logging equipment, data acquisition and processing, details regarding data interpretation, and preparation of the data presentations. Discussions regarding the development of the contamination plume modeling and visualizations are presented in Section 9.0, "Development of the Visualizations." The visualizations of the contamination plumes in the T Tank Farm are discussed on a tank-by-tank basis in Section 10.0, "Discussion of Results." Results are summarized in Section 11.0, "Summary of Results," and conclusions and recommendations are presented in Section 12.0, "Conclusions" and Section 13.0,"Recommendations," respectively.

3.0 Radionuclides of Interest

Radionuclide contamination distributions and their impacts or implications relative to contamination sources are the primary focus of this project. Although only the presence of the gamma-ray-emitting radionuclides are detected during this characterization project, the presence, potential distributions, and implications of other radionuclides and chemical contaminants should be considered by the reader, based on the distributions of the gamma-ray-emitting radionculides.

The radionuclide contamination in the vadose zone can be considered to present both a short-term occupational exposure risk to operations workers and a long-term risk to the public and the environment. The types of possible risks depend on a variety of factors that are specific to each radionuclide, including the decay half-life of the nuclide, its mobility in the vadose zone (and ultimately in the groundwater), and its specific activity and/or biological toxicity.

Long-term human health risks arise primarily from a potential pathway whereby an individual is exposed by ingesting contaminated groundwater and from a pathway involving direct exposure of an individual to contaminated sediment that is uncovered or otherwise brought to the surface in the distant future, after the end of an institutional control period. Long-term risk scenarios are usually evaluated by using vadose zone contaminant-transport modeling to produce performance assessments that estimate potential doses for different pathways. Radionuclides of concern would be those with long half-lives and those that are mobile in the vadose zone and could contribute to groundwater contamination.

Short-term risk scenarios involve inhalation of radionuclides or direct exposure to workers during remediation or other operations that would uncover or bring the vadose zone contamination to the surface in the near future. The radionuclides of concern are those that are easily suspended in air and the high specific-activity radionuclides that present an exposure problem.

Boothe (1996) presents a review of the radionuclide inventory of the tank wastes and the relative risk levels associated with each radionuclide.

Many radionuclides in the original tank wastes that have short half-lives have decayed away and are no longer detectable. Some of the radionuclides of interest are identified in the following sections. These radionuclides include those that are detectable with the SGLS, those whose occurrences can be inferred from the SGLS data, and radionuclides that are related to those detected with the SGLS.

The information in the following sections was obtained from a variety of sources, including National Low-Level Waste Management Program documents (Rudin and Garcia 1992a, 1992b; Rudin et al. 1992), nuclear physics references including Lederer and Shirley (1978), GE (1989), Erdtmann and Soyka (1979), and Hanford Site contractor documents including Dresel et al. (1995) and Johnson (1993).

3.1 Cesium-137 (^{137}Cs)

^{137}Cs is one of the highest specific-activity radionuclides in the tank wastes and is present at high concentrations. This radionuclide originated as a high-yield fission product and accounts for a high percentage of the total radioactivity in irradiated fuel assemblies. ^{137}Cs was a major component of the process waste stream generated by the plutonium and uranium separations processes.

^{137}Cs has a half-life of 30.2 years and is the longest-lived high-yield fission-product. It decays with the emission of beta particles (511 and 1176 kilo-electron-volts [keV]) to produce barium-137 (^{137m}Ba), which in turn produces a 661.6-keV gamma-ray photon with an intensity of 84.62 gamma photons per 100 decays (Erdtmann and Soyka 1979). As a result of the gamma photon emission, ^{137}Cs is easily detected and quantified with HPGe spectral gamma-ray detection equipment. The minimum detectable level (MDL) of ^{137}Cs is about 0.1 pCi/g with the present SGLS equipment and logging acquisition rates utilized for this vadose zone characterization project.

Because of its relatively long half-life and high concentration in the tank waste, ^{137}Cs is the most abundant radionuclide in the vadose zone around the SSTs. This contaminant is easy to detect and quantify with passive gamma logging and was detected in most of the boreholes within the T Tank Farm. ^{137}Cs is reported to have a high sorptive capacity in sediment. However, in the presence of competing positive ions such as from the dissolved radioactive salts present in the SSTs, the sorption of ^{137}Cs decreases (Carboneau et al. 1994b). At low concentrations, ^{137}Cs is more strongly adsorbed to the sediment, particularly if pH values are greater than 4.0, as is typical of the Hanford sediment.

^{137}Cs was detected around numerous T Tank Farm tank monitoring boreholes. The most extensive and highly concentrated ^{137}Cs occurs along the southeastern quarter of tank T-106.

^{137}Cs is absorbed by humans and animals through the digestive tract and behaves chemically in the body similar to potassium (Carboneau et al. 1994b). The EPA-mandated maximum contaminant level (MCL) for ^{137}Cs in groundwater is 200 picocuries per liter (pCi/L) (PNNL 1998).

3.2 Cobalt-60 (^{60}Co)

^{60}Co is generated in nuclear reactors by neutron activation of stable ^{59}Co. ^{60}Co occurs in relatively high concentrations in the cladding of irradiated reactor fuel elements and was present in the waste stream products sent to the SSTs from the plutonium and uranium separation processes. ^{60}Co was originally present in the tanks at significant activities, but much of the ^{60}Co has since decayed away because it has a relatively short half-life of 5.27 years.

^{60}Co decays via beta emission to create stable nickel-60 (^{60}Ni). About 95 percent of the beta particles emitted during the decay of ^{60}Co have energies equal to or below 314 keV, but beta particle energies as high as 1480 keV can be generated. During the decay to stable ^{60}Ni, ^{60}Co also emits two high-energy gamma rays: one at 1173 keV and the other at 1333 keV. The production of these gamma rays is 99.8 and 99.9 percent, respectively (Erdtmann and Soyka 1979). Under favorable conditions, these gamma rays make the presence of ^{60}Co easy to detect and quantify with passive spectral gamma measurement equipment. The MDL of ^{60}Co is about 0.1 pCi/g with the present SGLS equipment and logging acquisition rates utilized for this vadose zone characterization project.

^{60}Co was detected around numerous T Tank Farm tank monitoring boreholes. The most extensive ^{60}Co contamination occurs along the southeastern quarter of tank T-106.

The human exposure risk for ^{60}Co is relatively high because this radionuclide emits both beta particles and gamma rays during decay that are relatively high-energy and because it has a high specific activity of 1.1×10^3 curies per gram [Ci/g] (DOE 1993). The specific activity of a substance is defined as the activity per unit mass of the radioisotope sample.

When ^{60}Co comes in contact with the soil and groundwater, most of it will become fixed in the soil and will not migrate appreciably from the original source site (Adams 1995). Adams (1995) cites several experiments that describe the soil and groundwater conditions that affect the mobility of this nuclide in the environment. ^{60}Co is generally immobile; however, spectral gamma logging at the tank farms has consistently shown that ^{60}Co is more mobile and more uniformly distributed than ^{137}Cs.

The EPA-mandated MCL for ^{60}Co in drinking water is 100 pCi/L (PNNL 1998).

^{60}Co is considered an exposure risk to workers because of the intense gamma rays emitted during decay, but it does not need to be considered in long-term performance assessments because of its relatively short half-life. Nevertheless, this contaminant is monitored in the vadose zone because it is easily detected and assayed, and it can be correlated with some of the moderately mobile, less easily detected radionuclides. Monitoring contamination plumes for changes in ^{60}Co concentrations may indicate changing conditions of a plume that are due to remobilization from precipitation infiltration or new tank releases, or to changes merely reflecting the decay rate of ^{60}Co.

3.3 Europium

^{154}Eu originates from the activation of europium-153 (^{153}Eu), which is a fission product. It is not as abundant in the irradiated fuel or the processing waste streams as ^{137}Cs, but it is present in irradiated fuel at high enough concentrations to significantly contribute to the total radiation flux from the fuel.

^{154}Eu decays by emission of a beta particle to stable gadolinium-154 (^{154}Gd) and has a half-life of only 8.59 years. The most intense gamma rays emitted during decay include 123 keV

(40.5 percent), 723 keV (19.7 percent), 1004 keV (17.6 percent), and 1274 (35.5 percent) (Erdtmann and Soyka 1979). The MDL of ^{154}Eu is about 0.3 pCi/g with the present SGLS equipment and logging acquisition rates utilized for this vadose zone characterization project.

^{152}Eu is an activation product with a half-life of 13.5 years. It decays by electron capture and positron emission to samarium-152 (^{152}Sm) and by beta emission to gadolinium-152 (^{152}Gd) with the release of a number of possible gamma rays, the most intense of which include 344 keV (27 percent), 779 keV (13 percent), 964 keV (14.6 percent), 1112 keV (13.6 percent), and 1408 keV (21 percent) (Erdtmann and Soyka 1979). The MDL of ^{152}Eu is less than 1 pCi/g with the present SGLS equipment and logging acquisition rates utilized for this vadose zone characterization project.

Europium in the tank wastes includes the isotopes ^{152}Eu and ^{154}Eu. These isotopes were detected together around numerous T Tank Farm tank monitoring boreholes. The most extensive ^{152}Eu and ^{154}Eu contamination occurs along the southeastern quarter of tank T-106.

Few references were found that describe the mobility of europium in the vadose zone sediments. Monitoring results at approximately 50 crib sites at the Hanford Site showed that europium is more mobile than ^{137}Cs but not as mobile as ^{60}Co (Brodeur et al. 1993). This conclusion is based strictly on a comparison of the contaminant distribution patterns at the crib sites, which may differ significantly from the distribution patterns at the SSTs in terms of types, quantities, and concentrations of waste streams and how effluent was released to the vadose zone.

Significant quantities of europium have not been detected in the unconfined aquifer beneath the 200 Areas (Dresel et al. 1995; Johnson 1993), indicating that it is retained in the vadose zone sediments.

^{154}Eu presents a short-term exposure risk because of the gamma radiation, but it is not considered a long-term risk because of its relatively short half-life. The EPA-mandated MCL for ^{154}Eu in drinking water is 200 pCi/L (PNNL 1998).

3.4 Strontium-90 (^{90}Sr)

^{90}Sr is similar to ^{137}Cs because it is also a high-yield, long-lived fission product with a half-life of about 29 years. Unlike ^{137}Cs, ^{90}Sr decays with emission of a beta particle but no gamma-ray photons. ^{90}Sr decays to yttrium-90 (^{90}Y) by relatively low beta emission. ^{90}Y has a short half-life (64 hours) and decays to stable zirconium-90 (^{90}Zr) by a high energy (2.2 MeV) beta emission. Because of the short half-life of ^{90}Y, the high energy beta emission is usually associated with the parent radionuclide ^{90}Sr.

Although ^{90}Sr cannot be detected directly by gamma spectroscopy, the beta particles from ^{90}Y are so energetic that when present at sufficient concentrations, bremsstrahlung radiation may be detected in a borehole with spectral gamma-ray detectors. Bremsstrahlung or "braking" radiation is incoherent gamma radiation produced by interactions between fast electrons and matter. It is

characterized in a gamma-ray spectrum by a low-energy continuum that decreases in intensity with increasing energy, in a log-linear manner, and covers an energy range from the x-ray region to about 300 keV. If ^{90}Sr is present at about 1,000 pCi/g or greater, it can be identified but not readily quantified with the spectral gamma-ray detection equipment.

The inventory of ^{90}Sr generated in a reactor increases linearly with the fuel fission rate, and essentially all the ^{90}Sr produced still remains in the fuel when it is extracted from the reactor and processed. At the time of processing, ^{90}Sr represents only about 0.05 percent of the total fission product activity but accounts for 20 percent of the total remaining radioactivity after 100 years.

Strontium is a divalent (Sr^{2+}) element that behaves like the other alkaline-earth metals (e.g., magnesium, calcium, and barium) (Carboneau et al. 1994a). The behavior of ^{90}Sr in the environment is dictated by its chemical properties. It forms an ionic bond with negatively charged elements and is easily dissolved in water. Strontium retention is very sensitive to the presence of calcium in the soil. When dissolved in liquid effluent and released into sediments, strontium will readily adsorb onto sediment grains or clay particles and can replace Ca^{2+} in $CaCO_3$ (Carboneau et al. 1994a).

^{90}Sr is dissolved easily during the fuel dissolution process, the first stage of fuel rod processing, and it stays in solution throughout the separation process. Consequently, ^{90}Sr is always a component in the effluent waste products of the separation processes, and ^{90}Sr is the second most abundant radionuclide (^{137}Cs is the most abundant) in the tank waste material.

^{90}Sr is a significant health risk because it replaces calcium and is deposited in bone material, where it becomes fixed. Once deposited in the body, damage is caused by the high-energy beta radiation emitted during decay.

In groundwater, ^{90}Sr tends to stay in soluble form and migrates farther than other fission products such as ^{137}Cs. ^{90}Sr is often a risk-limiting radioisotope because of the relatively high mobility of ^{90}Sr in both the vadose zone sediment and the groundwater and because of its high health risk relative to other nuclides. The EPA-mandated MCL for ^{90}Sr in drinking water is 8 pCi/L (PNNL 1998).

3.5 Antimony-125 (^{125}Sb)

^{125}Sb is a fission product originating from slow neutron fission of uranium-235 (^{235}U) or plutonium-239 (^{239}Pu). Because its yield is low, ^{125}Sb does not account for a large percentage of the total fission product. The half-life of ^{125}Sb is 2.8 years.

^{125}Sb decays with the emission of a beta particle to a metastable state of tellurium-125 (^{125m}Te), then to the stable end product tellurium-125 (^{125}Te), from which the measured gamma ray results. Gamma rays emitted during the decay of ^{125}Sb include 428 keV (29.6 percent), 600 keV (18 percent), and 636 keV (11 percent) (Erdtmann and Soyka 1979).

^{125}Sb was detected in two T Tank Farm tank monitoring boreholes; one along the southeastern quarter of tank T-103 and one along the southeastern quarter of tank T-106.

^{125}Sb is an important radionuclide for vadose zone characterization and monitoring work. ^{125}Sb is more mobile than some of the other gamma-emitting radionuclides and because it is easily measured, it can be tracked and monitored for contaminant migration studies. Brodeur et al. (1993) observed that ^{125}Sb was more mobile than ^{137}Cs and it was detected deeper in the vadose zone than ^{137}Cs.

^{125}Sb poses minimal risk because of its generally low abundance, but it may represent a short-term exposure risk because it can be inhaled. The EPA-mandated MCL for ^{125}Sb in drinking water is 300 pCi/L (PNNL 1998).

3.6 Technetium-99 (^{99}Tc)

^{99}Tc is an abundant fission product that is long-lived and is considered to be mobile in the environment. It is an important radionuclide in long-term risk assessments and can result in high calculated risk values.

^{99}Tc has a fission yield from fissionable isotopes of uranium and plutonium of about 6 percent (out of 200 percent), which is equivalent to that of ^{137}Cs. As a result, it is as abundant in terms of mass content as ^{137}Cs in effluent streams and SST wastes at Hanford. However, ^{99}Tc is present in the tank waste at a lower curie content (by many orders of magnitude) because ^{137}Cs has a much higher specific activity.

^{99}Tc has a half-life of 2.1×10^5 years, which is one of the reasons for its high risk rating in long-term performance assessments. It decays by 293-keV beta emission to stable ruthenium-99 (^{99}Ru) without the emission of gamma rays that are detectable with the logging system; therefore, it cannot be detected or assayed through the boreholes.

The mobility of ^{99}Tc in soil is highly dependent on its chemical form, which is governed by the oxidation-reduction potential of the soil. Rudin et al. (1992) state that, if sufficient reducing conditions exist in the sediment, technetium will precipitate out of solution as a sulfide or hydrated oxide. If oxidizing conditions exist, technetium will be present as a pertechnetate ion, which studies have shown will migrate at a rate of 88 percent of the groundwater velocity or greater (Rudin et al. 1992).

The EPA-mandated MCL for ^{99}Tc in groundwater is 900 pCi/L (PNNL 1998). ^{99}Tc is highly mobile in the groundwater at Hanford and has been detected in the groundwater samples obtained in groundwater monitoring boreholes near the T Tank Farm (refer to Section 4.8 of this report).

3.7 Uranium

Uranium isotopes are long-lived and can be mobile in both the groundwater and vadose zone. Boothe (1996) lists uranium isotopes as a groundwater hazard that should be included in a performance assessment.

Uranium isotopes in tank wastes primarily include ^{238}U and ^{235}U, with minute quantities of ^{232}U, ^{233}U, ^{234}U, and ^{236}U. Uranium isotopes in the irradiated fuel elements are separated from the fission and activation products in the chemical processes (except for the early bismuth phosphate [$BiPO_4$] process). Consequently, waste effluent sent to the SSTs after the $BiPO_4$ processing ceased does not usually contain much uranium.

^{238}U, by far the most abundant uranium isotope, occurs naturally in the Earth's crust and is routinely assayed for stratigraphic correlation purposes. ^{238}U has a long half life (4.5×10^9 years) and decays through a long and complex chain with emission of alpha and beta particles as well as gamma rays. Although ^{238}U does not directly emit gamma rays, it can be assayed by measuring its gamma-emitting daughter products, which include protactinium-234 (^{234m}Pa), radium-226 (^{226}Ra), lead-214 (^{214}Pb), and bismuth-214 (^{214}Bi) under the assumption that secular equilibrium exists throughout the decay chain. Typically, the 609-keV or 1764-keV peaks associated with ^{214}Bi are used to determine ^{238}U.

When ^{238}U is not in secular equilibrium with its post-radium daughter nuclides, such as when it has been chemically separated, it can be assayed by using the 1001-keV gamma ray associated with ^{234m}Pa, which is the second daughter in the uranium decay chain. The intensity of the 1001-keV ^{234m}Pa line is low relative to the 609-keV ^{214}Bi line (0.6% vs. 47%). Therefore, significant activity at 1001-keV, without a correspondingly greater activity at 609 keV is an indication of "processed" ^{238}U.

^{235}U, the second most abundant uranium isotope, is the fissile isotope present in enriched reactor fuel. It is also long-lived, with a half-life of 7.0×10^8 years. ^{235}U can be measured with a gamma ray at 185.7 keV. Although this line overlaps the 185.99-keV line associated with ^{226}Ra, a correction can be made by evaluating other lines in the ^{238}U series.

^{238}U and ^{235}U were detected at approximately the same depth interval in one borehole near the northeast quarter of tank T-106. ^{238}U was also detected in two other boreholes near the southeast quarter of tank T-103.

The chemistry and geochemistry of uranium have been widely studied and the behavior of uranium in the vadose zone and in groundwater is well known. Uranium can exist in several oxidation states depending on the Eh and pH of the geological and hydrological media. Uranium can be one of the more mobile radionuclides at Hanford, and a large quantity of water may flush it through the vadose zone sediments. In terms of a long-term performance assessment, uranium is often one of the higher risk radionuclides for groundwater contamination. The proposed EPA-mandated MCL for uranium in groundwater is 20 micrograms per liter (μg/L) (PNNL 1998).

3.8 Niobium-94 (^{94}Nb)

^{94}Nb has a half-life of about 20,000 years and decays by beta particle emission to stable molybdenum-94 (^{94}Mo). The primary source of ^{94}Nb in the environment has been low-level radioactive waste material generated from the neutron activation of stable niobium-93 (^{93}Nb).

In general, ^{94}Nb is easily adsorbed by soils and is not easily leached into the groundwater. When ^{94}Nb comes into contact with soil and groundwater, most of it will become fixed in the soil and will not migrate appreciably from the original site.

^{94}Nb was detected in two T Tank Farm tank monitoring boreholes located near the southeastern quarter of tank T-103.

The human exposure risk for ^{94}Nb is relatively high because this radionuclide emits both beta particles and gamma rays during decay that are relatively high-energy. The 500-keV maximum energy beta particle emitted from the decay of ^{94}Nb is relatively strong and can result in a beta dose to some internal organs. Each ^{94}Nb decay also results in two high-energy gamma rays, 700 and 870 keV, both of which are more energetic than the 660-keV gamma ray associated with the decay of ^{137}Cs.

^{94}Nb presents a short-term exposure risk because it can be inhaled.

3.9 Tin-126 (^{126}Sn)

^{126}Sn, a fission product, has a half-life of 100,000 years and decays by beta emission to ^{126m}Sb, and then to ^{126}Sb (12.4 day half-life), which decays by beta emission to stable ^{126}Te. It can be detected by gamma ray lines at 414.7, 666.3, and 695 keV.

^{126}Sn was detected in several monitoring boreholes located along the southeastern and southwestern quarters of tank T-106. ^{126}Sn was also detected in one other borehole near the southeast quarter of tank T-103.

Because of its relatively long half life, ^{126}Sn, with its daughters (^{126m}Sb and ^{126}Sb), is the predominant gamma emitter in tank waste on a long-term basis.

3.10 Plutonium, Americium-241 (^{241}Am), Neptunium-237 (^{237}Np), Iodine-129 (^{129}I), Ruthenium-106 (^{106}Ru)

Other nuclides and elements of interest and/or concern with this project include plutonium, ^{241}Am, ^{129}I, ^{237}Np, and ^{106}Ru. Because none of these nuclides or elements were detected in the vadose zone at the T Tank Farm, they will be discussed only in short summaries in this report.

Plutonium isotopes are an inhalation exposure risk. These isotopes are reported to be strongly adsorbed onto the sediment, but, in some cases, organic compounds may enhance their mobility (Carboneau and Garcia 1994). Several plutonium isotopes are present in small quantities in the tank waste and most can be detected and assayed to some degree with gamma spectroscopy measurements if these isotopes are present at high enough concentrations.

^{241}Am has a long half-life (433 years) and can be mobile under low pH conditions. It has an intense gamma ray with an energy of 59.5 keV, which is too low in energy to be detected and assayed with the SGLS. ^{241}Am decays by alpha particle emission to ^{237}Np, which is more mobile than americium. Both of these nuclides may pose a high long-term risk mainly because of the mobility of neptunium (Winberg and Garcia 1995).

^{237}Np is produced from the decay of ^{241}Am and in a reactor by neutron reaction with uranium. ^{237}Np emits a gamma ray with an energy of 311 keV and can be detected with the SGLSs to a lower level of about 2.0 pCi/g; it was not detected in any of the T Tank Farm monitoring boreholes.

Most of the iodine isotopes generated in nuclear reactors are short lived and may be a short-term exposure problem. However, ^{129}I is a long-lived isotope with a half-life of 1.6×10^7 years that is mobile in the vadose zone and groundwater, and it can be a significant long-term risk. Although ^{129}I does emit gamma rays during decay, the energy levels are between 4 and 40 keV, which is too low to be detectable with the SGLS in steel-cased boreholes. The EPA-mandated MCL for ^{129}I is 1 pCi/L (PNNL 1998).

^{106}Ru is a fission product that was abundant in the nuclear waste. ^{106}Ru decays to rhodium-106 (^{106}Rh), which in turn immediately decays to palladium-106 (^{106}Pd) and emits intense gamma rays at 512 keV and 622 keV. When the waste was first placed in the tanks, ^{106}Ru was a major contributor to the total gamma activity of the waste. Because ^{106}Ru has a half-life of only 368 days, it has now decayed to low levels and is generally not detectable. ^{106}Ru was thought to have been a primary target nuclide for vadose zone leak-detection schemes; however, spectral gamma data show that in many cases gamma-ray activity from ^{137}Cs, ^{60}Co, or ^{238}U, in addition to ^{106}Ru, was detected with the gross gamma logging systems (in intervals of elevated gross gamma activity). There are many instances where the SGLS did not detect any man-made gamma emitting radionuclides in regions of boreholes where historical gross gamma log data indicate elevated count rates. These can generally be attributed to ^{106}Ru. In some cases, plots of historical gross gamma activity exhibit a decline in count rates consistent with a short-lived radionuclide such as ^{106}Ru. The EPA-mandated MCL for ^{106}Ru in groundwater is 30 pCi/L (PNNL 1998).

4.0 Geology and Hydrology

The geology of the Hanford Site has been described in detail in numerous documents. The following sections are summaries of information presented in Price and Fecht (1976), Caggiano and Goodwin (1991), Delaney et al. (1991), Lindsey et al. (1992), and Lindsey et al. (1994).

4.1 Regional Geology

The Columbia Plateau is a part of the North American continental plate and lies in a back-arc setting east of the Cascade Range (see Figure 14-2). It is bordered on the east by the Rocky Mountains and Idaho Batholith, on the north by the Okanogan Highlands, and on the south by the High Lava Plains. The Columbia Plateau is divided into three informal structural subprovinces: the Blue Mountains, the Palouse Slope, and the Yakima Fold Belt (Tolan and Reidel 1989) (see Figure 14-3). The Hanford Site lies within the Pasco Basin, one of the largest structural basins in the Columbia Plateau, near the junction of the Yakima Fold Belt and the Palouse subprovinces. Figures 14-2 and 14-3 show the location of the Hanford Site relative to the major regional geologic features in the Pacific Northwest.

The Pasco Basin is bounded on the north by the Saddle Mountains, on the west by the Umtanum Ridge, the Yakima Ridge, and the Rattlesnake Hills, and on the south by Rattlesnake Mountain and the Rattlesnake Hills. The locations of these features are shown in Figure 14-4. All of these uplifts are major structural anticlines within the basalt basement rock. The eastern boundary of the Pasco Basin is a structural monocline with the bedrock dipping to the west and covered with sediments that constitute the Palouse Slope.

4.2 Structural Geology of the Pasco Basin

The major structural features in the Pasco Basin are shown in Figure 14-4. Distinctive features of the Yakima Fold Belt are a series of segmented, narrow, asymmetrical anticlines that are generally east-west trending, and they are within the basalt basement rock. The northern limbs generally dip steeply to the north and are vertical or overturned. The southern limbs generally dip to the south at shallow angles. The anticlinal ridges are separated by broad synclines or basins that may contain thick accumulations of sediments. The Umtanum-Gable Mountain anticline divides the Pasco Basin into the Wahluke and Cold Creek synclines. The Cold Creek syncline is asymmetrical and is a relatively flat-bottomed structure. The Hanford Site 200 Areas are situated on the northern limb of the Cold Creek syncline where bedrock dips to the south at an angle of approximately 5 degrees. In the vicinity of the T Tank Farm, approximately 380 ft of sediments overlie the dipping basalt bedrock.

4.3 General Stratigraphy of the Hanford Site

The general stratigraphy of the Hanford Site consists of basalt flows and associated sedimentary interbeds that constitute the Columbia River Basalt Group and Ellensburg Formations. The

Columbia Basin basalts are overlain by younger sedimentary units consisting of the Ringold Formation, the Plio-Pleistocene unit, the Early Palouse soil, the Hanford formation, and Holocene surficial deposits. Figure 14-5 illustrates the generalized stratigraphy of the Hanford Site.

4.3.1 Basement Basalt and Sedimentary Units

The basement rocks at the Hanford Site consist of a series of basalt flows that are a part of the Columbia River Basalt Group. These flows are continental flood basalts of Miocene Age that extend from north-central Washington, south into Oregon, and east into Idaho, covering an area of more than 63,000 square miles. Interbedded with and overlying many of the basalt flows are sedimentary units constituting the Ellensburg Formation. Sediments of the Ellensburg Formation consist of epiclastic and volcanoclastic materials.

4.3.2 Suprabasalt Sediments

The suprabasalt sediments are dominated by laterally extensive deposits of the late Miocene to middle Pliocene Age Ringold Formation and the Pleistocene Age Hanford formation. Locally occurring strata of the Plio-Pleistocene unit and early Palouse unit separate the Ringold Formation and the Hanford formation.

4.3.2.1 Ringold Formation

Overlying the Columbia Basin basalts are fluvial-to-lacustrine deposits of the Ringold Formation, which include granular to cobble gravels with a sandy matrix, cross bedded and laminated sands, and plane to cross-laminated clay and silt. Deposition in a fluvial environment where post-depositional erosion and truncation are common has resulted in sediments that exhibit extreme and abrupt changes in materials over short lateral distances (Caggiano and Chou 1993).

Lindsey (1995) performed a detailed investigation into the stratigraphy of the Ringold Formation. During the preparation of that report, surface outcrops of Ringold Formation sediments were investigated and mapped, lithologic logs of cores acquired in several Hanford Site boreholes were analyzed, and geologic logs (based on drill cuttings) and cutting samples for several hundred boreholes within and surrounding the Hanford Site were reviewed. On the basis of those data, Lindsey divided the Ringold Formation stratigraphy into five facies based on depositional environment as follows: fluvial gravel, fluvial sand, overbank-paleosol deposits, lacustrine deposits, and basaltic alluvium. These facies are described in detail in Lindsey (1995). The Ringold Formation is also divided into three informal members: Wooded Island (lowermost), Taylor Flats, and Savage Island. The stratigraphic designations of the Ringold Formation are shown in Figure 14-6.

The lower half of the Ringold Formation (Wooded Island member) contains five separate stratigraphic intervals dominated by fluvial gravels. These gravels, which are designated units A,

B, C, D, and E, are separated by basinwide intervals containing deposits typical of the overbank and lacustrine facies associations (see Figure 14-6). Above the Wooded Island member lies the Taylor Flats member. Sediments in the Taylor Flats member consist of mixed fluvial sand and overbank deposits that are commonly referred to as the Ringold Formation upper unit. Overlying the Taylor Flats member is the Savage Island member, which consists primarily of lacustrine facies.

The Ringold Formation is the most extensive suprabasalt sedimentary unit at the Hanford Site. This formation is as much as 600 ft thick south of the 200 West Area. It is absent in the north and northeastern portions of the 200 East Area and adjacent areas to the north, where it pinches out against structural highs in the uppermost basalt flows.

4.3.2.2 Plio-Pleistocene Sediments

The Plio-Pleistocene unit sediments unconformably overlie the Ringold Formation in the 200 West Area. This unit is laterally discontinuous and pinches out in the northern, eastern, and southern boundaries of the 200 West Area. The sediments consist of locally derived basaltic alluvium and pedogenic calcium-carbonate-rich material; both of these facies may be present at some locations. The basaltic material consists of weathered and unweathered locally derived basaltic gravel containing varying amounts of sand and silt. The carbonate-rich sediments consist of calcium-carbonate cemented silt, sand, and gravel interfingering with carbonate-poor sediments. The Plio-Pleistocene unit generally dips to the south-southwest.

The thickness of the Plio-Pleistocene unit varies; it is thickest in the southwest, southeast, and north-central portions of the 200 West Area. These sediments may be as much as 82 ft thick.

4.3.2.3 Pre-Missoula Gravels

The pre-Missoula gravels consist of quartzose to gneissic clast-supported pebble to cobble gravel with quartzo-feldspathic sand matrix that underlies the Hanford formation in the east-central region of the Cold Creek syncline and at the east end of Gable Mountain anticline east and south of the 200 East Area. These gravels do not occur in the region of the T Tank Farm.

4.3.2.4 Early Palouse Soil

A compact, massive loess-like silt with minor fine-grained sand unit may overlie the Plio-Pleistocene unit. This unit is designated the "Early Palouse soil," and it can range to tens of feet thick. The Early Palouse sediments can grade upward into sediments similar to those at the base of the overlying Hanford formation, making the contact between these two lithologic units indistinguishable.

This unit pinches out in the west-central portion of the 200 West Area and near the southern, eastern, and northern boundaries. Limited lithological data acquired in boreholes west of the

200 West Area suggest the Early Palouse soil may extend to the west. The Early Palouse soil is thickest in the southwest and southeast portions of the 200 West Area, where it reaches a maximum thickness of 65 ft.

4.3.2.5 Hanford Formation

The Hanford formation sediments consist of pebble-to-boulder gravel, fine- to coarse-grained sand, and silt. These deposits are divided into three facies: gravel-dominated, sand-dominated, and silt-dominated. These facies are referred to as the coarse-grained deposits, the plane-laminated sand facies, and the rhythmite facies, respectively (Baker et al. 1991). The Hanford formation is thickest in the 200 East and 200 West Areas, where it is as much as 350 ft thick, and it is absent on ridges more than 1,160 ft above sea level. These sediments were deposited during several episodes of cataclysmic flooding that resulted from drainage of glacial lake Missoula in the Pleistocene Age (Baker et al. 1991).

The gravel-dominated facies generally consists of coarse-grained basaltic sand and granule-to-boulder gravel, and ranges from well sorted to poorly sorted. In outcrop, these sediments display massive bedding, planar to low-angle bedding, and large-scale planar cross-bedding. Gravels dominate the Hanford formation in the 100 Areas north of Gable Mountain, the northern portion of the 200 East Area, and the eastern portion of the Hanford Site. The gravel-dominated facies was deposited by high-energy flood waters in or immediately adjacent to the main flood channel.

The sand-dominated facies consists of fine- to coarse-grained sand and granule gravel. In outcrop, these sediments display plane lamination and bedding, and, less commonly, plane bedding and channel-fill sequences. These sands may contain small pebbles or pebble-gravel interbeds less than 8 inches (in.) thick. The silt content of the sands is variable, but where it is low, an open framework texture occurs. The sands are typically basaltic, displaying a salt-and-pepper appearance. The sand-dominated facies is transitional between the gravel-dominated facies to the north and the rhythmite facies to the south, and it is present in the 200 Areas. The laminated-sand facies was deposited adjacent to the main flood channelway as it spilled out of the main channel, or it may have been deposited during the diminishing stages of flooding.

The rhythmite facies sediments were deposited under slack water conditions and in back-flooded areas remote from the main flood channelway. These sediments consist of thinly bedded, plane-laminated and ripple cross-laminated silt and fine- to coarse-grained sand and commonly display normally graded rhythmites a few centimeters to several tens of centimeters thick (Baker et al. 1991; DOE 1988). This facies dominates the Hanford formation occurrence along the western, southern, and northern margins of the Pasco Basin, within and south of the 200 Areas.

Clastic dikes are present in the Hanford formation as well as in other sedimentary units in the Pasco Basin (Black 1980). These dikes normally cross-cut bedding, although locally they do parallel bedding. They usually consist of thin alternating vertical to subvertical layers of silt, sand, and granules. Clastic dikes are more common in the finer grained facies and rare in the open-framework gravels (Connelly et al. 1992). Where the dikes intersect the ground surface,

distinct patterned ground is observed. Fecht et al. (1998) provide a summary of the current understanding of clastic dikes in the Pasco Basin.

4.3.2.6 Holocene Surficial Sediments

Holocene surficial deposits consist of silt, sand, and gravel that form a thin layer across much of the Hanford Site. These sediments were deposited by a combination of aeolian and alluvial processes. During construction activities at several areas of the Hanford Site (such as the tank farms), these surficial sediments were removed and replaced with a gravel cover that prevented establishment of vegetation for both operation purposes and radiological controls.

4.4 Geology of the 200 West Area

The 200 West Area is situated on the generally southward-dipping north limb of the Cold Creek syncline, which is a gently sloping low-relief surface that resulted from two geomorphological processes: Pleistocene cataclysmic flooding and Holocene eolian activity. Pleistocene cataclysmic flooding resulted when glacially created dams failed and drainage from the dammed lakes flowed across the Columbia Plateau. These floods led to deposition of sand and gravel in the waters that were impounded (with the formation of Lake Lewis) behind Wallula Gap. Deposition of sand and gravel created Cold Creek bar, a prominent feature on which the 200 West Area is located (Figure 14-7). The northern boundary of the Cold Creek bar is an east-southeast trending erosional channel that formed during waning stages of flooding as floodwaters drained from the basin (Bjornstad et al. 1987). Since the Pleistocene, winds have locally reworked the surface of the glacio-fluvial sediments, depositing a thin veneer of eolian sand in places. Holocene deposits consist of fine- to medium-grained sand and occasionally silt that were deposited in thin sheets less than 3 meters (m) thick (Lindsey et al. 1992). As discussed previously, the Holocene surficial deposits were removed during construction of the tank farm excavation.

The general stratigraphy of the 200 West Area consists of basalt flows and sedimentary interbeds that constitute the Columbia River Basalt Group and Ellensburg Formations. Overlying the Columbia River basalts are sediments that consist of fluvial-to-lacustrine deposits of the Ringold Formation. The Ringold Formation is subdivided into several stratigraphic units; however, erosion by the ancestral Columbia River and later cataclysmic flooding has removed the Savage Island Member and most of the Taylor Flat Member from the Ringold Formation over most of the Hanford Site (DOE 1988; Tallman et al. 1979).

The cataclysmic flooding that eroded the Ringold Formation sediments also deposited the unconsolidated sands, gravels, and silt that are informally designated the Hanford formation. These deposits are as much as 150 ft thick beneath the 200 West Area. Figure 14-8 is a map depicting the surface geology and major structural features in the Pasco Basin.

4.5 T Tank Farm Geology

A description of the geology beneath the T Tank Farm was first completed in 1976 after 36 tank monitoring boreholes and 7 groundwater monitoring wells were drilled in and around the T Tank Farm. The geology, which was described from sediment samples collected at 1- to 5-ft depth intervals during drilling, is presented in Price and Fecht (1976). Cross sections based on these data are shown in Figures 14-9 and 14-10.

Price and Fecht (1976) provide detailed descriptions of the geologic conditions beneath the T Tank Farm. Caggiano and Goodwin (1991) provide geologic cross sections and further descriptions of geologic conditions based on a review of historical data and data from newly drilled groundwater monitoring wells. Lindsey (1993) provides a summary of the geology and hydrogeology of the T Tank Farm based on information from Price and Fecht (1976) and Caggiano and Goodwin (1991) and data from newer RCRA groundwater monitoring wells, surface mapping, and older wells. Figure 14-11 is a summary diagram of Lindsey's conclusions in the vicinity of the T Tank Farm. The following description of the T Tank Farm geology is a summation of data from these documents using the stratigraphic nomenclature proposed in Lindsey (1993).

The three major stratigraphic units present within the vadose zone at the T Tank Farm from top to bottom are 1) the unconsolidated sand, silt, and gravel of the Hanford formation, 2) the early Palouse soil and the Plio-Pleistocene unit, and 3) the semiconsolidated sediments of the Ringold Formation.

The Hanford formation was deposited during the Pleistocene epoch by numerous cataclysmic flooding events caused by periodic ruptures of ice dams holding back large glacial lakes. The Hanford formation sediments consist of coarse to very coarse gravel, fine- to coarse-grained sand, and silt. Three distinct facies have been recognized by Lindsey (1993): gravel-dominated, sand-dominated, and silt-dominated (ordered from top to bottom of the Hanford formation).

In the vicinity of the T Tank Farm, the upper portion of the Hanford formation consists of gravelly deposits typical of the gravel-dominated facies of the Hanford formation. Much of this material in the immediate vicinity of the tank farm has been excavated and redeposited as backfill material around the tanks. This material is poorly sorted and consists predominantly of cobbles, pebbles, and coarse to medium sand with silt. The backfill extends from the ground surface to a depth of about 38 ft (i.e., from the surface elevation of about 671 ft to an elevation of about 633 ft above mean sea level) (Price and Fecht 1976). A sand-dominated interval of the Hanford formation primarily composed of very coarse to medium sand with some pebbles occurs beneath the backfill material (Price and Fecht 1976). Generally, this interval tends to become finer grained in the downward direction with the frequency of silt beds increasing. The base of this unit lies about 75 to 100 ft below the ground surface. The contact appears to be irregular and generally slopes to the west and east (Lindsey 1993).

Clastic injection dikes are commonly found in the Hanford formation. These clastic injection dikes consist of thin, alternating vertical to subvertical layers of silt, sand, and granules that

generally cross-cut bedding. Clastic injection dikes are common in the vadose zone beneath the Hanford Site, although they are difficult to detect. Where present, clastic injection dikes can act as barriers or pathways to fluid transport, depending on the content of the dike and the type of sediment through which it passes (Lindsey 1993).

Locally occurring strata separating the Pleistocene-aged Hanford formation and the Miocene- to Pliocene-aged Ringold Formation are informally defined as the early Palouse soil, the pre-Missoula gravels, and the Plio-Pleistocene unit. The pre-Missoula gravels are not present in the vicinity of the T Tank Farm and will not be discussed further.

The Palouse soil and the Plio-Pleistocene unit contain similar sedimentary textures and are often difficult to differentiate on the basis of texture alone. Available data from wells in the vicinity of the T Tank Farm are generally inadequate to distinguish between these units (Caggiano and Goodwin 1991). However, a deep exploratory borehole (50-06-18) was drilled adjacent to tank T-106 in 1993. On the basis of detailed lithologic information derived from the drilling log of this borehole, Freeman-Pollard et al. (1994) have identified and determined the local depth and thickness of each unit in this area. This information is included in the description of each unit.

The early Palouse soil horizon is encountered at a depth of about 80 ft and is approximately 10 ft thick in the vicinity of tank T-106 (Freeman-Pollard et al. 1994). This unit consists of massive, brown-yellow and compact, loess-like silt and minor fine-grained sand (Lindsey and Horton 1991). The upper contact of the unit is poorly defined, and it may grade up-section into silty strata commonly found in the lower portion of the sand-dominated facies of the Hanford formation. Magnetic polarity data indicate the unit to be early Pleistocene in age (Lindsey and Horton 1991).

The Plio-Pleistocene unit underlies the early "Palouse" soil and extends from about 91 to 105 ft in the vicinity of tank T-106 (Freeman-Pollard et al. 1994). This laterally discontinuous unit is divided into the sidestream alluvium facies and the calcic paleosol facies (Lindsey and Horton 1991). These facies are inferred to be late Pliocene to early Pleistocene in age on the basis of stratigraphic position and the magnetic polarity of interfingering loess units. Weathered and unweathered basaltic gravels dominate the sidestream alluvium facies. The calcic paleosol facies consist of massive calcium-carbonate-cemented silt, sand, and gravel (caliche) to interbedded caliche-rich and caliche-poor silts and sands. The caliches are moderately to highly fractured. Two prominent caliche layers are found within the Plio-Pleistocene unit below the T Tank Farm. The upper layer occurs from about 91 to 93 ft and the lower layer occurs from about 100 to 103 ft. The lower caliche layer is better developed than the upper caliche layer (Price and Fecht 1976).

The Plio-Pleistocene unit unconformably overlies the Ringold Formation. Beneath the T Tank Farm, the Ringold Formation consists of both the upper unit and Unit E. The upper unit consists of up to 25 ft of coarse- to fine-grained sand with lenses of interbedded silt. The upper unit may pinch out near the southeast corner of the T Tank Farm. The Ringold Unit E underlies the Ringold upper unit, where present, or the Plio-Pleistocene unit. The Ringold Unit E consists of

fluvial gravels with muddy zones and cemented zones above the water table that may form local perched water conditions (Lindsey 1993).

When possible, the SGLS ^{40}K, ^{238}U, and ^{232}Th concentration data were used to identify lithologic features and to determine lateral correlation of these features between boreholes. Often, contacts between lithologic units were not distinctive, or they were not penetrated by the monitoring boreholes. Furthermore, the T Tank Farm boreholes are double-cased and the annular space between the casings is filled with grout. This configuration significantly affected the SGLS data acquisition by attenuating gamma rays and introduced an undetermined error to the calculated concentrations. However, some insight into the lithology beneath the T Tank Farm can be inferred from these data. Figures 14-12 and 14-13 are log plots of the SGLS KUT concentration data and total gamma plots for boreholes 50-00-03 and 50-00-10, respectively.

The major stratigraphic units that are distinguishable using the KUT data include the Hanford formation, the Early Palouse Soil, the Plio-Pleistocene Unit, and the Upper Unit and Unit E of the Ringold Formation. The identification of these units is based strictly on a correlation of the published geological information with the KUT log profile characteristics and not on quantitative evaluation of sediment or formation properties such as chemical composition and grain size. The reader is encouraged to consult the individual Tank Summary Data Reports (DOE 1995d, 1995e, 1998c, 1998d, 1998e, 1998f, 1999a, 1999b, 1999c, 1999d, 1999e, and 1999f), where the KUT concentration plots are included in the report appendices. The Tank Summary Data Reports also include discussions describing lithologic features in context with contaminant distribution, where these correlations exist. More often than not, these lithology/contaminant correlations are borehole specific and do not relate to adjacent boreholes.

4.6 T Tank Farm Hydrology

The Hanford Site is underlain by a multiaquifer system consisting of four hydrologic units that correspond to the three uppermost formations of the Columbia River Basalt Group and the suprabasalt sediments (DOE 1988; Delaney et al. 1991). The groundwater beneath the Hanford Site occurs under confined, semi-confined, and unconfined conditions.

The confined aquifers are located in the sedimentary interbeds of the Ellensburg Formation, flow-top breccias, and in permeable interflow zones that occur between basalt flows (Figures 14-5 and 14-6). Dense regions within the interiors of the basalt flows of the Columbia Basin Basalt Group separate the flow tops and interflow zones and act as aquitards. The shallow basalt aquifers are generally located in the Saddle Mountains and upper Wanapum Basalts. Recharge to these aquifers occurs through infiltration of precipitation and runoff along the margins of the Pasco Basin. Groundwater from the shallow basalt aquifers most likely discharges to the overlying sediments and to the Columbia River.

The unconfined aquifer is the uppermost aquifer in the area of the T Tank Farm and is the focus of groundwater monitoring at the Hanford Site. At the T Tank Farm, the aquifer is contained in the Ringold Unit E Formation, which consists of fluvial gravels with muddy zones and cemented

zones above the water table that may form local perched water conditions (Lindsey 1993). The water table occurs at a depth of about 218 ft (Hodges 1998).

Groundwater flow directions in the vicinity of the T Tank Farm have varied over time as a result of the influence of various effluent discharge sites in the 200 West Area. Before the start of Hanford operations, groundwater flow was predominantly east or northeast, driven by recharge in the Cold Creek Valley and topographically high areas along the western boundary of the Pasco Basin. During the late 1940s and early 1950s, groundwater flow was affected by discharges to the T Pond, located northwest of the T Tank Farm. Groundwater mounding beneath T Pond resulted in a gradient to the south or southeast. With the closure of T Plant processing operations in 1956, discharges to the T Pond decreased and other recharge sources (U Pond and Z Cribs) became more important, such that flow direction changed to the north or northeast (Hodges 1998).

The hydraulic gradient in the vicinity of the T Tank Farm is 0.0013, which was calculated between monitoring wells 299-W10-16 and 299-W11-28. The estimated groundwater-flow velocity is 0.13 m/day (PNNL 1998) (see Figure 14-14). Figure 14-15 presents a water table map of the Hanford Site for June 1997. Presently, groundwater flow is generally in a northeast direction and is controlled by the U Pond groundwater mound to the south. The U Pond groundwater mound has been dissipating since the U Pond was deactivated in 1984. A comparison of groundwater levels indicates that the groundwater table dropped more than 5 ft from 1985 to 1990. The June 1990 water level in the vicinity of the T Tank Farm is reported as 464 ft above mean sea level (a depth of about 207 ft) (Caggiano and Goodwin 1991). The June 1997 water table beneath the T Tank Farm was reported at an approximate elevation of 453 ft (a depth of about 218 ft) (Hodges 1998). The groundwater flow direction under the T Tank Farm was primarily to the north when the groundwater mound developed beneath the U Pond. As the mound dissipated following decommissioning of the U Pond in 1985, the groundwater flow direction shifted from the north to the northeast. With further decline of the recharge mound, the groundwater flow direction is expected to shift toward the regional west to east direction (PNNL 1998).

Natural recharge of the unconfined aquifer is by rainfall and runoff from the hills bordering the Hanford Site, by infiltration from small ephemeral streams, by water infiltration through faults and fractures in the underlying basalts, and by infiltration from the Columbia and Yakima Rivers. At the Hanford Site, recharge of the unconfined aquifer by precipitation is highly variable depending on the seasons, vegetative cover, and surface and near-surface soil types.

Artificial recharge of the uppermost aquifer occurs from the disposal of waste water at the Hanford Site and from large-scale agricultural irrigation that surrounds the Site. At the present time, large-scale waste-water disposal on the Hanford Site occurs only at the Treated Effluent Disposal Facility, which is located southeast of the 200 East Area, and at the State Approved Land Disposal System (SALDS), which is located north of the 200 West Area.

Natural recharge through the unsaturated (vadose) zone has been studied at various locations at the Hanford Site. The most recent study estimating recharge rates at the Hanford Site is documented in Fayer and Walters (1995); average long-term recharge rates vary from 2.6 millimeters per year (mm/yr) to 127 mm/yr (annual amounts of precipitation range from 76 to 291 mm). Figure 14-16 presents a map depicting the estimated annual recharge from infiltration from precipitation from PNNL (1998). In the 200 East and 200 West Areas, the highest values are associated with areas of greatest surface disturbance, such as at the tank farms and burial grounds.

Recharge rates are highest in coarse-grained sediments with little or no vegetative cover, which is the present surface condition at the T Tank Farm. The tank farm surface covers are designed to restrict vegetative growth and control accumulation of radioactive surface contamination. These functions are accomplished by removing all vegetation, applying gravel covers, and in some cases by applying a surface sealant to control dust.

Unsaturated (vadose) conditions across the Hanford Site show variations in hydrologic properties similar to those observed in the uppermost aquifer system. Sediments in the vadose zone vary from open-framework gravels of the gravel-dominated facies and interbedded sand and silt of the silt-dominated facies of the Hanford formation to calcium-carbonate-rich deposits of the Plio-Pleistocene unit to cemented gravels of the Ringold Formation. These sediments are characterized by numerous lateral discontinuities, such as pinchouts and erosion truncations, and flow patterns are irregular. If clastic dikes are present, they may alter vertical flow patterns.

Knowledge of vadose zone hydraulic properties is important for predicting the fate and transport of contaminants through the vadose zone sediments and for determining the potential for recharge of the vadose zone through precipitation. Laboratory results have indicated a high degree of variability in the moisture retention data; however, there is a paucity of data from some of the lithologic units encountered in the vadose zone at the 200 West Area. The reader is advised to reference Connelly et al. (1992), DOE (1993), and Myers et al. (1998) for the details and results of the analyses performed on samples of specific vadose zone sediments.

4.7 Groundwater Monitoring

Groundwater beneath the T Tank Farm is monitored under a RCRA groundwater monitoring program that is currently administered by PNNL. The T Tank Farm is designated Waste Management Area T (WMA-T).

The groundwater beneath WMA-T is monitored with a network of four RCRA monitoring wells that surround this tank farm. Figure 14-14 shows the locations of these monitoring wells. Well 299-W10-16 was installed as an upgradient monitoring well, and wells 299-W10-15, 299-W11-27, and 299-W11-28 were installed as downgradient monitoring wells for WMA-T. The RCRA standard monitoring wells were all constructed to monitor the top portion (approximately 15 to 20 ft) of the unconfined aquifer. Additional information regarding these monitoring wells is provided in Caggiano and Chou (1993). The other monitoring wells shown in Figure 14-14 are used only to acquire ground water level measurements.

Groundwater-level measurements are acquired in all the monitoring wells quarterly, and groundwater samples for chemical and radiological analyses are acquired in the RCRA-standard wells semiannually. The results of the data analyses are presented annually in a report prepared by PNNL. *Hanford Site Groundwater Monitoring for Fiscal Year 1997* (PNNL 1998), an example of the most recent presentation of the monitoring data, summarizes the results of groundwater and vadose zone monitoring activities that were conducted at the Hanford Site during fiscal year (FY) 1997.

4.8 Groundwater Contamination in the Area of the T Tank Farm

The following discussions are the results of groundwater monitoring at WMA-T during FY 1997 that are presented in PNNL (1998). No attempt was made to review the specific groundwater data or to provide additional evaluation and interpretations. The reader is encouraged to review the referenced documents for additional discussions regarding contaminant distributions, for details regarding analytical methods and quality assurance for sample analyses, and for discussions of further interpretations of results.

A large tritium plume covers the northern half of the 200 West Area and is shown on Figure A-1 in Appendix A. The plume extends to the northeast, beyond the 200-West Area boundary. Tritium values exceeded the interim DWS of 20,000 pCi/L in WMA-T monitoring wells 299-W10-15, 299-W10-16, and 299-W11-28. The maximum tritium concentration (62,900 pCi/L) was detected in monitoring well 299-W11-28.

A ^{99}Tc plume is centered over the area of the TX and TY Tank Farms, designated as Waste Management Area TX-TY (WMA-TX-TY), and is shown on Figure A-2 in Appendix A. However, the maximum ^{99}Tc concentration (21,700 pCi/L) was measured in WMA-T downgradient monitoring well 299-W11-27 located along the western edge of the plume. This concentration is approximately 24 times greater than the interim DWS of 900 pCi/L.

Gross beta concentrations exceeded the interim DWS of 50 pCi/L in all of the WMA-T monitoring wells. The maximum gross beta concentration (13,700 pCi/L) was measured in monitoring well 299-W11-27.

A ^{106}Ru concentration of 31.6 pCi/L was measured in WMA-T downgradient monitoring well 299-W10-15. This value slightly exceeded the interim DWS of 30 pCi/L.

A chromium plume is located over the central portion of WMA-T and is shown on Figure A-3 in Appendix A. Chromium was detected at concentrations slightly above the interim DWA of 100 μg/L in downgradient monitoring wells 299-W10-15 (106 μg/L) and 299-W11-28 (115 μg/L). Chromium concentrations in downgradient monitoring well 299-W11-27, which exhibited a peak in FY 1996, remained below the interim DWS in FY 1997.

Fluoride was detected in a number of wells in the vicinity of WMA-T. A flouride plume is centered near the northern edge of WMA-T and is shown on Figure A-4 in Appendix A. The

maximum fluoride concentration of 4.46 milligrams per liter (mg/L) was measured in downgradient monitoring well 299-W10-15; this concentration is above the interim DWS of 4 milligrams per liter (mg/L).

The groundwater beneath much of the northern portion of the 200 West Area contains elevated nitrate concentrations that are above the 45 mg/L MCL. The distribution of the nitrate plumes are shown on Figure A-5 in Appendix A. Nitrate concentrations exceeded the interim DWS of 10 mg/L in all of the WMA-T monitoring wells. The maximum nitrate concentration (69.8 mg/L) was measured in downgradient monitoring well 299-W10-15. There are many possible sources for the extensive nitrate contamination in the vicinity of WMA-T but a specific source or sources has not been determined.

The specific conductance in monitoring well 299-W10-15 remained high, although the values were below the critical mean for WMA-T during FY 1997 (1,175 microsiemens per centimeter [μS/cm]). The elevated specific conductance for groundwater in this well is principally the result of elevated concentrations of sodium and nitrate.

Specific conductance in monitoring well 299-W11-27 exceeded the critical mean for WMA-T during FY 1997, with a maximum value of 1,267μS/cm measured in November 1996. This increase in specific conductance is the result of increases in calcium, magnesium, nitrate, and sulfate and was accompaied by increases in ^{99}Tc, tritium, and chromium. Reported ^{60}Co concentrations of 29 and 26 pCi/L were measured in May and August 1997, respectively, indicating that ^{60}Co is a co-contaminant.

The sodium:calcium ratio provides information on a potential contaminant source. Although the waste in the SSTs contain considerable sodium, the sodium:calcium ratio will be reduced for low-volume discharges as a result of ion exchange with vadose zone sediments. Sodium:calcium ratios in downgradient monitoring well 299-W11-27 dropped to as low as 0.13, much lower than upgradient and area background ratios (3:6), and are consistent with a low-volume tank-waste source that cannot overwhelm the ion-exchange capacity of the vadose zone. In addition, the tritium:^{99}Tc ratio has fallen as low as 0.2, distinct from the upgradient and area background numbers and consistent with the magnitude of ratios expected in tank waste.

The contaminants affecting groundwater quality in downgradient monitoring well 299-W11-27 represent a very narrow plume. Downgradient wells 299-W10-8 and 299-W11-23, which bracket well 299-W11-27 and are separated by approximately 55 m, are unaffected by the plume. This lack of lateral dispersion, which indicates a nearby source, coupled with the observed chemistry, offers strong indication that the groundwater contamination observed in well 299-W11-27 originated within WMA-T.

5.0 Review of Tank Farm History

5.1 Tank Construction

The T Tank Farm tanks were constructed between 1943 and 1944 and are located in the northwestern portion of the 200 West Area (Figure 14-1). The 16 tanks in the T Tank Farm are SSTs of two design types; Type I and Type II. There are four Type I tanks that are 20 ft in diameter, have a 3-ft radius knuckle at the junction of the tank's bottom and side walls, and have a 0.5-ft dished bottom (the perimeter of the tank bottom is 0.5 ft above the center of the tank bottom). At the maximum waste capacity of 55,000 gal per tank, the level of the waste in each tank is about 18 ft above the bottom of the tank base. There are twelve Type II tanks which are 75 ft in diameter, have a 4-ft radius knuckle at the junction of the tank's bottom and side walls, and have a 1-ft dished bottom. At the maximum waste capacity of 530,000 gal per tank, the level of the waste in each tank is about 18 ft above the tank bottom. The tops of the Type I and Type II tanks are about 11 ft and 7 ft below the finished grade of the tank farm surface, respectively; the bases of the tanks are at a depth of about 40 ft below the ground surface. The T Tank Farm is one of the original tank farm designs along with the B, C, and U Tank Farms. Figure 14-17 presents a plan view of the T Tank Farm showing the 16 waste tank locations. This figure also shows the locations of the monitoring boreholes around the large Type II tanks. Details regarding the construction of the Type II tanks were derived from construction details outlined in *Specifications for Construction of Composite Storage Tanks Bldg. No. 241* (DOE 1944). The following discussion of tank construction is based on this information.

Each tank consists of a steel-reinforced concrete shell approximately 1 ft thick and a carbon-steel inner liner that covers the bottom and sides of the shell. The dome of each tank was also constructed with reinforced concrete approximately 1 ft thick. The thicknesses of the bottom section of liner plating and both wall sections of plating are 1/4 in. The steel tank sides are joined to the steel liner of the tank bottom by rounded knuckle sections of 3/8-in.-thick steel plating formed to a 4-ft radius. The knuckle sections allowed for expansion of the base liner. Six steel angle stiffeners are welded horizontally around the interior of the tank walls. The specifications for liner plating and protective membrane composition are outlined in Drawing W-71387, which is available from the Lockheed Martin Services, Inc., Microfiche Library, Richland, Washington.

The tanks are sited at slightly different elevations, creating a gradient that allows liquids to flow from one tank to another as they are filled. The tanks are arranged in four cascades, each consisting of a three-tank cascade series with the receiving tank 1 ft lower than the feed tank. For example, one three-tank cascade series consists of tanks T-101, -102, and -103, where T-101 cascades into T-102 and tank T-102 cascades into T-103. The height of the cascade line outlets from the tank bottoms controls the maximum capacity of the tanks. The cascade inlet and overflow connections are sleeved and welded to the tank steel liners about 2 ft below the top of the liner, which is about 21 ft below the ground surface. The cascade lines are set on reinforced

concrete beams that bridge the distance between the tanks, and the beams are reinforced at the concrete tank shells.

Each tank is equipped with four spare 3-in.-diameter inlet nozzles. These nozzles are located at an azimuth of about 135 degrees at the same height as the cascade line connections to the tanks. It is unknown if these nozzles are capped or connected to piping; however, as will be discussed later, these nozzles have been determined to be sources of leaks.

The domes of the tanks are penetrated by several risers that allow access to the tank interiors. Tanks T-104, -110, and -111 have liquid observation wells (LOWs) that penetrate the wastes in these tanks. The LOWs are used to monitor the interstitial water levels in the waste solids by logging with neutron-neutron and gamma probes. A cross section of a typical SST with associated risers and access ports is shown on Figure 14-18; Brevick et al. (1995) provide information specific to each T Tank Farm tank.

All of the T Farm tanks, except tanks T-102 and T-105, contain thermocouple trees that are used to monitor the temperatures of the wastes. Several thermocouples are installed on a single tree to allow the waste to be more effectively monitored at several specific depth locations. The data are automatically transmitted from the thermocouple trees to tank farm operations via the Tank Monitor and Control System (TMACS).

Transfer lines connect the tanks to each other as well as to other facilities at the Hanford Site. Most of the lines are constructed of 3-in.-diameter steel piping with welded joints. These lines are generally below the ground surface and some are contained within reinforced concrete encasements that allow capture and diversion of leaked waste liquid to appropriate catchment tanks. Diversion boxes contain the switching mechanisms that allow transfers from one transfer line to another. The diversion boxes are constructed of concrete and are buried below the ground surface to a depth of about 12 ft; like the transfer-line encasements, drainage from the diversion boxes is directed to catchment tanks. Several diversion boxes are located within the T Tank Farm; these diversion boxes drain into the 241-T-301 Catch Tank at the south end of the T Tank Farm. This tank is 20 ft in diameter and 13.5 ft high. The tank has a concrete domed lid that lies approximately 10 ft below the ground surface. Other receiver tanks and vaults associated with T Tank Farm operations are described in detail in DOE (1992). These facilities also have a potential to contribute to shallow vadose zone contamination at the T Tank Farm.

Limited construction information was located for the four Type I auxiliary tanks located in the southwest portion of the tank farm. However, DOE (1944) indicates that the construction of the Type I tanks was similar to that of the Type II tanks.

Several inches of gravel were placed on top of the backfilled sediments to provide protection and retard establishment of vegetation that could bring subsurface contamination up to the ground surface. The ground layer also helped prevent or reduce exposure to personnel from contaminated near-surface sediment and pipelines. Unfortunately, the lack of vegetation inhibits evapotranspiration of precipitation and may promote infiltration of precipitation into the subsurface at the farm.

The major driving forces for pushing contaminants through the vadose zone at WMA T, other than their own volumes and densities, appear to be surface infiltration through the gravels that cover the WMA and surface runoff, principally from rapid snow melt (Hodges 1998). WMA T is located at the bottom of a natural depression that tends to catch any surface runoff and cause water to pond within the T Tank Farm. Slopes immediately adjacent to the WMA, particularly along the east side, tend to funnel surface runoff directly into the tank farm. A rapid snow melt event in February 1979 caused widespread flooding of the T Tank Farm. The extent of the flooding is illustrated by photos in Hodges (1998). There is little doubt that this is not the only event of this type that has occurred (Hodges 1998).

Additional details regarding the construction of the T Tank Farm tanks are presented in Brevick et al. (1995).

5.2 Tank Waste Constituents

Anderson (1990) provides general information regarding the history and contents of the T Tank Farm tanks. More information specific to this tank farm and each tank is provided in a compilation of historical monitoring information that is assembled in several volumes of reports prepared by Brevick et al. (1995) and by Agnew (1997) and Agnew et al. (1995).

The *Supporting Document for the Historical Tank Content Estimate for T Tank Farm, Vol. 1 and 2* (Brevick et al. 1995) specifically addresses the T Tank Farm. This document presents historical waste inventories for each of the T Tank Farm tanks. The authors compiled most of the available operational and monitoring information for the tanks and provided detailed summaries of tank construction and configuration, in-tank photographs, and other data. Much of the information presented in this section of this report is from Brevick et al. (1995). General descriptions of the types of wastes discharged to and stored in the T Tank Farm tanks are provided in Table 1.

Table 1. General Waste Information, T Tank Farm

Tank No.	Waste Description	Service Period
T-101	Bismuth phosphate metal waste, tributyl phosphate waste, supernatant containing coating waste, B Plant low-level waste, decontamination waste, evaporator feed and bottoms waste, ion-exchange waste, REDOX ion-exchange waste, REDOX high-level waste, PNL laboratory waste, and 224-U waste.	1944-1979
T-102	Bismuth phosphate metal waste, coating waste, B Plant low-level waste, evaporator bottoms waste, ion-exchange waste, REDOX ion-exchange waste, and wastewater.	1945-1976

Table 1 (continued). General Waste Information, T Tank Farm

Tank No.	Waste Description	Service Period
T-103	Bismuth phosphate metal waste, coating waste, B Plant low-level waste, evaporator bottoms waste, ion-exchange waste, REDOX ion-exchange waste, and wastewater.	1945-1974
T-104	Bismuth phosphate first-cycle decontamination waste.	1946-1976
T-105	Bismuth phosphate first- and second-cycle decontamination waste, coating waste, B Plant low-level waste, decontamination waste, ion-exchange waste, wastewater, and Hanford laboratory operations waste.	1946-1976
T-106	Bismuth phosphate first- and second-cycle decontamination waste, coating waste, B Plant low-level waste, decontamination waste, ion-exchange waste, and wastewater.	1947-1973
T-107	Bismuth phosphate first-cycle decontamination waste, tributyl phosphate waste, coating waste, B Plant low-level waste, evaporator feed waste, ion-exchange waste, uranium recovery waste, and wastewater.	1944-1976
T-108	Bismuth phosphate first-cycle decontamination waste, tributyl phosphate waste, B Plant low-level waste, evaporator bottoms waste, ion-exchange waste, PNL laboratory waste, Hanford laboratory operations waste, wastewater, and salt cake.	1945-1974
T-109	Bismuth phosphate first-cycle decontamination waste, tributyl phosphate waste, B Plant low-level waste, evaporator bottoms waste, ion-exchange waste, PNL laboratory waste, and salt cake.	1945-1974
T-110	Bismuth phosphate second-cycle decontamination waste, 224-U waste, and wastewater.	1944-1976
T-111	Bismuth phosphate second-cycle decontamination waste, and 224-U waste.	1945-1974
T-112	Bismuth phosphate second-cycle decontamination waste, coating waste, B Plant low-level waste, decontamination waste, evaporator feed waste, ion-exchange waste, 224-U waste, PNL laboratory waste, and wastewater.	1946-1976
T-201	224-U waste, and evaporator feed waste.	1952-1976
T-202	224-U waste.	1952-1976
T-203	224-U waste, and evaporator feed waste.	1952-1976
T-204	224-U waste.	1952-1976

The T Tank Farm began receiving waste from T Plant processing operations in December 1944. Three main waste types were produced by the bismuth-phosphate process used in T Plant until 1956. The first waste type was metal waste that was produced when irradiated uranium fuel elements were dissolved in acid and plutonium was extracted. The metal waste contained all of the uranium from the irradiated uranium fuel elements and 90 percent of the fission products (i.e., no effort was made to extract the uranium or fission products from the waste and they were disposed to the tanks) (Brevick et al. 1995). Two decontamination cycles were performed to purify the plutonium product once the plutonium was extracted by the bismuth-phosphate process. ("Decontamination" is used to describe the removal of contaminants from the plutonium product.) The first decontamination cycle produced a waste stream (known as first-cycle decontamination waste) that contained almost 10 percent of the fission products from the original irradiated uranium fuel elements. The second decontamination cycle produced a waste stream (known as second-cycle decontamination waste) that contained about 0.1 percent of the fission products from the original irradiated uranium fuel elements (DOE 1993).

The wastes in the T Tank Farm tanks consist of sludge and liquids (depicted in Figure 14-18). Sludge is composed of solid (hydrous metal oxides) precipitate that resulted from the neutralization of acidic wastes. The nitric acid solutions of metals that result from dissolution of the irradiated fuel elements during processing were neutralized with sodium hydroxide before they were transferred to the tanks. The sludge forms the solids component of the tank waste. Liquids are present as supernatant and interstitial liquid. Supernatant liquid rests on top of the tank solids, while interstitial liquid fills the interstitial spaces within the waste solids. Interstitial liquid may be drainable if it is not held in the void spaces by capillary forces. Tank content quantities of sludge and liquids are summarized monthly in the *Waste Tank Summary Report* (Hanlon 1999).

The chemical composition of the waste is complex and an ongoing program is characterizing the tank wastes through retrieval and analyses of cores of the waste. Sampling data obtained from the WHC Waste and Retrieval Group are presented in Brevick et al. (1995). Agnew (1997) also provides details regarding the waste content of the tanks. These data indicate the anions are predominantly carbonates, nitrates, nitrites, and sulfates; cations include Na^{+}, Al^{+3}, Fe^{+3}, Cr^{+3}, Ni^{+2}, Pb^{+2}, Bi^{+3}, Zr^{+2}, La^{+3}, and other metals include uranium, plutonium, and americium. Radionuclides contained in the wastes include $^{89\text{-}90}Sr$, ^{137}Cs, ^{134}Cs, ^{60}Co, ^{125}Sb, ^{106}Ru, ^{144}Ce, ^{95}Zr, and ^{239}Pu, and isotopes of uranium (^{235}U and ^{238}U) and europium (^{152}Eu and ^{154}Eu). These chemical constituents and radionuclides were introduced into the tanks in solution, and through evaporation and in-tank reactions, they precipitated as sludge and salt cake.

The first cascade series (tanks T-101, -102, and -103) received metal waste and was full by February 1946. The second cascade series (tanks T-104, -105, and -106) began receiving second-cycle decontamination waste in early 1946 and was full by August 1946. The third cascade series (tanks T-107, -108, and -109) began receiving first-cycle decontamination waste in 1945 and was full by March 1946. The remaining cascade series (tanks T-110, -111, and -112) began receiving second-cycle decontamination waste in 1945 and was full by July 1946 (Brevick et al. 1995).

Waste was pumped from tanks T-107, -108, and -109 in 1951 and 1952 to create storage space for tributyl phosphate (TBP) waste. TBP waste was produced at U Plant during the reprocessing of metal waste with TBP to recover uranium. Tanks T-107, -108, and -109 began receiving TBP waste in 1952 and were full by January 1953 (Brevick et al. 1995).

Also during 1952, 224-Waste was added to tanks T-110, -111, -112, -201, -202, -203, and -204. 224-Waste was produced by the bismuth-phosphate process used to extract plutonium at the 224-Building of B Plant. Because tanks T-110, -111, and -112 were already full, supernatant liquid cascaded to tank T-111 and then to tank T-112 as the 224-Waste was added to tank T-110. The supernatant liquid was eventually pumped from tank T-112 to a crib (Brevick et al. 1995).

Additional first-cycle decontamination waste from the bismuth-phosphate process was added to the third cascade series (tanks T-107, -108, and -109) in 1953. Metal waste was added to the first cascade series (tanks T-101, -102, and -103) in 1955 (Brevick et al. 1995).

In 1956, tanks T-101, -102, and -103 were sluiced to make room for additional metal waste from T Plant and future coating waste from the Reduction and Oxidation Extraction Facility (REDOX). REDOX was built in 1950 and 1951 and used methyl-isobutyl ketone (also known as hexone) to extract uranium and plutonium from irradiated fuel slugs.

In 1956, tanks T-105 and T-106 received coating waste from REDOX, and tank T-108 received evaporator bottoms transferred from tank TX-117 (TX Tank Farm). Coating waste was produced by the dissolution of aluminum and zircaloy cladding from the fuel elements before processing. Evaporator bottoms were produced at the 242-T Evaporator, which processed tank wastes to reduce waste volumes and reclaim tank space for additional wastes (Brevick et al. 1995).

In 1957, evaporator bottoms waste from the 242-T Evaporator was transferred to tank T-109 from tank TX-117. In 1965, a cross-site transfer of coating waste from tank C-102 (C Tank Farm) was received by tanks T-102 and T-103. In 1967, coating waste was transferred to tank T-107 from tank C-102 (Brevick et al. 1995). In 1967, first-cycle decontamination waste from tanks T-105, -107, -108, and -112 was transferred to tank TX-118 for processing at the 242-T Evaporator.

Tanks T-101 and T-105 received B Plant ion-exchange waste from tanks BX-101 and BX-104 (BX Tank Farm) in 1972 (Brevick et al. 1995). B Plant ion-exchange waste was produced at the 221-B Building by passing supernatant and sluicing liquids through ion-exchange columns to remove cesium (DOE 1993). Additional B Plant ion-exchange waste was transferred to tank T-107 from tank BX-104 in 1973 (Brevick et al. 1995).

In 1974, tanks T-101, -102, and -105 received coating waste and ion-exchange waste from tank S-110 (S Tank Farm). The final recorded activity in the T Tank Farm was receipt of coating waste from tank SX-106 (SX Tank Farm) into tank T-101 in 1975 (Brevick et al. 1995).

5.3 Current Status

The tanks in the T Tank Farm contain a total volume of 1,867,000 gal of waste consisting of 1,839,000 gal of sludge and 28,000 gal of supernatant; the sludge contains 174,000 gal of drainable interstitial liquid (Hanlon 1999).

The evaluation of leaks from tanks and transfer lines in the T Tank Farm is complicated by the presence of deliberate discharges of tank wastes to the vadose zone in cribs and trenches adjacent to the tank farm. These discharges and their potential impact to the groundwater beneath WMA-T are discussed in detail in Section 6, "Adjacent Waste Site Information."

The following seven tanks in the T Tank Farm are classified assumed leakers: tanks T-101, T-103, T-106, T-107, T-108, T-109, and T-111 (see Figure 14-17). Hanlon (1999) reports the following leak volumes for these tanks: 7,500 gal for tank T-101, less than 1,000 gal for tank T-103, 115,000 gal for tank T-106, 8,000 gal for tank T-107, less than 1,000 gal for tank T-108, less than 1,000 gal for tank T-109, and less than 1,000 gal for tank T-111. According to Hanlon (1999), with the exception of tank T-107, these estimates were based solely on the observed liquid-level decreases in these tanks. This is considered the most accurate method for estimating leak volumes. However, the accuracy of the leak volume estimate for tank T-107 is believed to be poor because it was derived from a gross estimate of 150,000 gal that was subsequently distributed among tank T-107 and 18 other tanks in eight different tank farms. Furthermore, because several tanks have leak volumes estimated to be very small (less than 1,000 gal), the current leak status of these tanks may be questionable.

All of the tanks in the T Tank Farm have been removed from service, and, with the exception of tanks T-104 and T-110 (which are both designated sound tanks), are designated stabilized. In addition, tanks T-102, T-103, T-105, T-106, T-108, T-109, T-112 and tanks T-201 through T-204 are designated to be in an intrusion prevention status, meaning that they have undergone measures to minimize the potential for addition of liquids to the tanks (Hanlon 1999).

Some SSTs are added to a Watch List because the waste in the tanks may be in a potentially unsafe condition, and handling and storage of the wastes require corrective action or special monitoring to reduce or eliminate the hazard. Resolution of the safety issues has been codified under Public Law 101-510 (generally known as the Wyden Amendment). Tank T-110 is currently on the Hydrogen (Flammable Gas) Watch List because this tank is suspected of having a significant potential for hydrogen/flammable gas generation, entrapment, and release. The waste in tank T-110 is monitored for trends of increasing temperature.

Table 2 presents a summary of general T Tank Farm information. This table indicates current leak detection monitoring reported in Hanlon (1999). Discussions regarding details of the monitoring are presented in Section 5.5, "Leak-Detection Monitoring."

Table 2. General T Tank Farm Information [a]

Tank	Total Waste Volume (1,000 gal)	Drainable Liquid (1,000 gal)	Primary Leak Detection Method	Tank Monitoring Methods	Input Method	Leaker (Y/N)	Original Leak Determination
T-101	102	17	None	ENRAF[b]	M[c]	Y	1992
T-102	32	13	ENRAF	ENRAF	A[d]	N	N/A[e]
T-103	27	4	None	ENRAF	M	Y	1974
T-104	326	31	LOW[f]	ENRAF	M	N	N/A
T-105	98	23	None	ENRAF	M	N	N/A
T-106	21	2	None	ENRAF	M	Y	1973
T-107	173	22	ENRAF	ENRAF	A	Y	1984
T-108	44	0	ENRAF	ENRAF	M	Y	1974
T-109	58	0	None	ENRAF	M	Y	1974
T-110	350	35	LOW	ENRAF	A	N	N/A
T-111	446	34	LOW	ENRAF	M	Y	1979, 1994[g]
T-112	67	7	ENRAF	ENRAF	M	N	N/A
T-201	29	4	Manual Tape	None	N/A	N	N/A
T-202	21	2	Manual Tape	None	N/A	N	N/A
T-203	35	4	None	None	N/A	N	N/A
T-204	38	4	Manual Tape	None	N/A	N	N/A

[a] Data are compiled from Hanlon (1999).
[b] Surface level measurement device manufactured by ENRAF Incorporated.
[c] Manually entered into the Tank Monitor and Control System (TMACS) and electronically transmitted to the Surveillance Analysis Computer System (SACS).
[d] Automatically entered into TMACS and electronically transmitted to SACS.
[e] Not applicable.
[f] In-tank liquid observation well.
[g] Tank T-111 was declared an assumed re-leaker in 1994.

5.4 Unplanned Releases

Three documented unplanned releases (UPRs) that occurred within the vicinity of the T Tank Farm were investigated to determine if they may have been the source(s) of some of the surface or near-surface contamination detected during the vadose zone characterization logging. These releases are discussed in the following sections, and Figure 14-19 shows their locations.

5.4.1 UPR-200-W-7

This release occurred in 1950 and resulted from work that was being performed on the 241-T-151 and 241-T-152 Diversion Boxes, which are located approximately 200 ft southeast of the T Tank Farm and about 100 ft southwest of the 207-T Retention Basins. An unknown amount of soil was contaminated, some of which was removed and placed at an unknown location. The remaining contamination was covered in-place with a 1-ft-thick layer of clean soil material.

5.4.2 UPR-200-W-147

This release occurred in 1973 and documents contamination associated with tank T-103. This contamination was discovered during drilling of monitoring wells that were to be used to evaluate the extent of migration of the tank T-106 leak. Additional investigation indicated the leakage may have resulted from a failed seal on one of the tank T-103 spare tank inlets. The volume of contaminated soil was estimated at about 5 cubic meters (m^3) (DeFord and Carpenter 1995). Data collected during the investigation indicated that the contamination penetrated into the vadose zone to a depth of about 75 ft and that the contamination moved southeastward.

5.4.3 UPR-200-W-148

This release documents leakage from tank T-106 that occurred in April 1973. The leak was assumed to have occurred in April 1973 during a routine filling operation, but was not discovered until June 1973. An estimated 115,000 gal of liquid waste containing approximately 40,000 Ci of ^{137}Cs, 14,000 Ci of ^{90}Sr, 4 Ci of plutonium, and other fission products leaked into the vadose zone sediments (Routson et al. 1979). The leak contaminated approximately 25,000 m^3 of soil (Freeman-Pollard et al. 1994). Subsequent investigations into the leak suggest the source may have been failure of the steel tank liner that was caused by corrosion by caustic waste contents. Additional investigation via borings indicated the plume was essentially stable though some lateral migration to the southeast was observed (Deford and Carpenter 1995).

5.5 Leak-Detection Monitoring

The SSTs have been monitored for leak-detection purposes throughout the years using either liquid-level measurements, solid-level measurements, or direct detection of contamination in the vadose zone with gross gamma logging. Section 5.7, "Gross Gamma Logging," presents a discussion of previous gross gamma logging programs used to detect contamination in the vadose zone via the boreholes surrounding the tanks. The primary leak-detection monitoring for the SSTs is currently based on solid- and liquid-level measurements acquired within the tanks. The following discussions provide details regarding the leak-detection monitoring conducted at the T Tank Farm.

Solid- and liquid-level measurements are made by direct access to the surface of the waste inside the tanks through surface riser ports built into the tank's domed tops. Instruments lowered down to the waste surface to determine the level include simple instruments like weighted hand-held measuring tapes, sparker probes, electronic tapes, and, more recently, automated ENRAF gauges. The wastes contained in all of the 100-series T Farm tanks are monitored with ENRAF gauges. These devices, which are manufactured by ENRAF Incorporated, monitor waste levels by detecting variations in the weight of a displacer that is suspended in the tank waste. In the T Tank Farm, data acquired with the ENRAF gauges from tanks T-102, T-107, and T-110 are automatically entered into the Tank Monitor and Control System (TMACS) and electronically transmitted to the Surveillance Analysis Computer System (SACS). The data acquired with the ENRAF gauges from the remaining tanks in T Farm are recorded on field data sheets and manually entered into SACS by surveillance personnel (Hanlon 1999). The precision of the measurements or potential problems likely to be encountered are described in Welty (1988), Scott (1993), and Catlin (1980).

Sealed fiberglass or TEFZEL-reinforced (TEFZEL is a trademark of E.I. du Pont de Nemours & Company) epoxy-polyester resin casings were inserted into the waste solids (sludge and salt cake) in tanks to allow access for borehole monitoring tools (Hanlon 1999). These bottom-sealed casings are called liquid observation wells (LOWs). Only three tanks in the T Tank Farm, tanks T-104, T-110 and T-111, are equipped with LOWs. The monitoring tools used in LOWs include very low-efficiency gamma-ray detection probes (Geiger-Mueller detectors) to measure the variations in gamma flux and neutron-neutron probes to measure variations in the hydrogen content profile. These tools are intended to detect changes in the solid-to-liquid interface level, and, thus, changes in the liquid level. They are particularly important for detecting leaks because most tanks now have relatively solid sludge and salt-cake waste components and the liquid is only found in the interstices or pores of the solid material. Therefore, a surface-level measurement will not detect changes in the interstitial liquid level. Scott (1993), Isaacson (1982), and Catlin (1980) describe the instrumentation used to measure interstitial liquid levels in the tanks.

Determining the liquid level in a tank is not an easy task. In addition to uncertainties or errors associated with the instrumentation, physical changes can occur in the waste that create changes in the measured solid or liquid level. Scott (1993) provides some understanding of the precision of the liquid-level measurement instrumentation, but that understanding has not yet been applied to assessing tank-leak volumes or to determining the uncertainty of the tank leak-volume estimates.

5.6 Vadose Zone Monitoring Boreholes

All of the SST farms, including the T Tank Farm, have monitoring boreholes installed around the tanks. These boreholes were installed and used as part of a tank-leak detection monitoring program where gamma-ray detectors were lowered into the boreholes to detect the presence of gamma-ray-emitting radionuclides in the sediments surrounding the tanks. The majority of the 67 monitoring boreholes in the T Tank Farm were drilled in the early to mid 1970s to depths between about 80 and 100 ft and were completed with 6-in.-diameter casing. Figure 14-17

shows the locations and identification of the monitoring boreholes surrounding tanks in the T Tank Farm.

Beginning in 1977, selected monitoring boreholes in the T Tank Farm were deepened and all boreholes were modified, apparently to eliminate the potential for downward contaminant migration along the casings. During the modifications, the original 6-in.-diameter casing was perforated generally along the upper 20 ft of the borehole and for a few feet near the bottom of the borehole. After perforation, a 4-in.-diameter casing with a metal cap welded on the bottom was installed within the 6-in.-diameter casing, and the annular space between the casings was filled with grout. The T Tank Farm is the only farm where essentially all of the boreholes have been modified in this manner.

The purpose of the borehole modification was to create a seal around the casing near the surface so that pooled rainwater or snow melt would not drain down the outside of the casing, but would instead infiltrate evenly across the farm. The borehole modification was also designed to create a seal at the bottom of the boreholes so that any flood water draining into the boreholes from the surface would be prevented from directly infiltrating into the deeper portion of the vadose zone. The seals were effective because throughout the 1980's, many of the boreholes required pumping before gross gamma monitoring work could be performed. However, during the time that the bottoms of the boreholes were not sealed, it is possible that surface flood waters drained into the them and carried contamination down into the deep vadose zone.

Unfortunately, the double layer of casing and the unknown thickness of grout limit the accuracy of in-situ log assays and change the spatial resolution. It is possible to compensate for the double layer of casing but it is not possible to correct for the unknown thickness of grout. These borehole modifications also decreased the sensitivity of the gross gamma leak-detection monitoring instruments, but they were still effective in detecting large, high concentration plumes.

The construction of most of the boreholes is documented in the form of drilling logs, most of which provide some degree of detail and description regarding the drilling operations, geologic descriptions of sediments penetrated by the drilling, and explanation of the construction configurations of the "as-built" boreholes. Although in most instances the information provided in the drilling logs is limited in scope, these logs provide information on when and how the boreholes were drilled and they document the occurrences of radiological contamination when it was encountered during drilling. Determination of the intensity of radiological contamination was made at the drill site using hand-held instrumentation with a higher MDL than a HPGe detector or laboratory analysis; therefore, contamination levels in sediments at the time of drilling may have been below the MDL of the hand-held instrumentation but are at levels that are capable of being detected with the SGLSs. All of the drilling logs are available in borehole archive files maintained by Waste Management Federal Services Northwest Operations. Details regarding borehole construction and casing configurations are provided in the Tank Summary Data Reports (DOE 1995d, 1995e, 1998c, 1998d, 1998e, 1998f, 1999a, 1999b, 1999c, 1999d, 1999e, and 1999f).

All of the vadose zone monitoring boreholes were drilled using cable-tool methods. At the Hanford Site, samples are collected by using a slip-jointed drill stem suspended from a cable to drive an open-ended drive barrel into the sediments below the casing. The filled drive barrel is removed from the borehole and struck to remove the sediments. When sediments are encountered that do not remain in the drive barrel as it is removed from the borehole, water is added to the borehole to improve cohesion between the sediments and the drive barrel.

As the drive barrel is driven downward and the sediments are removed to create the borehole, the borehole is open along the sampling interval. A carbon-steel casing is driven downward into the slightly undersized, open portion of the borehole, and the drilling process proceeds over another drilling interval. The first sediments retrieved after casing advancement are generally materials sheared off the formation wall into the borehole as the casing was advanced.

During cable tool drilling, there is a possibility that the borehole wall will collapse before the steel casing can be driven into place. If this occurs, a void may remain behind the borehole casing.

Voids behind the casing or a highly rugose borehole can create a pathway for migration of contaminants down the outside of the borehole casing when temporary saturated conditions occur within the vadose zone. Movement of contaminated sediment could also occur as sloughed material sifted downward within the gap between the outside of the casing and the formation. The pounding action of the cable tool during drilling would amplify the sifting action along the casing.

Based on the interpretation of the contaminant distributions for each borehole, three contaminant migration scenarios are considered in the Tank Summary Data Reports and in this report. These scenarios include: 1) the potential for contamination to adhere to the outside of the casing and be driven downward as the casing is advanced during the drilling process, 2) contamination distributed on the inside of the casing as contaminated materials fall from the drive barrel during withdrawal from the borehole, and 3) contamination carried downward by migration of surface water along the annular space between the outside of the casing and the formation sediments.

All of the borehole casings were cut off at the top of the surface collars; the casings are at most only a few inches above the surface grade of the tank farm. Plugs or caps were put into the boreholes to keep dust, contaminants, and water out of the boreholes, but the caps are not watertight and were meant merely to keep objects from inadvertently falling into the boreholes. If ponding of water occurred at the ground surface, there is potential for water and contaminated sediments to enter and migrate down the inside of the borehole casings even though the cap is installed on the top of the casing. If a borehole cap is removed for a significant amount of time, contaminated sand or silt can be blown into the borehole and settle to the bottom of the hole. When low-level contamination is present at the bottom of a borehole with contamination-free regions above it, it is generally assumed that the contamination is on the inside of the borehole casing and not deposited in the vadose zone sediments.

Casing may also have been contaminated by wind-driven contamination as it was stored on the ground at the drill site. Contamination deposited on the rust scale of metal is difficult to remove and may have remained both on the inside and outside of the casing as the borehole was drilled.

Log Data Reports accompany the log plots in the Tank Summary Data Reports. The borehole data presented in the Log Data Reports contain information regarding borehole drilling details, geological information, well construction configuration, and other pertinent information found in the documentation on file.

5.7 Gross Gamma Logging

A gross gamma logging program was the primary means of detecting leaks from the SSTs for many years. The intent of the logging program was to detect a leak front that was thought to produce high concentrations of radionuclides in the formation intersected by tank monitoring boreholes. Gross gamma logs were acquired from all but one of the T Tank Farm boreholes (borehole 50-06-18) according to a schedule specified in Welty and Vermeulen (1989) and Welty (1988). In the past, logging was performed more frequently because it was often the only leak-detection method available or in-tank measurement precision was poor. More recently, this program has been discontinued in favor of upgraded and more precise in-tank measurements, and consequently, the reliance on the gross gamma logging for leak detection has been eliminated for all of the SSTs.

Gross gamma logging of some fashion began at Hanford in the 1960s by making stationary measurements with Geiger-Mueller detectors that were lowered by hand into the boreholes. Almost no documentation is available about this work, other than references to the monitoring in some daily operations logs of the health physics technicians.

In the mid-1970s, the gross gamma logging program was upgraded to more automated systems installed in vans; descriptions of this equipment are presented in Isaacson (1982). These logging systems were used to create a large monitoring database. The systems used three different downhole gamma-ray detector probes that sent pulses up a cable to a pulse counter. The counter tallied the pulses and output a total count value to a computer every second. The downhole probes were withdrawn from the borehole at a set rate, thereby summing the counts over a series of equal depth intervals in a borehole.

The three downhole probes consisted of a 1-in.-diameter by 1-in.-long sodium-iodide detector, a lower efficiency probe containing three Geiger-Mueller tubes, and a low-efficiency probe containing a small, shielded Geiger-Mueller tube. The intent of the three probes was to be able to cover a large gamma-ray flux range without saturating the instrumentation. These systems were effective at covering the high range of activity but were not effective at detecting lower activities where radionuclide concentrations are less than 10 pCi/g equivalent ^{137}Cs.

Boreholes were logged at a set rate of 45 feet per minute (ft/min). With a counting time of 1 s and a delay required to save the data, the resulting data acquisition interval was 1 ft. These

logging systems recorded the total number of gamma-ray photons detected throughout the 1-ft intervals and recorded the top depth of the data acquisition interval.

Data were presented as plots of the gross count rate in counts per second as a function of depth. Spatial count-rate activity peaks were compared visually with previous data to determine, in a qualitative manner, if changes had occurred. No additional processing or analysis were performed on the data. If a change was suspected, the borehole was relogged or the monitoring frequency was increased. An increasing count-rate activity trend in the data was used to identify a potential leak from a tank.

Determinations of contaminant migration were made on the basis of changes in gamma-ray flux rather than radionuclide concentrations because the logging instrumentation was not calibrated to a radionuclide concentration response. Relative changes in detected count rate were sometimes related to leaks from tanks.

Review and visual comparison of gross gamma log data over time have been useful in the evaluation of changes in contaminant profiles that may be indicative of migration. However, poor depth control and small changes in the position of the borehole probe between log runs can result in apparent peak movement and/or large variations in the peak count rates.

When evaluating any gross gamma log data, the sensitivity of the instruments to the presence of ^{137}Cs must be considered. Comparison of the Tank Farms gross gamma log data to the ^{137}Cs concentration plots suggests that an anomalous gross gamma response can only be expected when ^{137}Cs is present at concentrations of 10 pCi/g or more. ^{60}Co and other lower specific activity nuclides each have higher levels of response.

Despite the limitations, the gross gamma logging database is the only historical record of the vadose zone contamination around the SSTs. Because the boreholes were consistently logged, an extensive and fairly comprehensive library of gross gamma activity is available for many of the boreholes. Once the limitations of these data are understood, the data library may be useful for assessing some of the history of the vadose zone contamination.

At the present time, no gross gamma-ray logging is being conducted in the monitoring boreholes surrounding the tanks in the T Tank Farm. Leak detection is conducted through acquisition of in-tank measurements within LOWs and/or by surface level measurements of the solid waste within the tank using an ENRAF gauge.

The most recent procedures for leak detection are outlined in the *Operating Specifications for Tank Farm Leak Detection* (WHC 1994).

6.0 Adjacent Waste Site Information

Several facilities into which millions of gallons of liquid waste and wastewater were discharged to the soil column and several underground storage tanks containing high-level radiological waste are located adjacent to the T Tank Farm. These facilities are discussed in the following sections, and Figure 14-17 presents a plan view map showing their locations relative to the T Tank Farm.

Geophysical logging was conducted in monitoring wells and boreholes within and around these facilities as early as 1958, and subsequent evaluations were performed that report the interpretation of the log data. An evaluation of gross gamma-ray log data acquired in vadose zone monitoring boreholes and groundwater monitoring wells at several of these waste disposal facilities was presented in the *T Plant Source Aggregate Area Management Study Report*. (DOE 1992). Along with summaries of these gross gamma-ray log evaluations, DOE (1992) provides detailed descriptions of the methodology of the gross gamma logging and details of the log data interpretations.

Brodeur et al. (1993) present the results of spectral gamma-ray logging that was conducted in selected boreholes at waste disposal facilities located throughout the 200 East and 200 West Areas. Results and interpretations of these data that are pertinent to the waste disposal facilities adjacent to the T Tank Farm are included in the following discussions.

Details regarding the construction configurations, operational histories, and waste components that are presented in the following sections were derived from DOE (1992). The reader is advised to reference that document for additional information.

Radiological waste constituents presented in the following sections are derived from waste inventories presented in DOE (1992). The following radionuclides are included in the inventory listings: ^{60}Co, ^{90}Sr, ^{137}Cs, ^{106}Ru, promethium-147 (^{147}Pm), isotopes of plutonium (^{238}Pu, ^{239}Pu, ^{240}Pu, and ^{241}Pu), tin-113 (^{113}Sn), isotopes of uranium (^{234}U, ^{235}U, ^{238}U), ^{129}I, ^{241}Am, and tritium (^{3}H). Total alpha and beta activities are also included in the inventories.

6.1 216-T-3 Reverse Well

The 216-T-3 Reverse Well is located approximately 1,200 ft east of the T Tank Farm. Reverse wells are boreholes lined with casing that is perforated or open at the bottom to allow liquids to migrate into the surrounding sediments. These facilities were used to discharge liquids deeper into the vadose zone than cribs and trenches. The 216-T-3 Reverse Well is constructed with 10-in.-diameter casing and is 206 ft deep.

The 216-T-3 Reverse Well was in service for 1 year (1945-1946). During this period, it received about 30 million gal of waste from T Plant, as well as overflow from the adjacent 241-T-361 Settling Tank. The major radionuclides in this waste are plutonium, ^{137}Cs, and ^{90}Sr.

Groundwater monitoring wells 299-W11-1, 299-W11-7, 299-W11-64, and 299-W11-67, located near the 216-T-3 Reverse Well, have been logged with gross gamma-ray probes. Well 299-W11-7 is the closest, located approximately 13 ft to the north. Log data acquired from this well in 1959, 1970, 1976, 1986, and 1987 reveal three zones of probable radionuclide contamination between 10 and 123 ft. The data indicate that the radionuclides present have long half-lives and that little or no vertical migration has occurred. The data are inadequate to define any lateral migration trends. Gross gamma data collected from wells 299-W11-1, 299-W11-64, and 299-W11-67 reveal no significant radionuclide contamination.

A spectral gamma-ray survey was conducted in monitoring well 299-W11-7 in May 1992, the details of which are provided in Brodeur et al. (1993). ^{137}Cs was detected from 3 to 169 ft, with the majority of the contamination occurring in three distinct intervals between depths of 10 to 20 ft, 40 to 80 ft, and 100 to 110 ft. The maximum concentration of ^{137}Cs was about 1,000 pCi/g at a depth of 15 ft.

Borehole 299-W11-79 was identified directly south of the 216-T-3 Reverse Well. Chamness and Merz (1993) indicate this borehole was completed to a depth of 142 ft in 1983, but was later grouted, suggesting that it has been abandoned. It is unknown whether gross gamma data were collected from this borehole.

6.2 216-T-4-1D Ditch

The 216-T-4-1D Ditch is located about 200 ft north-northeast of the T Tank Farm. This facility transported wastewater from T Plant and the 207-T Retention Basin to the 216-T-4A and 216-T-4B Ponds, which were located about 1,200 ft northwest of the T Tank Farm. The 216-T-4-1D Ditch was approximately 850 ft long by 8 ft wide by 4 ft deep.

The 216-T-4-1D Ditch was active from November 1944 until May 1972 and was interim stabilized in September 1995 (Smith 1996). During its service life, it received approximately 11.2 billion gal of process cooling water and steam condensate from T Plant and the 242-T Evaporator (this is a total waste volume designated for the 216-T-4-1 and 216-T-4-2 Ditches and the 216-T-4-A and 216-T-4-B Ponds). Numerous leaks in the T Plant building resulted in contamination of the 216-T-4-1 Ditch and the 216-T-4-A Pond. The bottom of the ditch was contaminated to a maximum of 20,000 counts per minute (c/m), and the ditch contains an estimated 1.41 g of plutonium (DeFord and Carpenter 1995).

There are no vadose zone boreholes or monitoring wells associated with the 216-T-4-1D Ditch.

6.3 216-T-4-2 Ditch

The 216-4-2 Ditch was constructed to replace the 216-T-4-1D Ditch, and the materials excavated for this ditch were used to cover the 216-T-4-1D Ditch. The 216-T-4-2 Ditch, which is 1,750 ft long by 8 ft wide by 4 ft deep, transported steam condensate and condenser cooling water from the 242-T Evaporator and nonradioactive wastewater from T Plant air conditioners and floor

drains. Some of the initial course of the 216-T-4-2 Ditch uses the same channel as the deactivated 216-T-4-1 Ditch.

The 216-T-4-2 Ditch was put into service in May 1972 and was active to July 1995. It was interim stabilized in September 1995 (Smith 1996). A radiation survey conducted in January 1978 showed the ditch to be free of radioactivity except for the first 50 ft of the ditch, the portion that coincides with the old ditch.

There are no vadose zone boreholes or monitoring wells associated with the 216-T-4-2 Ditch.

6.4 216-T-4-A Pond

The 216-T-4-A Pond (also referred to as the 216-T-4-1 Pond) was active during the same period as the 216-T-4-1 Ditch. It was located about 1,200 ft northwest of the T Tank Farm. The 216-T-4-A Pond was L-shaped and covered an area of approximately 16 acres (DeFord and Carpenter 1995).

The 216-T-4-A Pond was in service from November 1944 to May 1972, when it was backfilled. The waste sources for this facility are the same as those described for the 216-T-4-1 Ditch. Contaminated wastewater from T Plant resulted in contamination of the 216-T-4-1 Ditch and the 216-T-4-A Pond. Monitoring along the shoreline of the pond indicated radiation readings of 2,000 to 15,000 c/m. The site was stabilized in 1972 by backfilling; however, in 1973, 6 to 9 in. of soil material was removed from the bottom surface of the pond and was placed in the 218-W-2A Burial Ground. The pond was covered with clean soil, and in 1975, was seeded to stabilize the surface.

There are no vadose zone boreholes or monitoring wells associated with the 216-T-4-A Pond.

6.5 216-T-4-B Pond

The 216-T-4-B Pond (also referred to as the 216-T-4-2 Pond) was constructed 200 ft east of the 216-T-4-A Pond. The 216-T-4-B Pond covered an area of 1.5 acres and was 1,760 ft long by 8 ft wide and 3 to 6 ft deep. It was separated from the site of the older 216-T-4-A Pond by an earthen dike.

The 216-T-4-B Pond was constructed in 1972 and was fed via the 216-T-4-2 Ditch; therefore, the wastes sent to this pond are the same as those described for the 216-T-4-2 Ditch. The gradient of the 216-T-4-2 Ditch was relatively low and the liquid sank into the soil in the upper one quarter of the ditch and did not reach the pond; the pond was considered dry since 1977. Interim stabilization was completed on the 216-T-4-B Pond in September 1995 (Smith 1996).

There are no vadose zone boreholes or monitoring wells associated with the 216-T-4-B Pond.

6.6 216-T-5 Trench

The 216-T-5 Trench is located about 300 ft west of the T Tank Farm. This facility consisted of a 50-ft-long by 10-ft-wide by 12-ft-deep excavation.

The 216-T-5 Trench was in service for 1 month during May 1955. This was a specific retention facility and was deactivated when a prescribed volume of liquid was discharged to the soil column. During its 1 month of operations it received about 680,000 gal of second-cycle decontamination waste from T Plant via tank T-112 in the T Tank Farm. The major radionuclides in this waste are ^{137}Cs and ^{90}Sr.

The 216-T-5 Trench is monitored by well 299-W10-1. Gross gamma log data acquired from this well showed no elevated gamma radiation levels. This well was not logged with spectral gamma-ray logging equipment.

6.7 216-T-6 Cribs

The 216-T-6 Cribs (216-T-6-1 and 216-T-6-2) are located about 900 ft east of the T Tank Farm. Each of these cribs is a wooden structure 14 ft long by 14 ft wide with a liquid disposal point 16 ft below ground surface. The 216-T-6-1 Crib was designed to overflow into the 216-T-6-2 Crib. The centers of the cribs are 62 ft apart.

The 216-T-6 Cribs were built in 1946 and were in service until June 1951. During their service lives they received about 12 million gal of liquid waste primarily from T Plant. The cribs also received overflow waste from the 241-T-361 Settling Tank. The primary radionuclides contained in the wastes discharged to the 216-T-6 Cribs are plutonium, ^{137}Cs, and ^{90}Sr.

The 216-T-6 Cribs are monitored by well 299-W11-1 and vadose zone boreholes 299-W11-54 through 299-W11-67. The monitoring well and all of the vadose zone boreholes are located in or near the 216-T-6-1 Crib except borehole 299-W11-60, which is located in the 216-T-6-2 Crib. High levels of gamma radiation were detected beneath the 216-T-6-1 Crib and it appears this plume is elongate to the south and extends to the east, under the 216-T-6-2 Crib. The data are inadequate to define the lateral extent of the radionuclides and there is no evidence of vertical contaminant migration. There is no evidence that radionuclide contamination reached the groundwater in this area.

A spectral gamma-ray survey was conducted in vadose borehole 299-W11-61 in April 1992, the details of which are provided in Brodeur et al. (1993). Low concentrations of ^{137}Cs, ranging from 0.2 to 1.2 pCi/g, were detected from the ground surface to a depth of 6 ft. A prominent zone of ^{137}Cs contamination was detected between 15 and 50 ft. The maximum concentration of ^{137}Cs within this zone (2,800 pCi/g) was encountered at a depth of 27 ft.

6.8 216-T-7 Crib and Tile Field

The 216-T-7 Crib and Tile Field are located at the southwestern corner of the T Tank Farm. The crib is located within the perimeter fencing of the tank farm and the tile field is located immediately outside the tank farm fencing. The crib is a 12-ft-long by 12-ft-wide wooden structure with a liquid release point 20 ft below ground surface. The tile field is 310 ft long and 84 ft wide and contained four 80-ft-long 10-in.-diameter pipes.

The 216-T-7 Crib and Tile Field were in service between April 1948 and November 1955. During their service lives, the crib and tile field received almost 30 million gal of second-cycle decontamination waste and cell drainage from T Plant and waste from the 224-T Building. The major radionuclides contained in the waste are ^{137}Cs and ^{90}Sr.

The 216-T-7 Crib is monitored by well 299-W10-3 and vadose zone boreholes 299-W10-59 through 299-W10-68 and 299-W10-74. The 216-T-7 Tile Field is monitored by well 299-W10-2 and vadose zone boreholes 299-W10-69 through 299-W10-72, and 299-W10-77 through 299-W10-81. A region of high gamma radiation more than 100 ft thick was detected beneath the 216-T-7 Crib and Tile Field. Most of the vadose zone boreholes are too shallow to fully penetrate the contaminant plume, indicating that the radionuclide contamination may have reached the groundwater below the site. There is evidence of downward migration of radionuclides within Hanford formation sediments and of lateral migration of radionuclides within the underlying Early Palouse soil and the Plio-Pleistocene unit, as far south as the 216-T-36 Crib (DOE 1992).

Monitoring well 299-W10-3 was logged with the SGLS in July 1998 as part of the baseline characterization of the T Tank Farm. A brief synopsis of the log data results and interpretations is provided; the information was derived from a letter report yet to be published.

^{137}Cs, ^{60}Co, and ^{154}Eu were detected by the SGLS around monitoring well 299-W10-3 during the 1998 logging run described previously. The ^{137}Cs contamination was detected along almost the entire length of the borehole. The highest concentrations of ^{137}Cs occurred from 40 to 70 ft in depth; the maximum ^{137}Cs concentration (874 pCi/g) was encountered at a depth of 41.5 ft. The ^{60}Co contamination was detected intermittently from 214 ft to the bottom of the logged interval (229 ft). The maximum ^{60}Co concentration (0.22 pCi/g) was detected at a depth of 228.5 ft. The ^{154}Eu contamination was detected continuously between 45 and 52 ft at low concentrations ranging from 0.21 to 0.95 pCi/g.

The radionuclide contamination detected in the vadose zone around monitoring well 299-W10-3 likely resulted from the discharge of waste to the 216-T-7 Crib and Tile Field. ^{137}Cs and ^{60}Co contamination was detected at the depth of the water table and a small zone of ^{60}Co contamination was detected approximately 8 ft below the water table, indicating contamination released to the 216-T-7 Crib and Tile Field has migrated downward through the vadose zone and reached groundwater in this area. A review of the SGLS data presented in the Tank Summary Data Reports for nearby tanks T-109 and T-112 (DOE 1998d, 1998f) shows no correlation

between the radionuclide contamination detected around the tank farm monitoring boreholes and the ^{137}Cs and ^{60}Co contamination detected around monitoring well 299-W10-3, indicating that the waste originating from the 216-T-7 Crib and Tile Field has not commingled with the vadose zone contamination related to T Tank Farm activities.

6.9 216-T-14 through 216-T-17 Trenches

The 216-T-14 through 216-T-17 Trenches are located approximately 300 ft northeast of the T Tank Farm. Each of these facilities is 275 ft long by 10 ft wide by 10 ft deep.

The trenches were in service for less than 1 year during 1954 and received first-cycle supernatant waste from T Plant via tanks T-104, T-105, and T-106 in the T Tank Farm. The 216-T-14 through 216-T-16 Trenches received 264,000 gal of waste and the 216-T-17 Trench received 207,000 gal of waste. The primary radionuclides contained in the wastes are ^{137}Cs and ^{90}Sr. Each trench was deactivated when it received the volume of the prescribed liquid retention capacity of the soil, the above ground piping was removed, and the trenches were backfilled.

The 216-T-14, 216-T-15, 216-T-16, and 216-T-17 Trenches are monitored by vadose zone boreholes 299-W11-69, 299-W11-68, 299-W11-80, and 299-W11-81, respectively. Historical gross-gamma data from borehole 299-W11-81 indicate the presence of man-made radionuclides associated with the 216-T-17 Trench. Increasing gamma activity with depth occurs at the bottom of 299-W11-81, suggesting that this borehole does not fully penetrate the zone of potential contamination. Currently, the gamma radiation levels in boreholes 299-W11-68, 299-W11-69, and 299-W11-80 are at or near background levels; however, historical gross gamma data from borehole 299-W11-68 indicate moderate to low levels of gamma radiation associated with the 216-T-14 Trench were present in the past.

A spectral gamma-ray survey was conducted in vadose borehole 299-W11-81 in May 1992, the details of which are provided in Brodeur et al. (1993). ^{137}Cs was encountered along the entire length of the borehole from the ground surface to a depth of 48 ft. The most prominent zone of ^{137}Cs contamination occurred from about 10 to 30 ft. The maximum concentration of ^{137}Cs detected within this zone was 19,000 pCi/g at a depth of 15 ft.

6.10 216-T-32 Crib

The 216-T-32 Crib is located along the west side of the T Tank Farm. This facility consists of two 12-ft-long by 12-ft-wide by 4-ft-deep wooden sumps within a 68-ft-long by 14-ft-wide by 26-ft-deep structure. The 216-T-32 Crib was fed by a single pipeline from the 241-T-201 tank in the T Tank Farm.

The 216-T-32 Crib was in service between November 1946 and May 1952, and during this period received almost 8 million gal of waste from the 224 T Building. The primary radionuclides in these wastes are plutonium, ^{137}Cs, and ^{90}Sr.

The 216-T-32 Crib is monitored by vadose zone boreholes 299-W10-52, -56, -57, -58, -64, -65, -73, -75, and -76. A thin interval of low-level radionuclide contamination was detected within the Hanford formation sediments beneath the 216-T-32 Crib. This region of radionuclide contamination merges with that detected beneath the 216-T-7 Crib and Tile Field to the south; however, there is no evidence of vertical or lateral radionuclide migration within the plume.

None of the vadose zone boreholes were logged with the spectral gamma-ray logging equipment.

6.11 216-T-36 Crib

The 216-T-36 Crib is located near the southwest side of the T Tank Farm. This facility consists of a 160-ft-long by 10-ft-wide by 15-ft-deep structure. The 216-T-36 Crib was fed by a single pipeline that discharged approximately 11 ft below grade.

The 216-T-36 Crib was in service between May 1967 and February 1968. During this period it received approximately 140,000 gal of waste from the 221-T and 221-U Buildings. The primary radionuclides in these wastes are ^{137}Cs and ^{90}Sr.

The 216-T-36 Crib is monitored by wells 299-W10-2 and 299-W10-4. Currently, the gamma radiation levels in this borehole are at background levels; however, historical gross gamma data collected between 1963 and 1976 showed low to moderate levels of radionuclide contamination within the Early Palouse soil and the Plio-Pleistocene unit. The source of these elevated readings is attributed to lateral migration of contaminants from the 216-T-7 Crib and Tile Field.

Monitoring wells 299-W10-2 and 299-W10-4 were not logged with the spectral gamma-ray logging equipment.

6.12 TX and TY Tank Farms

The TX and TY Tank Farms are located directly south of the T Tank Farm (see Figure 14-17). Both of these tank farms contain SSTs, some of which are leakers.

The TY Tank Farm is located 700 ft south of the T Tank Farm. This facility contains six 758,000-gal single-shell tanks. Five of the tanks are designated assumed leakers with a combined estimated leak volume of 60,400 gal (Hanlon 1999). The major contributors to this leak volume are tanks TY-105 (35,000 gal) and TY-106 (20,000 gal). Hanlon (1999) provides a listing of the assumed leakers, dates declared or confirmed leakers, and estimated leak volumes for each tank. The listing also cites references of the leak-volume estimates.

The TX Tank Farm is located 1,150 ft south of the T Tank Farm. This facility contains eighteen 758,000-gal single-shell tanks. Eight of the tanks are designated assumed leakers with a combined estimated leak volume of 58,500 gal (Hanlon 1999).

The tanks in both of these tank farms are surrounded by numerous vadose zone monitoring boreholes that have been logged with gross gamma-ray logging systems as a means of leak detection for several decades. The data indicate contamination exists in the vadose zone throughout both of these tank farms. Many of the monitoring boreholes are only 100 to 125 ft deep, while the water table is at a depth of more than 200 ft; therefore, a large portion of the vadose zone is not monitored.

Tank monitoring boreholes in both the TX and TY Tank Farms were logged with spectral gamma-ray logging equipment. The TX Tank Farm Report (DOE 1997i) and the TY Tank Farm Report (DOE 1998g) present the spectral gamma logging results. Plumes of ^{137}Cs and ^{60}Co contamination were detected in the vadose zone sediments around and beneath both the TX and TY Tank Farm tanks. In addition, plumes of ^{154}Eu, ^{152}Eu, ^{235}U, and ^{238}U contamination were also detected beneath the TX Tank Farm tanks.

Groundwater beneath the TX and TY Tank Farms is monitored with networks of monitoring wells that are strategically located around these facilities. Widespread contamination plumes are associated with the tank farms and several waste disposal facilities adjacent to the TX and TY Tank Farms. The proximity of many potential sources makes identification of the impact of a single source or facility on groundwater quality difficult. Details regarding groundwater contamination beneath the TX and TY Tank Farms are presented in PNNL (1998).

7.0 Spectral Gamma-Ray Log Measurements

7.1 Equipment

Logging operations were conducted with two SGLSs (designated for identification purposes as Gamma 1 and Gamma 2), which were manufactured in 1993 by Greenspan, Inc., of Houston, Texas. They are a custom assemblage and adaptation of laboratory spectroscopy instrumentation and were designed specifically to perform laboratory-quality assays in boreholes. Complete documentation, including plans, system schematics, software documentation, and specific component manuals, are available in the MACTEC-ERS archive files.

Both logging units are completely self-contained systems composed of a downhole probe, a logging cable and delivery system, and surface computer electronics mounted in a cabin on a heavy-duty truck chassis. Figure 14-20 shows one of the SGLSs in a typical logging setup over a borehole.

These systems use HPGe gamma-ray detectors with efficiencies of 35 percent relative to a 3-in. by 3-in. cylindrical sodium-iodide detector standard. Germanium detectors are used because they provide a high-energy resolution that allows unique identification of a radioisotope source. Use of germanium detectors for both laboratory and field work is practical because of advances in portable electronic systems and because of developments by the manufacturers of the detection systems that made production of higher efficiency detectors more economical.

The detectors, which are installed in hollow-steel cylindrical housings or probes, are mounted in a portion of the housing with a decreased housing wall thickness that reduces the attenuation of the gamma-ray signal (by the steel housing). The downhole probes also contain a high-voltage power supply, a preamplifier, and a liquid nitrogen dewar and cryostat assembly. The liquid nitrogen dewar system is needed to cool the detector diode to liquid nitrogen temperatures. The dewar holds a quantity of liquid nitrogen that allows about 10 hours of logging between refills.

The probe is delivered downhole on a Kevlar-reinforced, multiconductor cable. The cable transmits the preamplified detector pulses and timing pulses uphole to the truck-mounted instrumentation. Conductors provide low-voltage power to the downhole power supply. The cable also has a vent tube for releasing nitrogen gas as the liquid nitrogen in the dewar vaporizes. The vent tube allows the downhole probe to be used in water-filled boreholes. Figure 14-21 shows a complete logging sonde suspended over a calibration borehole.

Sonde movement within a borehole is governed by a servo-controlled hydraulic winch that receives its control signal from the uphole system computer. The probe position in the borehole is measured with a digital rotary encoder mounted on a sheave wheel hanging from a boom (Figure 14-20). The boom is used to position the detector over the borehole.

The surface instrumentation, which is mounted in standard instrument racks inside the rear cabins of the logging trucks, consists of a high-count-rate nuclear spectroscopy amplifier interfaced to a computer-controlled multichannel analyzer. Spectral log data are recorded by computers onto hard disks.

All instrumentation control, winch control, tool positioning, safety interlocks, and other functions are under computer control using a data acquisition and control program written by the manufacturer of the system and designated "LOG." The extensive computer control and automation of the system allow it to operate much faster than a nonautomated system, thus making the characterization operation cost effective.

7.2 Calibration

The calibration of the SGLSs is specified in a calibration plan (DOE 1997a) and reported in a calibration report (DOE 1995a). Koizumi et al. (1991), Brodeur et al. (1991), and Koizumi et al. (1994) provide more general information on calibration methods and procedures for germanium logging systems.

The logging systems are calibrated by several processes that include a base calibration, periodic recalibrations at the Hanford calibration site, and daily field verifications. The schedule for periodic recalibrations was revised in 1998 from a biannual (semi-annual) to an annual basis.

The base calibration that was completed in the spring of 1995 included initial testing and qualification of the logging systems. This calibration was performed using the DOE borehole calibration models at the DOE-GJO as standards. These models are concrete cylinders or

monoliths with large homogeneous regions where the concrete is enriched with known concentrations of the naturally occurring radionuclides ^{40}K, ^{238}U, and ^{232}Th. Boreholes pass through the enriched zones so the logging sonde can be lowered into these zones. When a logging tool is placed in the middle of the zone of enriched concrete, the measurement geometry is such that a homogeneous, isotropic medium of known radionuclide concentration is simulated. The response of the detector to the medium of the calibration zone is recorded, and the mathematical relationships between radionuclide concentration and count rate response are computed. The mathematical relationships constitute the system calibration factors.

During the base calibration, calibration factors were calculated to enable direct conversion of specific photon peak count rate responses to KUT concentration in picocuries per gram. In addition, the efficiency versus energy curve was calculated. This so-called efficiency curve allows direct calculation of the efficiency of the system at a specified photon energy, thus allowing determination of the concentration of man-made radionuclides that are not present in the calibration models, such as ^{137}Cs or ^{60}Co. Figure 14-22 presents an example of an efficiency calibration function.

The calculated radionuclide concentrations derived with these conversion factors may be as much as 14 percent higher than the actual in situ concentrations because the concentrations of the calibration models are expressed in terms of gamma-ray activity per unit-sample mass of *dry* bulk material. However, the measurements made in the calibration models were in a water-saturated environment. The conversion factors in the calibration reports are strictly applicable only when the logged formation has the same water content as the calibration-model test zones. The vadose zone contains pore-space water in various percentages of saturation from near 0 percent to near 100 percent, and the boreholes are logged dry. Corrections for pore-space water cannot presently be applied to the vadose zone measurements because the in situ water content is not being measured.

The base calibration also determined the environmental corrections that are used to correct for logging in a nonstandard borehole environment. For instance, steel casing installed in a borehole attenuates the gamma-ray signal from the formation to the detector. As a result, the detected count rate is lower than it would have been in an open (uncased) borehole measurement. An environmental correction is applied to the spectral peak intensities to correct for casing attenuation.

Environmental corrections were determined in the base calibration for a large range of casing thicknesses, for the effect of water in the borehole, and for a shield that can be used to intentionally lower the gamma-ray flux at the detector. Because the environmental corrections do not change with changes in the detection system, they need to be determined only once.

All of the T Tank Farm boreholes were double-cased and grouted. The grout was inserted in between the 4-in. and 6-in. casings and penetrated the formation through perforations at the top and the bottom of the boreholes. Because the grout thickness is unknown, it is not possible to calculate or otherwise measure the attenuation of the gamma-ray signal caused by the grout. Therefore, no compensation was made for the grout in the radionuclide concentration

calculations and the reported concentrations are under-estimated by the unknown amount of attenuation. For this reason, the reported radionuclide concentrations for the T Tank Farm are considered apparent concentrations.

The base calibration also determined the response of the system to high gamma-ray flux. This test enabled determination of a count-rate correction equation, sometimes called a dead-time correction, that is applied to all of the spectra data during data analysis.

During the initial acceptance and base calibration, the winch/cable systems were tested in order to determine accuracy in depth measurements and cable stretch. The results of the tests can be found in the acceptance test records. No discernable cable stretch was noted.

Field calibrations were performed biannually at the DOE borehole calibration models at the Hanford Site until 1998, when the frequency was changed to an annual schedule. The field calibration models are identical in status as calibration standards to the national standards in Grand Junction. They were constructed at the GJO and eventually moved to the Hanford Site in the late 1980s for use in Hanford environmental logging work. Koizumi (1993) presents descriptions of these calibration models. The field calibrations provide periodic confirmation of proper system performance, and ensure that every borehole measurement is bracketed in time by system calibrations.

Biannual field calibrations are used to quantify any small changes in the performance of the logging systems over time, and the following is a synopsis of the calibrations performed up to the completion of the T Tank Farm logging. The first field calibration was completed in April 1995, immediately after the base calibration was completed and before any logging operations began. This first field calibration is documented in the base calibration report (DOE 1995a). The first biannual calibration (second field calibration) was performed in October 1995 and is reported in DOE (1996c); the second biannual calibration (third field calibration) was performed in April and May 1996 and is reported in DOE (1996d); the third biannual calibration (fourth field calibration) was performed in October 1996 and is reported in DOE (1997g); the fourth biannual calibration (fifth field calibration) was performed in February and April 1997 and is reported in DOE (1998a); and the fifth biannual calibration (sixth field calibration) was performed in October and November 1997 and is reported in DOE (1998b). The data from the first and sixth field calibrations are pertinent to the T Tank Farm data in that these data verify the logging systems were performing within acceptable standards during the period of the T Tank Farm logging operations. The calibration constants derived from calibration data were used to calculate radionuclide concentrations from the T Tank Farm borehole data.

The efficiency of the logging systems is checked in the field calibrations by recalculating the direct conversion factors for KUT and by recalculating the energy versus efficiency function shown on Figure 14-22. The dead-time correction is confirmed by measuring the system response in calibration zones that have successively increasing radionuclide concentrations. Calibration uncertainties are calculated and incorporated in the analysis of borehole log data.

In addition to the base and field calibrations, the performance of each logging system is verified daily in the field, before and after acquiring log data. These field verifications are performed by recording the system response when the detector is surrounded by a cylindrical-shaped gamma-ray source. By placing the detectors in a consistent geometrical relationship with a verification photon source, it is possible to verify the efficiency of the system, as well as other performance factors, such as the energy resolution and system gain.

The field verifications are designed to quantify the system efficiency and energy resolution. These performance factors are subject to small changes over time and could be appreciably affected in the event of a logging-system malfunction.

During the performance of the T Tank Farm logging, an extensive database tracking the response of the SGLSs to the field verification sources was developed, and system performance guidelines were established on the basis of these data. These criteria are now being used as a quality-assurance measure that verify system performance in the field.

The field verification data have been analyzed and are reported in DOE (1995a) and DOE (1998b), respectively. The data show no statistically significant trend over time, verifying the stability and consistent performance of the system.

7.3 Logging Process and Procedures

Data acquisition or logging work is performed according to a logging procedure (DOE 1997d) and adherence to this procedure ensures consistent and documented operation of the logging systems. This procedure does not specify actual data acquisition parameters because those parameters may vary in the field according to the borehole environment encountered during the logging process. Parameters such as data acquisition interval, logging mode, logging speed, or counting time may be varied by the engineer in an effort to extract as much information from the borehole as possible. Requirements specify that all data acquisition parameters are recorded on Log Data Sheets so the borehole-specific data acquisition parameters are documented and available for data processing, analysis, and interpretation. Log Data Sheets are completed as the borehole is being logged and are transferred from the field site to the office upon completion of logging. Log Data Reports are created from data on the Log Data Sheets, and the Log Data Reports are provided with the log plots in the Tank Summary Data Reports for each tank.

Logging operations commence after an initial instrumentation warm-up time period and after completion of the pre-survey field verification. Under normal conditions with moderate to low man-made radionuclide concentrations, data acquisition is initiated with 100-s detector live time at 0.5-ft depth intervals along the length of the borehole. However, because the boreholes in the T Tank Farm are double-cased with cement grout in the annulus between the casings, a longer counting time was needed to compensate for the attenuation associated with the second casing and to improve the low-level detection capability for the man-made contaminants. As a result, a 200-s counting time at 0.5-ft depth intervals was used. These data acquisition parameters strike a reasonable compromise between the required spatial resolution, adequate counting statistics, and the time requirements and costs of the logging operations. At the end of the day, another field

verification spectrum is recorded. For the T Tank Farm, the routine count time was increased to 200 s to compensate for the effects of dual casing.

If high concentrations of contamination are encountered and the detector dead-time increases to a level greater than about 80 percent, the logging engineer will generally change to a real-time (clock time) logging mode. A real-time logging mode is used through zones of high radionuclide concentrations, but even then the system sometimes become saturated and unable to record data. Above a ^{137}Cs concentration of about 10,000 pCi/g, the SGLS becomes saturated and log data cannot be obtained using the current high-efficiency detectors. These zones are identified on the log plots.

The SGLSs have digital spectrum stabilizers that automatically adjust the gain and maintain the natural ^{40}K peak at 1460-keV within an established spectrum channel range. Occasional fine adjustments of the gain may be required throughout an 8-hour (hr) logging period to keep the 1460-keV peak in the established range and these adjustments are recorded on the Log Data Sheets. However, this adjustment does not affect the system's efficiency or the calculated radionuclide concentrations.

Each time the computer is set with specified data acquisition parameters and an automated data acquisition process is executed, it is defined as a separate log run. If the process is interrupted for any reason, such as when a high count-rate region is encountered or operations cease for the day, a new log run is established when logging continues. The logging parameters for each log run are recorded on Log Data Sheets.

The spectra recorded at each depth in the borehole are automatically transferred by the LOG program to nonvolatile memory on the computer hard disk as each spectrum recording is completed.

Upon completion of logging, the spectra recorded on hard disk are transferred to an optical disk. These optical disks are then transported into the field office where the data are transferred to the main computer database maintained in the office according to the Vadose Zone Characterization Project Working File Index. Log Data Sheets are completed as the borehole is being logged and are also transferred from the field to the office with the log data. The data on the Log Data Sheets are entered into a Paradox database created specifically for the log data; the Log Data Sheets are then copied and filed.

7.4 Data Management

All data and records are managed as specified in the *General Administrative Procedures Manual* (MACTEC-ERS 1996). Section 3.0, "Records Management," of that manual should be used in conjunction with the current revision of the Vadose Zone Characterization Project Working File Index for complete records management guidance.

The Vadose Zone Characterization Project Working File Index specifies management requirements for all project data, reports, memoranda, and miscellaneous information and governs recording and retention of data and records, copying the data to the computer database, and management and retention of the database.

7.5 Data Analysis

Data analysis can begin after logging of a borehole is completed and the log data are transferred to the office computer. Data analysis is the process of reducing the spectra data to individual peak count rates and converting those raw count rates to concentrations. The radionuclide concentration data are put into a log profile format and then plotted.

The data analysis work is accomplished with Pentium microprocessor-equipped personal computers and a combination of commercial and custom software. The data analysis process, instructions, software, and procedures are documented in the data analysis manual (DOE 1997b). All computer programs that are not commercial programs are verified and validated according to DOE standards.

Statistical uncertainties derived from the logging and calibration data by standard uncertainty propagation methods are converted in the analysis software to equivalent concentrations to produce an estimation of the uncertainty of the concentration determination. The estimated uncertainties provide a measure of the quality of the data and are shown on the log plots as error bars at the concentration data points. Discussion of the uncertainty estimation calculation method is provided in detail in the base calibration report (DOE 1995a).

The MDL is also plotted with the concentration values. Calculation of the MDL is described in the data analysis manual (DOE 1997b). The MDL represents the minimum concentration at which the radionuclide would have to be present for it to be represented by a statistically significant peak in the spectrum. It also represents the lowest radionuclide concentration that could be detected using the data acquisition parameters used to acquire the spectra.

The final step of the data analysis process is preparation of a Log Data Report. The Log Data Report is created to document the details of the logging operations and the analysis of the borehole log data. It is created using the Paradox database program with data from the vadose zone characterization database.

The Log Data Report provides information about the borehole construction and casing configuration and how the borehole was logged (log run information). It also includes information regarding data analyses and provides a description of the accompanying log plots. The Log Data Report is provided with the log plots so that others may independently interpret the results.

Upon completion of the data analysis, the original spectra data, the analyzed spectra data, the individual nuclide concentration versus depth data, and the log plots are archived in permanent data storage as specified in the data analysis manual.

A flow chart of the data analysis process is shown in Figure 14-23. The reader is encouraged to consult DOE (1997b) for additional details regarding the data analysis process.

8.0 Log Data Results

8.1 Instrumentation Performance

The two logging systems (Gamma 1 and Gamma 2) logged a total of 67 boreholes within the T Tank Farm within a cumulative period of approximately 10 months. An optimum production rate of 50-ft of borehole per day was logged, generally using an acquisition time of 200 s per 0.5-ft depth interval.

Field verification spectra were recorded before and after each day's work. The pre-log verification data were analyzed before the commencement of logging. All data were recorded on the computer as spectra, and logging information was recorded by the logging engineers on the Log Data Sheets (see DOE 1997b, 1997d). The entries on the Log Data Sheets were later entered into a Paradox database and used in the analysis of the spectra.

The casing thickness values used during log data analysis to correct for casing attenuation were generally based on the published thickness values for the 4-in. and 6-in. schedule-40 steel pipe used in the T Tank Farm boreholes. The casing thicknesses used to correct the data were recorded on the individual Log Data Reports (provided with the logs in Appendix A of each of the Tank Summary Data Reports). The original spectral data are saved in the data archive; therefore, the conversion from count rate to concentration can be recalculated for any borehole if the true casing thickness is determined to be different from the value assumed for data analysis.

The maximum radiation flux from which a quantifiable spectrum could be recorded was that from a ^{137}Cs concentration of about 10,000 pCi/g.

For the counting time of 200 s used in the T Tank Farm, the MDL for ^{137}Cs is consistently between 0.1 and 0.3 pCi/g. The MDL for ^{60}Co is consistently around 0.1 pCi/g; the MDL for ^{154}Eu is about 0.3 pCi/g; and the MDL for ^{152}Eu is less than 1 pCi/g. The MDL differs slightly for each spectrum depending on the concentrations of other radionuclides at the individual spectrum depth region, including the naturally occurring nuclides. In regions of higher man-made radionuclide concentrations, elevated Compton background continuum and peak interference will tend to increase MDL values.

The MDL values for all the radionuclides are plotted on the radionuclide concentration plots that are provided in the Tank Summary Data Reports for each T Tank Farm tank. An MDL value is plotted for each occurrence of a particular radionuclide, and the log plots show that the MDL values vary as the concentrations of the radionuclide vary.

8.2 Direct Gamma Radiation and Gamma-Ray Attenuation

The logging operations measured gamma-emitting radionuclide concentrations at the ground surface when the detector was centered at the 0-ft depth location in the boreholes. The zero depth reference mark, which is etched into the detector housing and ensures consistent depth measurements of the logging probe, is at the center of the HPGe detector. Radionuclide concentration values measured at the ground surface are not accurate for two reasons: the calibration of the logging systems makes the assumption of a homogeneous infinite medium, which is not the case near the ground surface, and the upper portion of the borehole casing is enclosed in a concrete collar that attenuates the gamma radiation to a greater degree than the soil.

When the SGLS detector is located near the ground surface, the detector is enclosed in an infinite half space (2 π geometry) and is affected by gamma rays emanating only from the lower half space, not the whole space (4 π geometry), which is the condition under which the detector was calibrated in the calibration models. Furthermore, when the detector is centered at or above ground surface, gamma rays originating from surface contamination far from the borehole can travel to the detector via a direct path, and they are not attenuated by any intervening soil or borehole casing material. If there is an appreciable amount of contamination on the ground surface, the reported radionuclide concentrations would be higher than the concentrations that are actually present in the formation.

A program was initiated in 1977 to deepen some of the boreholes in the T Tank Farm in order to further monitor contaminant plumes originating from leaking tanks (see Section 5.6). The program also included the modification of almost all T Farm boreholes as a means to eliminate the potential problem of downward contaminant migration along the casings. The boreholes were modified by perforating of the upper and lower regions of the original 6-in.-diameter casing, installing 4-in.-diameter casings within the 6-in.-diameter casing, and filling the annular space between the casings with grout. The calibration models used to develop the relationship between gamma-ray energy intensity and radionuclide concentration did not incorporate a correction for attenuation of the gamma-ray energy by the grout in the annular space between the casings. Because the attenuation of the grout was not factored into the casing correction, the concentrations reported for the double-cased boreholes are less than the actual concentrations and are reported as apparent concentrations.

Although the boreholes within the T Tank Farm are completed above the water table, surface water has invaded and accumulated inside many of the boreholes in varying amounts. The height of the water columns in these boreholes ranges from less than 1 ft to more than 120 ft (a situation where the borehole is entirely filled with water). Normally, an additional correction factor is applied to compensate for the change in the gamma-ray intensities detected within the water-filled portion of the borehole. Unfortunately, the appropriate water correction factors for the casing diameters encountered were not available; therefore, no compensation was applied to the water-filled intervals of the boreholes. Radionuclide concentrations calculated with uncorrected data tend to be systematically low. However, the errors associated with the lack of a water correction are minor compared with errors caused by uncorrected effects of double casing and grout because the gamma-ray attenuation due to the casing and grout is significantly greater than

that due to water. Calculated radionuclide concentrations are reported as apparent concentrations to acknowledge these systematic errors.

8.3 Radionuclides Detected

Detection of a nuclide is considered positive when the peak identification routine of the spectrum analysis software detects a photopeak associated with a gamma ray known to be emitted by the radionuclide and the intensity of the peak is statistically above the MDL. Radionuclides that emit multiple photons are confirmed by detection of two or more photopeaks associated with the characteristic gamma rays. When a photopeak is detected and the source radionuclide is identified, custom software converts the peak count rate to an equivalent concentration in picocuries per gram using certain assumptions (see DOE 1997b).

In the T Tank Farm, the most widespread contamination consists of ^{137}Cs, ^{60}Co, and ^{154}Eu, and, to a lesser degree, ^{152}Eu. These contaminants form large plumes within the vadose zone sediments that are distributed mainly along the east and southeast sides of tanks T-103 and T-106. In addition, a plume of highly concentrated ^{137}Cs contamination is distributed on the southeast side of tank T-101. Other radionuclides, including ^{94}Nb, ^{125}Sb, ^{126}Sn, ^{235}U, and ^{238}U, were detected along the middle portions of several boreholes located near tanks T-103 and T-106, within the contaminant plumes defined by ^{137}Cs, ^{60}Co, and ^{154}Eu.

8.4 Log Plots

Log data results are presented in the Tank Summary Data Reports as plots showing radionuclide concentration relative to depth in the boreholes. A set of plots for each borehole consists of a separate plot of any man-made radionuclides, a plot of the KUT concentrations, a plot showing shape factor analysis results where appropriate, and a combination plot showing logs of the man-made and naturally occurring radionuclides along with the total gamma log and the most recent historical gross gamma-ray log acquired with the Tank Farms logging system. The plots for the boreholes surrounding each of the tanks are provided in the appendix of the Tank Summary Data Reports for the individual tanks. The man-made radionuclide correlation plots for the boreholes surrounding each tank are provided in Appendix A of this report.

Each set of plots also includes a Log Data Report. The Log Data Reports provide all the information required to analyze and interpret the log data, including explanations of any anomalies or peculiarities in the data or the analysis process. The plots themselves do not provide enough information with which to assess the data; consequently, anyone reviewing the data should also review the Log Data Reports. The Log Data Reports are retained with the plots as required by the project quality assurance program.

The log plots and the nuclide-specific data files for each borehole are maintained in the vadose zone characterization computer database. These data will eventually be transferred to other Hanford databases to make the information more readily available.

8.5 Tank Summary Data Reports

A Tank Summary Data Report was prepared for each tank in the T Tank Farm. Each report provides a mechanism for reporting the results of the spectral gamma logging and places the data in the context of the documented tank history.

In addition to the log plots for the boreholes surrounding the tank, a Tank Summary Data Report provides a discussion of each borehole and the spectral gamma data analysis and interpretation for each borehole.

The Tank Summary Data Reports provide a correlation and discussion of the contamination around a tank and identify any geologic correlations. A correlation plot provided in the Tank Summary Data Reports shows the contamination concentration plots from each borehole around the tank in a single figure to aid in the cross-borehole correlation. The analysts also make conclusions, where appropriate, about the sources of the contamination in the vadose zone.

In general, the Tank Summary Data Reports provide a summary of the logging data, an assessment of the conditions of the vadose zone, and an analysis of the relationship between the vadose zone contamination and the tank. The Tank Summary Data Reports for the T Tank Farm tanks are listed in the reference section of this report.

8.6 Spectral Shape Factor Analysis

Insights into the distribution of the radionuclides identified by the SGLS can be provided by using an analytical method known as shape factor analysis (Wilson 1997, 1998). Shape factor analysis uses the Compton downscattering caused by the interaction of gamma rays with matter between the gamma-ray source and the detector to help determine the location of the source relative to the detector. Shape factor analysis is not generally applicable to spectral gamma measurements in boreholes in the T Tank Farm because most of the boreholes have a second 4-in.-diameter steel casing installed inside the original 6-in.-diameter casing. When the 4-in. casing was installed, the 6-in. casing was perforated near the bottom and top of the hole and an unknown amount and type of cement grout was added to the annular space between the two casings. The double casing thickness, annular grout, and unknown degree of grout penetration into the formation are all elements that attenuate gamma rays and distort the overall spectrum shape. At present, the effects of these elements on the various shape factors are not well known, and interpretation of shape factors under these conditions is likely to be inconclusive or misleading. However, there is one borehole (50-06-04) that was not completed with dual casings and grout, and another borehole (50-06-18) that has an interval of single casing. Shape factor analysis was applicable to the spectral gamma measurements collected under these conditions and yielded interpretable results for both boreholes.

Additional information on shape factor analysis theory is provided in Wilson (1997, 1998). For a more extensive discussion of shape factor analysis as it is applied to log data from single-cased, non-grouted boreholes, the reader is referred to the A Tank Farm Report (DOE 1999a).

8.7 Interpreted Data Sets

A data set called an "interpreted data set" is used for creating the T Tank Farm visualizations. The data set is a tabulation of ^{137}Cs contamination deemed to be distributed in the backfill materials and undisturbed sediments (beneath the base of the tank farm excavation) rather than being confined in the immediate vicinity of the borehole casings. This data set was created by editing the concentration data of all of the ^{137}Cs contamination detected in the course of the SGLS logging in the T Tank Farm boreholes. Because shape factor analysis could not be applied to the spectral gamma measurements collected from almost all of the boreholes in the T Tank Farm (except 50-06-04 and 50-06-18), this edited SGLS data set reflects interpretations of the distribution and nature of occurrence of contaminants as determined from general experience and familiarity with the distribution of ^{137}Cs in the course of reviewing many SGLS logs. Spectral shape factor analysis results from the single-cased intervals in boreholes 50-06-04 and 50-06-18 were also used to determine the distribution of the ^{137}Cs in borehole 50-06-04 and the ^{137}Cs and ^{60}Co in borehole 50-06-18. The edited SGLS concentration plots for each borehole are presented in the tank correlation plots included in Appendix B.

Most obvious in the interpreted data set revisions are those in the upper 20 ft of the boreholes. Surface spills and piping leaks occurred at the surface in the tank farm, and contamination from these releases migrated into the backfill materials to varying depths; furthermore, some of the contaminant distributions observed on the concentration profiles may have resulted from more than a single event. Some of the contamination in the upper 20 ft of the boreholes may also have resulted from dragdown of surface contamination during drilling when the boreholes were originally installed or later when they were deepened. Contaminant distributions are attributed to dragdown when the contaminant concentrations decrease rapidly with depth in the borehole because the contaminants being moved by the drilling become diluted as the drilling drive barrel entered uncontaminated backfill materials (or when the drive barrel entered uncontaminated formation sediments deeper in the boreholes). Additionally, some of the boreholes may have been (and may continue to be) conduits for contaminant migration along the inside and/or outside of the casings.

Because there are various mechanisms contributing to the contaminant distributions in the upper 20-ft interval of the boreholes and there is no positive method of conclusively identifying sources and distributions of contamination, an entire interval may be identified as a region of vadose zone contamination. Although there may be differing interpretations regarding the distribution of this near-surface contamination, (i.e., whether the contamination is distributed in the backfill materials [or undisturbed sediments] or on or within the borehole casings), these differences involve an insignificant portion of the total vadose zone contamination at the T Tank Farm.

Intermittent ^{137}Cs contamination was observed throughout some of the T Tank Farm monitoring boreholes. This contamination most likely resulted from dragdown during drilling or migration down the inside and/or outside of the casings, and these occurrences were removed from the SGLS data.

Occurrences of ^{137}Cs contamination (regardless of concentration) were not deleted when they were laterally correlatable between boreholes or when the contamination was continuous at depth with isolated, intermittent, or no other contamination in the upper regions of the boreholes. These intervals are interpreted to indicate the boreholes intersect a plume.

^{137}Cs contamination occurred at the bottoms of many of the boreholes. This contamination most likely occurred when contaminated matter entered the inside of the casings and migrated to the bottoms of the boreholes, and these occurrences of ^{137}Cs contamination were removed from the SGLS data.

The discussions presented in the following sections describe the rationale for the creation of the interpreted data set for all the intervals of contamination that were detected in the T Tank Farm tank monitoring boreholes. The locations of the T Tank Farm monitoring boreholes are shown in Figure 14-17, and the correlation plots for each of the tanks are presented in Appendix B. The Tank Summary Data Reports are referenced at the end of each tank section as a source for additional details regarding data interpretations for each borehole. Additional discussions regarding relationships between boreholes and specific plumes are presented in Section 10.0, "Discussion of Results."

8.7.1 Boreholes Associated with Tank T-101

Borehole 50-01-02

The ^{137}Cs contamination detected between the ground surface and 4 ft probably resulted from surface spills that migrated downward into the backfill sediments. The ^{137}Cs contamination detected below this zone (4.5 to 26 ft) was probably carried down during drilling activities or migrated down the inside and/or outside of the casing and was removed from the SGLS data set used to create the visualizations.

Borehole 50-00-03

The ^{137}Cs contamination detected between the ground surface and 3 ft probably resulted from surface spills that have migrated downward into the backfill sediments.

The isolated occurrences of ^{137}Cs contamination detected at 38, 66, and 99.5 ft were probably carried down during drilling activities or migrated down the inside and/or outside of the casing. The zone of continuous ^{137}Cs contamination detected at the bottom of the borehole (128 to 139 ft) is probably attributable to surface flood water that accumulated at the bottom of the borehole, leaving a ring of residual ^{137}Cs contamination on the inside of the casing. Both the isolated and continuous ^{137}Cs contamination were removed from the SGLS data set used to create the visualizations.

Borehole 50-01-04

The ^{137}Cs contamination detected between the ground surface and 3.5 ft probably resulted from surface spills that migrated downward into the backfill sediments. The ^{137}Cs contamination detected below this zone (4 to 19.5 ft) was probably carried down during drilling activities or migrated down the inside and/or outside of the casing and was removed from the SGLS data set used to create the visualizations.

The large zone of apparently continuous, highly concentrated ^{137}Cs contamination detected from 20 to 122.5 ft is probably the result of a leak from one or more of the spare fill lines on the southeast side of the tank that occurred when tank T-101 was overfilled during normal tank farm operations. The SGLS data suggest that the maximum vertical extent of the plume has not been determined because the contamination extends to the bottom of the logged interval in this borehole.

Borehole 50-01-06

The ^{137}Cs contamination detected between the ground surface and 2.5 ft probably resulted from surface spills that migrated downward into the backfill sediments. The ^{137}Cs contamination detected below this zone (3 to 36 ft) was probably carried down during drilling activities or migrated down the inside and/or outside of the casing and was removed from the SGLS data set used to create the visualizations.

Borehole 50-01-09

The ^{137}Cs contamination detected between the ground surface and 8.5 ft probably resulted from surface spills that migrated downward into the backfill sediments. The elevated ^{137}Cs contamination detected from 17.5 to 24 ft is probably associated with a leak originating from the cascade overflow line attached to tank T-101.

The zones of ^{137}Cs contamination detected from 12.5 to 17 ft and from 24.5 to 34 ft were either carried down during drilling activities or were caused by streaming gamma radiation originating from the contamination associated with the cascade overflow line leak described above. Both zones of ^{137}Cs contamination were removed from the SGLS data set used to create the visualizations.

Borehole 50-01-12

The ^{137}Cs detected at the ground surface is probably related to direct radiation from surface contamination. The isolated ^{137}Cs detected between 1.5 and 6 ft is probably surface contamination that was carried down during drilling activities or migrated down the inside and/or outside the casing. Each of these areas of ^{137}Cs contamination were removed from the SGLS data set used to create the visualizations.

8.7.2 Boreholes Associated with Tank T-102

Borehole 50-02-02

The ^{137}Cs detected at the ground surface is probably related to direct radiation from surface contamination. The isolated ^{137}Cs detected at the bottom of the borehole is most likely particulate matter that has fallen into the borehole from the ground surface. Both areas of ^{137}Cs contamination were removed from the SGLS data set used to create the visualizations.

Borehole 50-02-05

The ^{137}Cs contamination detected between the ground surface and 1.5 ft probably resulted from one or more surface spills that migrated downward into the backfill sediments. The elevated ^{137}Cs contamination detected from 37 to 42.5 ft is probably from an unidentified tank or pipeline leak associated with tank T-102 or T-105. The lower concentrations of ^{137}Cs detected above and below this zone may represent the outer fringe of a larger ^{137}Cs plume.

The isolated ^{137}Cs detected at 77 ft was probably carried down during drilling activities and was removed from the SGLS data set used to create the visualizations.

Borehole 50-02-08

The ^{137}Cs detected at the ground surface is probably related to direct radiation from surface contamination. The small zone of ^{137}Cs detected from 1 to 2 ft is probably surface contamination that was carried down during drilling activities or migrated down the inside and/or outside of the casing. Each of these areas of contamination were removed from the SGLS data set used to create the visualizations.

Borehole 50-02-09

The ^{137}Cs contamination detected between the ground surface and 5.5 ft probably resulted from one or more surface spills that migrated downward into the backfill sediments. The ^{137}Cs contamination detected between 6 and 87.5 ft was probably carried down during drilling activities or migrated down the inside and/or outside of the casing and was removed from the SGLS data set used to create the visualizations.

Borehole 50-02-10

The ^{137}Cs detected at the ground surface is probably related to direct radiation from surface contamination. The ^{137}Cs detected between 0.5 and 26.5 ft is probably surface contamination that was carried down during drilling activities or migrated down the inside and/or outside of the casing. Each interval of contamination was removed from the SGLS data set used to create the visualizations.

Borehole 50-00-12

The ^{137}Cs detected at the ground surface is probably related to direct radiation from surface contamination. The isolated zones ^{137}Cs detected between 0.5 and 140 ft are probably surface contamination that was carried down during drilling activities or migrated down the inside and/or outside of the casing. Each area of contamination was removed from the SGLS data set used to create the visualizations.

Borehole 50-02-12

The ^{137}Cs detected at the ground surface is probably related to direct radiation from surface contamination and was removed from the SGLS data set used to create the visualizations.

8.7.3 Boreholes Associated with Tank T-103

Borehole 50-03-01

The ^{137}Cs detected at the ground surface is probably related to direct radiation from surface contamination and was removed from the SGLS data set used to create the visualizations.

Borehole 50-03-04

The ^{137}Cs contamination detected from 1 to 4.5 ft probably resulted from one or more surface spills that migrated downward into the backfill sediments. The ^{137}Cs contamination detected directly below this zone (5 to 7 ft) and at 17 ft was probably carried down during drilling activities or migrated down the inside and/or outside of the casing and was removed from the SGLS data set used to create the visualizations.

The zone of ^{137}Cs contamination detected from 20 to 24.5 ft probably originated from a leak from a spare fill line on the southeast side of the tank.

Borehole 50-03-05

The ^{137}Cs contamination detected between the ground surface and 3 ft probably resulted from one or more surface spills that migrated downward into the backfill sediments. The ^{137}Cs contamination detected below this zone (3.5 to 6 ft) and at 29 ft was probably carried down during drilling activities or migrated down the inside and/or outside of the casing and was removed from the SGLS data set used to create the visualizations.

Borehole 50-03-06

The ^{137}Cs contamination detected at the ground surface and at 0.5 ft probably resulted from one or more surface spills that migrated downward into the backfill sediments. The ^{137}Cs contamination detected below this zone (1 to 12.5 ft) and at 98 ft was probably carried down

during drilling activities or migrated down the inside and/or outside of the casing and was removed from the SGLS data set used to create the visualizations.

Borehole 50-03-08

The ^{137}Cs detected at the ground surface is probably related to direct radiation from surface contamination. The small zones of ^{137}Cs detected between 0.5 and 2 ft are probably surface contamination that was carried down during drilling activities or migrated down the inside and/or outside of the casing. Each area of contamination was removed from the SGLS data set used to create the visualizations.

Borehole 50-03-10

The ^{137}Cs detected at the ground surface is probably related to direct radiation from surface contamination and was removed from the SGLS data set used to create the visualizations.

8.7.4 Boreholes Associated with Tank T-104

Borehole 50-04-03

The ^{137}Cs contamination detected between the ground surface and 9 ft probably resulted from one or more surface spills that migrated downward into the backfill sediments. The elevated ^{137}Cs contamination detected between 23 and 27 ft may have been driven downward through the backfill material into this region of the vadose zone by precipitation infiltration.

The ^{137}Cs contamination detected from 9.5 to 23 ft and between 28 and 78.5 ft was probably carried down during drilling activities or migrated down the inside and/or outside of the casing. The zone of continuous ^{137}Cs contamination detected at the bottom of the borehole (79 to 86.5 ft) is probably attributable to 1) surface flood water that accumulated at the bottom of the borehole, leaving a ring of residual ^{137}Cs contamination on the inside of the casing, 2) surface flood water that percolated downward along the outside of the borehole casing, carrying ^{137}Cs contamination to the depth of the early Palouse soil horizon, or 3) near-surface ^{137}Cs contamination that adhered to the outside of the borehole casing and was carried downward as the borehole was advanced. Each of these zones were removed from the SGLS data set used to create the visualizations.

Borehole 50-04-05

The ^{137}Cs contamination detected between the ground surface and 20.5 ft probably resulted from one or more surface spills that migrated downward into the backfill sediments. The ^{137}Cs contamination detected between 21.5 and 84.5 ft was probably carried down during drilling activities or migrated down the inside and/or outside of the casing and was removed from the SGLS data set used to create the visualizations.

Borehole 50-04-07

The ^{137}Cs contamination detected between the ground surface and 16 ft probably resulted from one or more surface spills that migrated downward into the backfill sediments. The elevated ^{137}Cs contamination detected from 22 to 26 ft may have been driven downward through the backfill material into this region of the vadose zone by precipitation infiltration.

The ^{137}Cs contamination detected from 17 to 21 ft and between 27 and 92 ft was probably carried down during drilling activities or migrated down the inside and/or outside of the casing and was removed from the SGLS data set used to create the visualizations.

Borehole 50-04-08

The ^{137}Cs contamination detected between the ground surface and 6.5 ft probably resulted from one or more surface spills that migrated downward into the backfill sediments. The ^{137}Cs contamination detected below this zone (between 7 and 22.5 ft) and at 87 ft was probably carried down during drilling activities or migrated down the inside and/or outside of the casing and was removed from the SGLS data set used to create the visualizations.

Borehole 50-04-10

The ^{137}Cs contamination detected between the ground surface and 2 ft probably resulted from one or more surface spills that migrated downward into the backfill sediments. The ^{137}Cs contamination detected below this zone (between 2.5 and 20.5 ft) and at 57.5 ft and 78 ft was probably carried down during drilling activities or migrated down the inside and/or outside of the casing and was removed from the SGLS data set used to create the visualizations.

8.7.5 Boreholes Associated with Tank T-105

Borehole 50-05-06

The ^{137}Cs contamination detected between the ground surface and 12.5 ft probably resulted from one or more surface spills that migrated downward into the backfill sediments. The ^{137}Cs contamination detected below this zone (between 13 and 37.5 ft) and at 116 ft was probably carried down during drilling activities or migrated down the inside and/or outside of the casing and was removed from the SGLS data set used to create the visualizations.

Borehole 50-05-07

The ^{137}Cs contamination detected between the ground surface and 9.5 ft probably resulted from one or more surface spills that migrated downward into the backfill sediments. The ^{137}Cs contamination detected below this zone (between 10 and 58 ft) was probably carried down during drilling activities or migrated down the inside and/or outside of the casing and was removed from the SGLS data set used to create the visualizations.

Borehole 50-05-11

The ^{137}Cs detected at the ground surface is probably related to direct radiation from surface contamination. The ^{137}Cs detected between 0.5 and 3.5 ft is probably surface contamination that was carried down during drilling activities or migrated down the inside and/or outside of the casing. Each area of contamination was removed from the SGLS data set used to create the visualizations.

8.7.6 Boreholes Associated with Tank T-106

Borehole 50-06-02

The ^{137}Cs contamination detected between the ground surface and 5 ft probably resulted from one or more surface spills that migrated downward into the backfill sediments.

The ^{137}Cs detected between 5.5 and 29.5 ft is probably surface contamination that was carried down during drilling activities or migrated down the inside and/or outside of the casing. The ^{137}Cs detected near the bottom of the borehole (between 118 and 123 ft) is most likely particulate matter that has fallen into the borehole from the ground surface. Both areas of ^{137}Cs contamination were removed from the SGLS data set used to create the visualizations.

Borehole 50-06-03

The ^{137}Cs contamination detected between the ground surface and 2.5 ft probably resulted from one or more surface spills that migrated downward into the backfill sediments. The thin zone of ^{137}Cs contamination detected from 19.5 to 21.5 ft probably resulted from a pipeline or cascade-line leak. The ^{137}Cs contamination detected from 33.5 to 40 ft most likely originated from the T-106 tank leak.

The ^{137}Cs contamination detected between 3 and 16 ft and from 27 to 27.5 ft was probably carried down during drilling activities or migrated down the inside and/or outside of the casing and was removed from the SGLS data set used to create the visualizations.

Borehole 50-06-04

The ^{137}Cs contamination detected between the ground surface and 1.5 ft probably resulted from one or more surface spills that migrated down into the backfill material. Shape factor analysis results indicate that this contamination is uniformly distributed in the backfill material.

Shape factor analysis results indicate that the ^{137}Cs detected from 2 to 11.5 ft is localized to the borehole casing, suggesting that it was probably carried down during the drilling of the borehole. This interval was removed from the SGLS data set used to create the visualizations.

The zones of elevated ^{137}Cs contamination detected from 12 to 14.5 ft and from 19 to 23 ft may be the result of further migration of contamination through the backfill material. Shape factor

analysis results indicate that the upper zone of contamination is uniformly distributed in the backfill material while the lower zone of contamination may be somewhat remote from the borehole.

Although shape factor results were inconclusive, the lower concentrations of ^{137}Cs detected from 15 to 18.5 ft and from 23.5 to 32 ft were probably carried down during the drilling of the borehole and were removed from the SGLS data set used to create the visualizations.

A zone of extremely high gamma radiation was detected from 35 to 40 ft that yielded no spectral gamma data. However, based upon the rate of decrease of the historical gross gamma activity, it was determined that ^{137}Cs is the predominant radionuclide present within this interval. The contamination originated from the T-106 tank leak, accumulated at the base of the tank farm excavation, and migrated laterally along the perimeter of the tank to the area penetrated by this borehole. The ^{137}Cs contamination detected above (32.5 to 34.5 ft) and below (40.5 to 42 ft) the zone of extremely high gamma radiation also originated from the T-106 tank leak.

Borehole 50-06-05

The ^{137}Cs contamination detected between the ground surface and 8 ft probably resulted from one or more surface spills that migrated down into the shallow backfill around this borehole. The zone of elevated ^{137}Cs contamination detected from 19.5 to 24 ft may be the result of a pipeline or transfer-line leak. The ^{137}Cs contamination detected below these zones (from 8.5 to 19 ft and from 24.5 to 31 ft) was probably carried down during the drilling of the borehole and was removed from the SGLS data set used to create the visualizations.

A zone of extremely high gamma radiation was detected from 33 to 93 ft. Based upon the rate of decrease of the historical gross gamma activity, it was determined that ^{137}Cs is the primary radionuclide present within this interval. The magnitude of contamination within this region of the vadose zone indicates that this contamination originated from the T-106 tank leak and that this borehole is very close to the leak source.

Below 93 ft, the SGLS detected very high concentrations of continuous ^{137}Cs contamination that extends to the bottom of the logged interval, indicating that the contaminant plume has migrated downward to a depth of at least 119 ft. However, the total vertical extent of the plume can not be ascertained because of the limited depth of the borehole.

Borehole 50-06-06

The ^{137}Cs contamination detected between the ground surface and 5 ft probably resulted from one or more surface spills that migrated down into the backfill material. The ^{137}Cs contamination detected from 5.5 to 32 ft, at 91 ft, and at 114.5 ft was probably carried down during drilling activities or migrated down the inside and/or outside of the casing and was removed from the SGLS data set used to create the visualizations.

A zone of extremely high gamma radiation was detected from 35 to 46 ft. Based upon the rate of decrease of the historical gross gamma activity, it was determined that ^{137}Cs is the predominant radionuclide present within this interval. The contamination originated from the T-106 tank leak, accumulated at the base of the tank farm excavation, and migrated laterally along the perimeter of the tank to this borehole. The ^{137}Cs contamination detected above (32.5 to 34.5 ft) and below (46.5 ft) the zone of extremely high gamma radiation also originated from the T-106 tank leak.

Borehole 50-06-08

The ^{137}Cs contamination detected between the ground surface and 3.5 ft probably resulted from one or more surface spills that migrated down into the shallow backfill around this borehole. The ^{137}Cs contamination detected from 4 to 22.5 ft and from 31.5 to 32 ft was probably carried down during the drilling of the borehole and was removed from the SGLS data set used to create the visualizations.

A zone of extremely high gamma radiation was detected from 35 to 41 ft. Based upon the rate of decrease of the historical gross gamma activity, it was determined that ^{137}Cs is the predominant radionuclide present within this interval. A large zone of moderate to high ^{137}Cs contamination extends from 46 ft to 81 ft around this borehole. No deep ^{137}Cs contamination was detected below 41 ft around adjacent borehole 50-06-06, which lies between this borehole and the suspected source of the contamination, suggesting that the ^{137}Cs did not migrate through the vadose zone sediments from the contaminant source. The data indicate that the contamination originated from the T-106 tank leak, accumulated at the base of the tank farm excavation, and migrated laterally along the bottom of the tank farm excavation to this borehole. It appears that some of this contamination then migrated downward, possibly by "fingering" or by some undetermined manner, to a depth of about 81 ft. It is postulated that the deeper ^{137}Cs contamination detected below about 81 ft was carried down during drilling activities and was removed from the SGLS data set used to create the visualizations.

Borehole 50-06-11

The ^{137}Cs detected at the ground surface is probably related to direct radiation from surface contamination. The ^{137}Cs detected at 0.5 ft and at 10.5 ft is probably surface contamination that was carried down during drilling activities or migrated down the inside and/or outside of the casing. Each area of contamination was removed from the SGLS data set used to create the visualizations.

Borehole 50-06-16

The ^{137}Cs contamination detected between the ground surface and 5 ft probably resulted from one or more surface spills that migrated down into the shallow backfill around this borehole. The zone of elevated ^{137}Cs contamination detected from 14 to 18.5 ft may represent near-surface contamination that migrated laterally along the surface of the tank dome into this region of the backfill material.

The relatively lower concentrations of ^{137}Cs detected from 5.5 to 13.5 ft and from 19 to 32.5 ft were probably carried down during the drilling of the borehole. The ^{137}Cs detected at the bottom of the borehole (86 ft) is most likely particulate matter that has fallen into the borehole from the ground surface. These areas of ^{137}Cs contamination were removed from the SGLS data set used to create the visualizations.

A zone of very high ^{137}Cs contamination was detected from 33 to 43 ft. The data indicate that the ^{137}Cs contamination originated from the T-106 tank leak, and it appears that the waste accumulated and spread along the base of the tank farm excavation to this borehole.

Borehole 50-06-17

The ^{137}Cs contamination detected between the ground surface and 18.5 ft probably resulted from one or more surface spills that migrated down into the shallow backfill around this borehole. The ^{137}Cs contamination detected below this zone from 19 to 32 ft was probably carried down during the drilling of the borehole and was removed from the SGLS data set used to create the visualizations.

A zone of extremely high gamma radiation was detected from 34.5 ft to the bottom of the logged interval (86.5 ft). Based upon the rate of decrease of the historical gross gamma activity, it was determined that ^{137}Cs is the predominant radionuclide present within this interval. Similar to borehole 50-06-05, the magnitude of contamination within this region of the vadose zone indicates that this contamination originated from the T-106 tank leak and that this borehole is very close to the leak source. The resulting contaminant plume has migrated downward to a depth of at least 86.5 ft. The ^{137}Cs contamination within the deeper portion of the plume (below 45 ft) does not appear to be laterally extensive to the west because deep ^{137}Cs contamination is absent around adjacent borehole 50-06-06.

Borehole 50-06-18

The ^{137}Cs contamination detected between the ground surface and 9 ft probably resulted from one or more surface spills that migrated down into the shallow backfill around this borehole. The zone of elevated ^{137}Cs contamination detected from 11 to 14 ft could be the result of a pipeline leak or may represent subsurface contamination that remobilized and migrated laterally along the surface of the tank dome into this region of the backfill material. The ^{137}Cs contamination detected from 16 to 23 ft may be the result of further migration of contamination through the backfill material. The ^{137}Cs contamination detected below this zone from 23.5 to 33 ft was probably carried down during the drilling of the borehole and was removed from the SGLS data set used to create the visualizations.

A zone of extremely high gamma radiation was detected from 35.5 to 44 ft. This zone was determined to contain high concentrations of ^{137}Cs contamination that originated from the T-106 tank leak. The ^{137}Cs contamination detected above (33.5 to 35 ft) and below (44.5 to 73 ft) the

zone of extremely high gamma radiation also originated from the T-106 tank leak and is suspected to be distributed primarily in the formation sediments around this borehole.

Borehole 50-00-09

The ^{137}Cs detected at the ground surface is probably related to direct radiation from surface contamination and was removed from the SGLS data set used to create the visualizations.

Borehole 50-00-10

The ^{137}Cs contamination detected from the ground surface to 17 ft is probably surface contamination that was carried down during drilling activities or migrated down the inside and/or outside of the casing. It is likely that the isolated ^{137}Cs contamination detected from 115.5 to 116 ft was also carried down during drilling as the borehole was telescoped to total depth. Each area of contamination was removed from the SGLS data set used to create the visualizations.

8.7.7 Boreholes Associated with Tank T-107

Borehole 50-07-03

The ^{137}Cs contamination detected between the ground surface and 1 ft probably resulted from one or more surface spills that migrated down into the backfill material. The zone of slightly elevated ^{137}Cs contamination detected from 5 to 15 ft may represent subsurface contamination that remobilized and migrated laterally along the surface of the tank dome into this region of the backfill material. The ^{137}Cs contamination detected below these zones (between 1.5 and 4.5 ft and between 15.5 and 81.5 ft) was probably carried down during drilling activities or migrated down the inside and/or outside of the casing and was removed from the SGLS data set used to create the visualizations.

Borehole 50-07-07

The ^{137}Cs contamination detected from 0.5 to 2.5 ft probably resulted from one or more surface spills that migrated down into the backfill material. The thin zone of elevated ^{137}Cs contamination detected from 42.5 to 45.5 ft may represent subsurface contamination that migrated down the tank wall and accumulated at the base of the tank farm excavation. The ^{137}Cs contamination detected between 4.5 and 29.5 ft and at 67 ft was probably carried down during drilling activities or migrated down the inside and/or outside of the casing and was removed from the SGLS data set used to create the visualizations.

Borehole 50-07-08

The ^{137}Cs contamination detected from 0.5 to 7.5 ft probably resulted from one or more surface spills that migrated down into the backfill material. The ^{137}Cs contamination detected between 8.5 and 83.5 ft was probably carried down during drilling activities or migrated down the inside

and/or outside of the casing and was removed from the SGLS data set used to create the visualizations.

8.7.8 Boreholes Associated with Tank T-108

Borehole 50-08-05

The ^{137}Cs contamination detected between the ground surface and 2.5 ft probably resulted from one or more surface spills that migrated down into the backfill material. The ^{137}Cs contamination detected from 11 to 18 ft and at 79 ft was probably carried down during drilling activities or migrated down the inside and/or outside of the casing and was removed from the SGLS data set used to create the visualizations.

Borehole 50-08-07

The ^{137}Cs contamination detected between the ground surface and 3 ft probably resulted from one or more surface spills that migrated down into the backfill material. The ^{137}Cs contamination detected at 101 ft and between 117.5 and 119 ft was probably carried down during drilling activities or migrated down the inside and/or outside of the casing and was removed from the SGLS data set used to create the visualizations.

Borehole 50-08-08

The ^{137}Cs contamination detected between the ground surface and 1 ft probably resulted from one or more surface spills that migrated down into the backfill material. The ^{137}Cs contamination detected between 3.5 and 7 ft was probably carried down during drilling activities or migrated down the inside and/or outside of the casing and was removed from the SGLS data set used to create the visualizations.

Borehole 50-08-09

The ^{137}Cs contamination detected between the ground surface and 4.5 ft probably resulted from one or more surface spills that migrated down into the backfill material. The ^{137}Cs contamination detected from 7 to 9.5 ft was probably carried down during drilling activities or migrated down the inside and/or outside of the casing and was removed from the SGLS data set used to create the visualizations.

Borehole 50-08-11

The ^{137}Cs contamination detected between the ground surface and 10.5 ft probably resulted from one or more surface spills that migrated down into the backfill material. The ^{137}Cs contamination detected between 85.5 and 97 ft may have originated from the T-106 tank leak and migrated downward through the vadose zone into the caliche layers of the Plio-Pleistocene unit. The ^{137}Cs

contamination detected below these zones (from 11 to 64 ft and between 103 and 135.5 ft) was probably carried down during drilling activities or migrated down the inside and/or outside of the casing and was removed from the SGLS data set used to create the visualizations.

Borehole 50-08-19

The ^{137}Cs contamination detected between the ground surface and 3 ft probably resulted from one or more surface spills that migrated down into the backfill material. The ^{137}Cs contamination detected between 8 ft and 11.5 ft was probably carried down during drilling activities or migrated down the inside and/or outside of the casing and was removed from the SGLS data set used to create the visualizations.

8.7.9 Boreholes Associated with Tank T-109

Borehole 50-09-01

The ^{137}Cs contamination detected between the ground surface and 6 ft probably resulted from a surface spill or a near-surface pipeline leak that migrated down into the backfill material. The ^{137}Cs contamination detected between 6.5 and 19.5 ft was probably carried down during drilling activities or migrated down the inside and/or outside of the casing and was removed from the SGLS data set used to create the visualizations.

Borehole 50-09-02

The ^{137}Cs contamination detected between the ground surface and 8 ft probably resulted from one or more surface spills that migrated down into the backfill material. The ^{137}Cs contamination detected between 8.5 and 34 ft was probably carried down during drilling activities or migrated down the inside and/or outside of the casing and was removed from the SGLS data set used to create the visualizations.

Borehole 50-09-05

The ^{137}Cs detected at the ground surface is probably related to direct radiation from surface contamination and was removed from the SGLS data set used to create the visualizations.

Borehole 50-09-07

The ^{137}Cs detected at the ground surface is probably related to direct radiation from surface contamination. The ^{137}Cs detected at 2 ft is probably surface contamination that was carried down during drilling activities or migrated down the inside and/or outside of the casing. Each area of contamination was removed from the SGLS data set used to create the visualizations.

Borehole 50-09-09

The ^{137}Cs detected at the ground surface is probably related to direct radiation from surface contamination. The ^{137}Cs detected between 0.5 and 2.5 ft is probably surface contamination that was carried down during drilling activities or migrated down the inside and/or outside of the casing. Each area of contamination was removed from the SGLS data set used to create the visualizations.

Borehole 50-09-10

The ^{137}Cs contamination detected between the ground surface and 9.5 ft probably resulted from one or more surface spills that migrated down into the backfill material.

The ^{137}Cs contamination detected between 10 and 23 ft and between 82 and 111.5 ft was probably carried down during drilling activities or migrated down the inside and/or outside of the casing. The ^{137}Cs detected at the bottom of the logged interval (from 117 to 119.5 ft) is most likely particulate matter that has fallen into the borehole from the ground surface. These areas of ^{137}Cs contamination were removed from the SGLS data set used to create the visualizations.

8.7.10 Boreholes Associated with Tank T-110

Borehole 50-10-05

The zone of slightly elevated ^{137}Cs contamination detected from 5 to 16 ft may represent subsurface contamination that remobilized and migrated laterally into this region of the backfill material. The ^{137}Cs contamination detected from the ground surface to 0.5 to 4.5 ft is probably surface contamination that was carried down during drilling activities or migrated down the inside and/or outside of the casing. The ^{137}Cs contamination detected from 16.5 to 28.5 ft was probably carried down during drilling activities. Both intervals were removed from the SGLS data set used to create the visualizations.

Borehole 50-10-07

The ^{137}Cs contamination detected from 0.5 to 1 ft, at 40.5 ft, and 83 ft is probably surface contamination that was carried down during drilling activities or migrated down the inside and/or outside of the casing and was removed from the SGLS data set used to create the visualizations.

Borehole 50-10-08

The ^{137}Cs contamination detected at 1 ft and at 2 ft is probably surface contamination that was carried down during drilling activities or migrated down the inside and/or outside of the casing and was removed from the SGLS data set used to create the visualizations.

Borehole 50-10-10

The ^{137}Cs contamination detected between the ground surface and 1.5 ft probably resulted from one or more surface spills that migrated down into the shallow backfill around this borehole. The ^{137}Cs contamination detected between 2.5 and 74.5 ft was probably carried down during drilling activities or migrated down the inside and/or outside of the casing and was removed from the SGLS data set used to create the visualizations.

Borehole 50-00-05

The ^{137}Cs contamination detected between 0.5 to 1.5 ft probably resulted from one or more surface spills that migrated down into the shallow backfill around this borehole. The ^{137}Cs contamination detected between 15 ft and the bottom of the logged interval (137 ft) was probably carried down during drilling activities or migrated down the inside and/or outside of the casing and was removed from the SGLS data set used to create the visualizations.

8.7.11 Boreholes Associated with Tank T-111

Borehole 50-11-05

The ^{137}Cs detected at the ground surface is probably related to direct radiation from surface contamination and was removed from the SGLS data set used to create the visualizations.

Borehole 50-11-07

The ^{137}Cs contamination detected between the ground surface and 6.5 ft probably resulted from one or more surface spills that migrated down into the backfill material. The ^{137}Cs contamination detected at 84 ft was probably carried down during drilling activities or migrated down the inside and/or outside of the casing and was removed from the SGLS data set used to create the visualizations.

Borehole 50-11-08

The ^{137}Cs contamination detected between the ground surface and 0.5 ft probably resulted from one or more surface spills that migrated down into the backfill material. The ^{137}Cs contamination detected at 10.5 ft and at 13.5 ft was probably carried down during drilling activities or migrated down the inside and/or outside of the casing and was removed from the SGLS data set used to create the visualizations.

Borehole 50-11-10

The ^{137}Cs contamination detected between the ground surface and 2.5 ft probably resulted from one or more surface spills that migrated down into the backfill material. No revisions were made to the SGLS data.

Borehole 50-11-11

The ^{137}Cs contamination detected between the ground surface and 13.5 ft probably resulted from one or more surface spills that migrated down into the backfill material. No revisions were made to the SGLS data.

Borehole 50-00-06

The ^{137}Cs contamination detected from 0.5 to 2 ft probably resulted from one or more surface spills that migrated down into the backfill material. The ^{137}Cs contamination detected between 111 and 145 ft was probably carried down during drilling activities or migrated down the inside and/or outside of the casing and was removed from the SGLS data set used to create the visualizations.

8.7.12 Boreholes Associated with Tank T-112

Borehole 50-12-05

The ^{137}Cs contamination detected between the ground surface and 19.5 ft is probably surface contamination that was carried down during drilling activities or migrated down the inside and/or outside of the casing and was removed from the SGLS data set used to create the visualizations.

Borehole 50-12-07

The ^{137}Cs contamination detected between the ground surface and 6 ft probably resulted from one or more surface spills that migrated down into the backfill material. The zone of slightly elevated ^{137}Cs contamination detected from 14.5 to 20 ft may be the result of further migration of contamination through the backfill material. The ^{137}Cs contamination detected below these zones (from 6.5 to 14 ft and from 20.5 to 24.5 ft) was probably carried down during drilling activities or migrated down the inside and/or outside of the casing and was removed from the SGLS data set used to create the visualizations.

Borehole 50-12-10

The ^{137}Cs detected at the ground surface is probably related to direct radiation from surface contamination and was removed from the SGLS data set used to create the visualizations.

Borehole 50-00-08

The ^{137}Cs contamination detected between the ground surface and 0.5 ft probably resulted from one or more surface spills that migrated down into the backfill material. The ^{137}Cs contamination detected at 75 ft was probably carried down during drilling activities or migrated down the inside and/or outside of the casing and was removed from the SGLS data set used to create the visualizations.

9.0 Development of the Visualizations

9.1 Introduction

An objective of this characterization project is to create visualizations of the major contamination plumes within the three-dimensional space that constitutes the vadose zone in the T Tank Farm and present those visualizations in this report. Because ^{137}Cs, ^{60}Co, and ^{154}Eu were the major contaminants in the T Tank Farm vadose zone, only these radionuclides were analyzed with the software and are depicted in the three-dimensional visualizations.

Creating the visualizations required developing geostatistical models of the ^{137}Cs, ^{60}Co, and ^{154}Eu distributions. The contamination models are considered to be empirical models, as contrasted with conceptual models or models developed from predicted calculations (e.g., contaminant transport calculations). The contaminant models are considered empirical models because they are based on data obtained by measuring the ^{137}Cs, ^{60}Co, and ^{154}Eu concentrations at discrete points in the subsurface.

The geostatistical models were developed only for the purpose of creating the visualizations of the ^{137}Cs, ^{60}Co, and ^{154}Eu distributions in the T Tank Farm. These empirical models are not intended to be used for quantitative calculations because of unavoidable limitations in the current geostatistical model, (i.e., the areal distribution of boreholes within the tank farm). The models are adequate to visually represent the contaminant distributions on a large scale. Future assessments may help to refine current model and describe the geostatistical structure of the data.

For each contaminant (^{137}Cs, ^{60}Co, and ^{154}Eu), a rudimentary geostatistical model was used in a process called "kriging" to estimate the grade or contaminant concentration at points on a three-dimensional grid. Once this concentration grid was developed, visualizations of the estimated concentration of each radionuclide could be produced that resulted in a solid surface model of the contamination. The visualization can be moved, rotated, and viewed from any angle or direction, and color pictorials of the visualization can be produced.

The software package from C Tech Development Corporation called "Environmental Visualization System" (EVS) was used to create the visualizations. Journel and Huijbregts (1978) and David (1977) explain the theory and application of geostatistics.

The radionuclide concentration data that constitute the SGLS data reported in the Tank Summary Data Reports for the T Tank Farm were placed in data files that defined the position in space of each data sample point and the nuclide-specific concentration for that point. The data file for ^{137}Cs was edited as described in Section 8.6, "Interpreted Data Sets," to remove intervals of contamination judged to be non-representative of contamination distribution in the formation, and the visualizations are based on these revisions to the SGLS radionuclide concentration data.

9.2 Geostatistical Structural Model

The EVS software determines a best fit of the geostatistical structure by calculating three-dimensional variograms which are plots of the variance of the data as a function of the distance between data points. A variogram is a basic geostatistical tool that describes the spatial correlation of data within a spatial domain (in this report the domain is the portion of the T Tank Farm vadose zone defined by the horizontal and vertical extents of the monitoring boreholes). The variogram is described by two parameters, the range and sill. The range is the distance beyond which the data points are no longer correlated (i.e., they are independent of one another), and the sill is the variance of all the data used in the variogram development.

For the T Tank Farm, the data did not show any significant decrease in variance as the data point-spacing decreased. This implies that spatial correlation is poor, and that more closely spaced data points are required to assess spatial variability. As a result, the geostatistical model takes on the form of the simple global variance value.

The total data domain of the calculations included all vadose zone boreholes within the T Tank Farm. The domain of the T Tank Farm was extended in the north-south and east-west directions to include the maximum and minimum borehole coordinate values. Borehole depths were converted to elevations, and the vertical parameter of the domain was set to include the highest and lowest sample points.

9.3 Three-Dimensional Plume Calculation and Visualizations

The kriging process calculates the average radionuclide concentrations of a volume of sediment by using the information from nearby sample points. The influence of each sample point is determined by proximity.

The kriging software applies a horizontal-to-vertical anisotropy ratio that allows the user to apply effects of anisotropy in the conductivity of soil matrices in fluid flow. The anisotropy ratio applies a biased weighting to data points in horizontal and vertical directions from a given data node. The program default is 10, which means that data points a given distance in the horizontal direction from a node will have an influence 10 times greater than data points at the same distance in a vertical direction. Analyses were performed at several anisotropy values for ^{137}Cs, ^{60}Co, and ^{154}Eu. Through trial and error, it was determined that an anisotropy value of 1 yielded results that best represented the measured ^{137}Cs distributions and an anisotropy of 10 yielded results that best represented the measured ^{60}Co and ^{154}Eu distributions.

For the three contaminants of interest (^{137}Cs, ^{60}Co, and ^{154}Eu) the MDL was generally on the order of 0.1 pCi/g. In the preprocessing module, a value of 0.01 pCi/g was substituted for non-detects in the data file. This allowed the presence of non-detects in the data set to have an impact on computation of nodal values during the kriging process. During post-processing, values less than 0.1 pCi/g were ignored.

In boreholes 50-01-04, 50-06-04, 50-06-05, 50-06-06, 50-06-08, 50-06-16, 50-06-17, and 50-06-18, detector saturation occurred over extended intervals of 5 to 50 ft and reliable concentration values could not be calculated from the data acquired within these intervals. Concentration values of 9,900 pCi/g (the approximate concentration of the highest reliable assay) were assumed for these intervals in the kriging operations.

The grids are constructed to encompass all data points in three-dimensional space. The horizontal extent of the grid is governed by the positions of the boreholes. The model does not extrapolate beyond the extent of either the range value or the kriging limit. As a result, both the grid and the associated visualizations can extend only to the maximum depth of the boreholes and the extent of the range.

In the visualization process, solid surfaces are created by connecting the three-dimensional points in space that have equal concentrations. The outermost solid surface of the plume is defined by a user-selected isolevel. To view an inner surface, a cut section is inserted through the solid surface plume. As the isolevel is increased, progressively higher radionuclide concentration surfaces can be visualized. Where a low concentration volume surrounds a zone of higher concentration, a cut surface is helpful in visualizing the variation in concentration.

Tanks were portrayed by creating solid three-dimensional surfaces at the location of the tank centers. In regions occupied by tanks, the model does not insert a contamination barrier so that contamination in a borehole can have some influence on concentrations on the opposite side of the tank. In a geostatistical estimation calculation, the closest boreholes will have the greatest influence and the model will be close to the actual distribution, except for areas where there are few or no boreholes.

9.4 Potential Uncertainties and Inaccuracies

The visualizations presented in this report are based on estimated ^{137}Cs, ^{60}Co, and ^{154}Eu concentrations determined by geostatistical estimation (kriging) procedures. In addition to the uncertainty associated with geostatistical estimation, there are other sources of uncertainty that must be considered. These include uncertainties in the assay calculation process as well as counting error. The uncertainty in assay calculation is discussed in the base calibration report (DOE 1995a) and subsequent recalibration reports. It is estimated by combining errors associated with the calibration efficiency determination, counting statistics of the calibration measurements, and uncertainties in the model concentration values. The counting error is associated with the random nature of the radioactive decay process.

Potential model inaccuracies are may also result from zones of high ^{137}Cs concentrations (and resultant detector saturation). Values of 9,900 pCi/g were entered into the concentration database for all 0.5-ft intervals within the each zone where detector saturation occurred. This method introduces a bias in the estimation results because actual concentrations in these areas may be considerably higher.

The calibration of the logging system assumes contamination uniformly distributed in a homogeneous medium that is effectively infinite in extent relative to the detector in both horizontal and vertical directions. This assumption is valid for most situations except at the very top and the bottom of the boreholes or where the concentration changes rapidly with depth or distance from the borehole. The data acquisition interval used to log the T Tank Farm boreholes (0.5 ft) provides adequate spatial resolution to characterize the situations where the contamination is not homogeneous in the vertical dimension. Contamination-zone edge effects can be removed if desired by spatial deconvolution methods described by Conaway and Killeen (1978). Changes in concentration with distance from the borehole may be identified by shape factor analysis under favorable conditions.

Near the ground surface, the source distribution is no longer an infinite medium; the inaccuracies associated with that distribution are discussed in Section 8.2, "Direct Gamma Radiation and Gamma-Ray Attenuation."

At the bottom of some of the boreholes, the lower end of the probe may come in direct contact with contaminated material that migrated down the inside of the borehole casing. Gamma rays emitted from these materials are not attenuated by the casing, but a casing attenuation factor is applied to the log data during processing. Therefore, the reported apparent concentrations at the bottom of the hole may be slightly high. ^{137}Cs contamination at the bottoms of boreholes that was interpreted to have resulted from migration down the inside of the casing was removed from the data to prevent creation of false plumes.

All of the above inaccuracies or errors in the visualizations are insignificant compared to the inaccuracy caused by the introduction of contamination along the borehole and the generation of so-called false plumes. However, the potential for the generation of a false plume from contaminated boreholes is considered during the interpretation process and is discussed in Section 10 of this report.

The visualizations are intended to provide the reader with an understanding of how the contamination from gamma-emitting contaminants that has leaked from the tanks may be distributed in the vadose zone sediments. They can also provide an assessment of the extent to which operations have contributed to contaminant distribution. A valuable attribute of the visualizations is that they can be utilized to define areas of concern that may be the subject of future comprehensive and more quantitative characterizations.

The ^{137}Cs, ^{60}Co, and ^{154}Eu contamination plumes presented in the visualizations were evaluated by comparing the visualizations with the spectral gamma-ray log data from the individual monitoring boreholes surrounding the tanks. The interpretation of each plume or group of plumes is discussed in Section 10.2, "Tank-by-Tank Discussion," where potential problems with each plume are also discussed.

10.0 Discussion of Results

The following sections present the results of the visualizations that were created with the data acquired from the T Tank Farm boreholes. The visualizations are provided in Section 14.0, "Figures," in the order in which they are discussed.

The background tank information regarding depth references for waste levels that is presented in the following sections was derived from illustrations and measurements provided in Brevick et al. (1995). Measurements that are reported in these documents, as well as those stated in Hanlon (1999), are relative to the top of the steel liner surface at the tank bottom. Estimated waste levels relative to the tank bases were derived from drawings presented in Brevick et al. (1995) and assumed a tank base thickness (liner and concrete) of 1 ft.

Figures 14-24 through 14-32 illustrate the man-made radionuclides that were identified during the course of the SGLS logging (^{137}Cs, ^{60}Co, ^{154}Eu, ^{152}Eu, ^{238}U, ^{235}U, ^{126}Sn, ^{94}Nb, and ^{125}Sb) as determined in the interpreted data set for all boreholes logged in the T Tank Farm. These figures show the 0.5-ft assays as spheres that are colored and sized to show the relative radionuclide concentration, and also indicate the spatial position at which the assays were acquired. The concentrations are presented with logarithmic color scales that range from 0.1 to as high as 10,000 pCi/g. The scales of the color bars were chosen for ease of estimating concentrations on a logarithmic scale, and sometimes the scale minimum value for a particular radionuclide may be lower than the MDL of the nuclide. The borehole identifications are indicated to facilitate correlation of the three-dimensional representation of the data in Figures 14-24 through 14-32 with the plan plot in Figure 14-17 and the correlation plots of the man-made radionuclides that are presented in Appendix B. The ^{137}Cs, ^{60}Co, and ^{154}Eu contamination intervals depicted in these figures were used to develop the geostatistical models and these figures can be compared directly with the contaminant plumes produced with the visualization software. A geostatistical model was not developed for the ^{152}Eu isotope because the ^{152}Eu isotope is chemically identical to and always associated with the ^{154}Eu isotope; both isotopes exhibit the same chemical characteristics in an unsaturated medium, and the ^{152}Eu contamination generally occurs at much lower concentrations than the ^{154}Eu within the vadose zone sediments. Essentially, the ^{154}Eu isotope provides the best representation of the nature and extent of europium contamination within the vadose zone. Because the ^{238}U, ^{235}U, ^{126}Sn, ^{94}Nb, and ^{125}Sb detected by the SGLS occurred in limited and isolated occurrences, these radionuclides were not modeled.

10.1 Radionuclide Contaminant Distribution

Figures 14-33 through 14-40 show horizontal planar slices at various depths in the T Tank Farm. The slices illustrate the distribution of radionuclide contaminants (^{137}Cs, ^{60}Co, and ^{154}Eu) that occur at concentrations greater than 0.2 pCi/g.

Figure 14-33, which is slice at a depth of 5 ft below the ground surface of the T Tank Farm, shows the ^{137}Cs contamination at this depth is present primarily in the central and eastern portions of the tank farm at concentrations ranging from 1 to 200 pCi/g. The maximum near-

surface ^{137}Cs contamination occurs in the east central portion of the tank farm between tanks T-104 and T-107. Figure 14-34, which is a slice at a depth of 10 ft below the ground surface, shows that the areal distribution of the ^{137}Cs contamination has decreased by more than half and the concentrations have also decreased. The ^{137}Cs contamination shown in Figures 14-33 and 14-34 is attributed to surface spills that have migrated downward into the backfill material surrounding the tanks. Figure 14-35, which is a slice at a depth of 18 ft, shows that most of the subsurface contamination resulting from surface spills has diminished and is isolated to the areas between tanks T-104 and T-107 and near tank T-106.

Figure 14-35 also shows ^{137}Cs contamination between tanks T-101 and T-102 and more highly concentrated ^{137}Cs contamination along the southeast side of tank T-101. Figure 14-36, which is a slice at a depth of 26 ft, shows the ^{137}Cs contamination near tanks T-101 and T-102 that was evident in Figure 14-35, but also shows a region of ^{60}Co and ^{154}Eu contamination along the southeastern side of tank T-103. The contamination detected within this depth interval probably originated from tanks T-101, -102, and -103, which are part of a cascade series. Between 1969 and 1973, these tanks were frequently filled beyond their design capacities, resulting in leakage from the spare fill lines located on the southeast side of each tank. The ^{137}Cs contamination detected between tanks T-101 and T-102 may also be the result of a leak from the cascade line connecting the two tanks (DOE 1999c).

Figure 14-37, which is a slice at a depth of 43 ft (the approximate depth of the base of the tanks), shows the contamination associated with the spare fill-line leaks from tanks T-101, -102, and -103. The ^{137}Cs contamination on the southeast side of tank T-101 has increased significantly in concentration. Low concentrations of ^{60}Co contamination are present at this depth between tanks T-101 and T-102; it appears that the ^{137}Cs contamination that was present in this area at a depth of 26 ft (Figure 14-36) has migrated southwestward along the base of the tank farm excavation and resides between tanks T-102 and T-105. The ^{60}Co and ^{154}Eu contamination along the southeastern side of tank T-103 has spread laterally to the southeast. Peak concentrations of these contaminants occur between 36 and 40 ft, suggesting that some of the contamination has accumulated near the base of the tank farm excavation (DOE 1999d). A broad area of highly concentrated ^{137}Cs contamination surrounds the southeast and southwest quarters of tank T-106. Smaller areas of ^{60}Co and ^{154}Eu contamination occur at this depth along the east and southwest sides of tank T-106 at much lower concentrations. The ^{137}Cs, ^{60}Co, and ^{154}Eu contamination is the result of the T-106 tank leak that occurred in 1973 (DOE 1999g). Zones of extremely high gamma radiation were encountered within most of the boreholes that intercepted the main portion of the contaminant plume from the T-106 tank leak and within the borehole that intercepted the contamination from the T-101 spare fill-line leak. The intensity of this radiation caused the SGLS detector to saturate during the logging of these zones, yielding no usable spectral data. However, historical gross gamma-ray data collected using a less sensitive Geiger-Mueller detector provided a representative profile of the highly contaminated regions around each borehole where the SGLS detector saturation occurred. On the basis of the rate of decrease in historical gross gamma activity, it is postulated that ^{137}Cs is the dominant radionuclide present in these intervals. Assumed values of 9,900 pCi/g (the approximate concentration of the highest reliable assay above and below the zone of detector saturation) were entered into the

concentration database for all 0.5-ft intervals within each zone of detector saturation. Actual concentrations are much higher.

Figure 14-38, which is a slice at a depth of 53 ft (approximately 10 ft below the base of the tanks), shows the increasing lateral spreading of the ^{60}Co and ^{154}Eu contamination related to the T-106 tank leak. The lateral extent of the ^{137}Cs contamination at this depth is somewhat reduced and concentrations have diminished within portions of the plume. The ^{60}Co and ^{154}Eu plume resulting from the T-103 spare fill-line leak appears to have merged with the T-106 leak plume. The low concentrations of ^{60}Co contamination between tanks T-102 and T-105 represent a remnant plume that probably resulted from a cascade line leak or a spare fill-line leak from tank T-102. The area of ^{60}Co and ^{154}Eu contamination between tanks T-101 and T-104 is probably related to the T-101 spare fill-line leak.

Figure 14-39, which is a slice at a depth of 72 ft, shows the lateral extent of the ^{137}Cs contamination related to the T-106 tank leak has decreased slightly but concentrations remain high within the remaining portions of the plume. The size and distribution of the ^{137}Cs contamination related to the T-101 spare fill-line leak remain unchanged. The extent of the ^{137}Cs plume on the southeast side of T-101 is poorly defined because there are relatively few data points in this area. Figure 14-39 also shows the maximum lateral extent of the ^{60}Co and ^{154}Eu contamination related to the T-106 tank leak. Because a portion of the ^{60}Co contamination was obscured by the ^{154}Eu contamination on the visualization, Figure 14-40 was generated to show the distribution and relative concentrations of ^{60}Co that were not visible on Figure 14-39. The ^{60}Co and ^{154}Eu contamination appear to have migrated laterally northward below most of tank T-106, westward to or beyond the western edge of the tank farm perimeter, southward below the northern and northwestern regions of tanks T-108 and T-109, and probably eastward below the western region of tank T-105. The ^{60}Co contamination has migrated further laterally than the ^{154}Eu contamination, extending southward beyond the southern end of tank T-108 and eastward below the southern and eastern portions of tank T-105. The ^{60}Co contamination that extends from the area between tanks T-101 and T-104 southwestward to the eastern side of tank T-105 most likely resulted from the T-101 spare fill-line leak. However, it is also possible that the some of ^{60}Co contamination detected between tanks T-104 and T-105 may represent the outer edge of the ^{60}Co plume that originated from the T-106 tank leak (DOE 1999e).

10.2 Tank-by-Tank Discussion

Figures 14-41 through 14-56 are three-dimensional visualizations that illustrate the major contamination plumes within the vadose zone of the T Tank Farm. These figures are discussed in detail in the following section.

The isolevel value applied to the visualization of a particular radionuclide indicates the lowest concentration of that radionuclide represented on the visualization. An isolevel value of 0.5 pCi/g was applied to the majority of visualizations presented in this report. However, to more clearly define the magnitude and extent of the relatively less concentrated ^{137}Cs and ^{60}Co contamination associated with tank T-102, an isolevel of 0.3 pCi/g was applied to the visualizations presented in Figures 14-49, 14-50, and 14-51.

Figures 14-41 through 14-44 show the plumes created with the EVS software superimposed over the SGLS data from the interpreted data set. In these four figures, the plumes are presented with a degree of transparency to view the SGLS data that define the plumes. Figures 14-41 and 14-42 show the distribution of the ^{137}Cs contamination viewed from below the tank farm from the southeast and from above the tank farm from the northwest, respectively. Figures 14-43 and 14-44 show the distribution of the ^{60}Co and ^{154}Eu contamination, respectively. In both figures, the contamination is viewed from below the tank farm from the southeast.

Figures 14-45 through 14-48 show different combinations of contaminant plumes in the T Tank Farm. Figures 14-45 and 14-46 show the distribution of the ^{137}Cs and ^{60}Co contamination; these views are from below the tank farm from the southeast from above the tank farm from the northwest, respectively. Figures 14-47 and 14-48 show the distribution of the ^{137}Cs and ^{154}Eu contamination; these views are also from below the tank farm from the southeast and from above the tank farm from the northwest, respectively.

Figure 14-49 is a visualization of the ^{137}Cs contamination in the vicinity of tanks T-101, T-102, and T-103, viewed from below the tanks from the south-southwest. Portions of the ^{137}Cs plumes in this region were cut by an east-west-trending vertical plane on the south side of these tanks to expose a cutaway view of the plume interiors. The ^{137}Cs plumes were superimposed over the SGLS data from the interpreted data set and are depicted with a degree of transparency to view the SGLS ^{137}Cs data that define the plumes.

Figures 14-50 and 14-51 are visualizations of the ^{137}Cs and ^{60}Co contamination and the ^{137}Cs and ^{154}Eu contamination, respectively, in the vicinity of tanks T-101, T-102, and T-103, viewed from below the tanks from the south-southwest. In each figure, the ^{137}Cs plumes were cut by an east-west-trending vertical plane on the south side of the tanks to expose a cross-sectional view of the relative ^{137}Cs concentrations detected around these tanks. The ^{60}Co plumes shown in Figure 14-50 and the ^{154}Eu plumes shown in Figure 14-51 were also cut by an east-west-trending vertical plane on the south side of the tanks to expose a cutaway view of the plume interiors. The respective plumes in each figure were superimposed over the representative SGLS data from the interpreted data set so that some of the SGLS data can be viewed through the cutaway portions of each plume.

Figure 14-52 is a visualization of the ^{137}Cs plume in the vicinity of tanks T-103, T-106, and T-109, viewed from below the tanks from the southeast. The ^{137}Cs plume was cut by a north-south-trending vertical plane on the east side of these tanks to expose a cutaway view of the plume interior. The ^{137}Cs plume was superimposed over the SGLS data from the interpreted data set; the plume is depicted with a degree of transparency to view the SGLS ^{137}Cs data that define it.

Figures 14-53 and 14-54 are visualizations of the ^{137}Cs and ^{60}Co contamination and the ^{137}Cs and ^{154}Eu contamination, respectively, in the vicinity of tanks T-103, T-106, and T-109, viewed from above the tanks from the southeast. In each figure, the ^{137}Cs plume was cut by north-south and east-west-trending vertical planes very close to the perimeter of tank T-106 to expose the region

of the ^{137}Cs contamination closest to the suspected leak source. The ^{60}Co plumes shown in Figure 14-53 and the ^{154}Eu plumes shown in Figure 14-54 were cut by a north-south-trending vertical plane on the east side of the tanks to expose a cutaway view of the plume interior. The respective plumes in each figure were superimposed over the representative SGLS data from the interpreted data set so that some of the SGLS data can be viewed through the cutaway portions of each plume.

Figures 14-55 and 14-56 are visualizations of the ^{137}Cs and ^{60}Co contamination and the ^{137}Cs and ^{154}Eu contamination, respectively, in the vicinity of tanks T-103 and T-106, viewed from above the tanks from the southeast. In each figure, the ^{137}Cs plume and the $^{60}Co/^{154}Eu$ plumes were cut by north-south and east-west-trending vertical planes very close to the perimeter of these tanks to expose a cross-sectional view of the relative contaminant concentrations in the immediate vicinity of suspected leak sources (i.e., the T-106 tank leak and the T-103 spare fill-line leak).

The visualizations that best portray the contaminant distribution around each tank will be discussed in the following subsections.

10.2.1 Tank T-101

Tank T-101 was placed into service in December 1944. The waste types contained in tank T-101 throughout its service life are summarized in Table 1, "General Waste Information, T Tank Farm." The tank was sluiced for recovery of metal waste in 1953 and again in 1956. Tank T-101 was removed from service in 1979 (DOE 1999b).

An unplanned release occurred in early 1969 when the tank was overfilled (539,000 gal) and an undetermined amount of tank waste overflowed to the soil column through a spare fill line (DOE 1999b).

In February 1975, an occurrence report (Jensen 1975a) documented a 0.5-in. decrease in the in-tank liquid level. The liquid-level decrease occurred after a 15-in. waste transfer was added to the tank. The in-tank waste volume at the time consisted of approximately 160,000 gal of liquid and 60,000 gal of sludge. The occurrence report concluded that the liquid-level decrease was caused by a dissipating crust surface or foam following the waste transfer rather than a tank leak (Jensen 1975a).

In October 1992, another occurrence report (Deaton 1992) documented a 2.6-in. decrease in the in-tank liquid level that occurred over a 2-month period from July to September 1992. Deaton (1992) postulates that corrosion caused the carbon steel liner to fail and the tank to leak. The liquid loss was reconciled as a leak to the vadose zone sediments even though no contamination was detected around the monitoring boreholes surrounding the tank.

Tank T-101 was classified as an assumed leaker in October 1992, solely on the basis of the observed in-tank liquid-level decrease that occurred from July to September 1992. The estimated total leak volume was 7,500 gal. As a result of the suspected leak, an emergency pumping

initiative transferred 25,300 gal of waste from the tank in late March 1993. The tank was interim stabilized in April 1993 (DOE 1999b).

Tank T-101 presently contains an estimated 102,000 gal of non-complexed waste that includes 101,000 gal of sludge, 1,000 gal of supernatant liquid, and 16,000 gal of drainable interstitial liquid within the sludge matrix (Hanlon 1999). The surface level of the waste in tank T-101 is approximately 3 ft above the center of the tank bottom (DOE 1999b).

Six boreholes exist around tank T-101 for vadose zone monitoring (see Figure 14-17). Boreholes 50-01-02, 50-01-04, 50-01-06, 50-01-09, 50-01-12, and 50-00-03 were drilled in 1973 to depths of 94 ft, 123 ft, 94 ft, 96 ft, 92 ft, and 148 ft, respectively. All the monitoring boreholes for tank T-101 were logged with the SGLS, and a correlation plot showing the man-made contaminant distributions in these boreholes is provided in Appendix B. Details regarding the borehole construction configurations, the logging operations performed, and the data acquired from each borehole are presented in the Tank Summary Data Report for tank T-101 (DOE 1999b).

Figures 14-41, 14-42, and 14-49 show the ^{137}Cs contamination in the vicinity of tank T-101. Figure 14-41 is a visualization of the T Tank Farm viewed from below the tanks from the southeast, Figure 14-42 is a visualization of the T Tank Farm viewed from above the tanks from the northwest, and Figure 14-49 is a visualization in the vicinity of tanks T-101, T-102, and T-103 viewed from below the tanks from the south-southwest. These figures show minor amounts of near-surface and shallow subsurface ^{137}Cs contamination in the vicinity of this tank, probably associated with surface spills or leaks that migrated into the backfill sediments. Some of this ^{137}Cs contamination may have also been carried down during drilling.

Zones of extremely high gamma radiation were encountered between 20 and 70 ft in borehole 50-01-04, which is located near the southeast side of tank T-101 (see Figure 14-17). The intensity of this radiation caused the SGLS detector to saturate during the logging of these zones, yielding no usable spectral data. However, based upon the rate of decrease of the historical gross gamma activity, it was determined that ^{137}Cs is the predominant radionuclide present in these intervals. Futhermore, high concentrations of ^{137}Cs were detected above and below the zones of detector saturation. In cases where a zone of detector saturation was encountered, ^{137}Cs concentration values of 9,900 pCi/g (the approximate concentration of the highest reliable ^{137}Cs assay above and below the zone of detector saturation) were placed into the database in these intervals to create the visualizations.

Figures 14-41, 14-42, and 14-49 show the ^{137}Cs contamination detected in borehole 50-01-04 as a vertically continuous plume that extends from 20 ft to the bottom of the logged interval (122.5 ft). However, there is no geostatistical structure defining the spatial distribution of the ^{137}Cs contamination shown on the visualizations around borehole 50-01-04. As a result, the volume of the contamination and the accuracy of the visualization in this region are unknown. This contamination is probably the result of a large volume of contamination that leaked to the soil column between 1968 and 1969, when the tank was overfilled during tank farm operations. Previous investigations have suggested the spare fill lines associated with tank T-101 are the

probable source of the leak. The maximum vertical extent of the plume has not been determined because very high concentrations of ^{137}Cs contamination extend to the bottom of the logged interval (DOE 1999b).

A large ^{60}Co and ^{154}Eu plume was identified around borehole 50-01-06 located between tanks T-101 and T-104. Figures 14-43, 14-45, 14-46, and 14-50 show the magnitude and extent of the ^{60}Co contamination; Figures 14-44, 14-47, 14-48, and 14-51 show the magnitude and extent of the ^{154}Eu contamination. Figures 14-43, 14-44, 14-45, and 14-47 are visualizations of the T Tank Farm viewed from below the tanks from the southeast. Figures 14-46 and 14-48 are visualizations of the T Tank Farm viewed from above the tanks from the northwest. Figures 14-50 and 14-51 are visualizations in the vicinity of tanks T-101, T-102, and T-103, viewed from below the tanks from the south-southwest. A 1975 investigation inferred that this plume originated from the direction of borehole 50-01-04, located near the southeast side of tank T-101 (Jensen 1975b), suggesting a leak from the spare fill lines associated with tank T-101 is the probable source of the contamination. More of this plume may be identified by deep ^{60}Co contamination detected west of tank T-104 around boreholes 50-04-08 and 50-04-10 (see Figure 14-17). Historical gross gamma data suggest that the ^{60}Co may have migrated laterally in a southwesterly direction from borehole 50-01-06 to 50-04-10 to 50-04-06 between 1973 and 1976. However, this does not rule out the possibility that the contamination detected around boreholes 50-04-08 and 50-04-10 may represent the outer edge of the ^{60}Co plume that originated from the T-106 tank leak. It is also possible that the ^{60}Co contamination originated from both sources (DOE 1999e).

The ^{137}Cs plume shown near the southeast side of T-101 is based primarily on data from borehole 50-01-04. The drilling log from 1973 was available for the interval from 47 to 87 ft; no radioactivity measurements are noted. However, Welty (1988) reports high levels of gamma activity from 20 ft to 87 ft (total depth) in the earliest available log data from 1973. The drilling log from the 1981 extension indicates that radioactivity was encountered in the sediment samples from 90 ft to at least 115 ft. Although the possibility exists that the borehole may have acted as a conduit and the observed contamination is highly localized, it appears likely that the contamination detected in borehole 50-01-04 was present prior to 1973, and that the plume shown in the visualizations is essentially correct. Boreholes 50-00-03 and 50-04-03 encountered low levels of ^{137}Cs at depth that were not included in the visualizations. Although these intervals are interpreted to be dragdown and/or borehole contamination, it is possible they represent the periphery of a plume emanating from the southeast side of T-101.

10.2.2 Tank T-102

Tank T-102 was placed into service in September 1945. The waste types contained in tank T-102 throughout its service life are summarized in Table 1. The tank was sluiced for recovery of metal waste in 1953 and again in 1956. Tank T-102 was removed from service in 1976 and was salt-well pumped from 1977 to 1978. The tank was administratively interim stabilized in March 1981, although the exact meaning of "administratively interim stabilized" is not known (DOE 1999c).

An unexplained in-tank surface-level increase that occurred in early 1979 was confirmed using several in-tank photographs taken between mid-1979 and late 1983. The suspected liquid-level increase was investigated and reported to be the result of rain water from periods of greater than normal rainfall (Dickman 1983). This water entered the tank via an unknown pathway.

Tank T-102 is categorized as sound and presently contains a total of 32,000 gal of non-complexed waste that includes 19,000 gal of sludge and 13,000 gal of supernatant liquids (Hanlon 1999). The surface level of the waste in tank T-102 is less than 1 ft above the center of the tank bottom (DOE 1999c).

Nine boreholes exist around tank T-102 for vadose zone monitoring (see Figure 14-17). Boreholes 50-02-02, 50-02-05, 50-02-08, 50-02-09, 50-02-10, 50-02-12, and 50-00-12 surround tank T-102 and were drilled in 1973 and 1974 to depths of 91 ft, 91 ft, 87 ft, 91 ft, 91 ft, 92 ft, and 151 ft, respectively. Borehole 50-01-09 is associated with tank T-101 and is discussed in Section 10.2.1. Borehole 50-05-11 is associated with tank T-105 and is discussed in Section 10.2.5. All of the monitoring boreholes for tank T-102 were logged with the SGLS, and a correlation plot showing the man-made contaminant distributions in these boreholes is provided in Appendix B. Details regarding the borehole construction configurations, the logging operations performed, and the data acquired from each borehole are presented in the Tank Summary Data Report for tank T-102 (DOE 1999c).

Figures 14-41, 14-42, and 14-49 show the ^{137}Cs contamination in the vicinity of tank T-102. Figure 14-41 is a visualization of the T Tank Farm viewed from below the tanks from the southeast, Figure 14-42 is a visualization of the T Tank Farm viewed from above the tanks from the northwest, and Figure 14-49 is a visualization in the vicinity of tanks T-101, T-102, and T-103 viewed from below the tanks from the south-southwest. Figures 14-42 and 14-49 show that only minor amounts of near-surface and shallow subsurface ^{137}Cs contamination exist in the vicinity of this tank. This contamination is probably associated with surface spills or leaks that migrated into the backfill sediments. Some of the ^{137}Cs contamination may have also been carried down during drilling.

^{137}Cs and ^{60}Co contamination was detected on the west side of tank T-101 around borehole 50-01-09 (see Figure 14-17) between 15 and 49 ft. This contamination was present in 1973 when the borehole was drilled and may be the result of a leak from the cascade overflow line connecting tanks T-101 and T-102. ^{137}Cs and ^{60}Co contamination was also detected on the southeast side of tank T-102 around borehole 50-02-05 (see Figure 14-17) between 38 and 73 ft. This contamination was present in 1974 when the borehole was drilled and may have resulted from a leak from the spare fill lines on the southeast side of the tank. Between 1969 and 1973, the tanks in the cascade series consisting of tanks T-101,-102, and -103 were occasionally filled beyond their design capacities of 530,000 gal. Tanks T-101 and T-103 are currently classified as assumed leakers, and there is strong evidence that suggests both tanks probably leaked from their spare fill lines. Because tank T-102 was part of the same cascade series and was operating under similar conditions during that time, it may also have leaked (DOE 1999c).

Figures 14-49 and 14-50 illustrate the magnitude and extent of the ^{137}Cs and ^{60}Co contamination, respectively, resulting from the suspected leaks described previously. Each figure is a visualization in the vicinity of tanks T-101, T-102, and T-103 viewed from below the tanks from the south-southwest.

Figure 14-49 shows an area of ^{137}Cs contamination between tanks T-101 and T-102 at a depth of about 20 ft. Figure 14-50 shows an area of deeper ^{60}Co contamination near the west side of tank T-101 at a depth of about 40 ft. The cascade overflow line connecting the tanks is the probable source of this contamination.

Figure 14-49 shows an area of ^{137}Cs contamination near the south side of the tank at a depth of about 40 ft. Figure 14-50 shows an area of ^{60}Co contamination located directly below the ^{137}Cs contamination. The ^{137}Cs and ^{60}Co contamination in these regions is probably the result of a leak from the T-102 spare fill lines. It appears that the ^{137}Cs contamination spread laterally to the south and west along the base of the tank farm excavation.

10.2.3 Tank T-103

Tank T-103 was placed into service in November 1945. The waste types contained in tank T-103 throughout its service life are summarized in Table 1. The tank was sluiced for recovery of metal waste in 1953 and again in 1955. During 1956, the supernatant was pumped from the tank and the remaining heel of sludge was sluiced. Intrusion prevention was completed for tank T-103 in August 1981. The tank was administratively interim stabilized in November 1983 (DOE 1999d).

In July and August 1973, several monitoring boreholes drilled near the southeast side of tank T-103 penetrated radioactive contamination. A subsequent investigation concluded that the contamination originated from a leak from a failed grout seal surrounding a spare fill line on the southeast side of the tank (ARH 1973). However, this fill line could only leak if the tank was overfilled. Welty (1988) reports the leakage occurred as a result of overfilling the tank. An examination of waste transaction records presented in Brevick et al. (1995) indicates this leakage probably occurred during the second quarter of 1973, when tank T-103 contained approximately 556,000 gal of liquid waste, which is about 26,000 gal more than the design capacity of the tank. The volume of the liquid lost during this leak was estimated by ARH (1973) to be on the order of 5 m^3 or 1,300 gal. However, the accuracy and precision of that estimate are not known.

Between November 1973 and February 1974, a liquid-level decrease in excess of 0.30 in. occurred, and tank T-103 was removed from service and declared an assumed leaker. Sample data collected from the tank in March and July 1974 indicate that the chemical contents of tank T-103 were primarily sodium nitrate and sodium nitrite, but the tank also contained significant quantities of plutonium, strontium, and cesium. Based solely on observed liquid-level decreases within the tank, Hanlon (1999) tentatively estimates the leak volume from tank T-103 to be less than 1,000 gal; however, this estimate probably does not include the volume of waste that leaked through the spare fill line, as discussed previously.

In March 1981, the liquid level within tank T-103 exceeded the established increase criterion (Lindsay 1981). The liquid-level increase was attributed to precipitation entering the tank through a pump pit (Welty 1988).

Tank T-103 is categorized as an assumed leaker and presently contains a total of 27,000 gal of non-complexed waste that includes 23,000 gal of sludge and 4,000 gal of supernate (Hanlon 1999). The surface level of the waste in tank T-103 is approximately 1.4 ft above the center of the tank bottom (DOE 1999d).

Eight boreholes exist around tank T-103 for vadose zone monitoring (see Figure 14-17). Boreholes 50-03-01, 50-03-04, 50-03-05, 50-03-06, 50-03-08, and 50-03-10 were drilled between 1973 and 1975 to depths of 92 ft, 123 ft, 123 ft, 123 ft, 91 ft, and 93 ft, respectively. Boreholes 50-02-08 and 50-02-10 are associated with tank T-102 and are discussed in Section 10.2.2. All of the monitoring boreholes for tank T-103 were logged with the SGLS, and a correlation plot showing the man-made contaminant distributions in these boreholes is provided in Appendix B. Details regarding the borehole construction configurations, the logging operations performed, and the data acquired from each borehole are presented in the Tank Summary Data Report for tank T-103 (DOE 1999d).

Figures 14-41, 14-42, 14-49, and 14-52 show the ^{137}Cs contamination in the vicinity of tank T-103. Figure 14-41 is a visualization of the T Tank Farm viewed from below the tanks from the southeast, Figure 14-42 is a visualization of the T Tank Farm viewed from above the tanks from the northwest, Figure 14-49 is a visualization in the vicinity of tanks T-101, T-102, and T-103, viewed from below the tanks from the south-southwest, and Figure 14-52 is a visualization in the vicinity of tanks T-103, T-106, and T-109, viewed from below the tanks from the southeast. These figures show that only minor amounts of near-surface and shallow subsurface ^{137}Cs contamination exist in the vicinity of this tank. This contamination is probably associated with surface spills or leaks that migrated into the backfill sediments. Some of the ^{137}Cs contamination may have also been carried down during drilling.

A distinct plume of radionuclide contamination was detected by the SGLS along the southeast and south sides of tank T-103 around boreholes 50-03-04, 50-02-08, 50-03-05, and 50-03-06. The contamination within this plume appears to be correlatable among these boreholes and is believed to be the result of the spare fill line leak on the southeast side of the tank described by ARH (1973). The primary constituents of the contaminant plume are ^{60}Co, ^{154}Eu, and ^{152}Eu. However, for reasons stated in Section 10.0, ^{152}Eu was not analyzed with the EVS modeling software. In one or more boreholes, occurrences of ^{94}Nb, ^{125}Sb, ^{126}Sn, and ^{238}U contamination were also detected within the main body of the plume; however, because the distribution of these contaminants was not extensive, they were also not analyzed with the EVS modeling software.

Figures 14-43, 14-50, 14-53, and 14-55 show the extent of the ^{60}Co contamination within the plume; Figures 14-44, 14-51, 14-54, and 14-56 show the extent of the ^{154}Eu contamination within the plume. Figures 14-43 and 14-44 are visualizations of the T Tank Farm viewed from below the tanks from the southeast. Figures 14-50 and 14-51 are visualizations in the vicinity of tanks

T-101, T-102, and T-103, viewed from below the tanks from the south-southwest. Figures 14-53 and 14-54 are visualizations in the vicinity of tanks T-103, T-106, and T-109, viewed from above the tanks from the southeast. Figures 14-55 and 14-56 are visualizations in the vicinity of tanks T-103 and T-106, viewed from above the tanks from the southeast.

The SGLS data collected from boreholes in the vicinity of the suspected leak indicate that the contaminant plume has migrated both downward and laterally away from the leak source. Fine-grained layers may exist within the Hanford formation and could possibly enhance the lateral spreading of the ^{60}Co and ^{154}Eu contamination within the plume (DOE 1999d). The visualizations portrayed in Figures 14-50 through 14-56 appear to illustrate that some of the ^{60}Co and ^{154}Eu contamination within the plume has migrated laterally to the south and has apparently intermingled with contamination resulting from the T-106 tank leak.

10.2.4 Tank T-104

Tank T-104 was placed into service in March 1946. The waste types contained in tank T-104 throughout its service life are summarized in Table 1. Tank T-104 was removed from service in 1976 and was primarily stabilized in 1978 following the completion of salt-well pumping. Tank T-104 is passively ventilated and has been partially interim isolated (DOE 1999e).

Pumping of the waste remaining in the tank T-104 resumed June 7, 1998, and is currently ongoing. Pumping operations during March 1999 required the addition of 4,087 gal of raw water to the tank. A total of 147,400 gal had been pumped from the tank as of the end of March 1999. Tank T-104 is classified as sound; however, interim stabilization has not yet been completed. The tank presently contains a total of 328,000 gal of non-complexed waste that consists of 328,000 gal of sludge and 31,000 gal of drainable, interstitial liquid within the sludge matrix (Hanlon 1999). The surface level of the waste in tank T-104 is approximately 14 ft above the center of the tank bottom (DOE 1999e).

Six boreholes exist around tank T-104 for vadose zone monitoring (see Figure 14-17). Boreholes 50-04-03, 50-04-05, 50-04-07, 50-04-08, and 50-04-10 were drilled in 1974 and 1975 to depths of 92 ft, 95 ft, 100 ft, 100 ft, and 93 ft, respectively. Borehole 50-01-06 is associated with tank T-101 and is discussed in Section 10.2.1. All the monitoring boreholes for tank T-104 were logged with the SGLS, and a correlation plot showing the man-made contaminant distributions in these boreholes is provided in Appendix B. Details regarding the borehole construction configurations, the logging operations performed, and the data acquired from each borehole are presented in the Tank Summary Data Report for tank T-104 (DOE 1999e).

Figures 14-41 and 14-42 show the ^{137}Cs contamination in the vicinity of tank T-104. Figure 14-41 is a visualization of the T Tank Farm viewed from below the tanks from the southeast and Figure 14-42 is a visualization of the T Tank Farm viewed from above the tanks from the northwest. These two figures show that a considerable amount of near-surface and shallow subsurface ^{137}Cs contamination exist in the vicinity of this tank. Figure 14-33, which is a horizontal planar slice at a depth of 5 ft below the ground surface of the T Tank Farm, shows that the maximum near-surface ^{137}Cs contamination occurs in the east central portion of the tank farm

between tanks T-104 and T-107. The near-surface and shallow subsurface ^{137}Cs contamination is probably associated with surface spills or leaks that have migrated as deep as 27 ft into the backfill sediments. Some of the ^{137}Cs contamination may have also been carried down during drilling.

A large ^{60}Co and ^{154}Eu plume was identified between tanks T-101 and T-104. This contamination is believed to have originated from a spare fill-line leak on the southeast side of tank T-101. Deep ^{60}Co contamination was detected in boreholes 50-04-08 and 50-04-10, located west of tank T-104 (see Figure 14-17). This contamination may demarcate the southernmost lateral extent of the ^{60}Co plume originating from a leak from tank T-101, or may demarcate the easternmost lateral extent of the ^{60}Co plume originating from the T-106 tank leak. It is also possible that the ^{60}Co contamination originated from both sources (DOE 1999e). A more detailed discussion of the origin of this contamination is provided in Section 10.2.1.

10.2.5 Tank T-105

Tank T-105 was placed into service in July 1946. The waste types contained in tank T-105 throughout its service life are summarized in Table 1. Tank T-105 was removed from service in 1976. The tank was administratively interim stabilized in June 1987 and intrusion prevention was completed in September 1988 (DOE 1999f).

Tank T-105 is categorized as sound and presently contains a total of 98,000 gal of non-complexed waste that includes 98,000 gal of sludge and 23,000 gal of drainable, interstitial liquid within the sludge matrix (Hanlon 1999). The surface level of the waste in tank T-105 is nearly 4 ft above the center of the tank bottom (DOE 1999f).

Six boreholes exist around tank T-105 for vadose zone monitoring (see Figure 14-17). Boreholes 50-05-06, 50-05-07, and 50-05-11 were drilled between 1973 and 1975 to depths of 87 ft, 120 ft, and 92 ft, respectively. Boreholes 50-05-06 and 50-05-11 were deepened between 1977 and 1981 to depths of 121.5 ft and 123 ft, respectively. In 1975, borehole 50-05-07 was backfilled with grout from 120 to 88 ft. Borehole 50-02-05 is associated with tank T-102 and is discussed in Section 10.2.2. Boreholes 50-04-08 and 50-04-10 are associated with tank T-104 and are discussed in Section 10.2.4. Borehole 50-06-03 is associated with tank T-106 and is discussed in Section 10.2.6. All the monitoring boreholes for tank T-105 were logged with the SGLS, and a correlation plot showing the man-made contaminant distributions in these boreholes is provided in Appendix B. Details regarding the borehole construction configurations, the logging operations performed, and the data acquired from each borehole are presented in the Tank Summary Data Report for tank T-105 (DOE 1999f).

Figures 14-41 and 14-42 show the ^{137}Cs contamination in the vicinity of tank T-105. Figure 14-41 is a visualization of the T Tank Farm viewed from below the tanks from the southeast and Figure 14-42 is a visualization of the T Tank Farm viewed from above the tanks from the northwest. Figure 14-42 shows a region of near-surface and shallow subsurface ^{137}Cs contamination around the southern half of this tank. This contamination is probably associated

with surface spills or leaks that have migrated as deep as 12 ft into the backfill sediments. Some of the ^{137}Cs contamination may have also been carried down during drilling.

Subsurface radionuclide contamination was detected in all of the boreholes surrounding tank T-105; however, it appears the contamination originated from adjacent tanks. ^{137}Cs and ^{60}Co contamination were detected around borehole 50-02-05 near the northeast side of the tank (see Figure 14-17). This contamination is interpreted to be the result of a spare fill-line leak from tank T-102 (DOE 1999c). A more detailed discussion of the origin of this contamination is provided in Section 10.2.2. Deep ^{60}Co contamination was detected in boreholes 50-04-08 and 50-04-10, located east of tank T-105 (see Figure 14-17). This contamination may represent the outer edge of the ^{60}Co plume that originated from the T-106 tank leak; however, it may have originated from tank T-101 (DOE 1999e). A more detailed discussion of the origin of this contamination is provided in Section 10.2.1. Deep ^{60}Co contamination was also detected in boreholes 50-05-06, 50-05-07, and 50-05-11, located on the south, southwest, and northwest sides of tank T-105, respectively (see Figure 14-17). This contamination most likely originated from the T-106 tank leak (DOE 1999f). A more detailed discussion of the origin of this contamination is provided in Section 10.2.6.

10.2.6 Tank T-106

Tank T-106 was placed into service in June 1947. The waste types contained in tank T-106 throughout its service life are summarized in Table 1. Tank T-106 was declared a confirmed leaker on June 8, 1973 (Freeman-Pollard et al. 1994) on the basis of observed decreases in the liquid level inside the tank and elevated radioactivity in borehole 51-08-11 (299-W10-51) in May and June 1973. The tank was removed from service and pumped to a minimum heel in June 1973. In July 1974, the tank was further pumped down to a residual layer of less than 6 in. Tank T-106 was interim stabilized and intrusion prevention was completed in August 1981 (DOE 1999g).

From in-tank liquid-level measurements, it was estimated that approximately 115,000 gal of liquid waste leaked from tank T-106 into the adjacent vadose zone sediments between April and June 1973. The liquid waste was estimated to contain 14,000 Ci of ^{90}Sr, 40,000 Ci of ^{137}Cs, 4 Ci of $^{239/240}Pu$, 267,000 Ci of ^{106}Ru, and about 3,000 Ci of radionuclides having half-lives of 3 years or less (Freeman-Pollard et al. 1994).

Shortly after the leak in the tank was confirmed, a total of 16 single-cased boreholes were installed between June and August 1973 to evaluate the conditions in the vadose zone beneath and in the vicinity of tank T-106. The results of this investigation were documented in a report prepared by Atlantic Richfield Hanford Company (ARH 1973). The report presents plume maps illustrating spatial distribution of ^{137}Cs, cerium-144 (^{144}Ce), and ^{106}Ru in the vadose zone around tank T-106. The results indicate that the deepest penetration of contamination was detected 87 ft below the ground surface, although the minimum detection level is not reported. The report concluded that further movement of the radioactivity from its present location would be negligible (ARH 1973).

Between 1973 and 1978, additional monitoring boreholes were installed and some existing boreholes were deepened in the vicinity of tank T-106. The boreholes were used to track the vertical and horizontal extents of the vadose zone contaminant plume associated with the tank leak. During this time, gross gamma-ray logs were routinely collected from all monitoring boreholes in the vicinity of tank T-106.

The 1978 status of the T-106 tank leak was summarized in a 1979 report prepared under Rockwell Hanford Operations (Routson et al. 1979). For this assessment, data from selected gross gamma-ray logs were used to delineate changes in the position of the leak boundary and to indicate the rate of radioactive decay of gamma-ray-emitting radionuclides in the leak plume area. In addition, in-situ measurements of gamma-emitting radionuclides were performed in existing boreholes using a borehole gamma energy analysis system, which provided information on the relative concentrations of ^{106}Ru, ^{144}Ce, ^{137}Cs, and ^{154}Eu. Sediment samples from new boreholes and boreholes that were deepened were also collected and analyzed for radionuclide content in the Rockwell Hanford Operations laboratory. The 1979 report concluded that the leak plume front moved horizontally between 1973 and 1974 but appeared to be relatively stationary from 1974 through 1978. The maximum penetration of waste (as defined by the 1 microcurie per liter [μCi/L] ^{106}Ru concentration) was 108 ft below the ground surface. On the basis of the known hydraulic properties of Hanford Site sediments at that time, the 1979 report concluded that it was unlikely that the leak would migrate through the unsaturated soils and reach the underlying aquifer during the "hazardous lifetime" of the radionuclides. However, the report did not consider the more mobile, long-lived radionuclides, such as ^{99}Tc (DOE 1999g) and it did not measure low concentrations of the less mobile radionuclides such as ^{137}Cs.

In 1989, the U.S. General Accounting Office (GAO) reviewed DOE's efforts to monitor the movement of leaked waste from SSTs and efforts to assess the environmental impacts of the leaks. As a result of this review, GAO recommended that DOE gather additional information to more accurately assess and evaluate risk of groundwater contamination resulting from SST leaks (GAO 1989). Upon completion of the 1989 GAO audit, DOE instructed Westinghouse Hanford Company (WHC) to perform additional soil characterization activities within the single-shell tank farms.

In 1992, tank T-106 was selected to undergo a limited vadose zone investigation in response to GAO audit finding GAO/RCED-89-157. The investigation was designed to fill in existing data gaps by providing current information on the nature and vertical extent of contaminant migration resulting from the T-106 tank leak. The field phase of the investigation consisted of drilling a telescoped cased borehole, identified in Figure 2 as borehole 50-06-18, to a depth of 180 ft. A total of 43 split-spoon soil samples were collected for chemical, radiological, and physical analysis. In addition, downhole spectral gamma-ray logging was performed eight times during borehole construction using the Radionuclide Logging System (RLS), which is the intrinsic germanium logging system that was the predecessor to the SGLS. The results of this investigation are presented in a 1994 report prepared by Bechtel Hanford, Inc. (Freeman-Pollard et al. 1994). On the basis of the soil sample and RLS data from this borehole, Freeman-Pollard et al. (1994) concluded that the waste from the 1973 T-106 tank leak is still confined to the

vadose zone and resides at least 69 ft above ground water (or 149 ft below the ground surface). Certain constituents in the leading edge of the plume have penetrated to the contact of the Ringold Unit E at 121 ft below the ground surface. In addition, ^{99}Tc contamination may have penetrated the upper portion of the Ringold Unit E to a depth of 145 ft, but the report contends that supporting data are ambiguous.

In 1997, PNNL conducted a Phase I, RCRA groundwater quality assessment for DOE under the requirements of the Hanford Federal Facility Agreement and Consent Order to determine if the Single-Shell Tank Waste Management Areas (WMAs) T and TX-TY have impacted groundwater quality. The results of that assessment are presented in a 1998 report prepared by PNNL (Hodges 1998).

Part of the Phase I assessment included the examination of contaminant patterns in monitoring well 299-W11-27, located immediately downgradient from the T Tank Farm. Hodges (1998) reports that drinking water standards in this well were exceeded for ^{99}Tc, tritium, nitrate, gross beta, and chromium. The largest exceedance was for ^{99}Tc, which was present at activity levels approximately 20 times the drinking water standard of 900 pCi/L. Cobalt was also recently detected in this well. On the basis of available evidence, Hodges (1998) concluded with a high degree of certainty that WMA T is the source of groundwater contamination in monitoring well 299-W11-27. Both contaminant chemistry and lack of lateral spreading in groundwater (dispersion) are indicative of a small volume, tank waste source within the tank farm (Hodges 1998). The study was not able to identify a specific tank as the source of the groundwater contamination.

Tank T-106 presently contains a total of 21,000 gal of non-complexed waste that includes 19,000 gal of sludge and 2,000 gal of supernate (Hanlon 1999). The surface level of the waste in tank T-106 is less than 6 in. above the center of the tank bottom (DOE 1999g).

Thirteen boreholes exist around tank T-106 for vadose zone monitoring (see Figure 14-17). Boreholes 50-06-02, 50-06-03, 50-06-04, 50-06-16, 50-06-05, 50-06-17, 50-06-06, 50-06-08, and 50-06-11 were drilled between 1973 and 1975 to depths of 92 ft, 100 ft, 93 ft, 126 ft, 94 ft, 122 ft, 100 ft, 92 ft, and 87 ft, respectively. Boreholes 50-06-02, 50-06-03, 50-06-05, 50-06-06, and 50-06-08 were deepened in 1977 to depths of 125 ft, 122 ft, 122 ft, 123 ft, and 123 ft, respectively. Boreholes 50-06-16 and 50-06-17 were backfilled with grout from 126 ft and 122 ft to 90 ft and 91 ft, respectively. Borehole 50-00-10 was drilled in 1944 to a depth of 150 ft; borehole 50-00-09 was drilled in 1977 to a depth of 122 ft; and borehole 50-06-18 was drilled in 1993 to a depth of 180 ft. Borehole 50-03-06 is associated with T-103 and is discussed in Section 10.2.3. All the monitoring boreholes for tank T-106 were logged with the SGLS, and a correlation plot showing the man-made contaminant distributions in these boreholes is provided in Appendix B. Details regarding the borehole construction configurations, the logging operations performed, and the data acquired from each borehole are presented in the Tank Summary Data Report for tank T-106 (DOE 1999g).

Figures 14-41, 14-42, and 14-52 show the ^{137}Cs contamination in the vicinity of tank T-106. Figure 14-41 is a visualization of the T Tank Farm viewed from below the tanks from the

southeast, Figure 14-42 is a visualization of the T Tank Farm viewed from above the tanks from the northwest, and Figure 14-49 is a visualization in the vicinity of tanks T-103, T-106, and T-109, viewed from below the tanks from the southeast. Figures 14-42 and 14-52 show regions of near-surface and shallow subsurface ^{137}Cs contamination around the southern, eastern, and northern sides of this tank. This contamination is probably associated with surface spills or leaks that have migrated as deep as 15 ft into the backfill sediments. Some of this contamination may have also been carried down during drilling. Small zones of elevated ^{137}Cs contamination detected at depths between 15 and 25 ft near the southeast side of tank T-106 may be the result of a pipeline or transfer line leak.

A broad plume of contamination was detected by the SGLS below about 33 ft in all of the monitoring boreholes surrounding the east, west, and south sides of tank T-106 (see Figures 14-41 and 14-52). This contamination is the result of the T-106 tank leak that occurred in 1973 (DOE 1999g). The primary constituents of the contaminant plume are ^{137}Cs, ^{60}Co, ^{154}Eu, and ^{152}Eu. However, for reasons stated in Section 10.0, ^{152}Eu was not analyzed with the EVS modeling software. In some of the boreholes, occurrences of ^{125}Sb, ^{126}Sn, ^{235}U, and ^{238}U contamination were detected within the main body of the plume; however, because the distribution of these contaminants was not extensive, they were also not analyzed with the EVS modeling software.

Zones of extremely high gamma radiation were encountered within most of the boreholes that intercepted the main part of this contaminant plume. The intensity of this radiation caused the SGLS detector to saturate during the logging of these zones, yielding no usable spectral data. However, based upon the rate of decrease of the historical gross gamma activity, it was determined that ^{137}Cs is the predominant radionuclide present in these intervals, but other radionuclides are certainly present. In cases where a zone of detector saturation was encountered, ^{137}Cs concentration values of 9,900 pCi/g (the approximate concentration of the highest reliable ^{137}Cs assay above and below the zone of detector saturation) were placed into the database in these intervals.

The magnitude and extent of the ^{137}Cs contamination within the plume resulting from the T-106 tank leak are shown in Figures 14-41, 14-42, and 14-52. The highest gross gamma count-rate activity, determined to represent primarily ^{137}Cs contamination, was measured around two boreholes (50-06-05 and 50-06-17) near the southeast side of the tank along the depth interval of about 32 to 42 ft. The magnitude of the ^{137}Cs contamination in this region of the vadose zone suggests that these boreholes are closest to the source of the leak and that the leak originated from an area near the bottom of the tank. The SGLS data indicate that the resulting contaminant plume has migrated downward to a depth of at least 119 ft around borehole 50-06-05; however, the total vertical extent of the plume cannot be determined because of the limited depth of this borehole (DOE 1999g).

The magnitude and extent of the ^{60}Co and ^{154}Eu contamination within the plume resulting from the T-106 tank leak are shown in Figures 14-43 and 14-44, respectively. The distribution of the ^{60}Co and ^{154}Eu contamination in relation to the ^{137}Cs contamination within the plume is shown on

Figures 14-45, 14-46, 14-53, and 14-55, and Figures 14-47, 14-48, 14-54, and 14-56, respectively. Figures 14-43, 14-44, 14-45, and 14-47 are visualizations of the T Tank Farm viewed from below the tanks from the southeast. Figures 14-46 and 14-48 are visualizations of the T Tank Farm viewed from above the tanks from the northwest. Figures 14-53 and 14-54 are visualizations in the vicinity of tanks T-103, T-106, and T-109, viewed from above the tanks from the southeast. Figures 14-55 and 14-56 are visualizations in the vicinity of tanks T-103 and T-106, viewed from above the tanks from the southeast.

The extensive ^{60}Co and ^{154}Eu contamination related to the T-106 tank leak has migrated downward and laterally from the leak source through the vadose zone sediments. In general, the maximum vertical extent of most of the ^{60}Co and ^{154}Eu within the plume could not be determined because of the limited depth of the boreholes (85 to 125 ft) in the T Tank Farm. The maximum lateral extent of these components of the plume is best illustrated by Figures 14-39 and 14-40, which depict a horizontal planar slice through the vadose zone sediments at a depth of 72 ft. The ^{60}Co and ^{154}Eu contamination at this depth appear to have migrated laterally northward below most of tank T-106, westward to near the western edge of the tank farm perimeter, southward below the northern and northwestern regions of tanks T-108 and T-109, and probably eastward below the western region of tank T-105. The ^{60}Co contamination at this depth has migrated a further lateral distance than the ^{154}Eu contamination, extending southward beyond the southern end of tank T-108 and eastward below the southern and eastern portions of tank T-105. The ^{60}Co contamination that extends from the area between tanks T-101 and T-104 southwestward to the eastern side of tank T-105 probably resulted from the T-101 spare fill-line leak. However, it is also possible that some of the ^{60}Co contamination detected between tanks T-104 and T-105 may represent the outer edge of the ^{60}Co plume that originated from the T-106 tank leak (DOE 1999e).

10.2.7 Tank T-107

Tank T-107 was placed into service in December 1944. The waste types contained in tank T-107 throughout its service life are summarized in Table 1. Tank T-107 was declared to be of questionable integrity and was removed from service in 1976, when gross gamma logging measurements in borehole 50-07-03 indicated an elevated radiation peak at 42 ft. Although surface-level data collected from within the tank showed no evidence of a leak, the tank was reclassified as an assumed leaker in 1984. The leak volume of this tank and 19 other tanks in eight different tank farms was estimated to be about 8,000 gal. This value is an average of 150,000 total gallons divided by 19 tanks and may be in error by as much as 100 percent or more (DOE 1995d).

A "White Paper" was issued May 21, 1991, (Raymond 1991) when the surface-level measurements of the tank fell from 61.2 to 55.15 in. during a 1-week period, indicating a leak. It was determined an instrument component had failed and caused the anomalous reading (Vermeulen 1991). Additional measurement readings indicated the profiles were consistent with the reference baseline, and no further action was taken.

Tank T-107 presently contains a total of 173,000 gal of non-complexed waste that includes 173,000 gal of sludge and 22,000 gal of drainable, interstitial liquid within the sludge matrix (Hanlon 1999). The surface level of the waste in tank T-107 is approximately 5 ft above the center of the tank bottom (DOE 1995d).

Five boreholes exist around tank T-107 for vadose zone monitoring (see Figure 14-17). Boreholes 50-07-03, 50-07-07, and 50-07-08 were drilled in 1974 and 1975 to depths of 92 ft, 94 ft, and 94 ft, respectively. Boreholes 50-04-07 and 50-04-05 are associated with tank T-104 and are discussed in Section 10.2.4. All of the monitoring boreholes for tank T-107 were logged with the SGLS, and a correlation plot showing the man-made contaminant distributions in these boreholes is provided in Appendix B. Details regarding the borehole construction configurations, the logging operations performed, and the data acquired from each borehole are presented in the Tank Summary Data Report for tank T-107 (DOE 1995d).

Figures 14-41 and 14-42 show the ^{137}Cs contamination in the vicinity of tank T-107. Figure 14-41 is a visualization of the T Tank Farm viewed from below the tanks from the southeast and Figure 14-42 is a visualization of the T Tank Farm viewed from above the tanks from the northwest. These two figures show that a considerable amount of near-surface and shallow subsurface ^{137}Cs contamination exists in the vicinity of this tank. Figure 14-33, which is a horizontal planar slice at a depth of 5 ft below the ground surface of the T Tank Farm, shows that the maximum near-surface ^{137}Cs contamination occurs in the east central portion of the tank farm between tanks T-107 and T-104. The near-surface and shallow subsurface ^{137}Cs contamination is probably associated with surface spills or leaks that have migrated as deep as 27 ft into the backfill sediments. Some of the ^{137}Cs contamination may have also been carried down during drilling.

^{60}Co was detected at low concentrations near the east side of tank T-107 around borehole 50-07-03. A small zone of ^{137}Cs contamination was detected near the south side of tank T-107 around borehole 50-07-07. Both radionuclides occur at approximately the depth of the bottom of the tank farm excavation (44 ft). The ^{137}Cs and ^{60}Co contamination is shown on Figures 14-24 and 14-25, respectively. The ^{137}Cs contamination is also visible on Figure 14-41.

The ^{60}Co contamination around borehole 50-07-03 is the likely cause of a historical gross gamma anomaly first detected in 1975. Anomalous activity was also detected around borehole 50-07-07 at about the same time. It is not known if the ^{60}Co contamination is from a surface or subsurface source and there is no direct evidence of a continuing flux or increase of contamination that would suggest a continuing leak source (DOE 1995d).

The ^{137}Cs contamination around borehole 50-07-07 may have resulted from a surface spill that migrated along the tank side and collected in the formation near base of the tank, or from a subsurface leak from the tank (DOE 1995d).

The rate of decrease of the measured gross gamma activity levels over time in boreholes 50-07-03 and 50-07-07 suggests that ^{60}Co was the major original constituent of the contaminant

source and has since decayed away because of its relatively short half life. However, it is not known if the contamination detected by the SGLS in these boreholes originated from a common source. Furthermore, it is not clear whether the source of this contamination is from a surface spill or a subsurface leak (DOE 1995d).

10.2.8 Tank T-108

Tank T-108 was put into service in September 1945. The waste types contained in tank T-108 throughout its service life are summarized in Table 1. Tank T-108 was declared to be of questionable integrity and was removed from service in 1974, on the basis of a 0.3-in. liquid-level decrease. The tank was administratively interim stabilized in 1978, and intrusion prevention was completed in 1981 (DOE 1998c).

Tank T-108 is classified as an assumed leaker and presently contains a total of 44,000 gal of sludge identified as non-complexed waste. The tank does not contain any supernatant or interstitial liquid (Hanlon 1999). The present waste level is approximately 1 ft above the center of the tank bottom (DOE 1998c).

Nine boreholes exist around tank T-108 for vadose zone monitoring (see Figure 14-17). Boreholes 50-08-05, 50-08-07, 50-08-08, 50-08-09, and 50-08-19 were drilled between 1973 and 1979 to depths of 93 ft, 94 ft, 100 ft, 87 ft, and 95 ft, respectively. Borehole 50-08-11 was drilled in 1944 to a depth of 136 ft. Borehole 50-05-06 is associated with tank T-105 and is discussed in Section 10.2.5; borehole 50-07-08 is associated with tank T-107 and is discussed in Section 10.2.7; and borehole 50-09-02 is associated with tank T-109 and is discussed in Section 10.2.9. All of the monitoring boreholes for tank T-108 were logged with the SGLS, and a correlation plot showing the man-made contaminant distributions in these boreholes is provided in Appendix B. Details regarding the borehole construction configurations, the logging operations performed, and the data acquired from each borehole are presented in the Tank Summary Data Report for tank T-108 (DOE 1998c).

Figures 14-41 and 14-42 show the ^{137}Cs contamination in the vicinity of tank T-108. Figure 14-41 is a visualization of the T Tank Farm viewed from below the tanks from the southeast, and Figure 14-42 is a visualization of the T Tank Farm viewed from above the tanks from the northwest. Figure 14-42 shows a region of near-surface and shallow subsurface ^{137}Cs contamination around the northern half of this tank. This contamination is probably associated with surface spills or leaks that have migrated as deep as 12 ft into the backfill sediments. Some of the ^{137}Cs contamination may have also been carried down during drilling.

Subsurface radionuclide contamination was detected in most of the boreholes surrounding tank T-108; however, no contamination in the vadose zone could be conclusively attributed to a leak from tank T-108 (DOE 1998c). Figure 14-39, which depicts a horizontal planar slice through the vadose zone sediments at a depth of 72 ft, illustrates plumes of ^{60}Co and ^{154}Eu contamination below the northern and western portions of the tank. Historical gross gamma and SGLS data indicate that the likely source of this contamination is the T-106 tank leak (DOE 1998c). A more detailed discussion of the origin of this contamination is provided in Section 10.2.6.

10.2.9 Tank T-109

Tank T-109 was put into service in December 1945. The waste types contained in tank T-109 throughout its service life are summarized in Table 1. Tank T-109 was declared to be of questionable integrity and was removed from service in 1974, on the basis of a gross gamma activity increase in borehole 50-09-01 below a depth of about 39 ft. The tank is estimated to have leaked less than 1,000 gal, based on a 0.35-in. liquid-level decrease between June 1973 and May 1974 (Walker 1988). The supernatant liquid was pumped from the tank in 1974 and salt-well pumping was completed by May 1978. The tank was administratively interim stabilized in 1984, and intrusion prevention has been completed although the date that it was performed is unknown (DOE 1998b).

Tank T-109 is classified as an assumed leaker and contains a total of 58,000 gal of sludge identified as non-complexed waste. The tank does not contain any supernatant or interstitial liquid (Hanlon 1999). The present waste level is approximately 2 ft above the center of the tank bottom (DOE 1998b).

Nine boreholes exist around tank T-109 for vadose zone monitoring (see Figure 14-17). Boreholes 50-09-01, 50-09-02, 50-09-05, 50-09-07, 50-09-09, 50-09-10, and 50-00-09 were drilled between 1973 and 1977 to depths of 90 ft, 89 ft, 94 ft, 94 ft, 121 ft, 121 ft, and 122 ft, respectively. Borehole 50-06-06 is associated with tank T-106 and is discussed in Section 10.2.6. Borehole 50-08-09 is associated with tank T-108 and is discussed in Section 10.2.8. All of the monitoring boreholes for tank T-109 were logged with the SGLS, and a correlation plot showing the man-made contaminant distributions in these boreholes is provided in Appendix B. Details regarding the borehole construction configurations, the logging operations performed, and the data acquired from each borehole are presented in the Tank Summary Data Report for tank T-109 (DOE 1998b).

Figures 14-41, 14-42, and 14-52 show the ^{137}Cs contamination in the vicinity of tank T-109. Figure 14-41 is a visualization of the T Tank Farm viewed from below the tanks from the southeast, Figure 14-42 is a visualization of the T Tank Farm viewed from above the tanks from the northwest, and Figure 14-52 is a visualization in the vicinity of tanks T-103, T-106, and T-109, viewed from below the tanks from the southeast. Figures 14-42 and 14-52 show regions of near-surface and shallow subsurface ^{137}Cs contamination along the northwestern and northeastern portions of the tank. This contamination is probably associated with surface spills or leaks that have migrated as deep as 10 ft into the backfill sediments. Some of this contamination may have also been carried down during drilling. A small zone of elevated ^{137}Cs contamination detected between 1 and 5 ft near the northeast side of tank T-109 may be the result of a near-surface pipeline leak.

Subsurface radionuclide contamination was detected in most of the boreholes surrounding tank T-109; however, it is not likely that any of the contaminants originated from tank T-109. Figure 14-39, which depicts a horizontal planar slice through the vadose zone sediments at a depth of 72 ft, illustrates plumes of ^{60}Co and ^{154}Eu contamination below the northern and eastern portions

of the tank. The distribution of these contaminants observed in the boreholes around tank T-109 indicates that the most likely source of the contamination was the T-106 tank leak (DOE 1998b). A more detailed discussion of the origin of this contamination is provided in Section 10.2.6.

10.2.10 Tank T-110

Tank T-110 was put into service in December 1944. The waste types contained in tank T-110 throughout its service life are summarized in Table 1. Tank T-110 was removed from service in 1976. The tank was primarily stabilized in 1978 and was partially isolated in December 1982 (DOE 1995e).

Pumping of the waste remaining in the tank T-110 began June 7, 1998, and is currently ongoing. Pumping operations during March 1999 required the addition of 3,906 gal of raw water to the tank. A total of 44,300 gal had been pumped from the tank as of the end of March 1999. Tank T-110 is classified as sound; however, interim stabilization has not yet been completed. The tank presently contains a total of 351,000 gal of non-complexed waste that consists of 351,000 gal of sludge and 37,000 gal of drainable, interstitial liquid within the sludge matrix (Hanlon 1999). The surface level of the waste in tank T-110 is approximately 12 ft above the center of the tank bottom (DOE 1995e).

Six boreholes exist around tank T-110 for vadose zone monitoring (see Figure 14-17). Boreholes 50-10-05, 50-10-07, 50-10-08, and 50-10-10 were drilled in 1974 and 1975 to depths of 95 ft, 94 ft, 93 ft, 94 ft, respectively, and borehole 50-00-05 was drilled in 1944 to a depth of 150 ft. Borehole 50-07-07 is associated with tank T-107 and is discussed in Section 10.2.7. All of the monitoring boreholes for tank T-110 were logged with the SGLS, and a correlation plot showing the man-made contaminant distributions in these boreholes is provided in Appendix B. Details regarding the borehole construction configurations, the logging operations performed, and the data acquired from each borehole are presented in the Tank Summary Data Report for tank T-110 (DOE 1995e).

Figures 14-41 and 14-42 show the ^{137}Cs contamination in the vicinity of tank T-110. Figure 14-41 is a visualization of the T Tank Farm viewed from below the tanks from the southeast, and Figure 14-42 is a visualization of the T Tank Farm viewed from above the tanks from the northwest. Both figures show that only minor amounts of near-surface and shallow subsurface ^{137}Cs contamination exist in the vicinity of this tank. This contamination is probably associated with surface spills or leaks that migrated into the backfill sediments. Some of the ^{137}Cs contamination may have also been carried down during drilling.

A small zone of weak ^{137}Cs contamination was detected around one borehole (50-07-07) near the north side of tank T-110 at approximately the depth of the bottom of the tank farm excavation (44 ft). This contamination most likely originated from tank T-107 (DOE 1995e). A more detailed discussion of the origin of this contamination is provided in Section 10.2.7.

10.2.11 Tank T-111

Tank T-111 was placed into service in October 1945. The waste types contained in tank T-111 throughout its service life are summarized in Table 1. Tank T-111 was declared to be of questionable integrity and was removed from service in 1974, on the basis of an unexplained in-tank liquid-level decrease of 0.30 in. The tank was reclassified as an assumed leaker in 1984 (DOE 1998e).

In 1994, tank T-111 was declared an assumed re-leaker because of a decreasing trend in the liquid-level measurements (Tucker 1994). On the basis of the observed in-tank liquid-level decrease, the volume of the tank leak was estimated to be less than 1,000 gal. On February 22, 1995, tank T-111 was declared interim stabilized after jet-pumping operations removed approximately 9,600 gal of supernatant liquid (Hanlon 1999).

Tank T-111 presently contains a total of 446,000 gal of non-complexed waste that consists of 446,000 gal of sludge and 34,000 gal of drainable, interstitial liquid within the sludge matrix (Hanlon 1999). The surface level of the waste in tank T-111 is approximately 14.5 ft above the center of the tank bottom (DOE 1998e).

Ten boreholes exist around tank T-111 for vadose zone monitoring (see Figure 14-17). Boreholes 50-11-05, 50-11-07, 50-11-08, 50-11-10, and 50-11-11 were drilled between 1974 and 1979 to depths of 93 ft, 94 ft, 94 ft, 100 ft, and 95 ft, respectively, and borehole 50-00-06 was drilled in 1944 to a depth of 150 ft. Boreholes 50-08-05 and 50-08-07 are associated with tank T-108 and are discussed in Section 10.2.8. Boreholes 50-10-08 and 50-10-10 are associated with tank T-110 and are discussed in Section 10.2.10. All of the monitoring boreholes surrounding tank T-111 were logged with the SGLS, and a correlation plot showing the man-made contaminant distributions in these boreholes is provided in Appendix B. Details regarding the borehole construction configurations, the logging operations performed, and the data acquired from each borehole are presented in the Tank Summary Data Report for tank T-111 (DOE 1998e).

Figures 14-41 and 14-42 show the ^{137}Cs contamination in the vicinity of tank T-111. Figure 14-41 is a visualization of the T Tank Farm viewed from below the tanks from the southeast, and Figure 14-42 is a visualization of the T Tank Farm viewed from above the tanks from the northwest. Both figures show that only minor amounts of near-surface and shallow subsurface ^{137}Cs contamination exist in the vicinity of this tank. This contamination is probably associated with surface spills or leaks that migrated into the backfill sediments. Some of the ^{137}Cs contamination may have also been carried down during drilling.

A zone of ^{60}Co contamination was detected around one borehole (50-08-07) located near the northwest side of tank (see Figure 14-40); however, this contamination can be directly correlated to contamination detected in monitoring boreholes surrounding tank T-108, and it is unlikely that it originated from tank T-111 (DOE 1998e). A more detailed discussion of the origin of this contamination is provided in Section 10.2.8.

Tank T-111 is classified both as a leaker and a re-leaker based upon in-tank liquid-level observations. However, because the tank leak volume estimate is less than 1,000 gal, the leak designation is probably based only on very small decreases in liquid level that may not be the result of a tank leak. Data from the SGLS and historical gross gamma monitoring data do not identify a tank leak. However, it is unlikely that a very small leak would be detected by external monitoring. Therefore, either the tank did not leak, or the leak plumes are limited in extent and have not been intercepted by any of the monitoring boreholes (DOE 1998e).

10.2.12 Tank T-112

Tank T-112 was placed into service in October 1945. The waste types contained in tank T-112 throughout its service life are summarized in Table 1. Tank T-112 was declared inactive in 1976. The tank was administratively interim stabilized in March 1981, and intrusion prevention was completed in June 1981 (DOE 1998f).

Tank T-112 is classified as sound and presently contains a total of 67,000 gal of non-complexed waste that consists of 60,000 gal of sludge and 7,000 gal of supernate (Hanlon 1999). The surface level of the waste in tank T-112 is approximately 2.5 ft above the center of the tank bottom (DOE 1998f).

Eight boreholes exist around tank T-112 for vadose zone monitoring (see Figure 14-17). Boreholes 50-12-05, 50-12-07, and 50-12-10 were drilled in 1974 and 1975 to depths of 100 ft, 94 ft, and 94 ft, respectively, and borehole 50-00-08 was drilled in 1944 to a depth of 148 ft. Boreholes 50-09-05 and 50-09-07 are associated with tank T-109 and are discussed in Section 10.2.9. Boreholes 50-11-08 and 50-11-10 are associated with tank T-111 and are discussed in Section 10.2.11. All of the monitoring boreholes for tank T-112 were logged with the SGLS, and a correlation plot showing the man-made contaminant distributions in these boreholes is provided in Appendix B. Details regarding the borehole construction configurations, the logging operations performed, and the data acquired from each borehole are presented in the Tank Summary Data Report for tank T-112 (DOE 1998f).

Figures 14-41 and 14-42 show the ^{137}Cs contamination in the vicinity of tank T-112. Figure 14-41 is a visualization of the T Tank Farm viewed from below the tanks from the southeast, and Figure 14-42 is a visualization of the T Tank Farm viewed from above the tanks from the northwest. Both figures show that only minor amounts of near-surface ^{137}Cs contamination exist in the vicinity of this tank. However, shallow subsurface ^{137}Cs contamination was detected as deep as 20 ft around one borehole (50-12-07) near the southwest side of the tank. The ^{137}Cs contamination is probably associated with surface spills or leaks that migrated into the backfill sediments. Some of the ^{137}Cs contamination may have also been carried down during drilling.

Data obtained from the SGLS and geologic and historical information do not identify any apparent subsurface contamination plumes that can be attributed to leaks from tank T-112 (DOE 1998f). However, a zone of weak ^{60}Co contamination was detected around one borehole (50-09-05) located near the northeast side of tank. This contamination correlates with

contamination detected in boreholes to the north and northeast and may demarcate the southernmost extent of the contaminant plume from the T-106 tank leak.

11.0 Summary of Results

Presentation and discussion of three-dimensional visualizations of contaminant distribution in the T Tank Farm are integral portions of this report. In preparing these visualizations, data sets were prepared for the three major contaminants (^{137}Cs, ^{60}Co, and ^{154}Eu) by compiling all SGLS data as a function of location and depth in the upper 125 ft of the T Tank Farm vadose zone, which is the approximate depth range of the monitoring boreholes. For ^{137}Cs, an "interpreted data set" was compiled that reflects interpretations regarding the distribution of the ^{137}Cs with respect to the borehole. The interpreted data set contains assays of ^{137}Cs that were deemed to be distributed in the backfill and undisturbed sediments (beneath the tank farm excavation), and excludes data deemed to be confined to the immediate vicinity of the borehole casing. This data set was created by evaluating all ^{137}Cs concentration data detected in the course of the SGLS logging in the T Tank Farm boreholes. Because spectral shape factor analysis could be applied to the SGLS data from only two of the boreholes in the T Tank Farm (boreholes 50-04-04 and 50-06-18), the interpreted ^{137}Cs data set generally reflects the analyst's interpretations of the distribution and nature of occurrence of contaminants based on experience gained from processing and reviewing a large volume of data during the vadose zone characterization at the Hanford Site SST farms.

Near-surface and shallow subsurface ^{137}Cs contamination was detected primarily in the central and eastern portions of the T Tank Farm. This contamination most likely resulted from surface spills or leaks from piping systems that were related to routine tank farm operations. There were three documented unplanned releases in the T Tank Farm; however, the extent of the ^{137}Cs contamination could not be attributed to these releases. The highest ^{137}Cs concentrations of (approximately 200 pCi/g) were detected within the near-surface backfill material in the east central portion of the tank farm between tanks T-104 and T-107. The thickest distributions of ^{137}Cs (27 ft) were also detected in this region around boreholes 50-04-03 and 50-04-07, suggesting a larger spill or several spills or leaks may have occurred in this area. Small ^{137}Cs peaks detected at a depth of about 20 ft in boreholes 50-06-03, 50-06-04, 50-06-18, and 50-06-05 may be the result of a transfer-line leak near the southeast side of tank T-106 (DOE 1999g).

A vertically continuous, elongate ^{137}Cs plume was detected near the southeast side of tank T-101 around borehole 50-01-04. The plume extends from 20 ft to the bottom of the logged interval (122.5 ft) and is probably the result of a large volume of contamination that leaked to the soil column in 1969, when the tank was overfilled during tank farm operations. Previous investigations have identified the spare fill lines located on the southeast side of tank T-101 as the probable source of the leak (DOE 1999b).

The horizontal extent of this plume is not known because the contamination was detected around only one borehole (50-01-04), resulting in a general lack of understanding of the spatial

variability of the plume. Contamination was not detected around borehole 50-00-03, which is located about 25 ft away from borehole 50-01-04, where high levels of ^{137}Cs contamination were detected. Therefore, it can be concluded that the horizontal extent of the plume is less than 25 ft. The maximum vertical extent of the ^{137}Cs plume has not been determined because very high concentrations of ^{137}Cs contamination extend to the bottom of the logged interval.

A large ^{60}Co and ^{154}Eu plume was identified near the south side of tank T-101 around borehole 50-01-06. A 1975 investigation inferred that this plume originated from the direction of borehole 50-01-04 (Jensen 1975b), suggesting the suspected leak from the spare fill lines on tank T-101 is the probable source of the contamination. More of this plume may be identified by deep ^{60}Co contamination detected west of tank T-104 around boreholes 50-04-08 and 50-04-10. Historical gross gamma data suggest that the ^{60}Co may have migrated laterally in a southwesterly direction from 50-01-06 to 50-04-10 to 50-04-08 between 1973 and 1976. However, this does not rule out the possibility that the contamination detected around boreholes 50-04-08 and 50-04-10 may represent the outer edge of the ^{60}Co plume that originated from the T-106 tank leak. It is also possible that the ^{60}Co contamination originated from both sources (DOE 1999e).

^{137}Cs and ^{60}Co plumes were detected near the west side of tank T-101 around borehole 50-01-09. This contamination was present in 1973 when the borehole was drilled and may be the result of a leak from the cascade overflow line connecting tanks T-101 and T-102 (DOE 1999c).

^{137}Cs and ^{60}Co plumes were also detected near the southeast side of tank T-102 around borehole 50-02-05. This contamination was present in 1974 when the borehole was drilled and may have resulted from a leak from the spare fill lines on the southeast side of the tank (DOE 1999c).

A distinct plume of radionuclide contamination, consisting primarily of ^{60}Co, ^{154}Eu, and ^{152}Eu, was detected along the southeast and south sides of tank T-103 around boreholes 50-03-04, 50-02-08, 50-03-05, and 50-03-06. The contamination within this plume appears to be correlatable among these boreholes and is described by ARH (1973) to be the result of a spare fill-line leak on the southeast side of tank T-103. Occurrences of ^{94}Nb, ^{125}Sb, ^{126}Sn, and ^{238}U contamination were also detected in one or more boreholes within the main body of the plume; however, the distribution of these contaminants was not extensive. The SGLS data indicate that the contaminant plume has migrated both downward and laterally away from the leak source. Historical gross gamma-ray data suggest that downward migration of ^{60}Co contamination has occurred within the plume around borehole 50-03-06 between 1975 and 1994. Furthermore, fine-grained layers may exist within the Hanford formation that could possibly enhance the lateral spreading of the ^{60}Co and ^{154}Eu contamination within the plume (DOE 1999d). This is evident on several visualizations, which show that some of the ^{60}Co and ^{154}Eu contamination within the plume has migrated laterally to the south and has apparently intermingled with contamination resulting from the T-106 tank leak.

A broad plume of contamination was detected below about 33 ft in all of the monitoring boreholes surrounding the east, west, and south sides of tank T-106. This contamination is the result of the T-106 tank leak that occurred in 1973 (DOE 1999g). The primary constituents of the contaminant plume are ^{137}Cs, ^{60}Co, ^{154}Eu, and ^{152}Eu. Occurrences of ^{125}Sb, ^{126}Sn, ^{235}U, and

^{238}U contamination were also detected in one or more boreholes within the main body of the plume; however, the distribution of these contaminants was not extensive.

Zones of extremely high gamma radiation were encountered within most of the boreholes that intercepted the main portion of the contaminant plume resulting from the T-106 tank leak. The intensity of this radiation caused the SGLS detector to saturate during the logging of these zones, yielding no usable spectral data. However, based upon the rate of decrease of the historical gross gamma activity, it was determined that ^{137}Cs is the predominant radionuclide present in these intervals, but other radionuclides are certainly present. The highest gross gamma count-rate activity, determined to represent primarily ^{137}Cs contamination, was measured near the southeast side of the tank around boreholes 50-06-05 and 50-06-17 along the depth interval of about 32 to 42 ft. The magnitude of the ^{137}Cs contamination in this region of the vadose zone suggests that these boreholes are closest to the source of the leak and that the leak probably originated from an area near the bottom of the tank. The deepest anomalous activity detected in borehole 50-06-17 corresponds closely with the depth of a caliche layer reported in the drilling log, suggesting that this caliche layer may retard the downward migration of the ^{137}Cs contamination in this region of the vadose zone to some degree. However, the SGLS data indicate that a portion of the ^{137}Cs plume resulting from the tank leak has migrated downward to a depth of at least 119 ft around adjacent borehole 50-06-05. Unfortunately, the total vertical extent of the plume cannot be determined because of the limited depth of this borehole (DOE 1999g).

Widespread ^{60}Co and ^{154}Eu contamination related to the T-106 tank leak was detected in boreholes 50-06-02, 50-06-03, 50-06-04, 50-06-16, 50-06-18, 50-06-06, 50-06-08, and 50-00-09. The contamination is correlatable between boreholes, indicating that a large plume consisting of these radionuclides has migrated downward and laterally from the leak source through the vadose zone sediments. In general, the maximum vertical extent of most of the ^{60}Co and ^{154}Eu within the plume could not be determined because of the limited depth of the boreholes in the T Tank Farm (DOE 1999g). The lateral extent of the ^{60}Co and ^{154}Eu within the plume is best illustrated by visualizations that depict horizontal planar slices through the vadose zone sediments. These visualizations show that the maximum lateral extent of these components of the plume occurs at a depth of approximately 72 ft. At this depth, the ^{60}Co and ^{154}Eu contamination appear to have migrated laterally northward below most of tank T-106, westward to near the western edge of the tank farm perimeter, southward below the northern and northwestern regions of tanks T-108 and T-109, and probably eastward below the western region of tank T-105. The ^{60}Co contamination has migrated a further lateral distance than the ^{154}Eu contamination, extending southward beyond the southern end of tank T-108 and eastward below the southern and eastern portions of tank T-105. A lobe of ^{60}Co contamination extends from the area between tanks T-101 and T-104 southwestward to the eastern side of tank T-105. This contamination probably resulted from the T-101 spare fill-line leak; however, it is also possible that some of the ^{60}Co contamination detected between tanks T-104 and T-105 may represent the outer edge of the ^{60}Co plume that originated from the T-106 tank leak (DOE 1999e).

Near the southeast side of tank T-106, the ^{60}Co contamination detected around borehole 50-06-18 terminates at 125 ft, which corresponds with the depth of the calcium-cemented gravels that

constitute the top of the Ringold Unit E. It should be noted that many of the boreholes drilled around tank T-106 met refusal at the top of this unit, preventing further penetration and limiting the total depth of these boreholes to 119 to 122 ft. It appears that the top of the Ringold Unit E may act as a barrier to the migration of radionuclide contamination; however, it is possible that contaminants have migrated through this zone along preferential pathways to the underlying, non-cemented gravels of the Ringold Unit E (DOE 1999g).

The available historical gross gamma log data suggest that the majority of the radionuclides that constitute the contaminant plume originating from the T-106 tank leak have remained stable and have not migrated through the formation sediments since 1974. However, some movement of the ^{60}Co component of the plume was detected around boreholes 50-06-02 and 50-06-03. In borehole 50-06-02, the data suggest that ^{60}Co contamination migrated downward within the plume from 1973 to 1992. In borehole 50-06-03, the data suggest that continued lateral migration of deep ^{60}Co contamination occurred between 1973 and 1994 (DOE 1999g).

A small zone of weak ^{137}Cs contamination was detected near the south side of tank T-107 around borehole 50-07-07 at approximately the depth of the bottom of the tank farm excavation (44 ft). This contamination may have resulted from a surface spill that migrated along the tank side and collected in the formation near base of the tank, from a subsurface leak from the tank, or from a combination of these sources (DOE 1995d).

Subsurface radionuclide contamination was detected in most of the boreholes surrounding tanks T-108 and T-109; however, it is not likely that any of the contaminants originated from these tanks. Historical gross gamma and SGLS data and the relative distribution of these contaminants indicate that the likely source of this contamination was the T-106 tank leak.

Tank T-111 is classified both as a leaker and a re-leaker based upon in-tank liquid-level observations. However, because the tank leak volume estimate is less than 1,000 gal, the leak designation is probably based only on very small decreases in liquid level that may not be the result of a tank leak. Data obtained from the SGLS and geologic and historical information do not identify any contamination that can be attributed to a leak from tank T-111. Therefore, either the tank did not leak, or the leak plumes are limited in extent and have not been intercepted by any of the monitoring boreholes (DOE 1998e).

The ^{137}Cs contamination related to the tank T-101 spare-fill line leak and the ^{137}Cs, ^{60}Co, and ^{154}Eu contamination originating from the T-106 tank leak were detected at the bottoms (depths of approximately 120 ft) of the boreholes in the vicinity of each respective plume. Because the depth to groundwater is about 220 ft below the T Tank Farm, about 100 ft of the vadose zone in this region is uncharacterized. The vertical extent of these contaminants has not been determined; therefore, the log data provide no basis for evaluating the potential for T Tank Farm waste to contaminate groundwater.

In 1997, a Phase I, RCRA groundwater quality assessment was implemented to determine if Single-Shell Tank Waste Management Areas (WMAs) T and TX-TY have impacted groundwater quality. The results of that assessment are presented in a 1998 report prepared by PNNL

(Hodges 1998). Part of this assessment included the examination of both spatial and temporal groundwater contaminant concentration patterns in monitoring well 299-W11-27, located immediately downgradient from the T Tank Farm. Hodges (1998) reports that elevated levels of ^{99}Tc, tritium, nitrate, and chromium were observed in this well. ^{60}Co was also recently detected in this well. On the basis of available evidence, Hodges (1998) concluded with a high degree of certainty that WMA T is the source of groundwater contamination in monitoring well 299-W11-27. Both contaminant chemistry and lack of lateral spreading in groundwater (dispersion) are indicative of a small volume, tank waste source within the tank farm (Hodges 1998).

The Phase I assessment results indicate that ^{60}Co contamination originating from T Farm tank waste is present in the groundwater downgradient from the T Tank Farm; however, there is no indication that the ^{137}Cs and ^{154}Eu contamination present in the vadose zone below the T Tank Farm has reached and contaminated groundwater.

Several uncertainties have the potential to impact some of the interpretations of the T Tank Farm data described above. First, there is an unknown thickness of the grout in the annular space between the casings of each borehole in the T Tank Farm as a result of the modification these boreholes in the late 1970s. As a result, it is not possible to compensate for the attenuation of the gamma-ray energy by the grout, which limits the accuracy of in-situ log assays and changes the spatial resolution. This results in calculated radionuclide concentrations that are less than actual, and are reported as apparent concentrations. Second, periodic flooding of the tank farm may have caused downward migration of contamination along the outside of the borehole casings prior to the modification of the T Farm boreholes. Moreover, flood waters may have also drained into the boreholes, which would function as conduits and allow contamination to directly infiltrate into the deeper portions of the vadose zone. Third, rudimentary geostatistical structural models were developed for the purpose of creating visualizations of the ^{137}Cs, ^{60}Co, and ^{154}Eu distributions in the T Tank Farm. These models are empirical and are not intended to be used for quantitative calculations because the areal distribution of the boreholes within the tank farm has created unavoidable limitations in the current geostatistical structural model.

12.0 Conclusions

The most widespread gamma-emitting contaminants detected in the vadose zone beneath the T Tank Farm are ^{137}Cs, ^{60}Co, and ^{154}Eu, and to a lesser degree, ^{152}Eu. The majority of the shallow subsurface ^{137}Cs contamination is associated with surface spills and/or leaks that migrated into the backfill sediments. Limited and relatively isolated occurrences of ^{94}Nb, ^{125}Sb, ^{126}Sn, ^{235}U, and ^{238}U were detected between 20 and 120 ft around several boreholes located near tanks T-103 and T-106.

The ^{137}Cs plume identified around borehole 50-01-04 indicates that a leak originated from the southeast quadrant of tank T-101 at a depth of about 20 ft, which corresponds to the location of

the spare fill lines. Evidence suggests that the leak occurred when the tank was overfilled during tank farm operations in 1969. The 1992 occurrence report (Deaton 1992) documenting a decrease in liquid-level measurements remains as the only evidence that the integrity of tank T-101 has failed and the justification for the tank's classification as an assumed leaker. The ^{137}Cs and ^{60}Co plumes detected near the west side of tank T-101 around borehole 50-01-09 may be the result of a leak from the cascade overflow line connecting tanks T-101 and T-102.

The ^{137}Cs and ^{60}Co plume identified around borehole 50-02-05, along with evidence that the adjacent tanks may have leaked under similar circumstances, suggest that a leak originated from the spare fill lines connected to tank T-102. It appears that the ^{137}Cs component of the plume spread laterally from the suspected leak source to the south and west along the base of the tank farm excavation. Although this contamination appears to have originated from tank T-102, a leak from tank T-105 cannot be entirely ruled out. However, tank T-105 is currently classified as sound.

The distinct plume of ^{60}Co, ^{154}Eu, and ^{152}Eu contamination intercepted by boreholes located near the southeast and south sides of tank T-103 is believed to have originated from a leak in the seal of a spare fill line on the southeast side of the tank, nearest to borehole 50-03-04. Some of the ^{60}Co and ^{154}Eu contamination within the plume has migrated laterally to the south and has apparently intermingled with contamination resulting from the T-106 tank leak. In addition, historical gross gamma-ray data from borehole 50-03-06 suggest that some downward migration of ^{60}Co contamination has occurred within the plume since 1975.

The very extensive plume of ^{137}Cs, ^{60}Co, ^{154}Eu, and ^{152}Eu contamination identified around and below the base of the tank T-106 originated from large leak from the tank in 1973. The leak source is located on the southeast side of the tank, nearest to boreholes 50-06-05 and 50-06-17. The plume extends radially outward as much as 100 ft from the leak source. Except for some movement of deep ^{60}Co contamination around boreholes 50-06-02 and 50-06-03, the data suggest that the majority of the radionuclides that constitute the contaminant plume have remained relatively stable since 1974. The vertical extent of the plume could not be determined because of the limited depth of most of the boreholes (90 to 120 ft).

The small zone of ^{137}Cs contamination detected near the south side of tank T-107 around borehole 50-07-07 may have resulted from a surface spill that migrated along the tank side and collected in the sediments near base of the tank, from a subsurface leak from the tank, or from a combination of these sources. The depth of the ^{137}Cs contamination corresponds with the base of the tank farm excavation and a lithology change at the interface between the backfill and undisturbed Hanford formation sediments.

The plumes of ^{60}Co and ^{154}Eu contamination that are interpreted to extend below tanks T-105, T-108, and T-109 probably originated from the T-106 tank leak. The deep ^{60}Co contamination detected between tanks T-104 and T-105 probably resulted from the T-101 spare fill-line leak; however, it is also possible that some of the ^{60}Co contamination may represent the outer edge of the ^{60}Co plume that originated from the T-106 tank leak.

Data obtained from the SGLS and geologic and historical information do not indicate leakage from tank T-111. The information obtained from in-tank liquid-level observations remains as the only evidence that tank T-111 ever leaked. However, the distribution and depth of monitoring boreholes are not sufficient to assure detection of all leaks. The contamination plumes that were identified in the vicinity of T-111 in boreholes 50-11-11 and 50-08-07 can be directly correlated to contamination detected in monitoring boreholes surrounding tank T-108.

Man-made radionuclide contamination occurs at the bottoms of several T Tank Farm monitoring boreholes; therefore, the vertical extent of these contaminants and their potential to contaminate groundwater below the farm is unknown. The logged depth of these boreholes is approximately 120 ft and the depth to groundwater in this region is about 220 ft, indicating that about 100 ft of the vadose zone below the T Tank Farm is uncharacterized.

Groundwater in the vicinity of the T Tank Farm is contaminated with several constituents, including tritium, ^{99}Tc, ^{106}Ru, chromium, fluoride, and nitrate. In addition, ^{60}Co contamination originating from T Farm tank waste is present in the groundwater downgradient from the T Tank Farm; however, there is no indication that the ^{137}Cs and ^{154}Eu contamination present in the vadose zone below the T Tank Farm has reached and contaminated groundwater.

13.0 Recommendations

13.1 Data Uses

The vadose zone characterization of the T Tank Farm was conducted to establish a baseline that defines the contamination from gamma-emitting radionuclides in the vadose zone sediments surrounding the tanks. This baseline will be used to compare with future monitoring data to determine if changes have occurred and to assess the potential causes of the changes. The data from this characterization project can also be correlated and compared with information other than concentration data, such as temperature and moisture data, and any relationships that are developed may provide insight as to the environment within which the contamination exists.

13.2 Tank and Tank Farm Characterization Data

It is recommended that additional work be conducted to collect, catalog, assess, and analyze historical documents, publications, and records pertaining to the tanks and tank farms. There is currently a paucity of accessible historical information about the tanks and tank farm operations. Some comprehensive work on collecting historical data was performed and is presented in a multivolume publication (Brevick et al. 1995). It is recommended that this work be continued and expanded to include more information that is not directly tied to tank contents information, such as some of the significant operational records. This work should also include assessments of the data that would be valuable to operations and remediation decision makers.

13.3 Future Vadose Zone Characterizations

This report presents the results of an initial baseline characterization effort based solely on spectral gamma logging in existing cased boreholes. The visualizations presented herein depict the subsurface distribution of gamma-emitting radionuclides in the upper portion of the vadose zone within the immediate vicinity of the single-shell tanks. These data must be evaluated in context with geologic data, historical gross gamma log data, and tank farms operational data to arrive at an understanding of the current state of vadose zone contamination. Major uncertainties exist with regard to the extent of many plumes, and with regard to the maximum contaminant concentration in zones of detector saturation. Moreover, available data provide little information regarding the distribution of beta-emitting radionuclides such as ^{90}Sr or ^{99}Tc or hazardous chemical constituents that do not emit gamma rays. Finally, although water is generally acknowledged to be the "driver" for contaminant movement, there is little information on the distribution of moisture in the vadose zone. Therefore, it is recommended that additional characterization of the vadose zone be performed. Many of the recommendations cited in this section are similar to the recommendations presented in the *TWRS Vadose Zone Contamination Issue Expert Panel Status Report* (DOE 1997h), which is related to the SX Tank Farm vadose zone characterization.

Although borehole geophysical methods do not provide all of the required characterization data, they are favorable for characterization because they are cost effective and safe and because there are numerous existing boreholes that allow access to the subsurface. Other borehole geophysical methods, such as neutron-neutron (moisture), temperature, and neutron capture logging, are recommended for development and implementation at the tank farms to provide better characterization data. These techniques should become part of an overall vadose zone characterization plan that includes adequate quality assurance so that data acquisition and analyses are fully documented.

The characterization effort and associated visualizations discussed herein are confined to approximately the top half of the vadose zone in the immediate vicinity of the 100-series single shell tanks in the T Tank Farm. This provides a very limited view of the state of vadose zone contamination in the vicinity of the T Tank Farm and does not characterize contaminant plumes from adjacent liquid waste disposal sites that are also part of the Single-Shell Waste Management Area (WMA) T. Expansion of the existing characterization effort to boreholes associated with other potential sources of contamination within the WMA is imperative in order to fully assess the nature and extent of contamination associated with the WMA and to evaluate existing and future groundwater contamination. This is especially important because tank waste is known to have been discharged to various other sites as discussed in Section 6.

As discussed in Section 9, the geostatistical models used in creating the visualizations of the ^{137}Cs, ^{60}Co, and ^{154}Eu distributions in the T Tank Farm are empirical models. However, analysis of the variograms, which are plots of the variance of the data as a function of the distance between data points, indicates that the spatial correlation of the data is poor and that more closely spaced data points are required to assess spatial variability. This would necessitate the drilling of a relatively large number of additional boreholes within the T Tank Farm to provide sufficient

data for even a simplistic geostatistical model. Given the present-day cost of drilling in the tank farm environment, it is highly unlikely that an adequate number of boreholes could be drilled to significantly improve the geostatistical model. Hence, it is recommended that a few additional boreholes, targeted to investigate specific anomalies, be drilled within the T Tank Farm. The proposed locations of these boreholes are discussed in the following section.

13.4 Specific Recommendations for Vadose Zone Investigation and Monitoring

Recommendations regarding future vadose investigation and monitoring presented in the Tank Summary Data Reports for each tank resulted from interpretation of the spectral gamma-ray data and review of historical information for the tanks. The following recommendations for future investigation and monitoring are based on the individual Tank Summary Data Reports, along with additional recommendations based on information and knowledge gained in the preparation of this report.

DOE is required to monitor the nature and extent of the contamination that leaks from the tanks as well as determine the extent of migration and stability of the contamination. Although the vadose zone monitoring should not be used as a primary leak-detection method (in-tank leak detection methods are considered to be more reliable) it may help confirm a leak, determine the degree of migration, and evaluate the stability of the contamination in the vadose zone.

Tank T-101

Tank T-101 is currently classified as an assumed leaker and is interim stabilized. Continued periodic monitoring of the boreholes surrounding this tank is recommended to identify temporal changes in the distribution of the vadose zone contaminants along the southeast side of tank T-101.

Borehole 50-01-04 should be relogged using high-rate logging equipment to better characterize the zone of high gamma radiation present around this borehole. In addition, a new borehole should be drilled adjacent to borehole 50-01-04 to identify the presence of other radionuclide contaminants, but more importantly, to confirm the ^{137}Cs contamination detected around borehole 50-01-04 is in the formation and not localized to the borehole casing. The new borehole should be drilled deep enough to determine the vertical extent of the contamination plume, if it is found to exist.

Tank T-102

Tank T-102 is currently classified as sound and is interim stabilized, but this classification should be reviewed in light of the ^{137}Cs contamination detected around borehole 50-02-05 near the base of the tank. Borehole 50-02-05 should be monitored annually to detect any changes in the magnitude and extent of this contamination. In addition, a new borehole should be drilled near

the location of the spare fill lines on the southeast side of tank T-102 to confirm these observations and to investigate the vertical extent of contamination near the source.

Tank T-103

Tank T-103 is currently classified as an assumed leaker and is interim stabilized. Although further leaks are unlikely, it is recommended that monitoring of boreholes 50-03-04, 50-03-05, 50-03-06, and 50-02-08 be continued annually to detect changes in the plume identified in this region of the vadose zone.

Tank T-104

Tank T-104 is currently classified as sound but is not interim stabilized. Because pumping of the waste from this tank is currently ongoing and water is being added to the tank to assist pumping operations, it is recommended that all of the boreholes surrounding this tank be monitored at least monthly to detect any potential leakage and/or remobilization of contamination until waste retrieval operations are completed. Boreholes 50-01-06, 50-04-08, and 50-04-10 should be monitored annually to detect any future changes in the contaminant plume encountered in this region of the vadose zone.

Tank T-105

Tank T-105 is currently classified as sound and is interim stabilized. Although available data discussed in this report do not dispute the current designation of tank T-105 as sound, there are questions regarding the sources of contaminants, particularly in boreholes 50-02-05 and 50-05-07. Additional monitoring in these boreholes is recommended. The installation of one or more new boreholes between tanks T-102 and T-105 is recommended to help identify the contaminant source and delineate the extent of the ^{137}Cs plume detected at the base of the tank farm excavation in this area.

Tank T-106

Tank T-106 is currently classified as an assumed leaker and is interim stabilized. Although further leaks are unlikely, it is recommended that monitoring of the boreholes surrounding tank T-106 be continued annually to detect changes in the plumes identified in this region of the vadose zone.

Selected intervals of boreholes 50-06-04, 50-06-05, 50-06-06, 50-06-08, 50-06-17, and 50-06-18 should be relogged using high-rate logging equipment to better characterize zones of high gamma radiation present around these borehole.

It is recommended that an analysis and interpretation be completed of the data acquired during the drilling of borehole 50-06-18 (299-W10-196). These data represent the only complete vertical profile of a tank farm contamination plume that has ever been obtained. Unfortunately,

those data were never fully assessed. Along with analysis and interpretation, the data should be correlated with the geology and with contamination data from nearby boreholes.

Because the T-106 tank leak volume is well known and the actual leak event is well documented, it represents an ideal case study that can be used to develop an understanding of how contaminants migrate through the vadose zone. Therefore, this plume should be the target of additional characterization. That characterization should start with the deepening of the boreholes around the tank, particularly boreholes 50-06-05 and 50-06-17. Sampling and laboratory analyses should be accomplished during the deepening of those boreholes. A specific objective of additional characterization of the T-106 tank leak should be to determine the depth and distribution of ^{99}Tc, a mobile, high-risk radionuclide, as well as other mobile radionuclides, such as the isotopes of uranium.

Finally, it is recommended that an evaluation be completed of the downhole germanium detector measurements that were completed in the late 1970s. There are some concerns with the quality of that data, and, in particular, with the calibration. To help answer those questions and improve the utility of those early assessments, it is recommended the "calibration" models located just west of the S Plant at Hanford be logged with the SGLS. Those models were constructed as a part of the 1970s T-106 work. Unfortunately, the models are assayed in terms of picocuries per unit volume instead of the generally accepted picocuries per unit mass, which self compensates for density variations. If the calibration can be adapted to a standard unit, it would greatly improve the utility and comparability of the older data.

Tank T-107

Tank T-107 is currently classified as an assumed leaker and is interim stabilized. Continued monitoring of the boreholes surrounding this tank is recommended because the tank is classified as an assumed leaker and still contains approximately 22,000 gal of drainable interstitial liquid (Hanlon 1999).

Tank T-108

Tank T-108 is currently classified as an assumed leaker and is interim stabilized. Continued monitoring of the boreholes surrounding this tank is recommended to identify changes in the distribution of the contaminant plume that originated from the T-106 tank leak.

Tank T-109

Tank T-109 is currently classified as an assumed leaker and is interim stabilized. Continued monitoring of the boreholes surrounding this tank is recommended to identify changes in the distribution of the contaminant plume that originated from the T-106 tank leak.

Additional characterization is recommended to determine the vertical extent of contamination on the north side of tank T-109.

Tank T-110

Tank T-110 is currently classified as sound but is not interim stabilized. Because pumping of the waste from this tank is currently ongoing and water is being added to the tank to assist pumping operations, it is recommended that all of the boreholes surrounding this tank be monitored at least monthly to detect any potential leakage and/or remobilization of contaminants until waste retrieval operations are completed.

Tank T-111

Tank T-111 is currently classified as an assumed leaker and is interim stabilized. However, as recently as 1994, tank T-111 was classified as an assumed re-leaker after additional unexplained liquid-level decreases were observed. Because approximately 34,000 gal of drainable interstitial liquid remain in the tank (Hanlon 1999), continued monitoring of the boreholes surrounding this tank is recommended to help identify future leaks or changes in the distribution of the vadose zone contaminants on the north side of tank T-111.

Tank T-112

Tank T-112 is currently classified as sound and is interim stabilized. Continued monitoring of the boreholes surrounding this tank is recommended because the tank still contains 7,000 gal of supernate.

14.0 Figures

This section contains the figures discussed in the text of the report in the order in which they were presented.

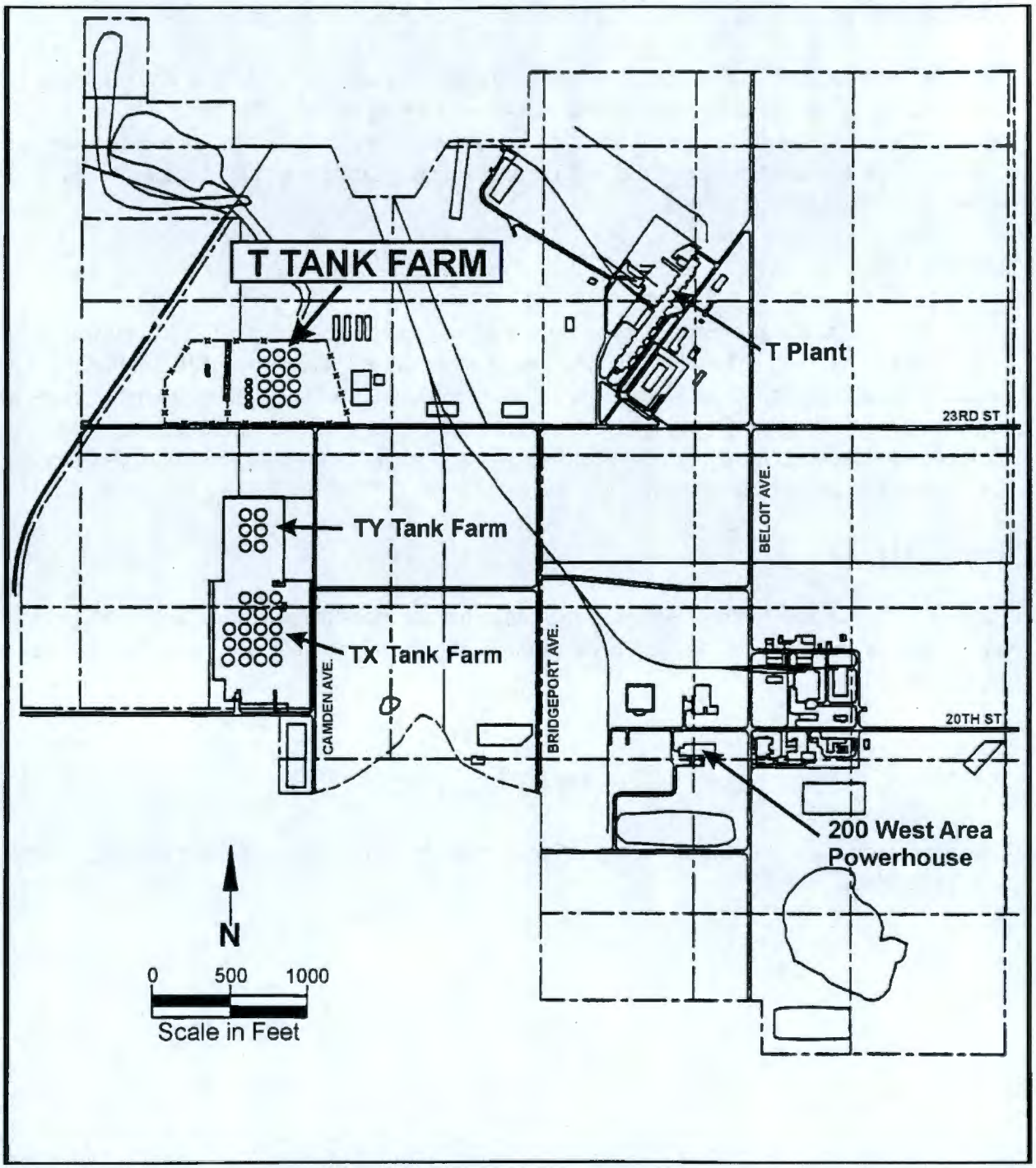

DOE (1992)

Figure 14-1. Map of the Northwestern Portion of the Hanford Site 200 West Area Showing the Location of the T Tank Farm

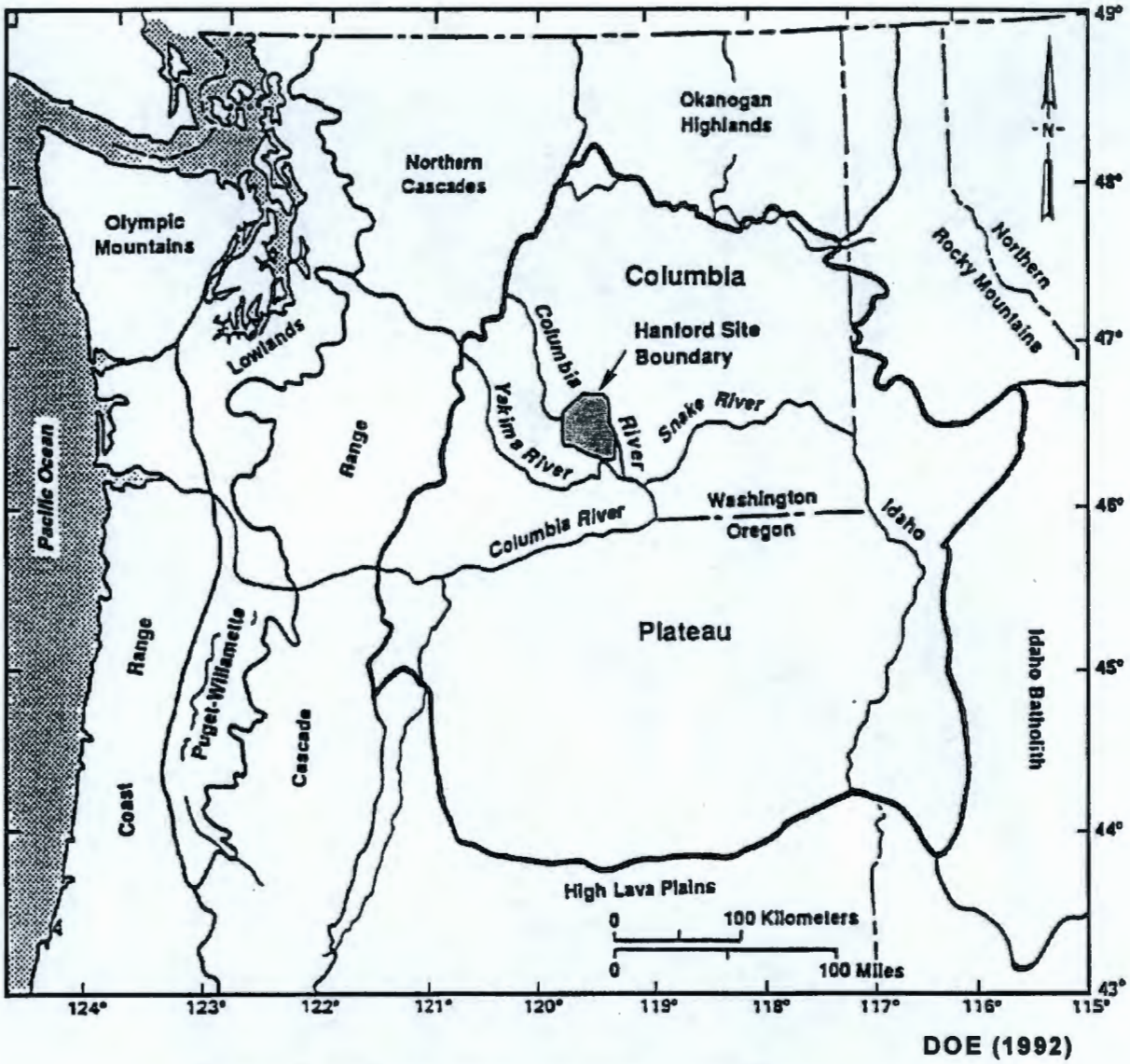

DOE (1992)

Figure 14-2. Columbia Plateau and Surrounding Structural Provinces

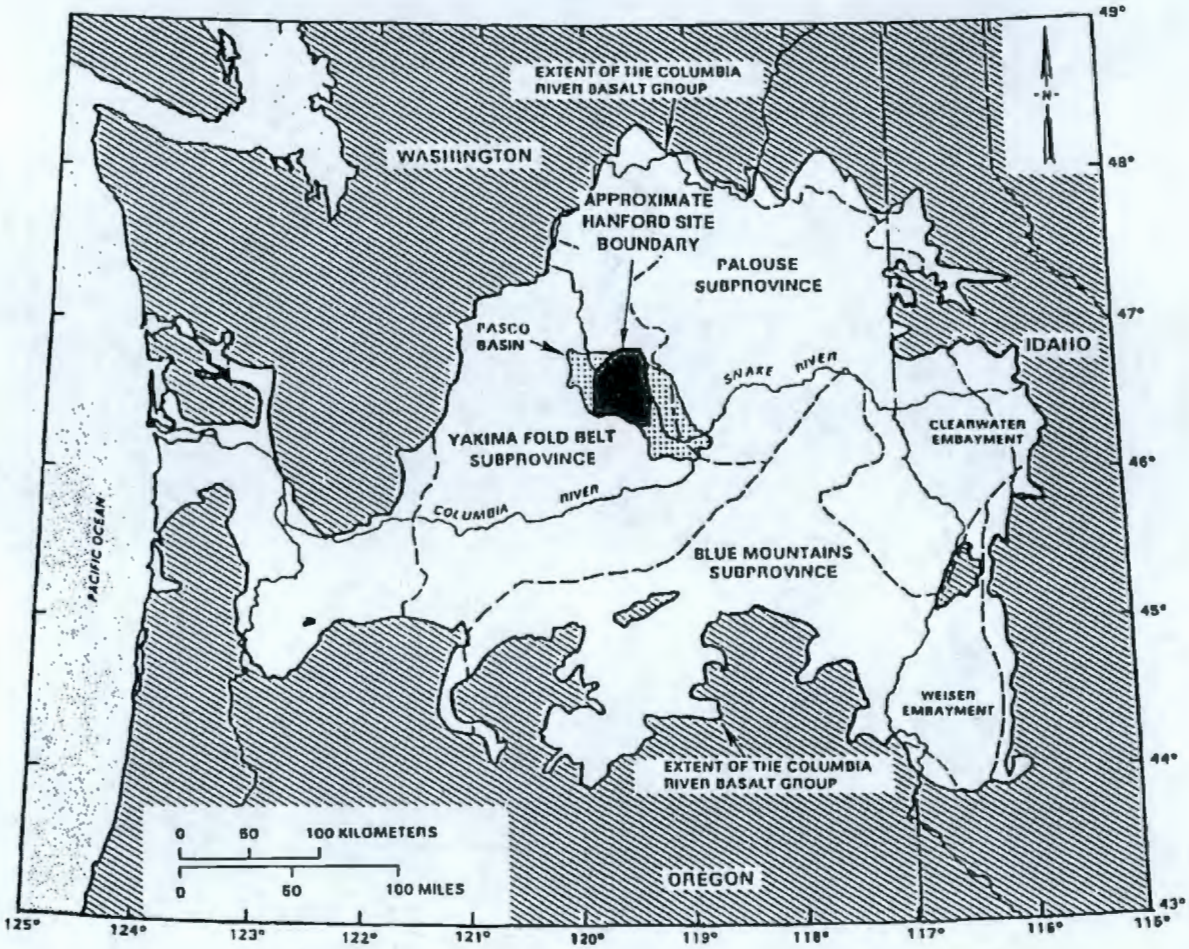

DOE (1992)

Figure 14-3. Structural Subprovinces of the Columbia Plateau

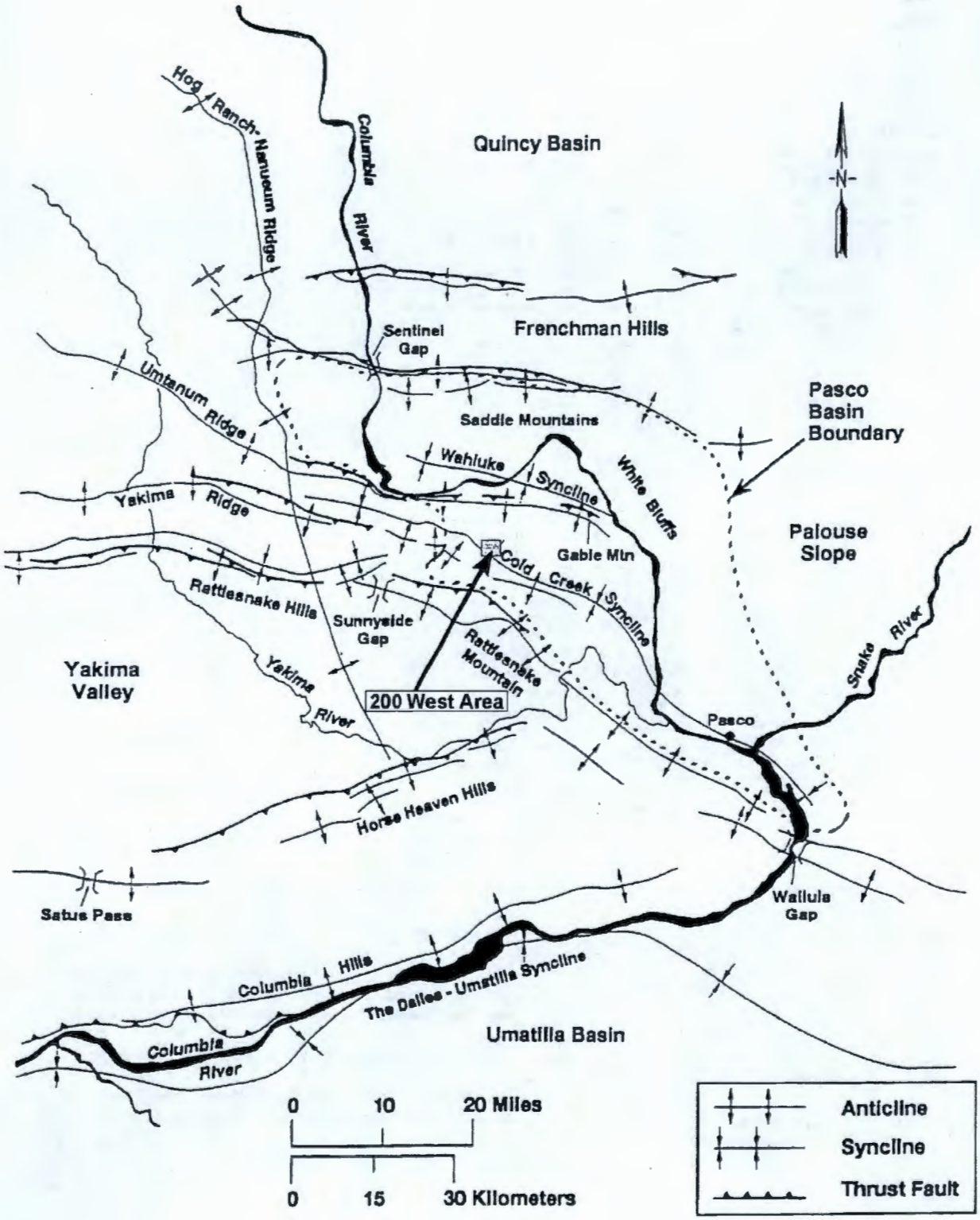

Lindsey (1995)

Figure 14-4. Geologic Structure of the Pasco Basin in the Vicinity of the Hanford Site

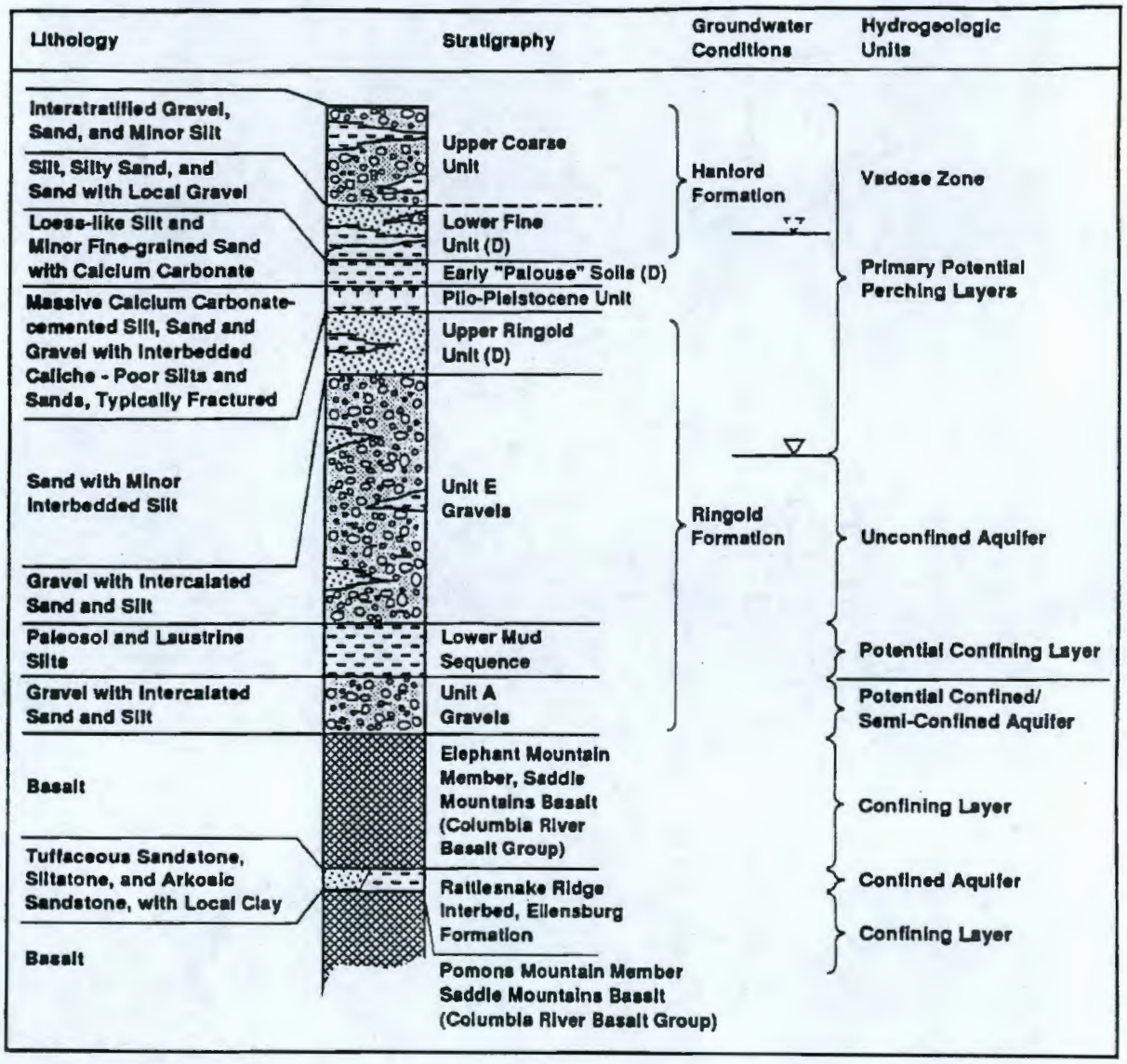

Figure 14-5. Conceptual Hydrogeologic Column for the Hanford Site

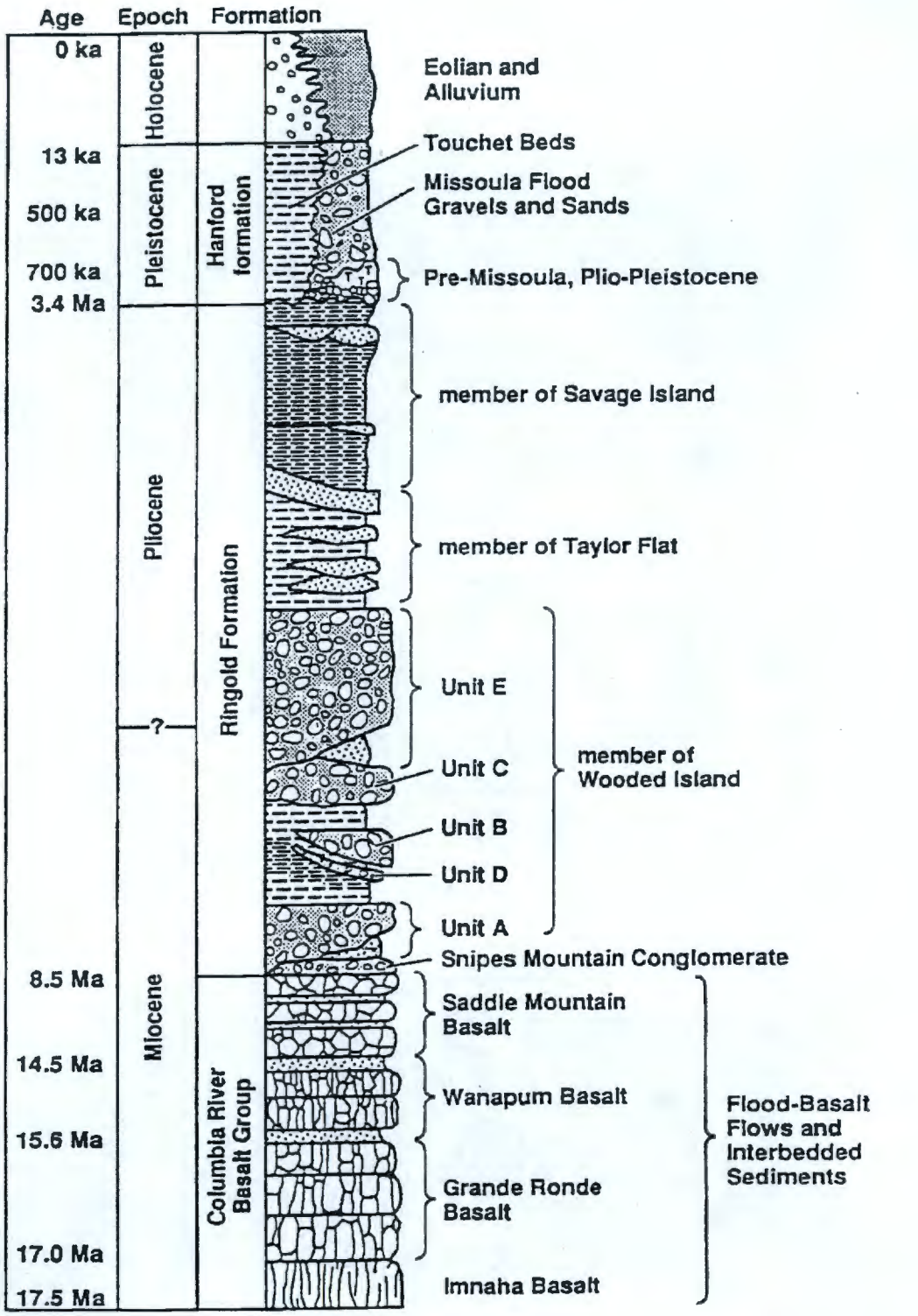

Figure 14-6. Late Neogene Stratigraphy of the Pasco Basin Emphasizing the Ringold Formation

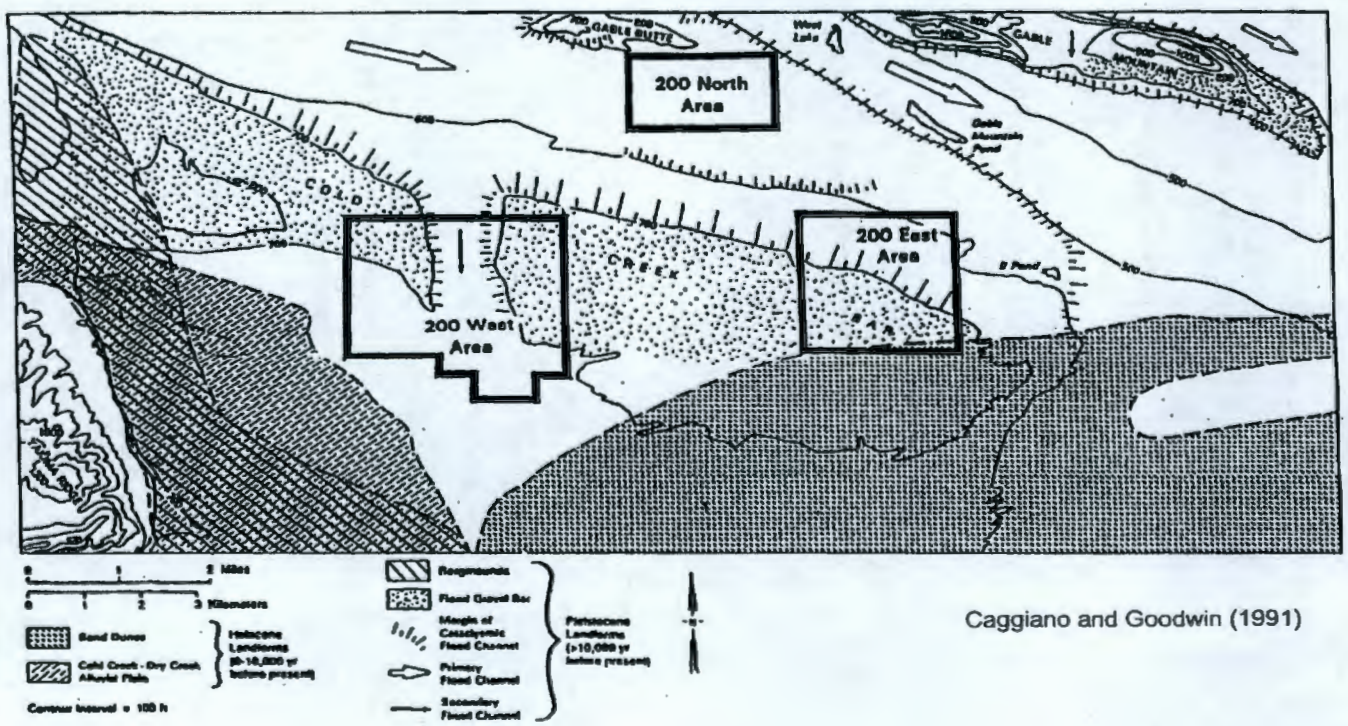

Figure 14-7. Geomorphological Map of the 200 East and 200 West Areas at the Hanford Site

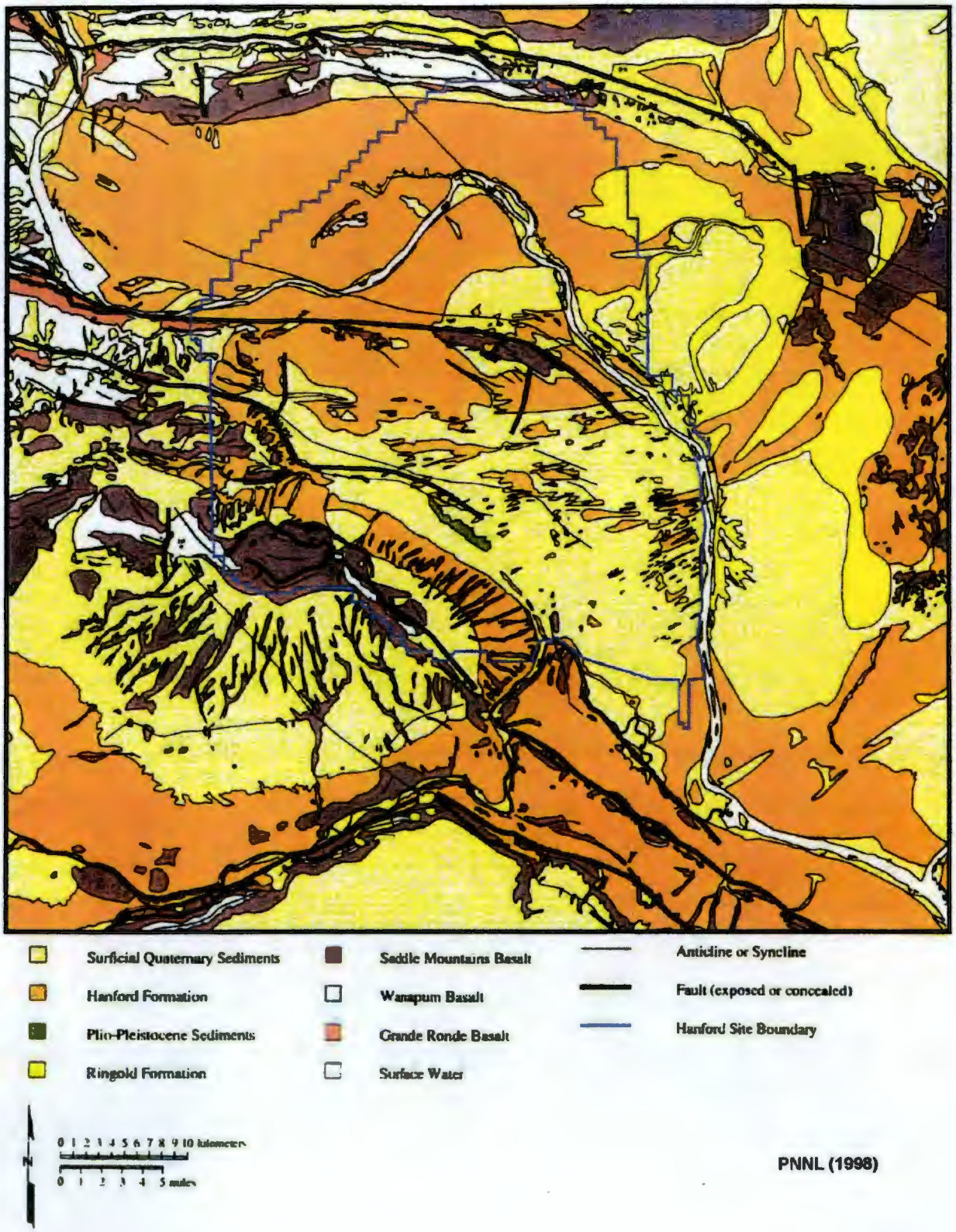

Figure 14-8. Pasco Basin Surface Geology and Structural Features

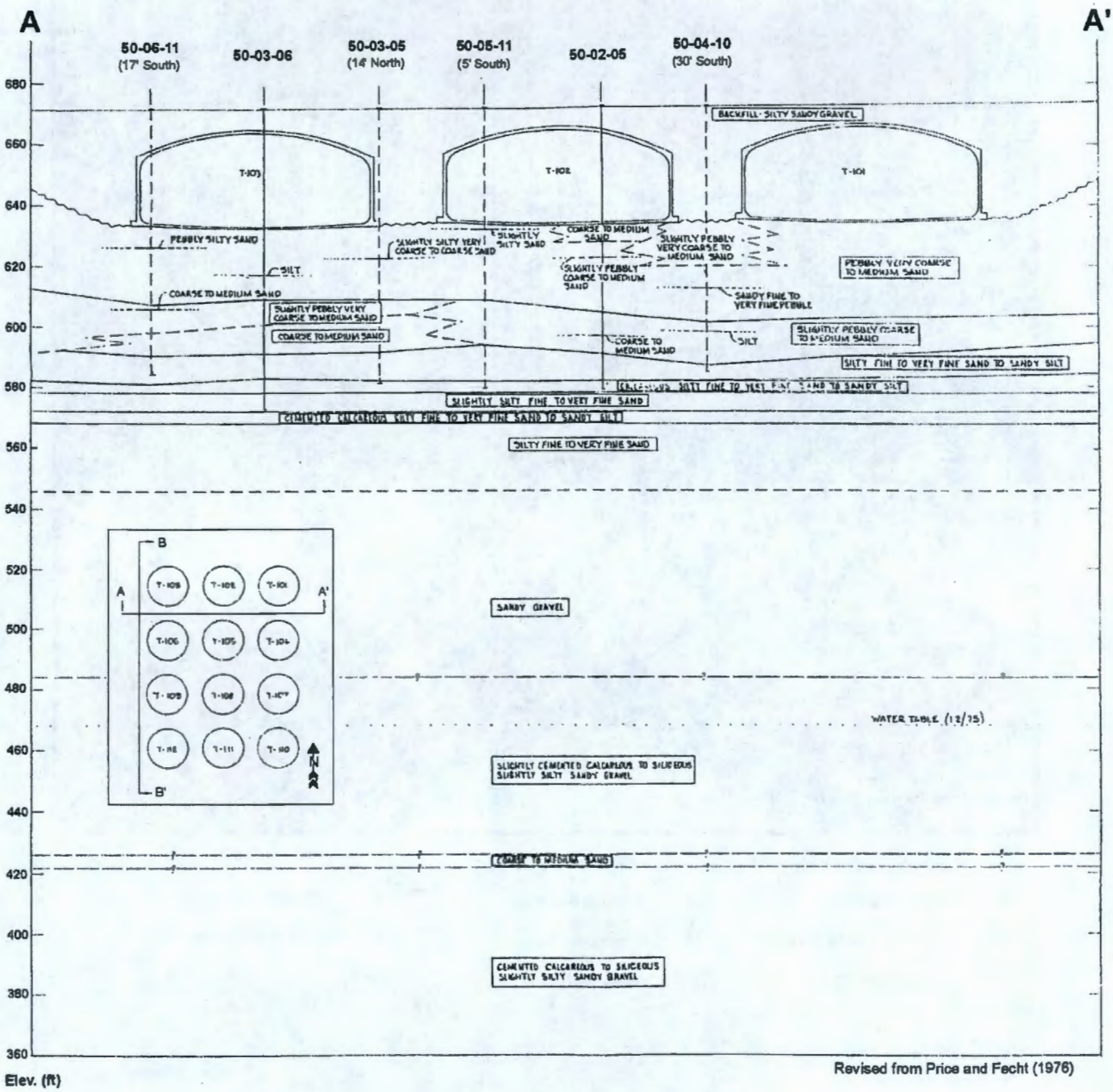

Figure 14-9. Cross Section AA' Across the T Tank Farm

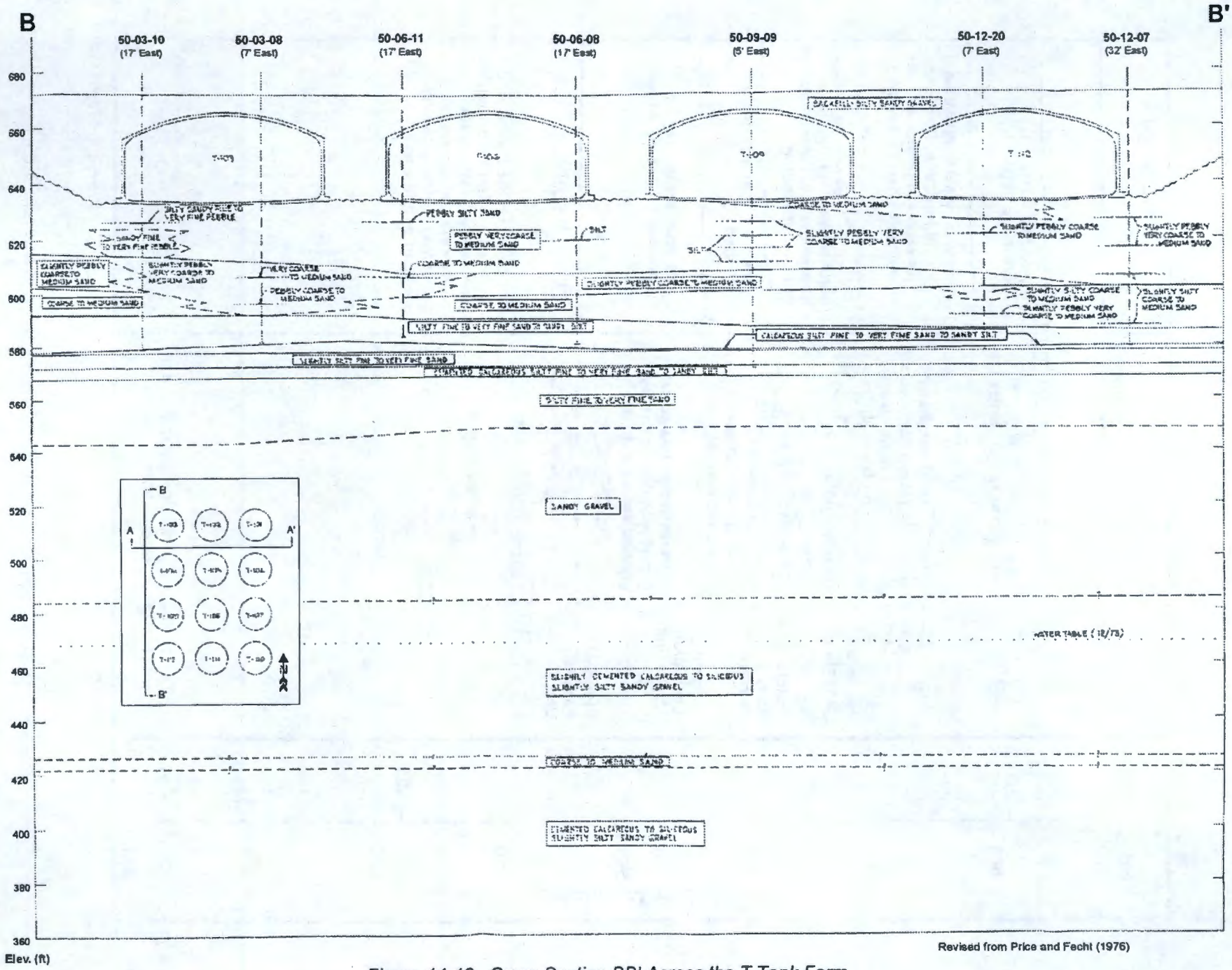

Revised from Price and Fecht (1976)

Figure 14-10. Cross Section BB' Across the T Tank Farm

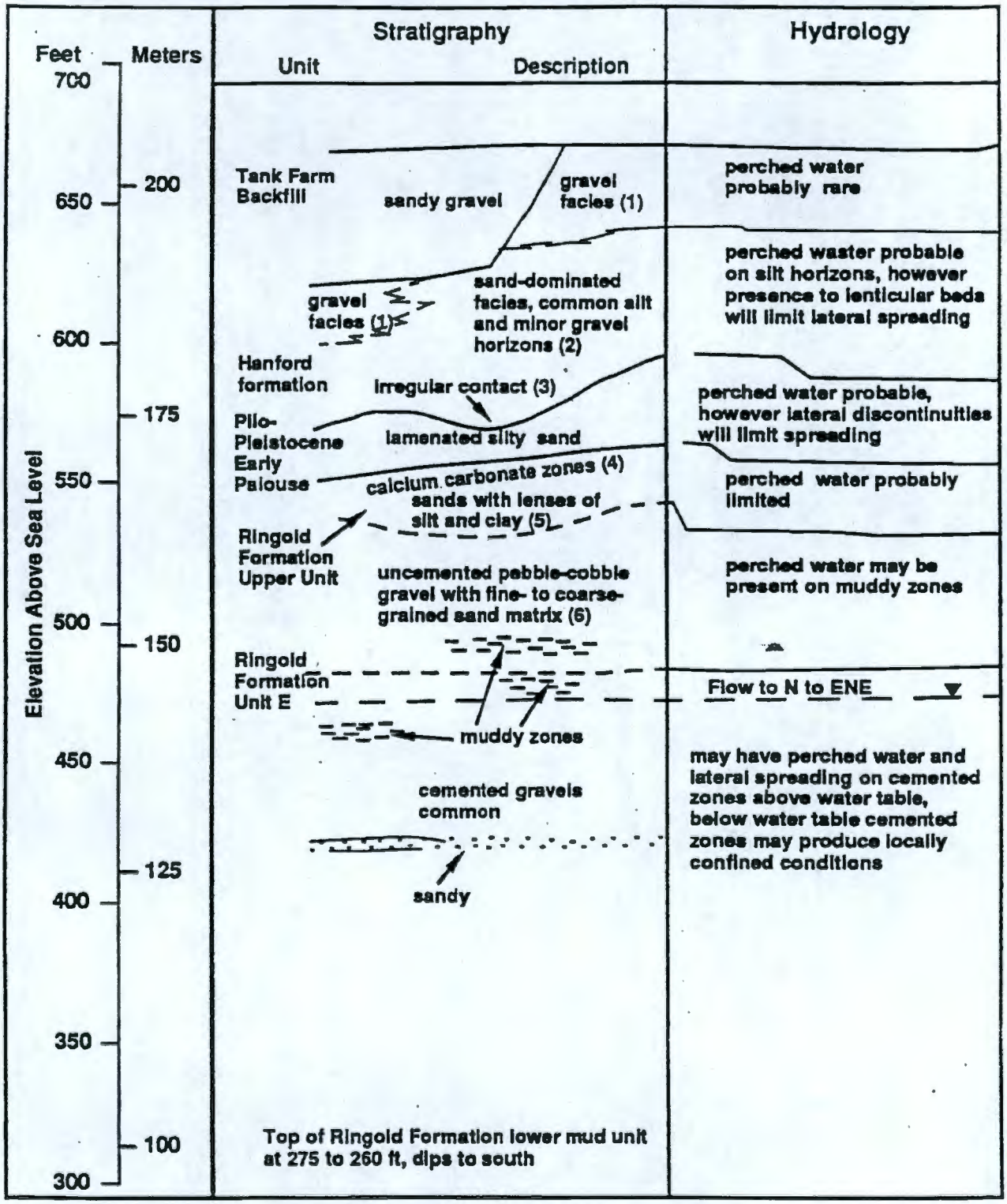

From Lindsey (1993)

Figure 14-11. Conceptual Geohydrological Setting of the T-TX-TY Tank Farms

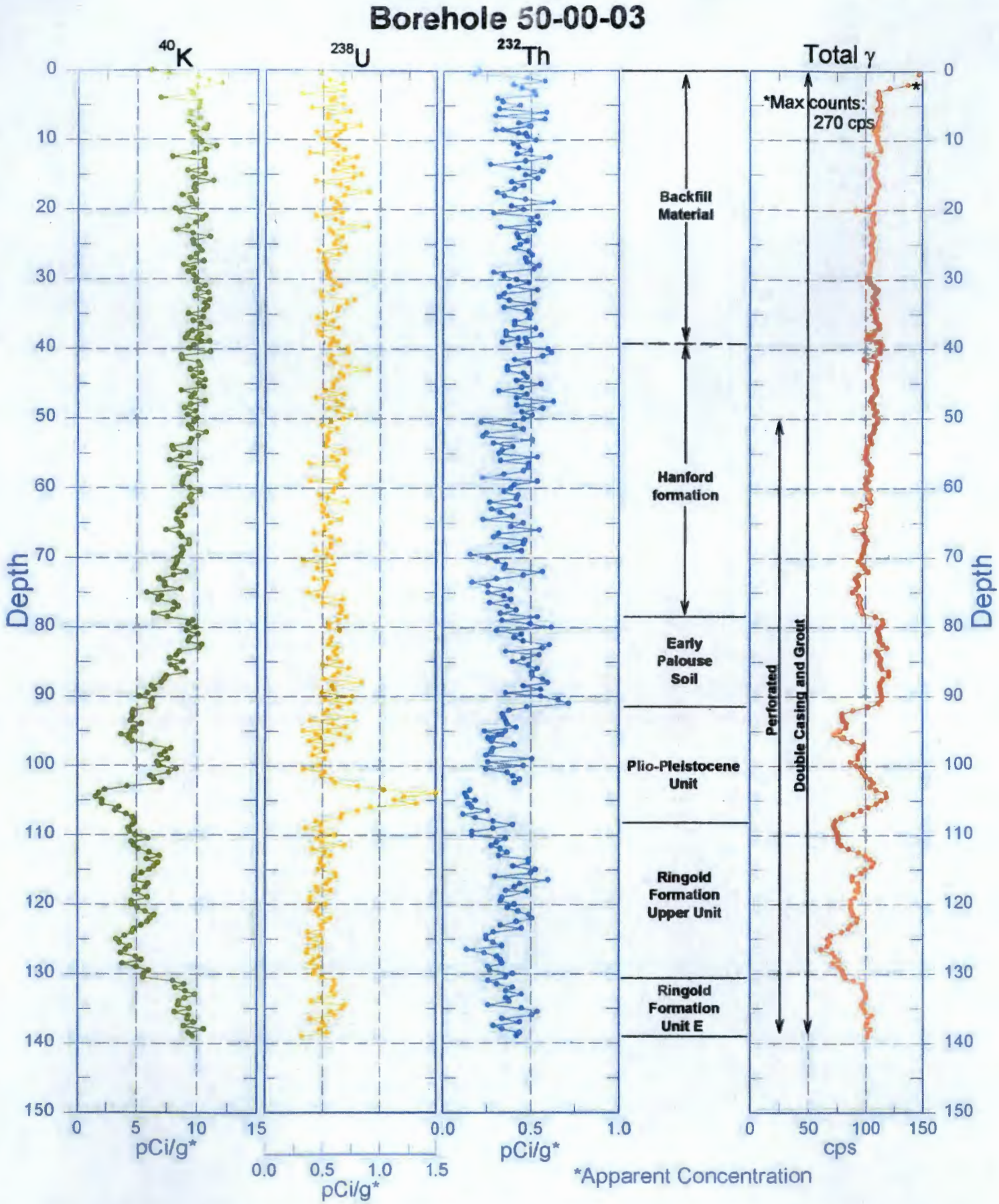

Figure 14-12. Lithological Features Identified From SGLS (KUT) Data From Borehole 50-00-03

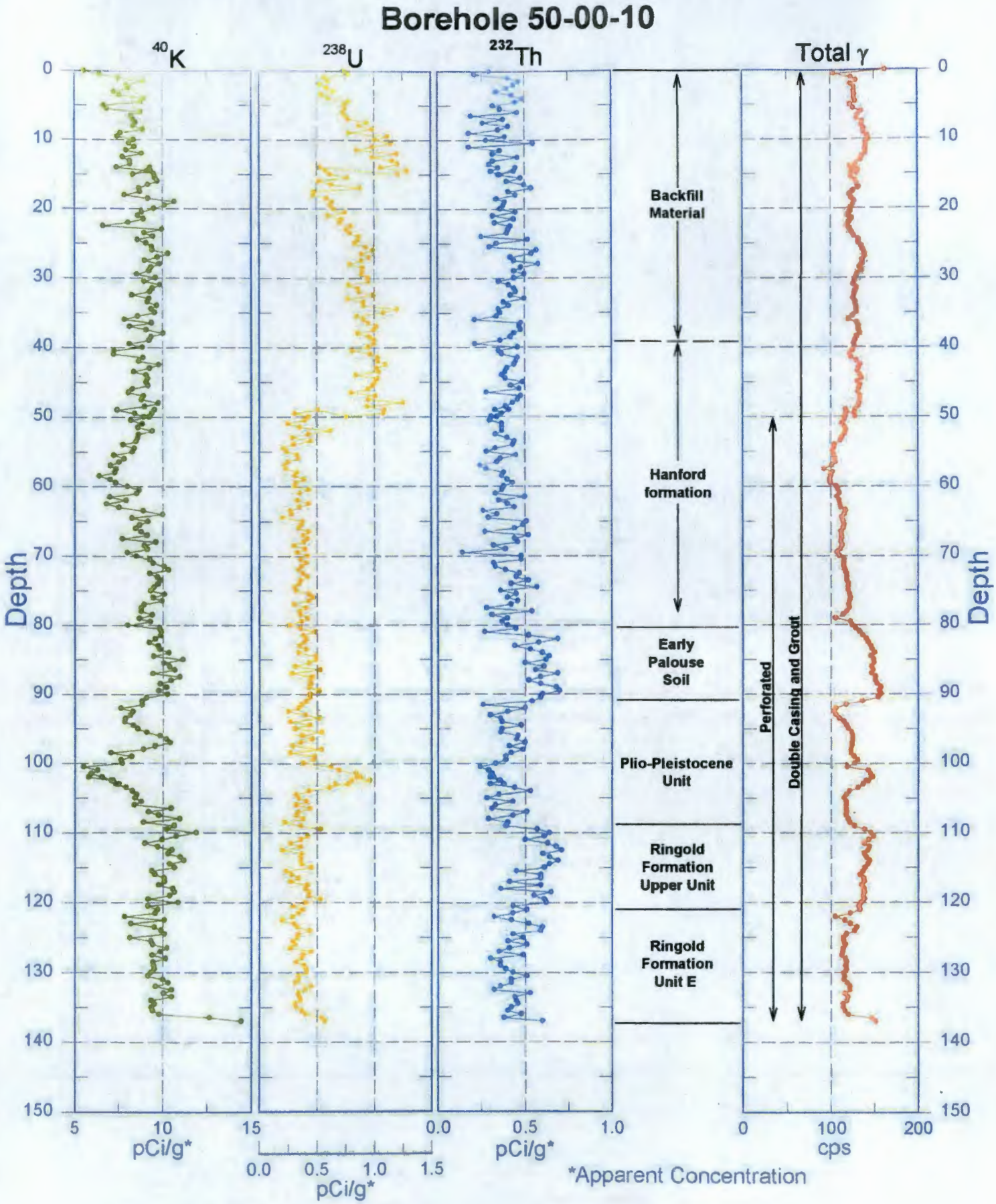

Figure 14-13. Lithological Features Identified From SGLS (KUT) Data From Borehole 50-00-10

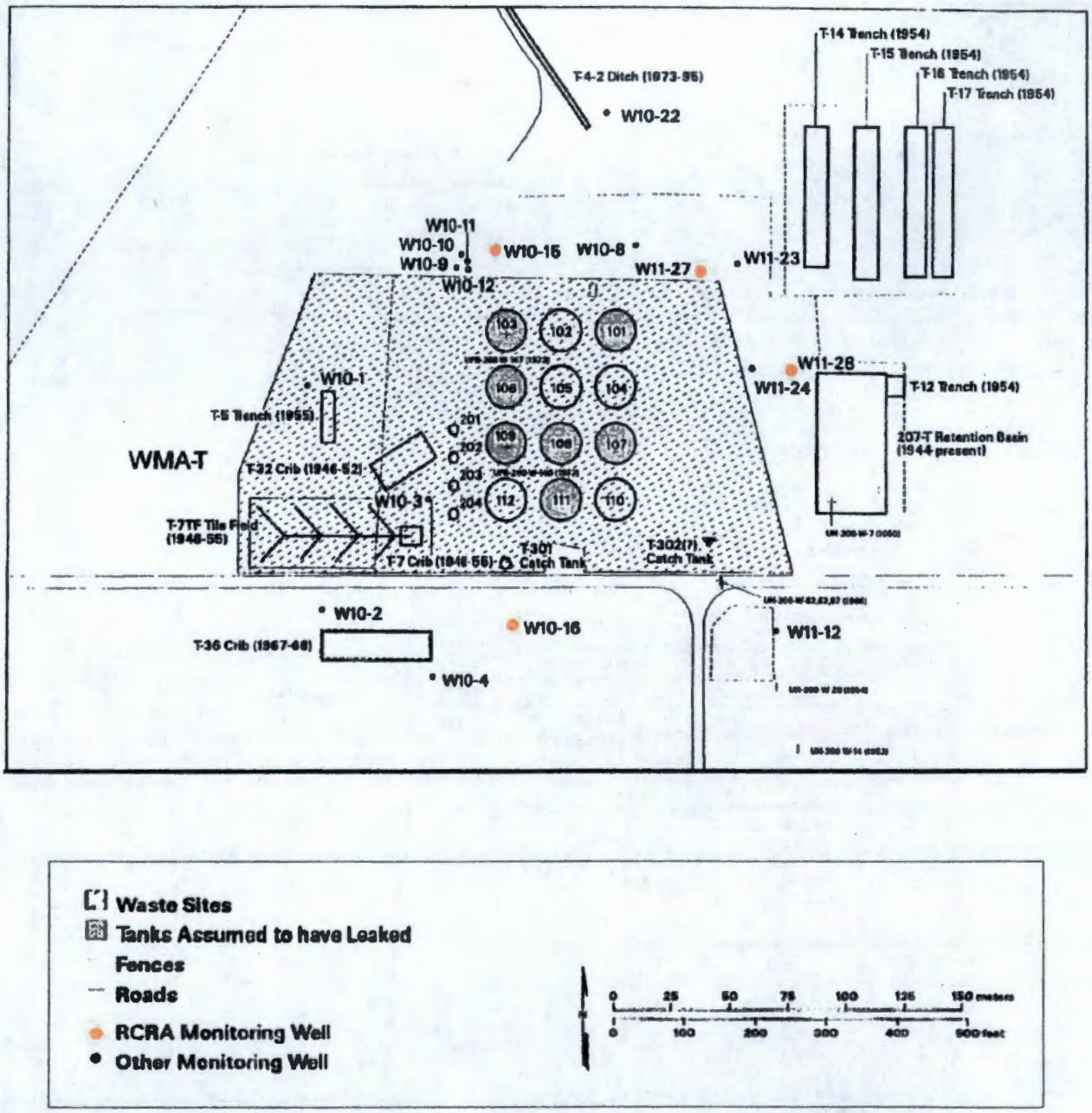

Figure 14-14. Plan Map of WMA-T Showing the Locations of the Groundwater Monitoring Wells

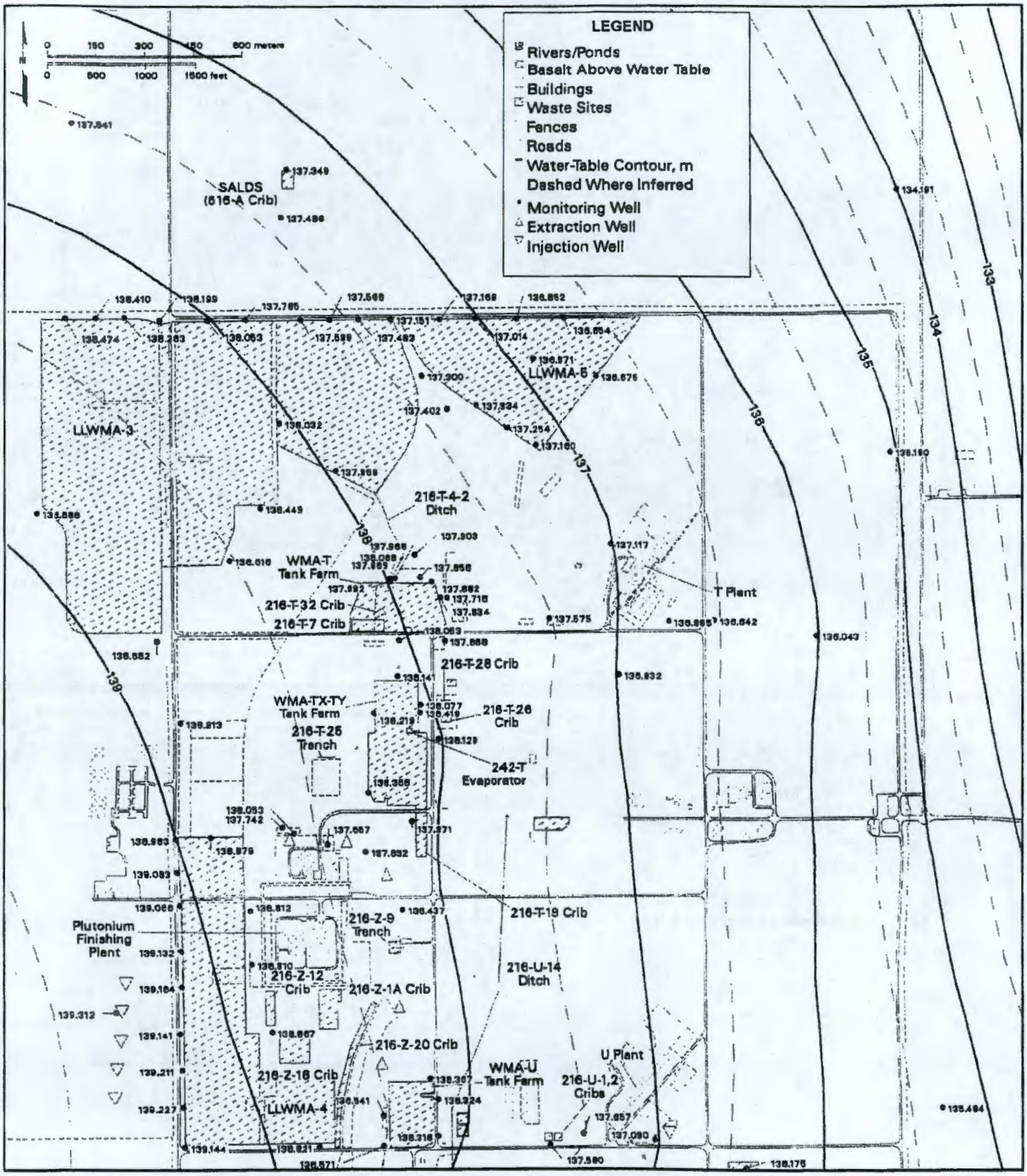

PNNL (1998)

Figure 14-15. 1997 Water Table Elevation Map for a Portion of the 200 West Area

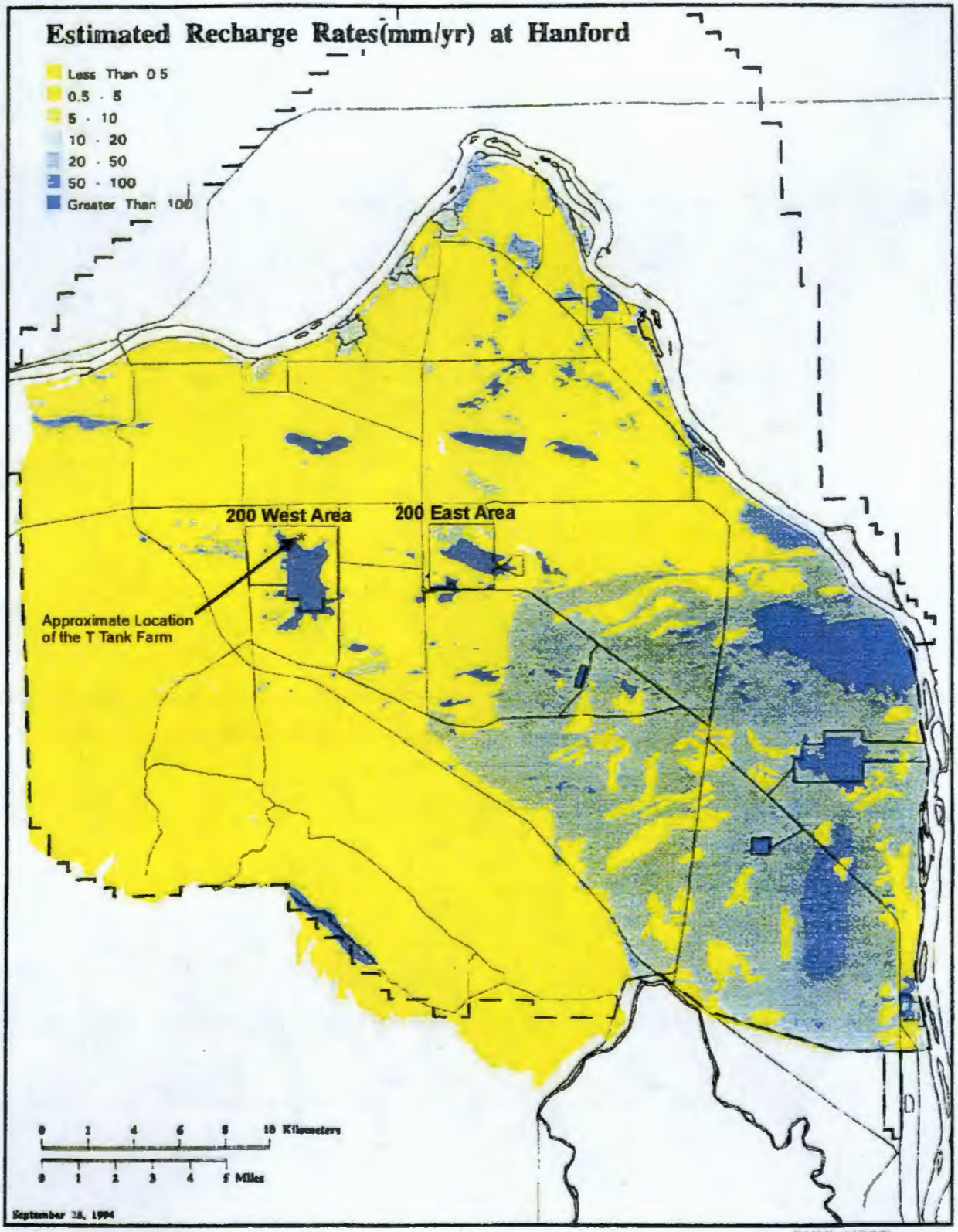

PNNL (1998)

Figure 14-16. Estimated Annual Recharge of Precipitation and Irrigation

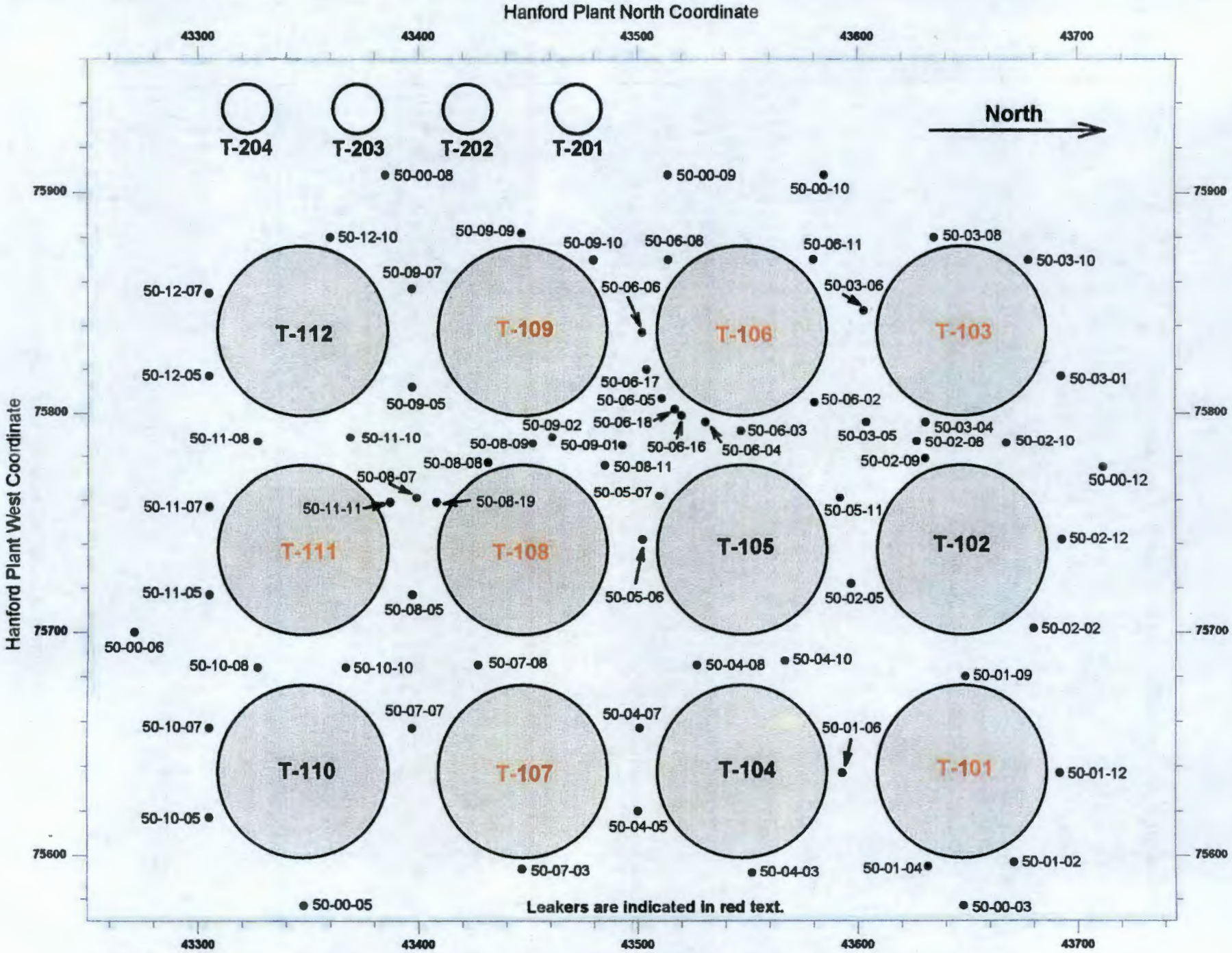

Figure 14-17. Plan Map of the T Tank Farm Showing the Location of the Tank Monitoring Boreholes

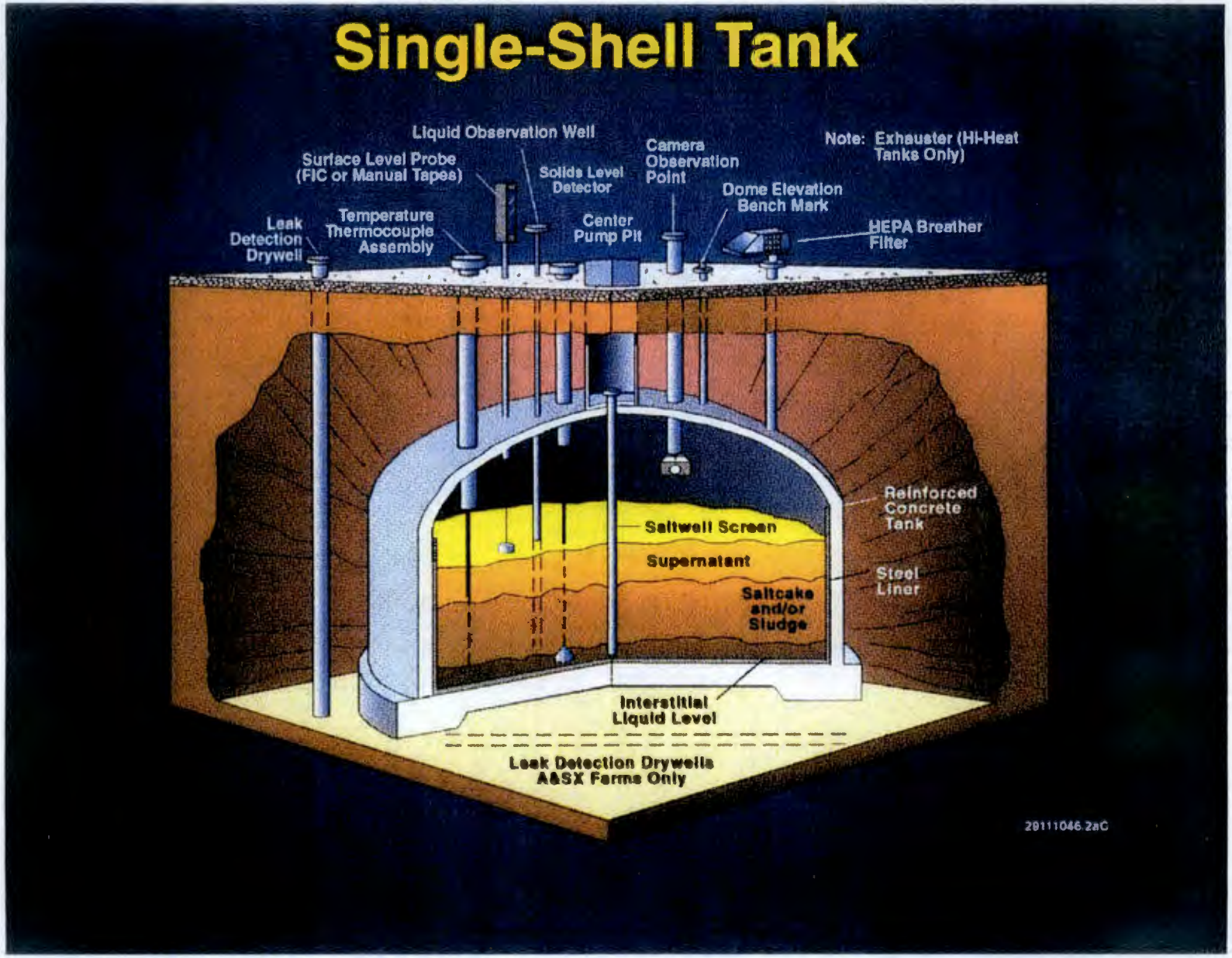

Figure 14-18. Cutaway Section of a Typical Single-Shell Tank Showing Tank Risers and Various Instrument Ports

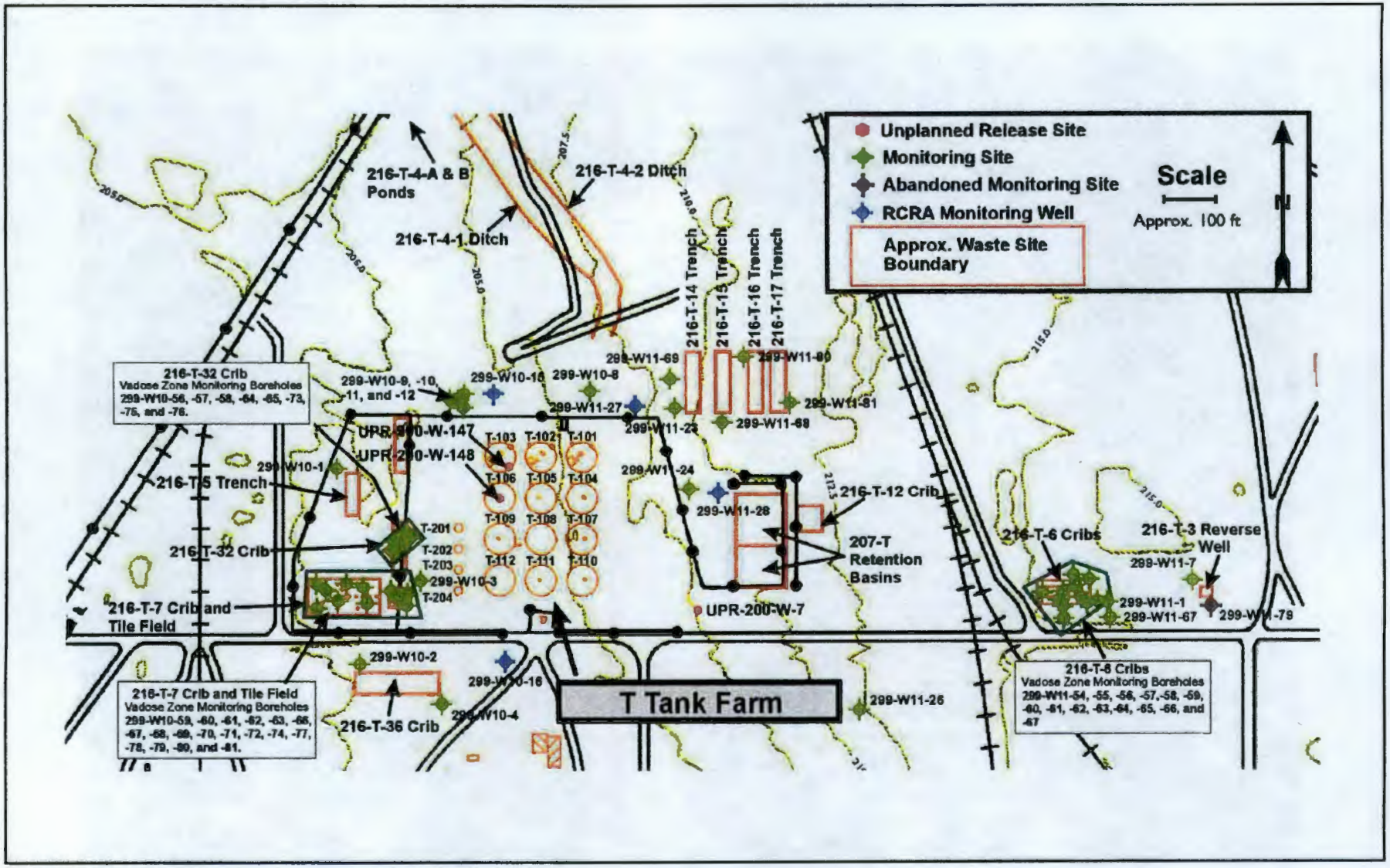

Figure 14-19. Plan Map of the 200 West Area in the Vicinity of the T Tank Farm Showing Adjacent Tank Farms, Waste Disposal Facilities, Unplanned Release Locations, and Monitoring Sites

Figure 14-20. View of a Spectral Gamma Logging System Rigged for Logging

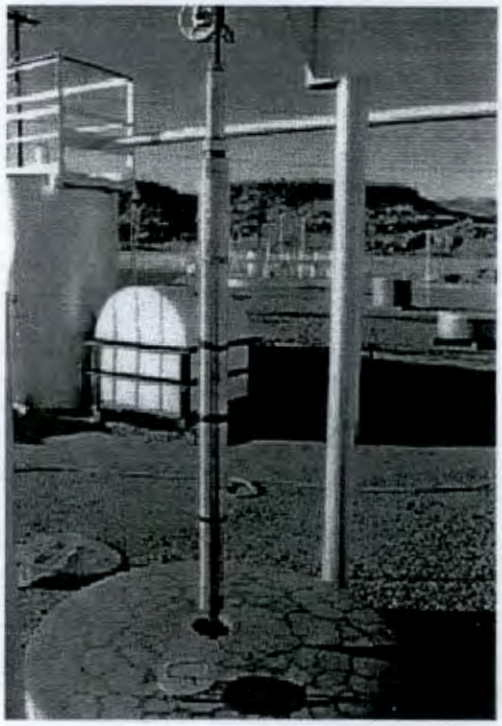

Figure 14-21. Probe With High-Purity Germanium Detector Suspended Over a Borehole

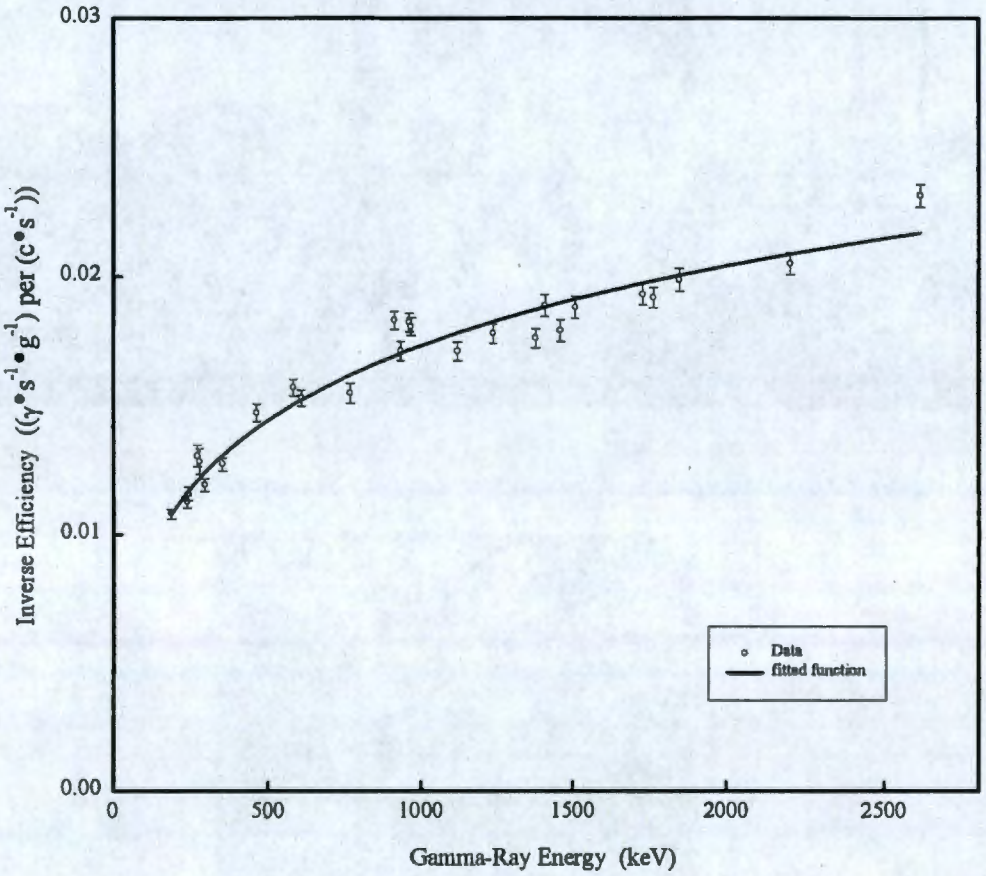

Figure 14-22. SGLS Base Calibration Efficiency Function

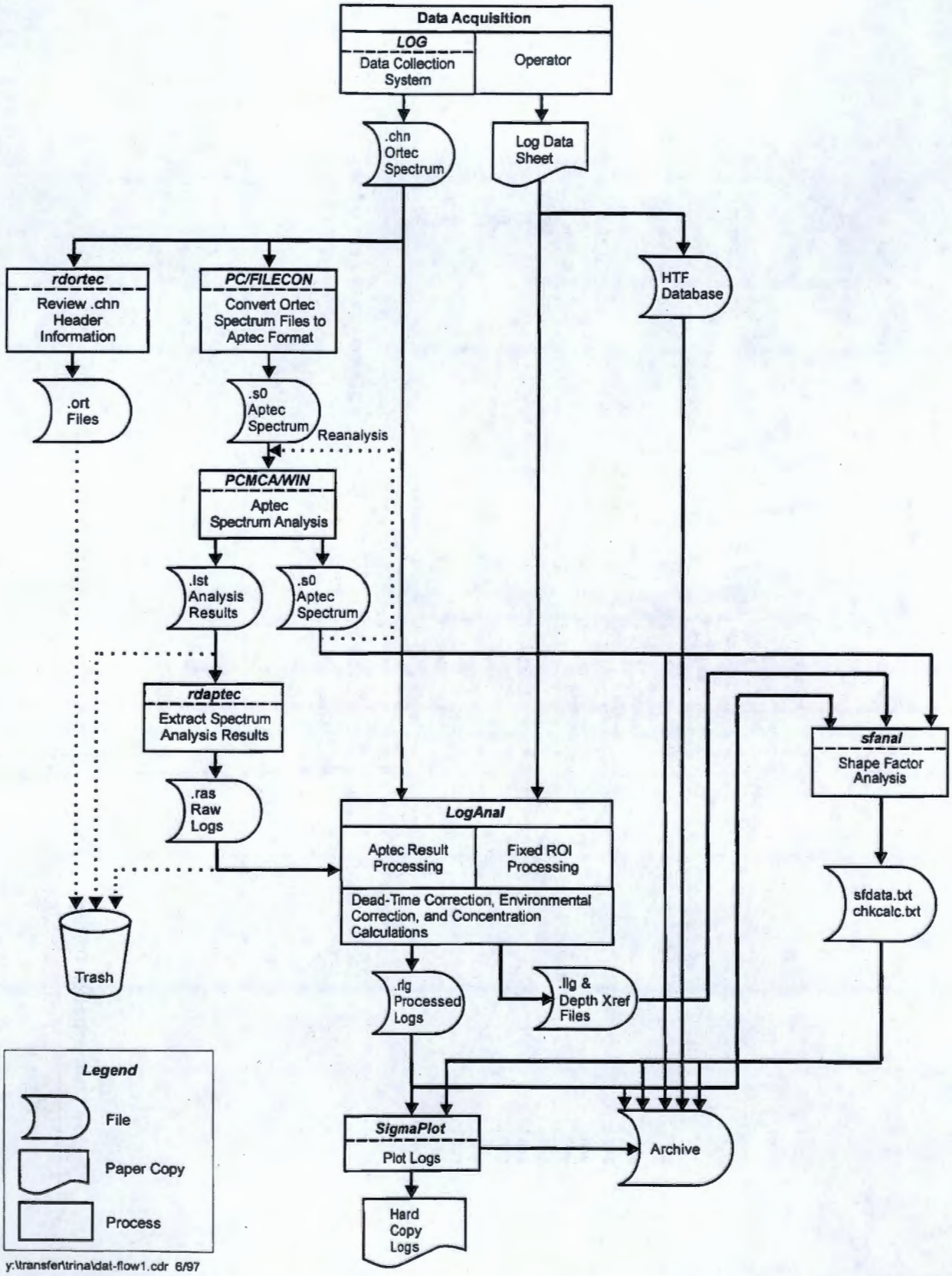

Figure 14-23. Hanford Tank Farm Vadose Zone Data Analysis Process

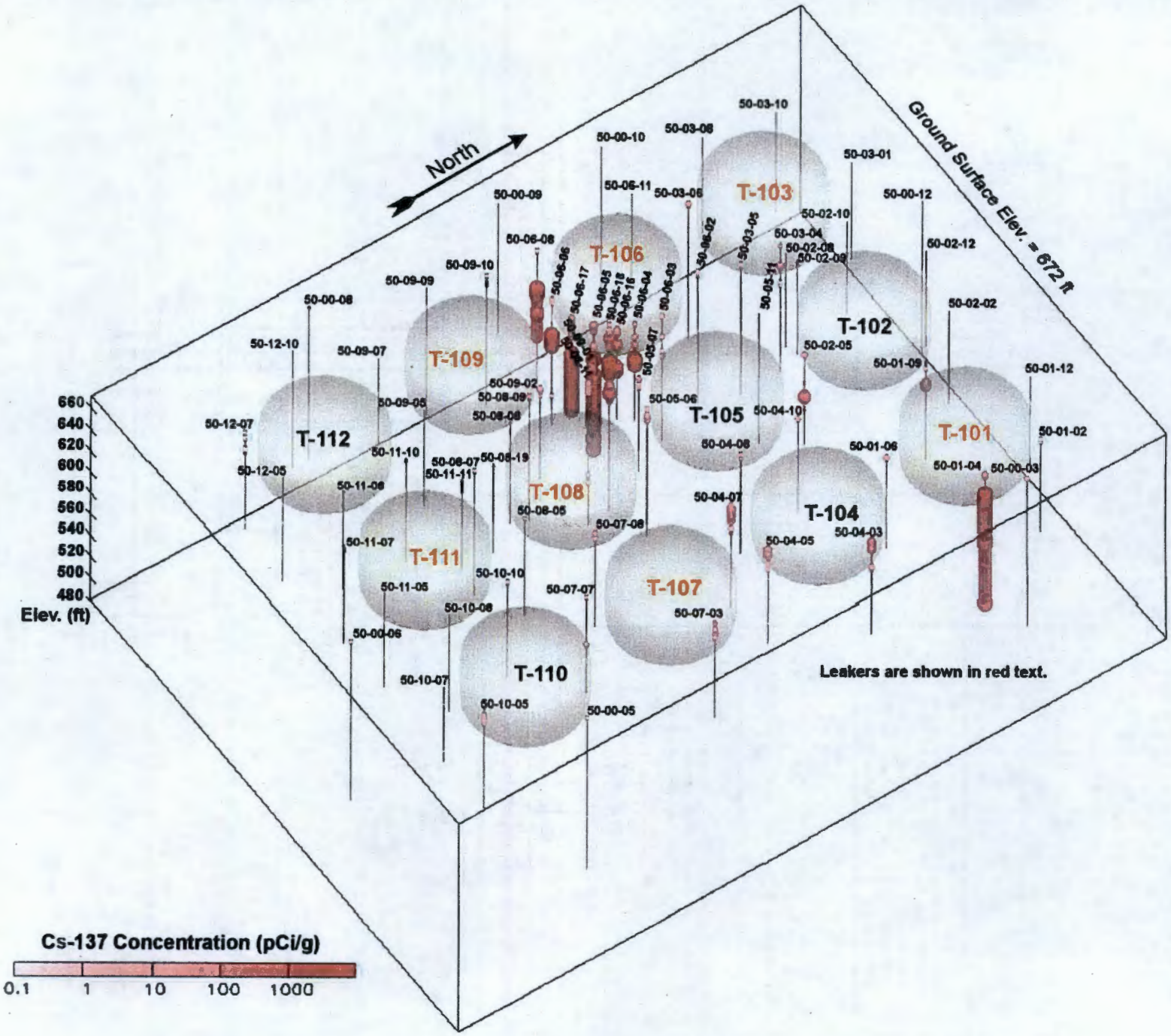

Figure 14-24. Visualization of ^{137}Cs SGLS Data Acquired at the T Tank Farm

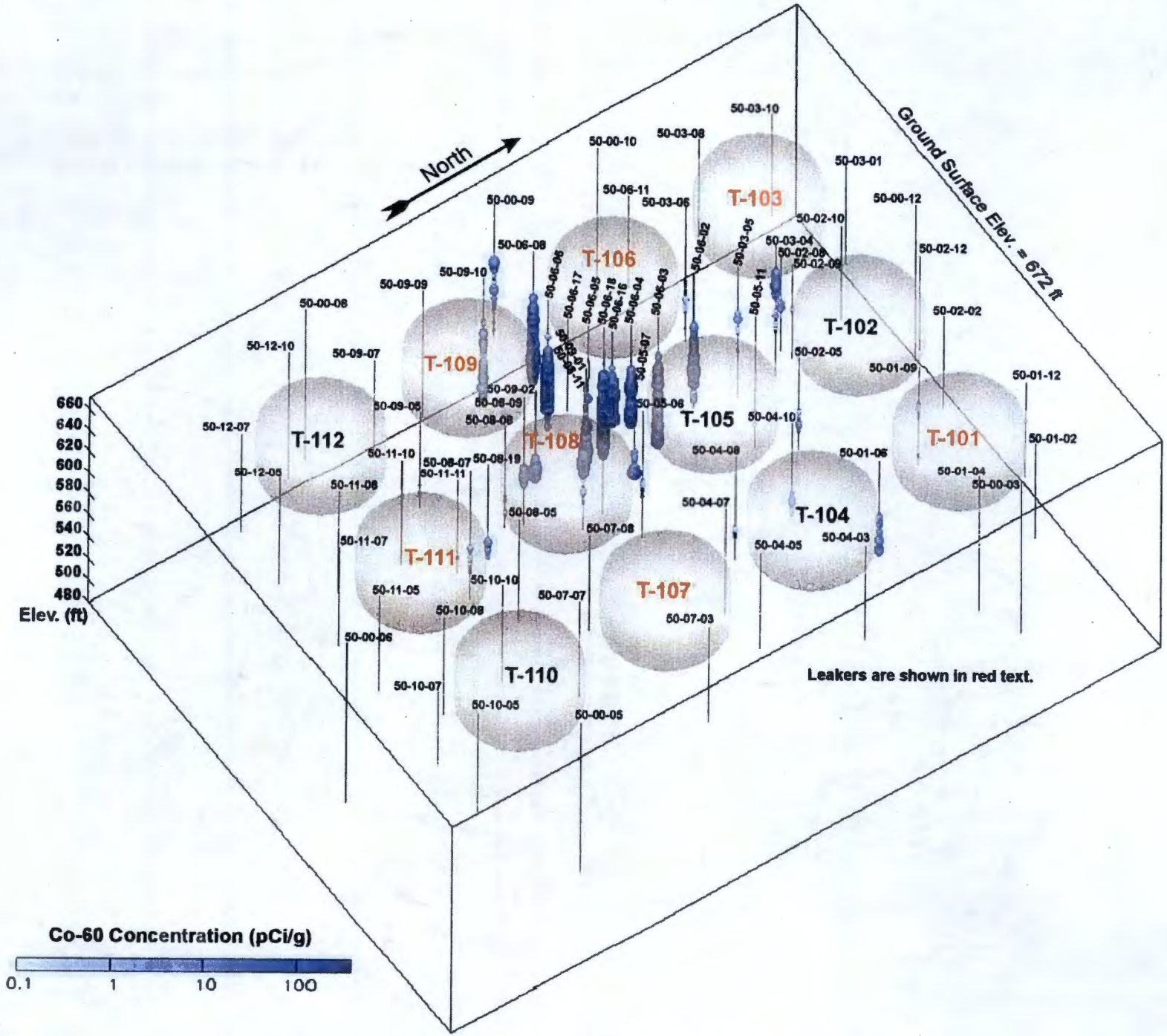

Figure 14-25. Visualization of ^{60}Co SGLS Data Acquired at the T Tank Farm

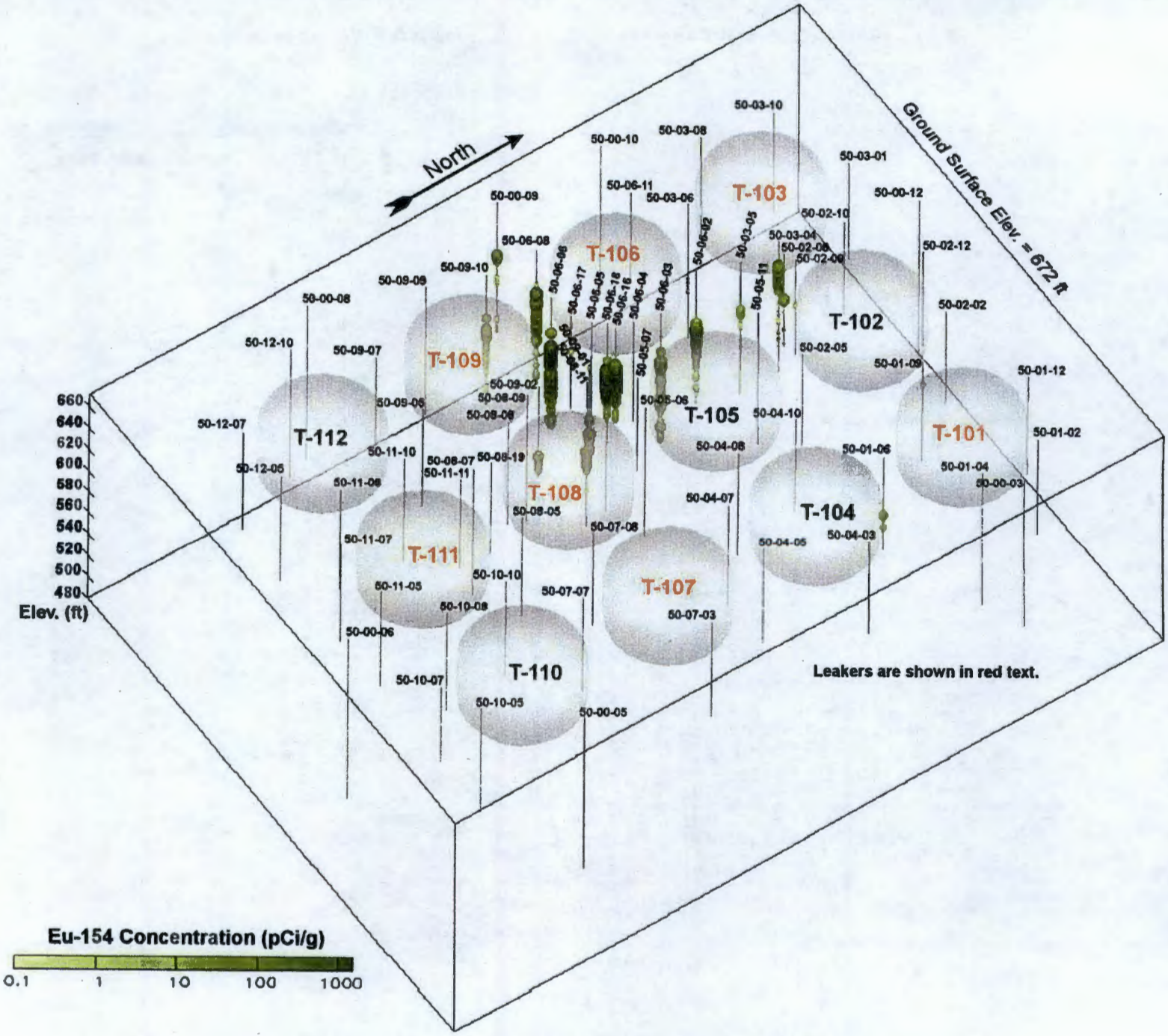

Figure 14-26. Visualization of ^{154}Eu SGLS Data Acquired at the T Tank Farm

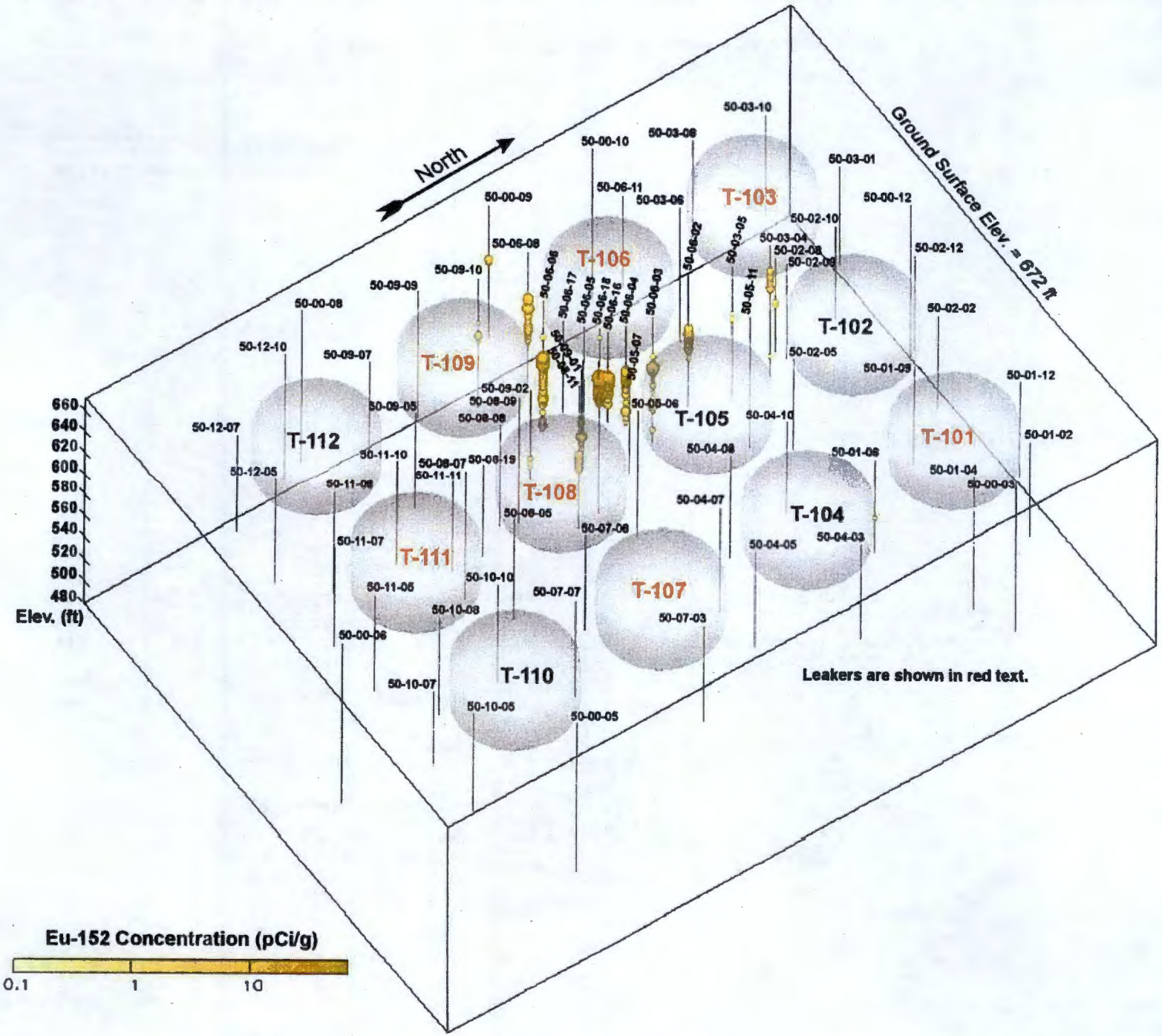

Figure 14-27. Visualization of ^{152}Eu SGLS Data Acquired at the T Tank Farm

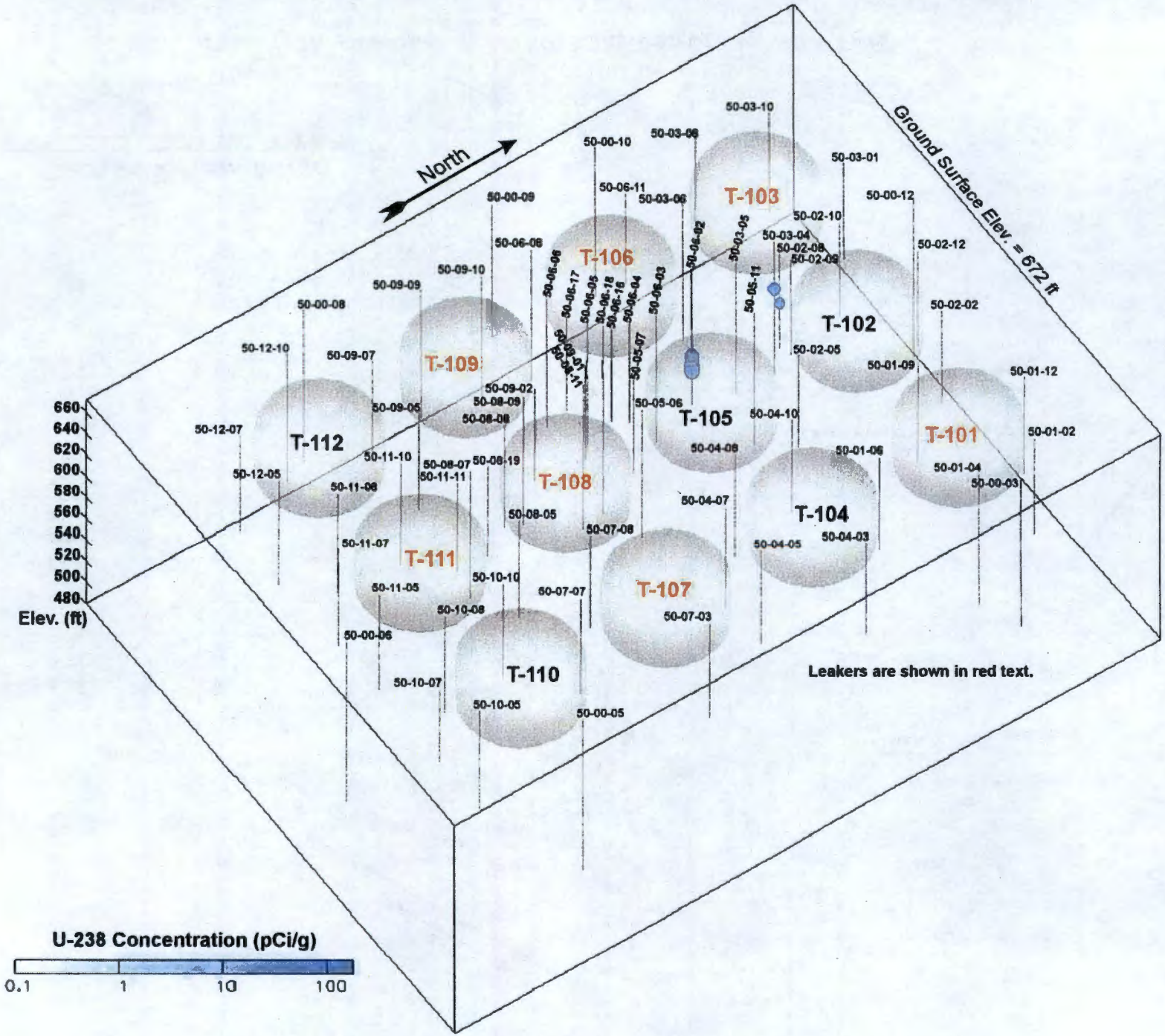

Figure 14-28. Visualization of ^{238}U SGLS Data Acquired at the T Tank Farm

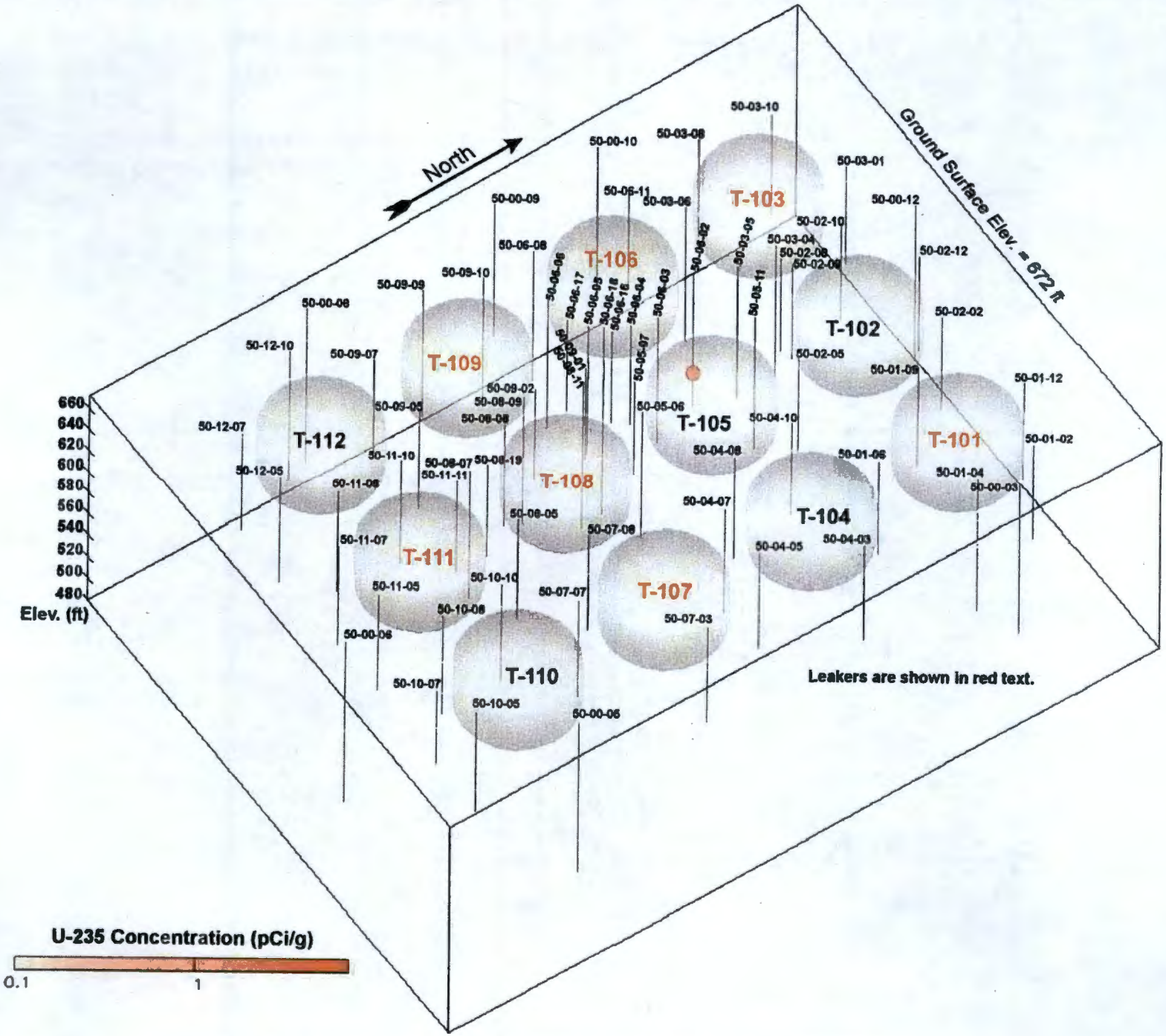

Figure 14-29. Visualization of ^{235}U SGLS Data Acquired at the T Tank Farm

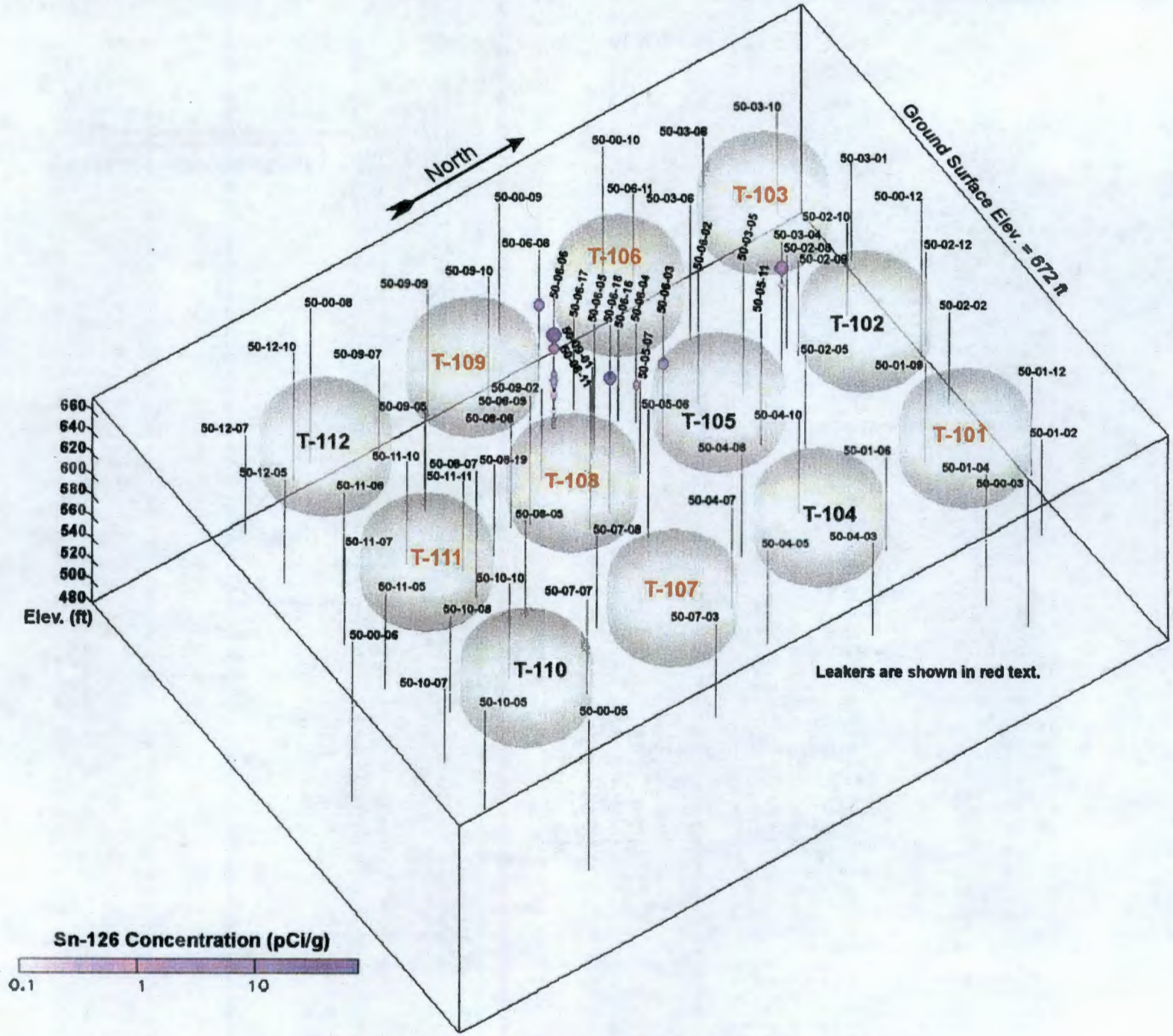

Figure 14-30. Visualization of ^{126}Sn SGLS Data Acquired at the T Tank Farm

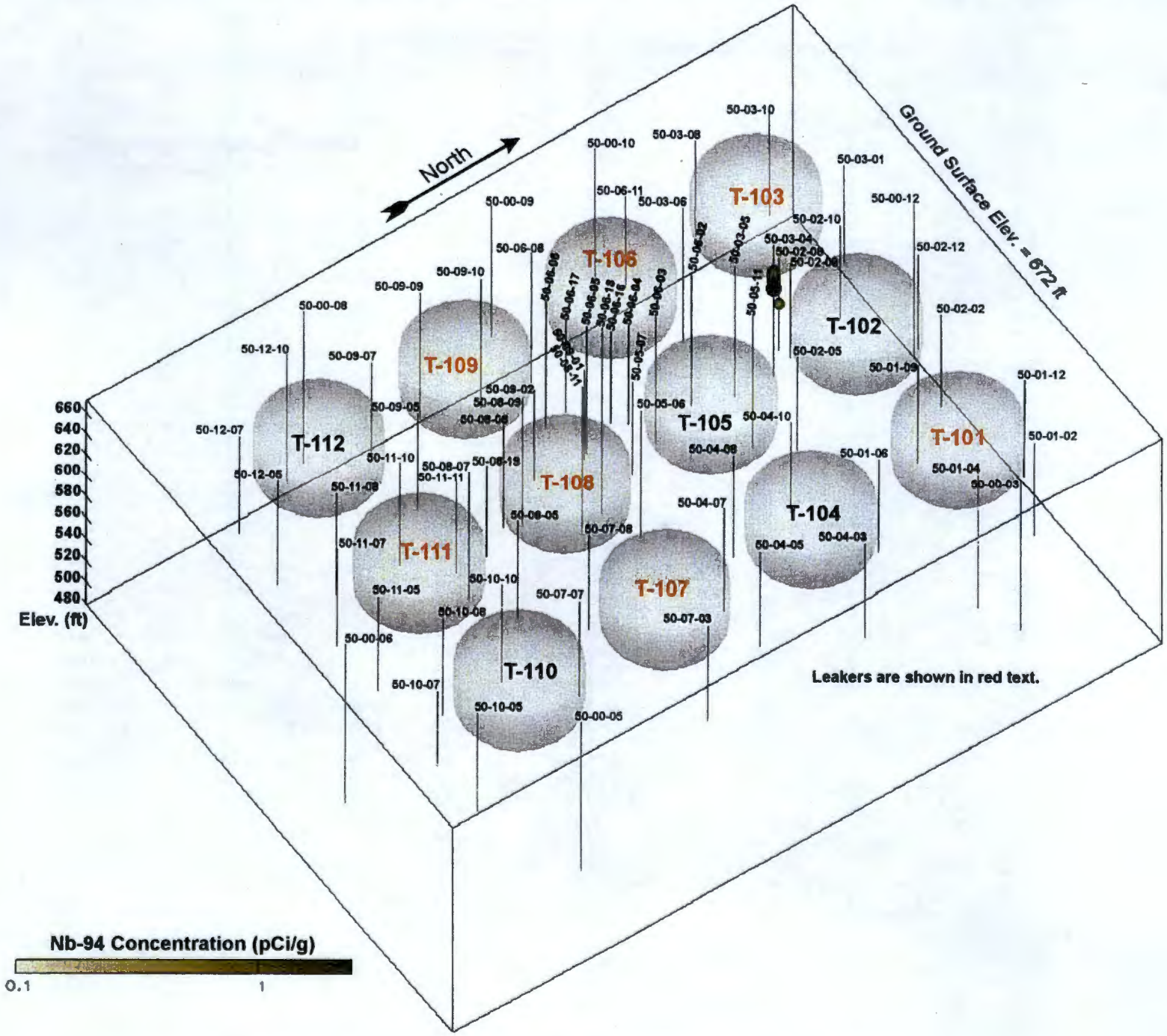

Figure 14-31. Visualization of ^{94}Nb SGLS Data Acquired at the T Tank Farm

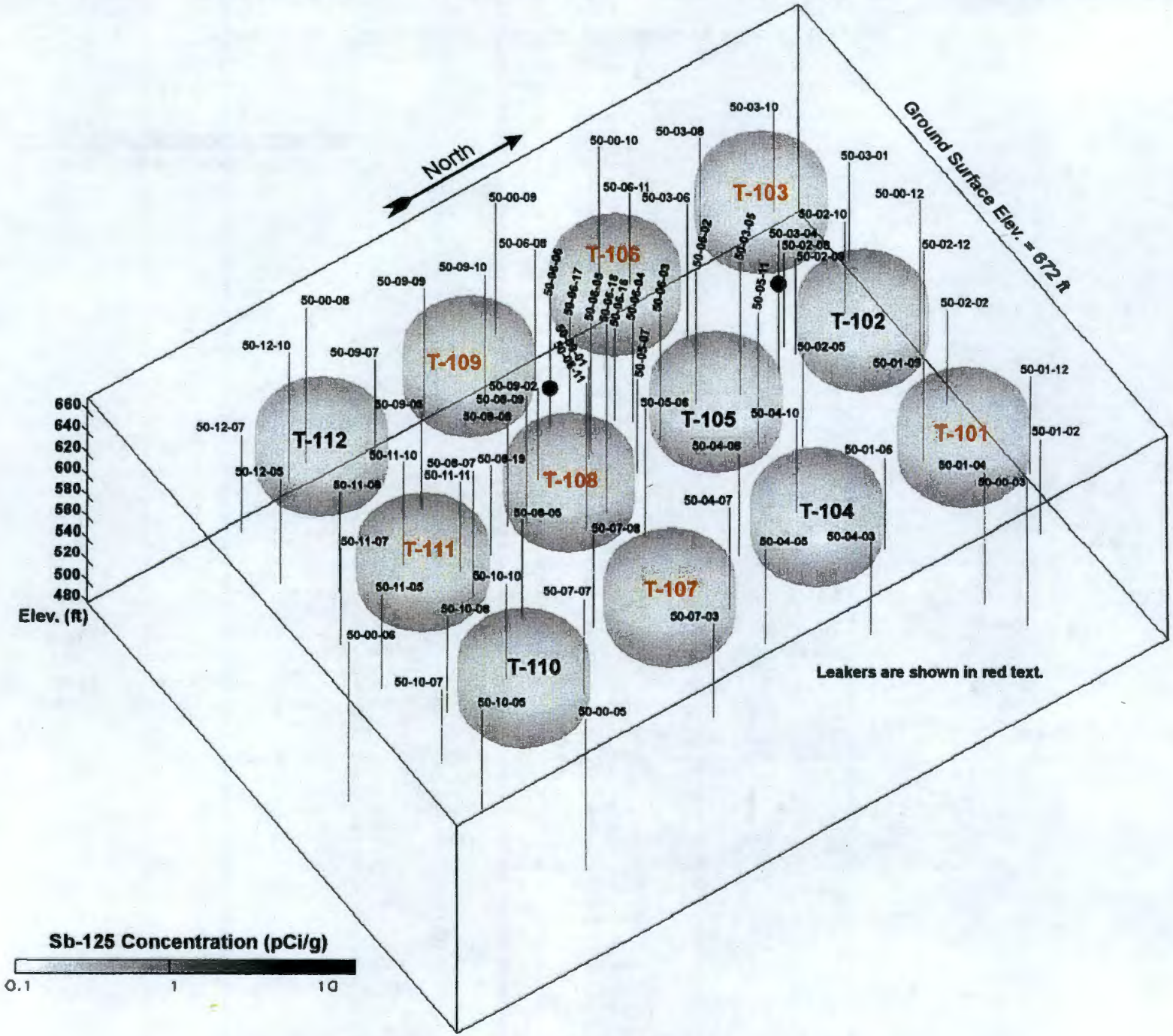

Figure 14-32. Visualization of ^{125}Sb SGLS Data Acquired at the T Tank Farm

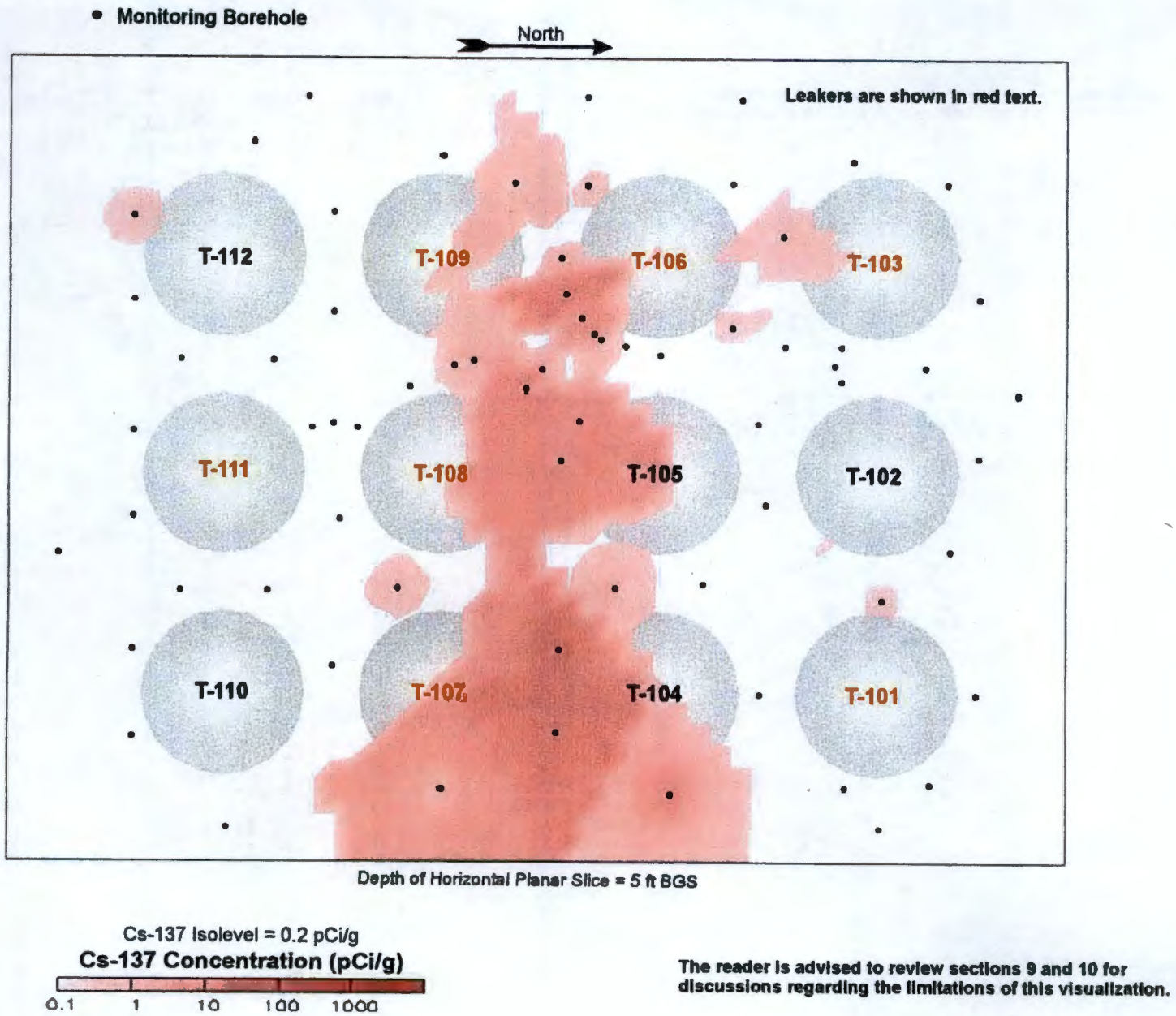

Figure 14-33. Visualization of ^{137}Cs Contamination at the T Tank Farm at a Depth of 5 Ft Below Ground Surface Viewed From Above the Tanks

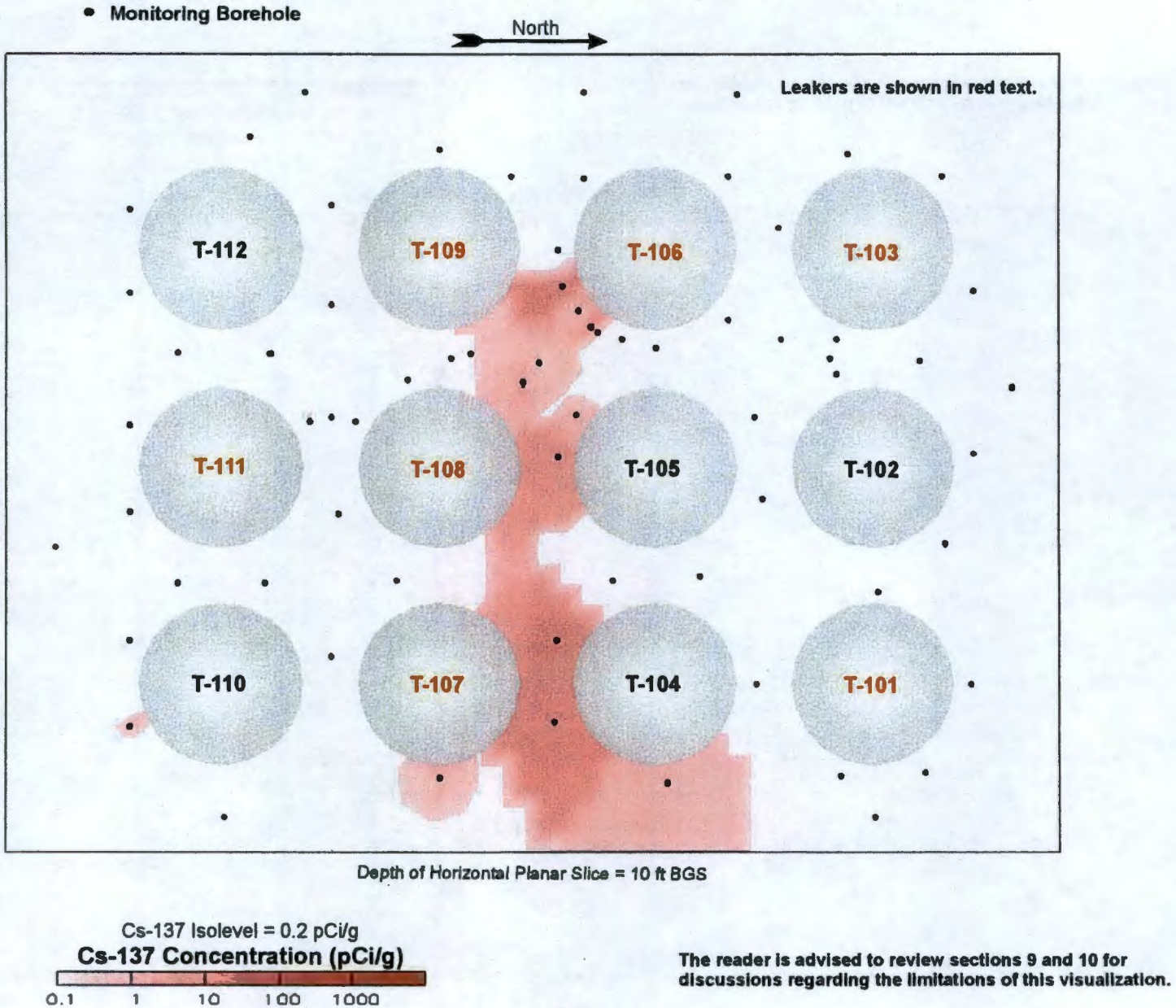

Figure 14-34. Visualization of ^{137}Cs Contamination at the T Tank Farm at a Depth of 10 Ft Below Ground Surface Viewed From Above the Tanks

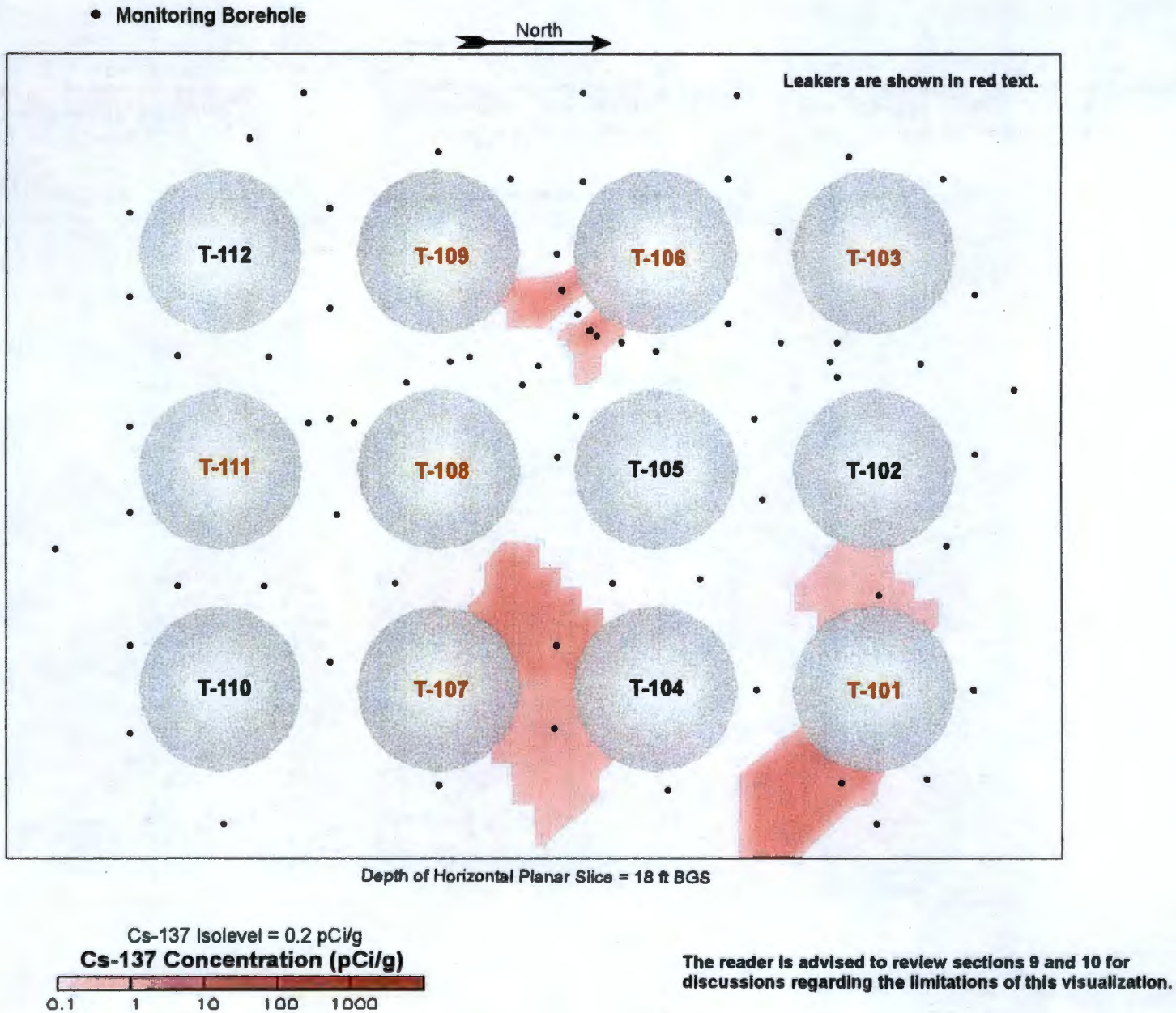

Figure 14-35. Visualization of ^{137}Cs Contamination at the T Tank Farm at a Depth of 18 Ft Below Ground Surface Viewed From Above the Tanks

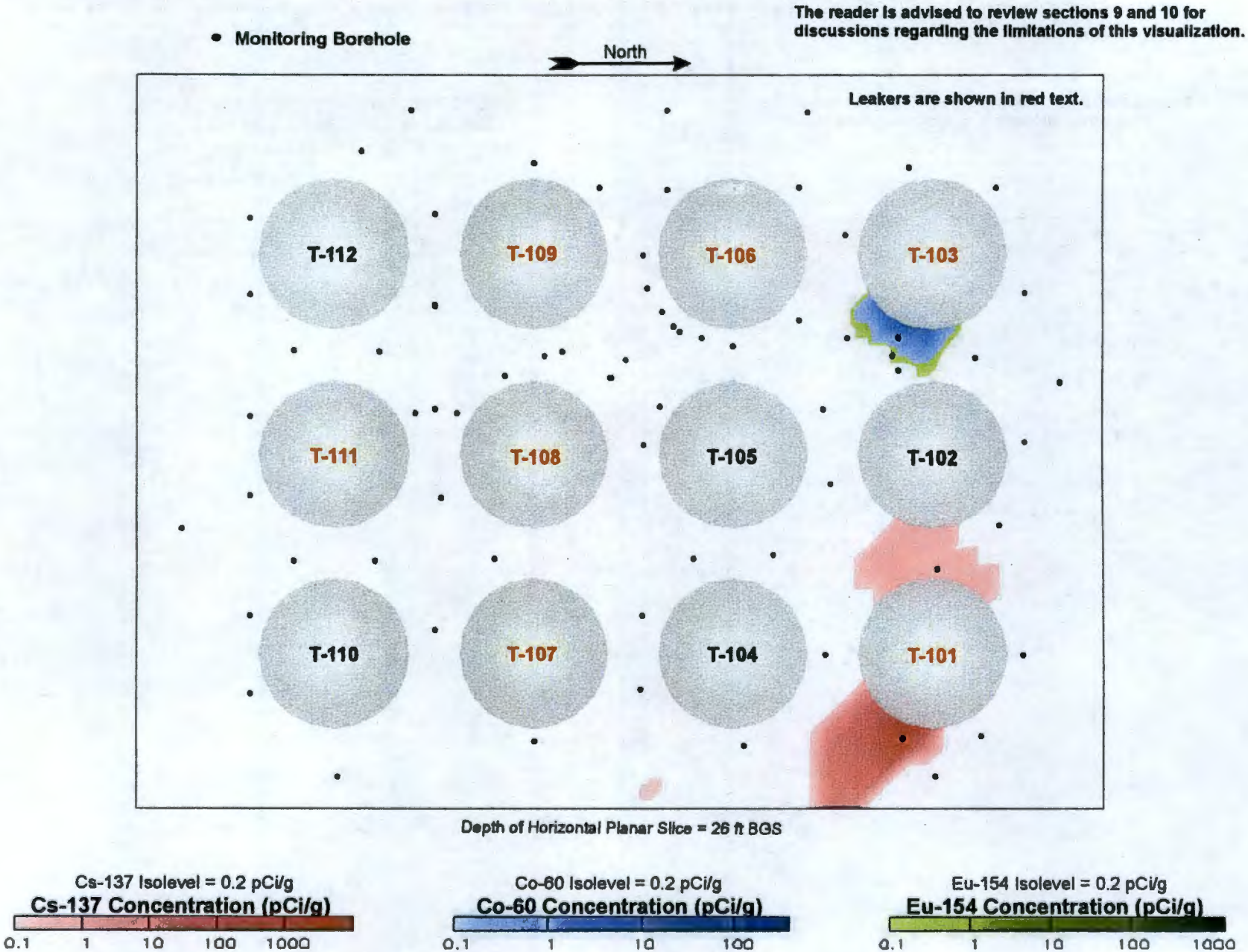

Figure 14-36. Visualization of ^{137}Cs, ^{60}Co, and ^{154}Eu Contamination at the T Tank Farm at a Depth of 26 Ft Below Ground Surface Viewed From Above the Tanks

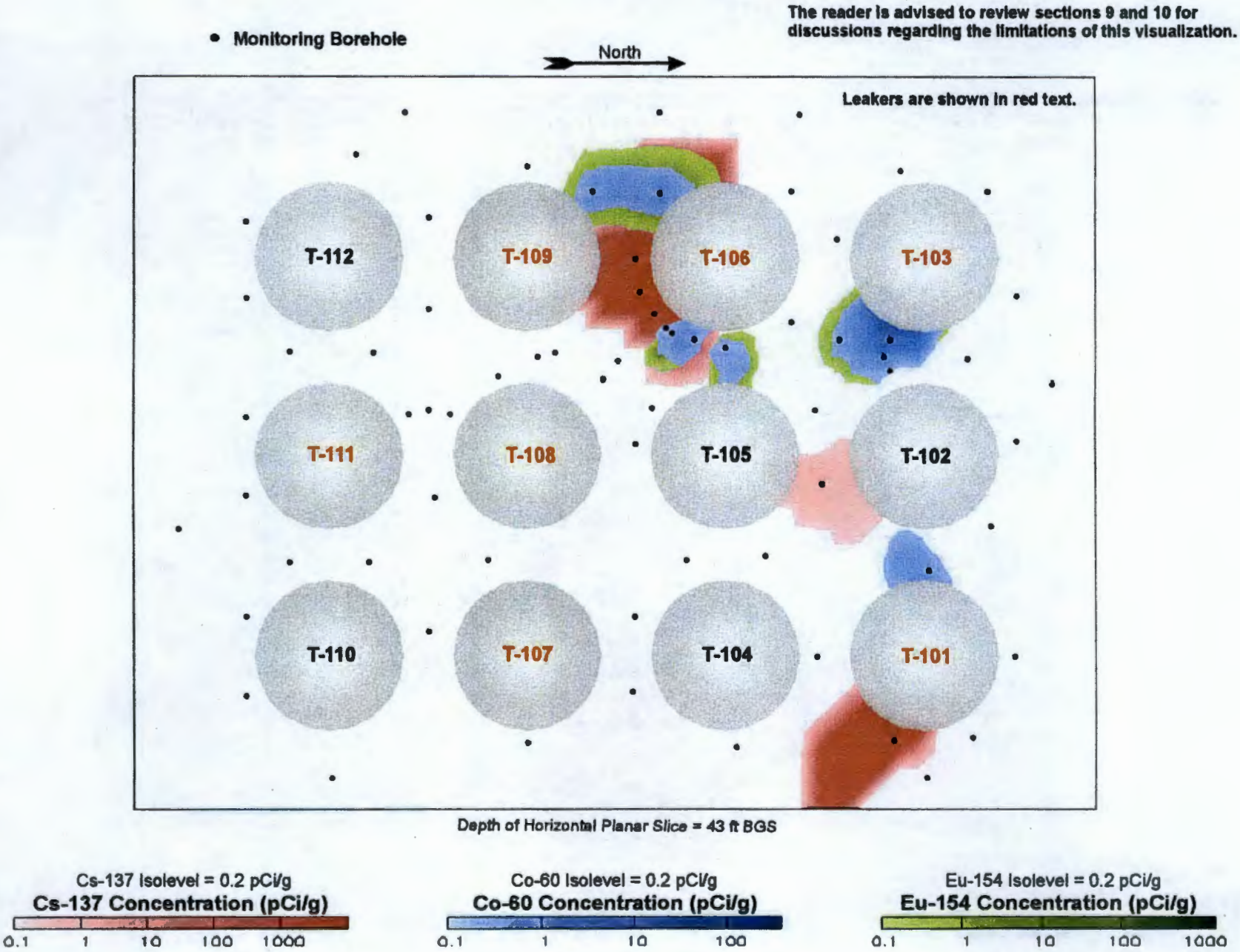

Figure 14-37. Visualization of ^{137}Cs, ^{60}Co, and ^{154}Eu Contamination at the T Tank Farm at a Depth of 43 Ft Below Ground Surface (Base of Tanks) Viewed From Above the Tanks

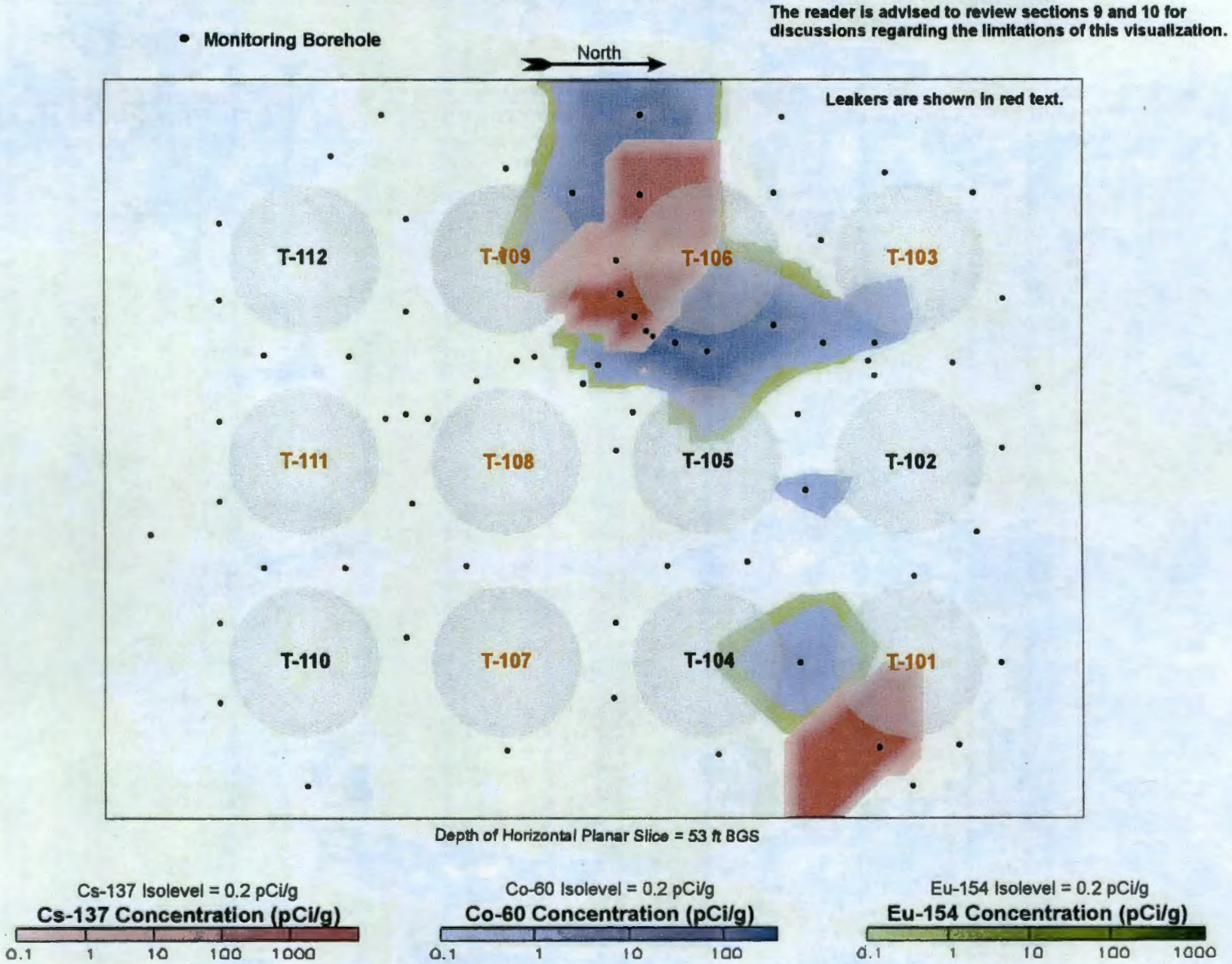

Figure 14-38. Visualization of ^{137}Cs, ^{60}Co, and ^{154}Eu Contamination at the T Tank Farm at a Depth of 53 Ft Below Ground Surface Viewed From Above the Tanks

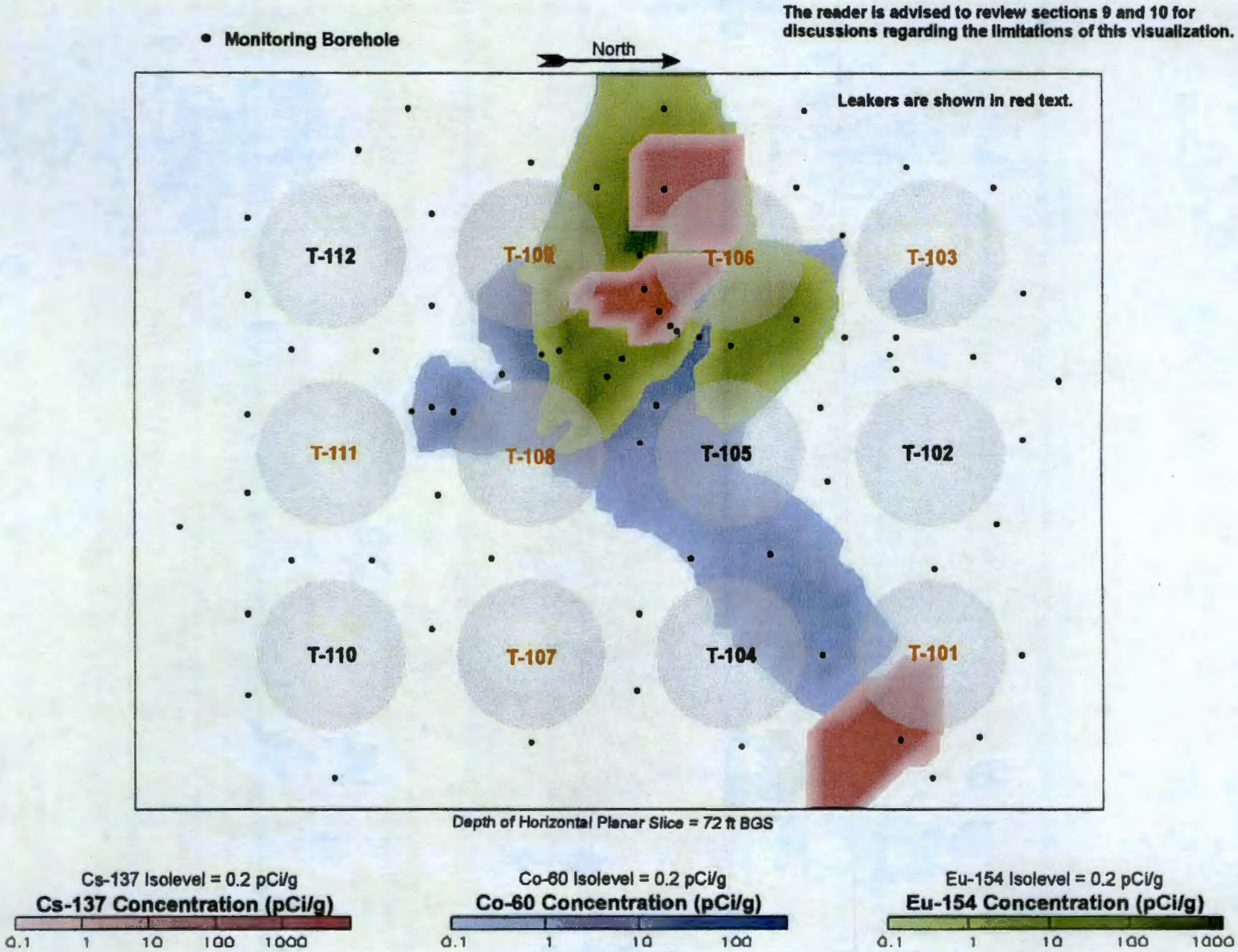

Figure 14-39. Visualization of ^{137}Cs, ^{60}Co, and ^{154}Eu Contamination at the T Tank Farm at a Depth of 72 Ft Below Ground Surface Viewed From Above the Tanks

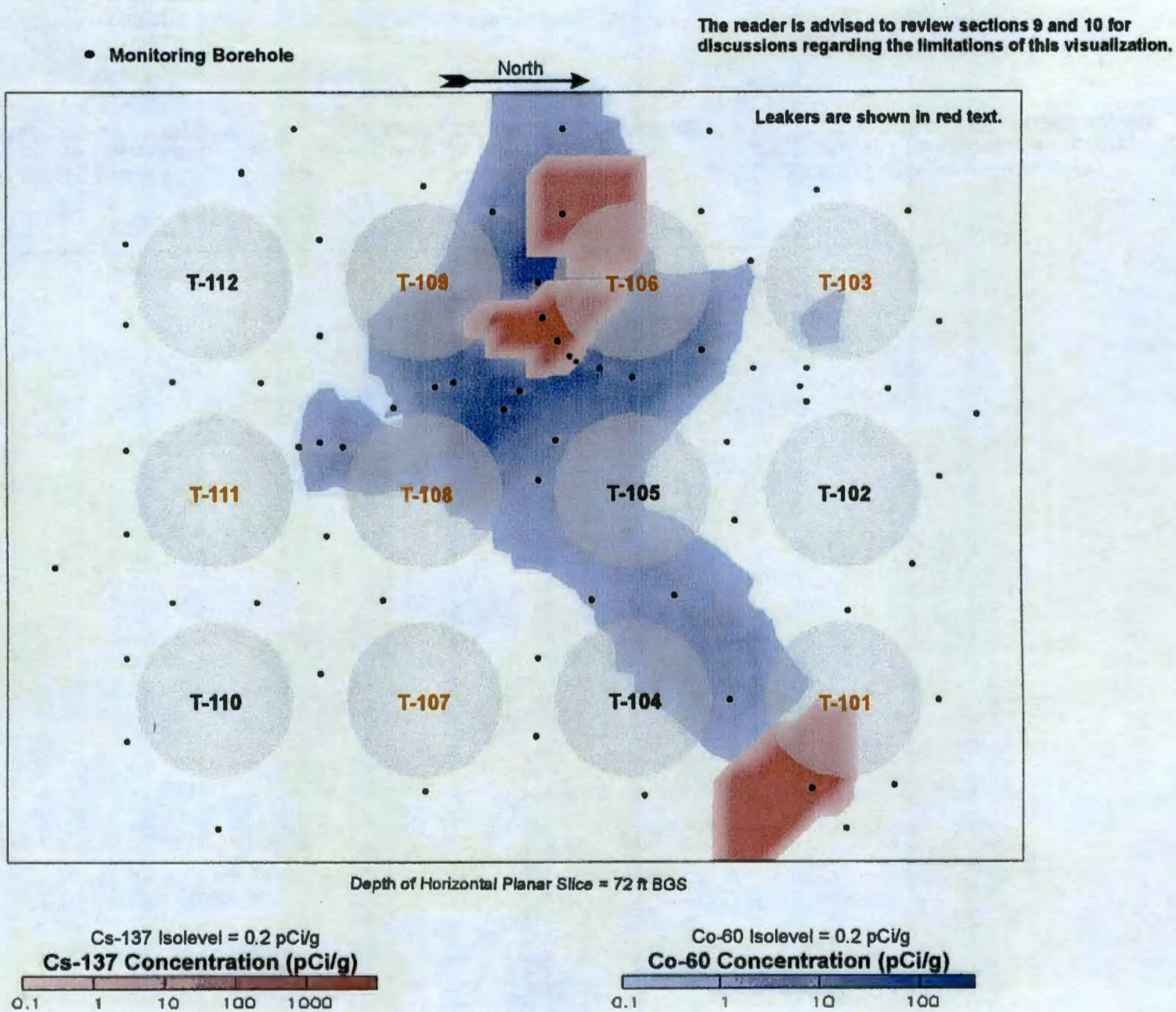

Figure 14-40. Visualization of ^{137}Cs and ^{60}Co Contamination at the T Tank Farm at a Depth of 72 Ft Below Ground Surface Viewed From Above the Tanks

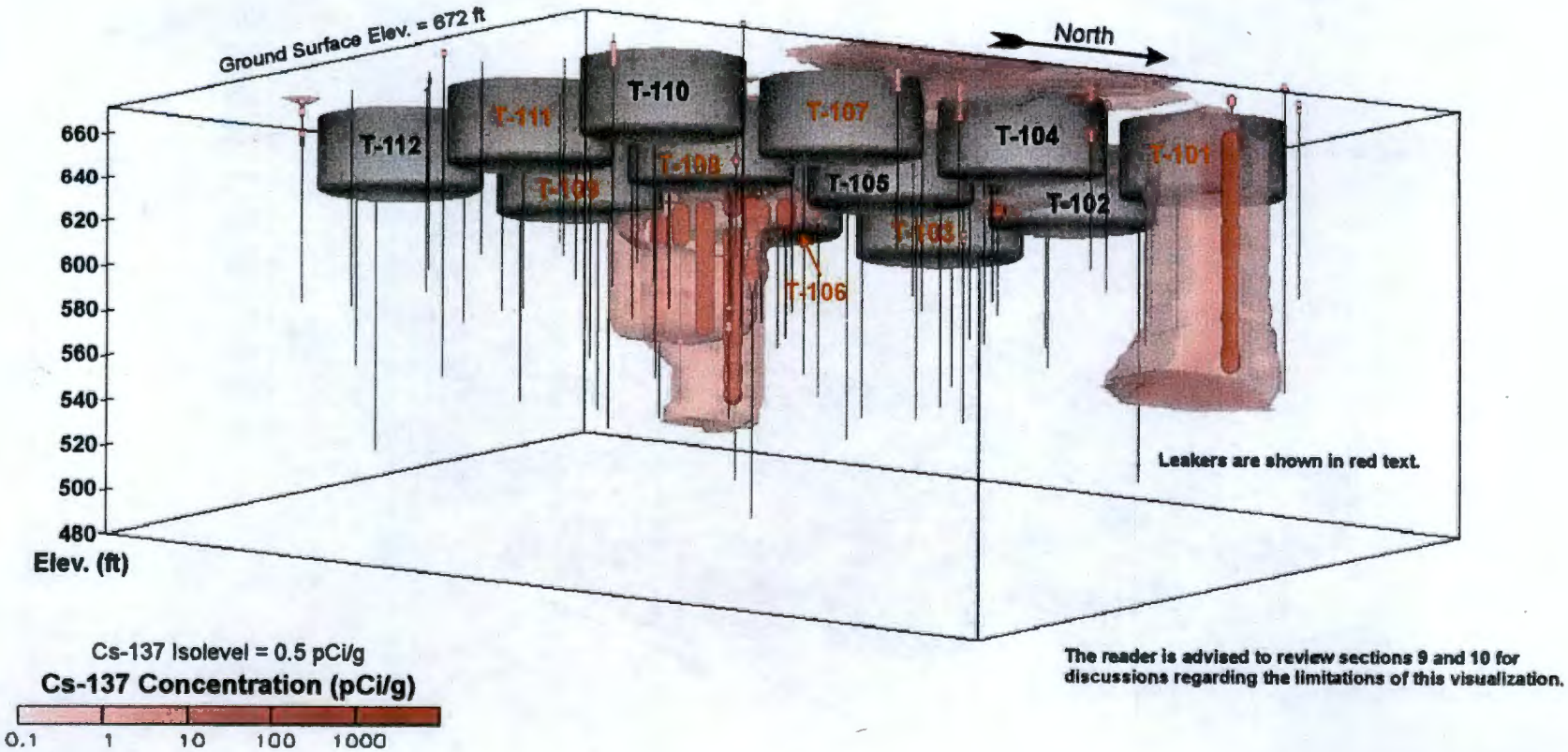

14-41. Visualization of ^{137}Cs Contamination Plumes at the T Tank Farm Superimposed Over the ^{137}Cs SGLS Data, Viewed From Below the Tanks From the Southeast

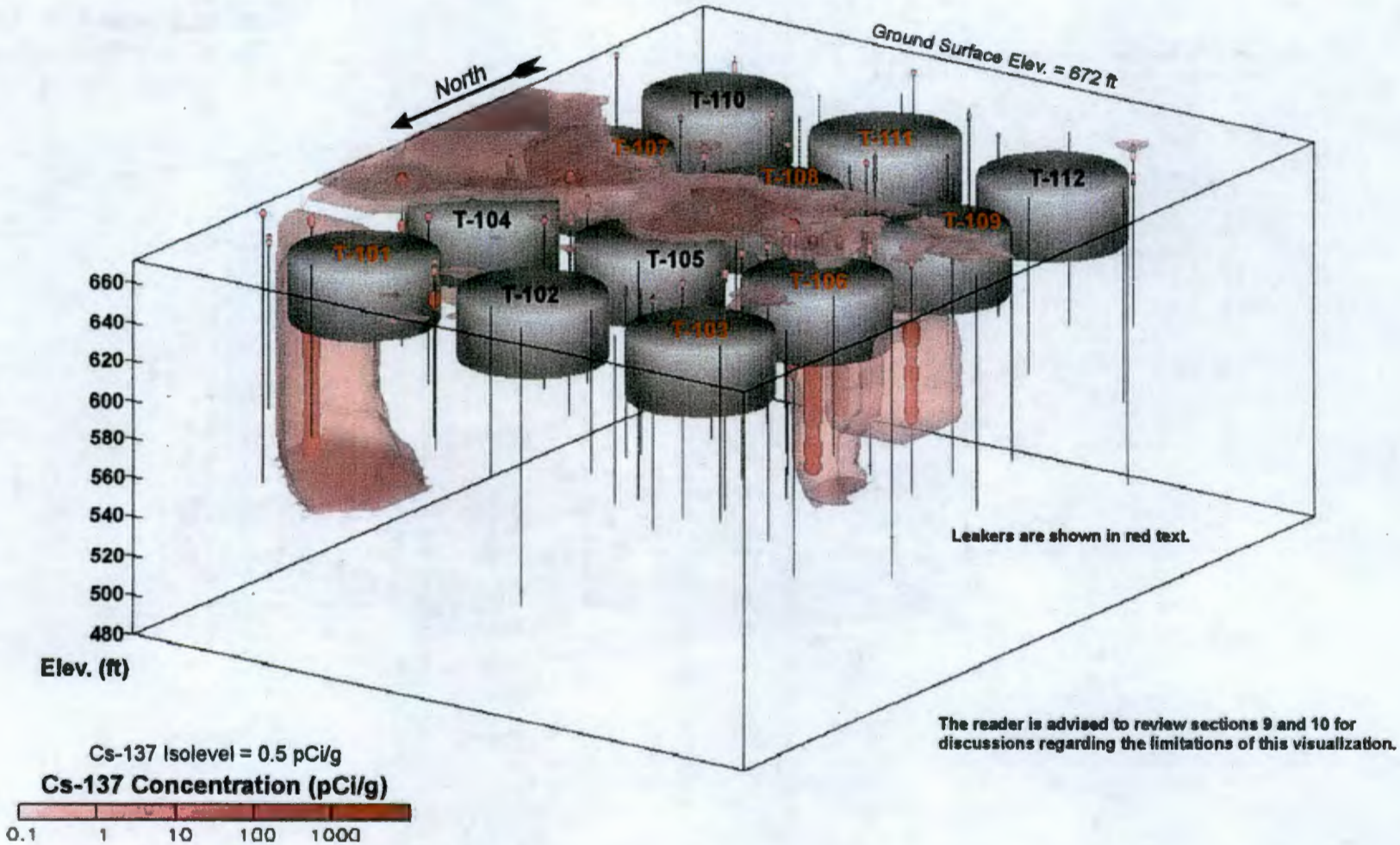

14-42. Visualization of ^{137}Cs Contamination Plumes at the T Tank Farm Superimposed Over the ^{137}Cs SGLS Data, Viewed From Above the Tanks From the Northwest

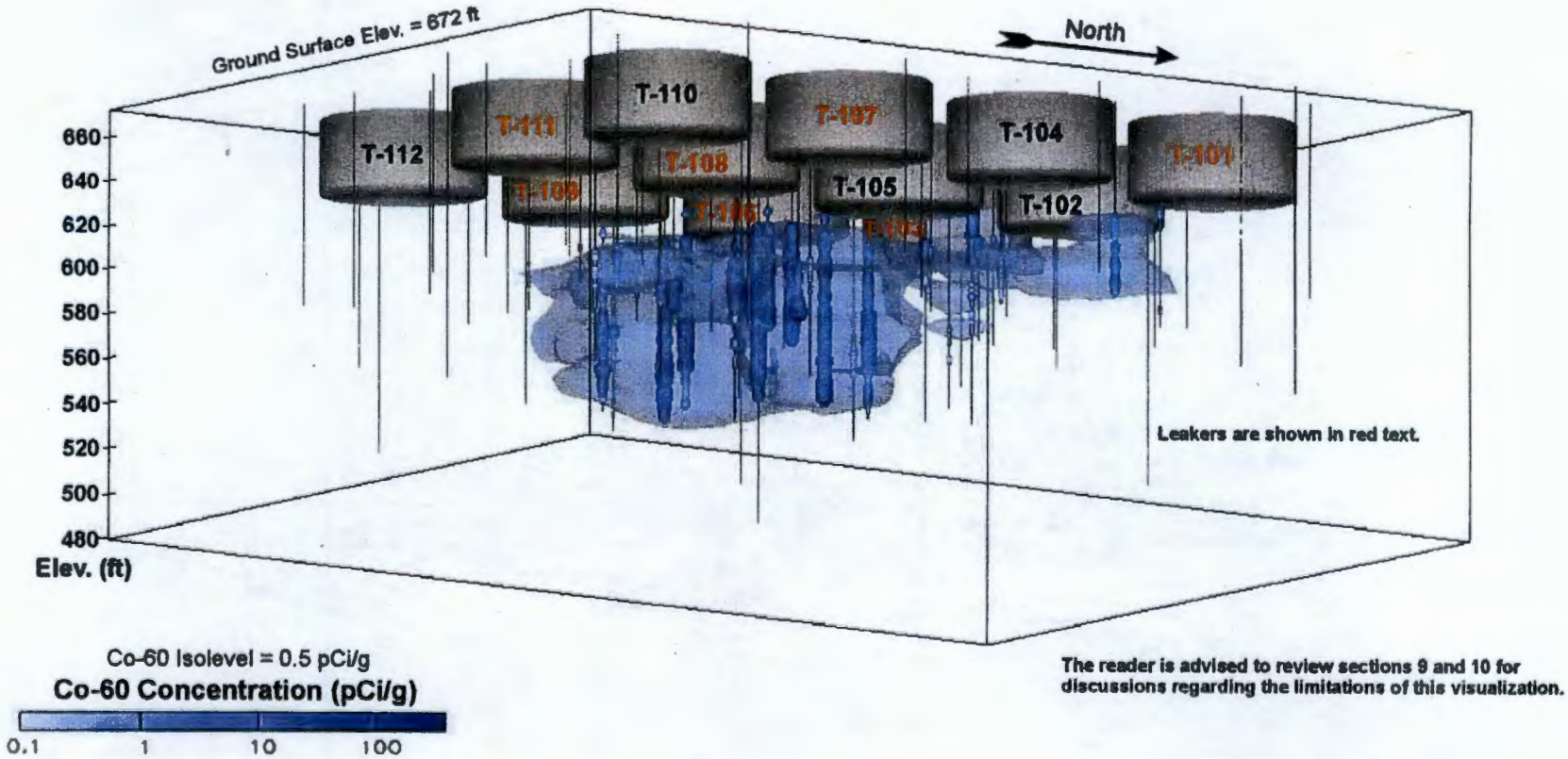

14-43. Visualization of ^{60}Co Contamination Plumes at the T Tank Farm Superimposed Over the ^{60}Co SGLS Data, Viewed From Below the Tanks From the Southeast

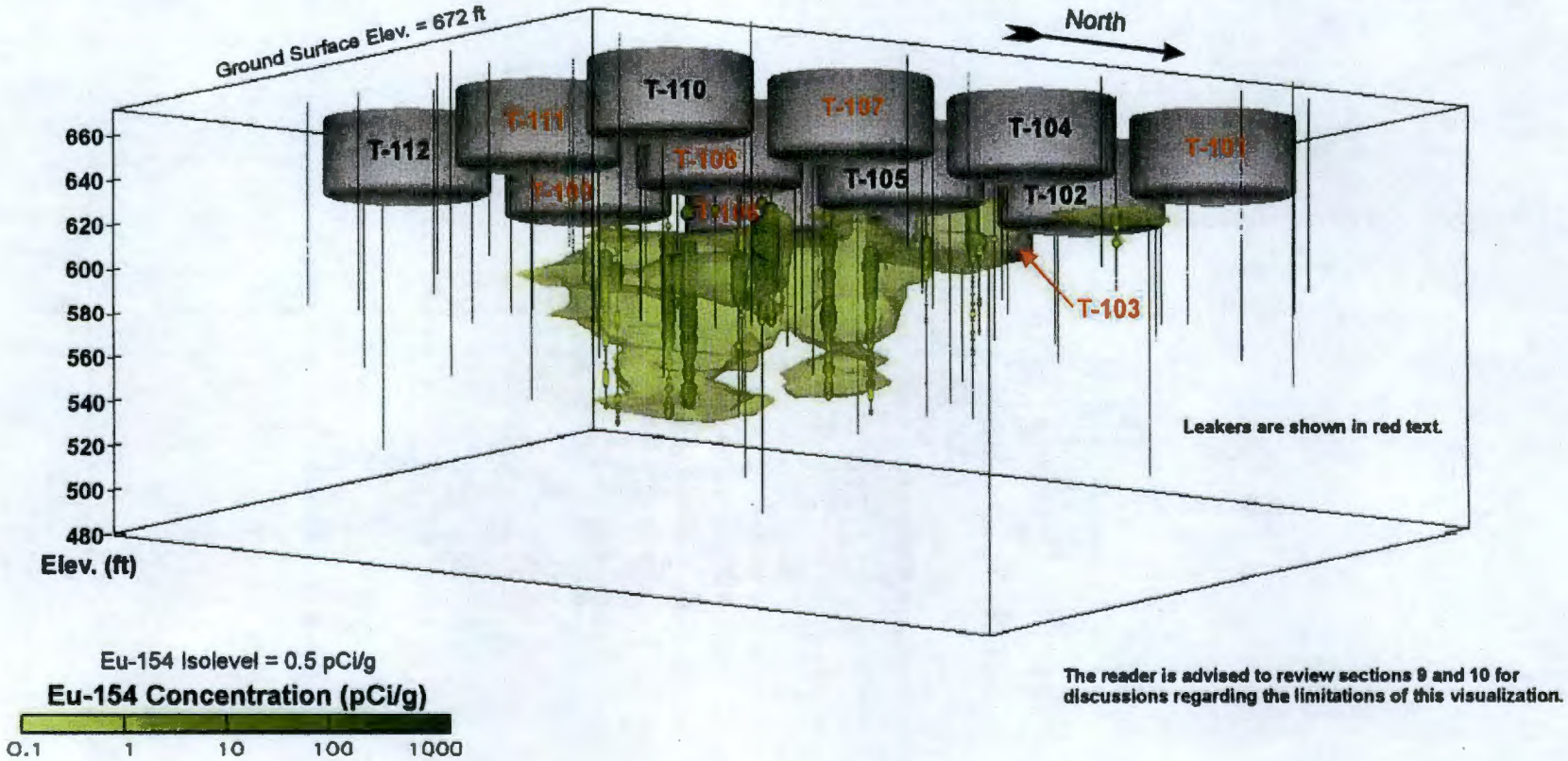

14-44. Visualization of ^{154}Eu Contamination Plumes at the T Tank Farm Superimposed Over the ^{154}Eu SGLS Data, Viewed From Below the Tanks From the Southeast

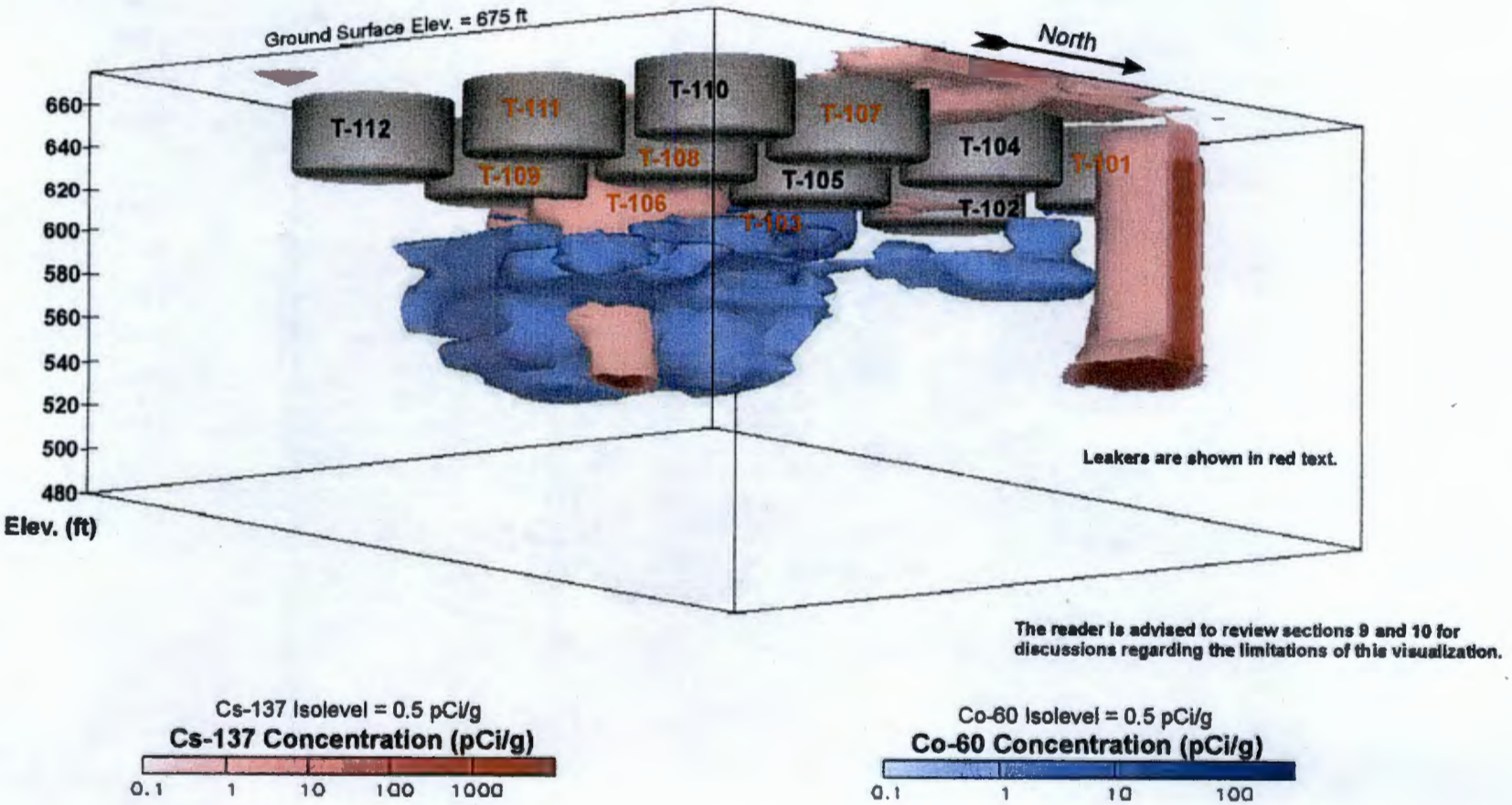

14-45. Visualization of ^{137}Cs and ^{60}Co Contamination at the T Tank Farm Viewed From Below the Tanks From the Southeast

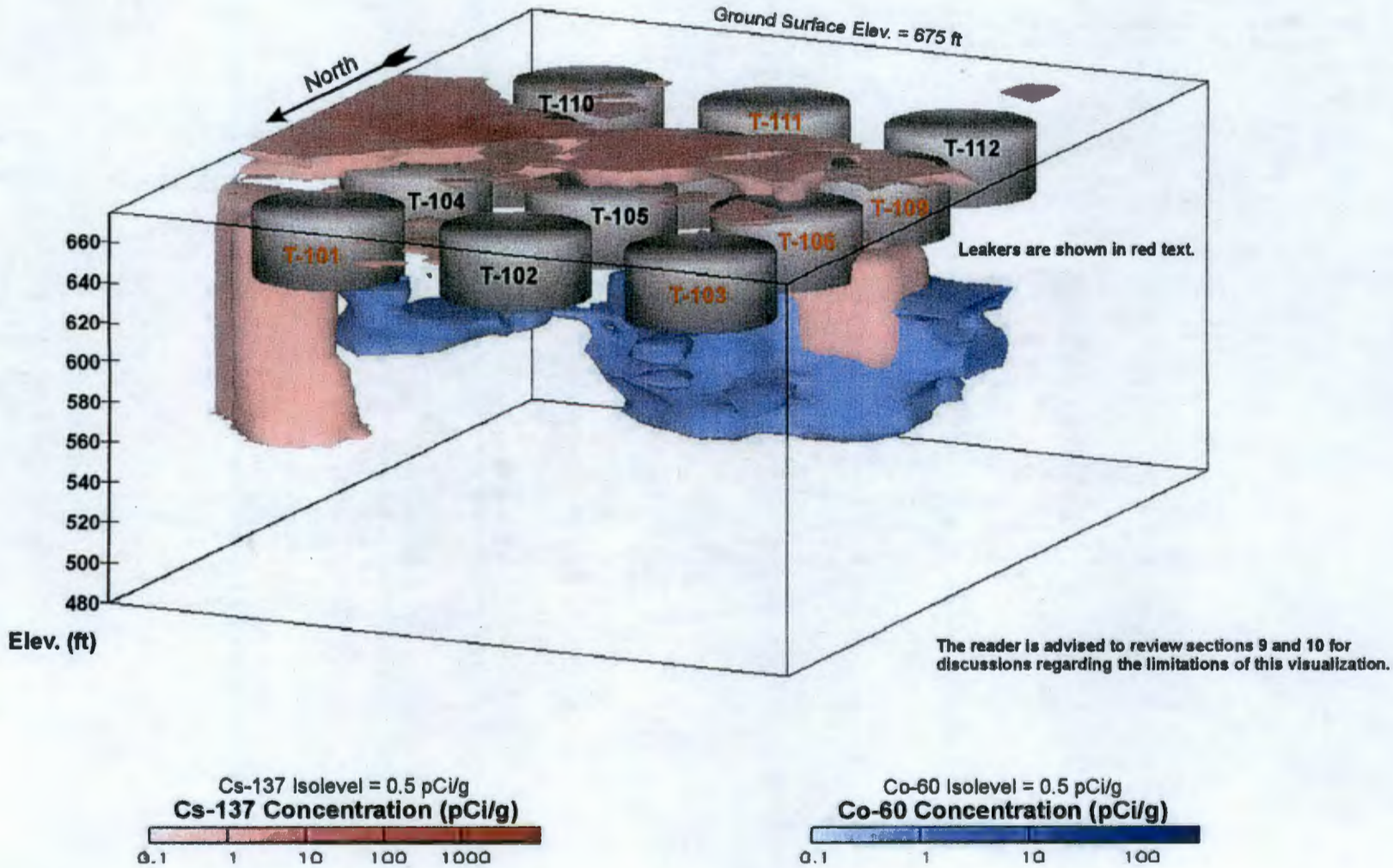

14-46. Visualization of ^{137}Cs and ^{60}Co Contamination at the T Tank Farm Viewed From Above the Tanks From the Northwest

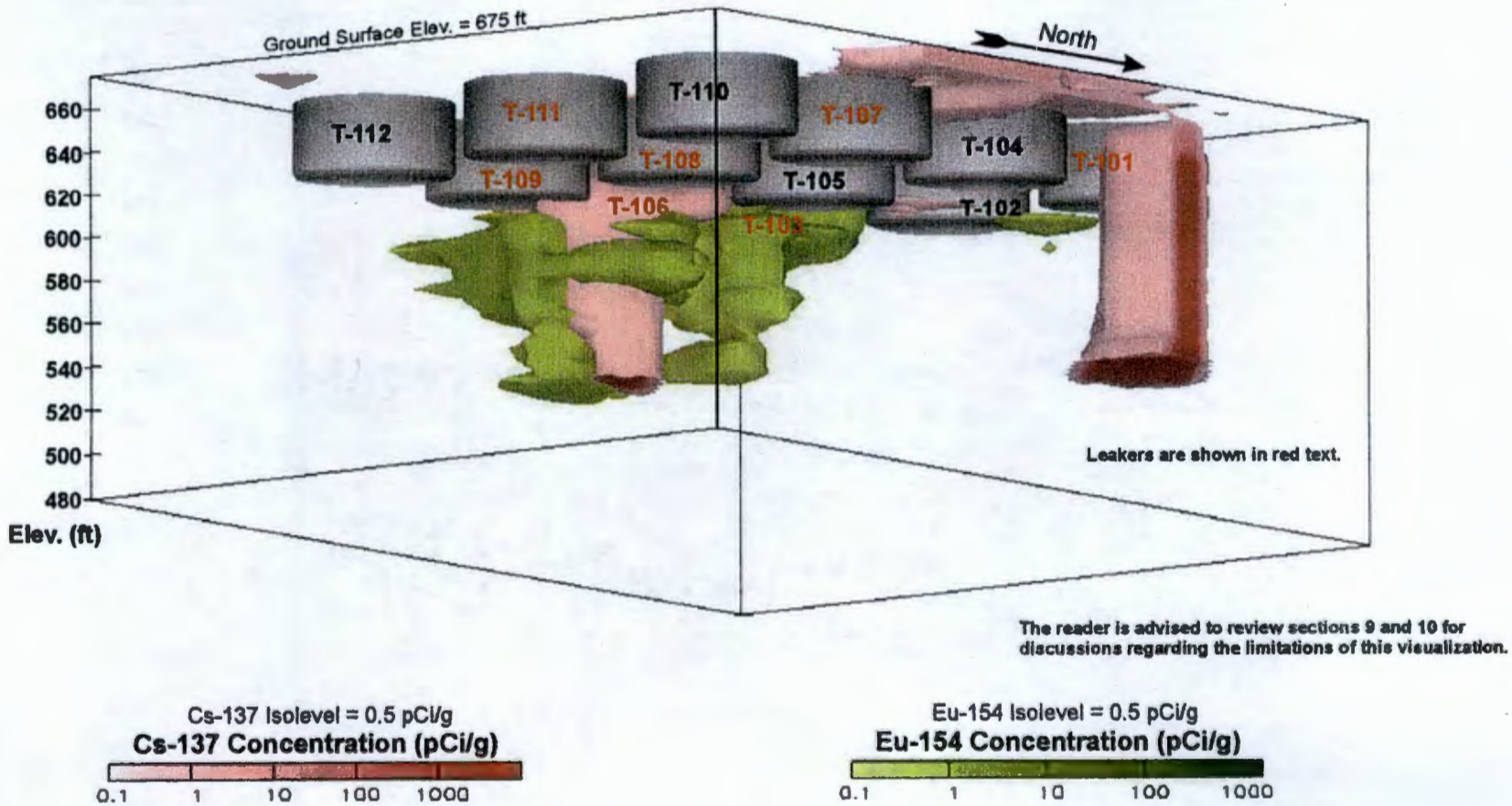

14-47. Visualization of ^{137}Cs and ^{154}Eu Contamination at the T Tank Farm Viewed From Below the Tanks From the Southeast

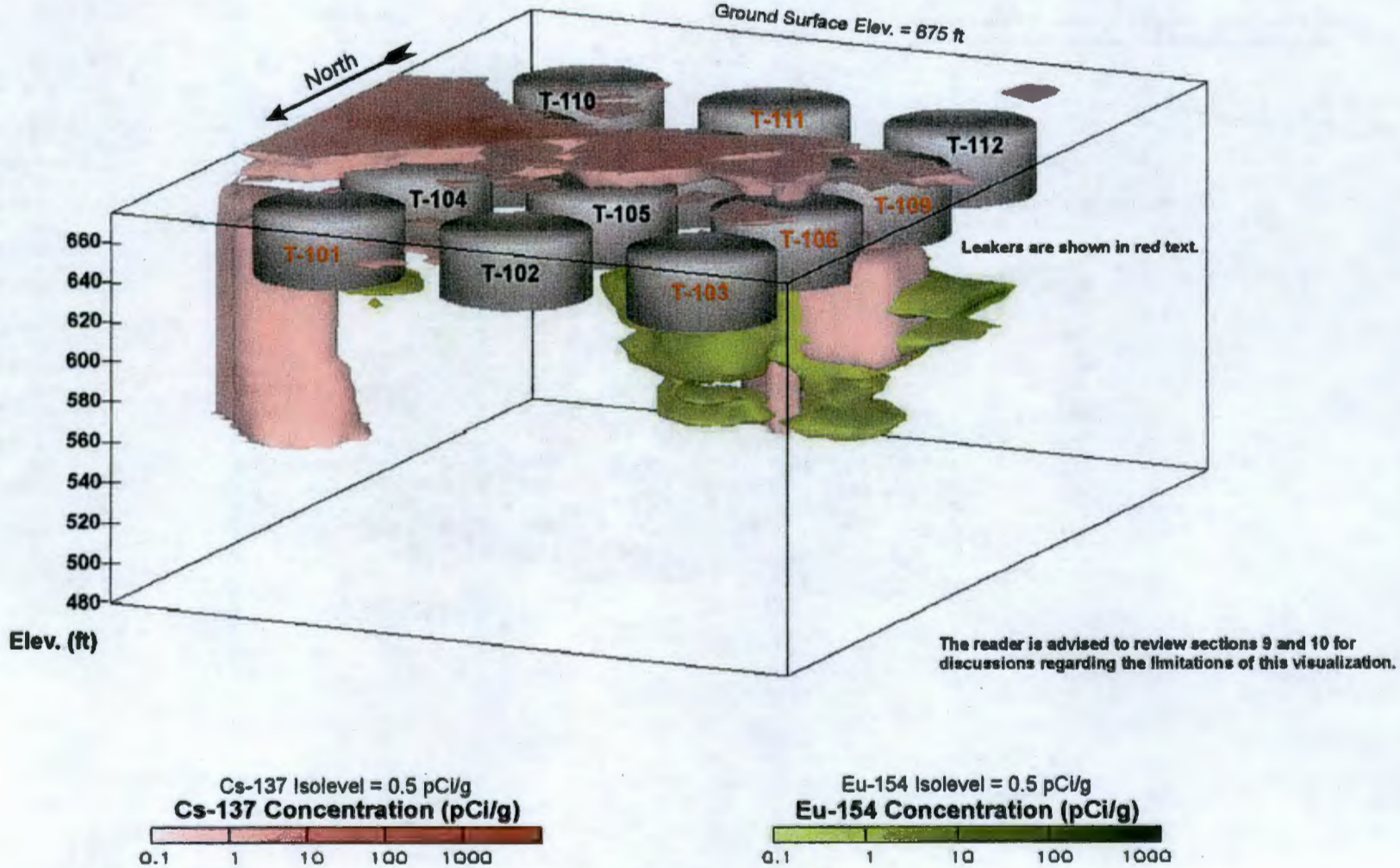

14-48. Visualization of ^{137}Cs and ^{154}Eu Contamination at the T Tank Farm Viewed From Above the Tanks From the Northwest

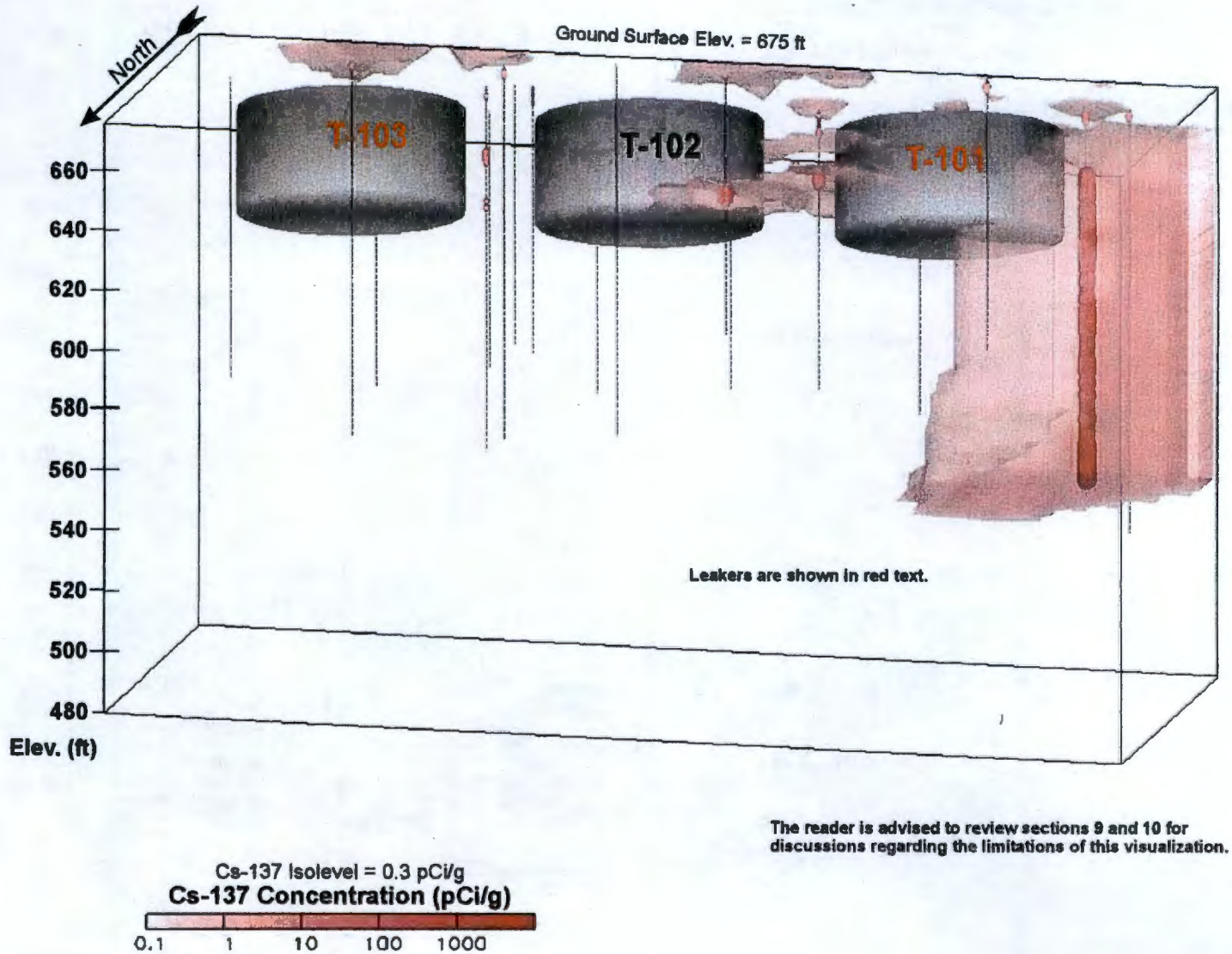

14-49. Visualization of ^{137}Cs Contamination in the Vicinity of Tanks T-101, T-102, and T-103 Superimposed Over the ^{137}Cs SGLS Data, Viewed From Below the Tanks From the South-Southwest

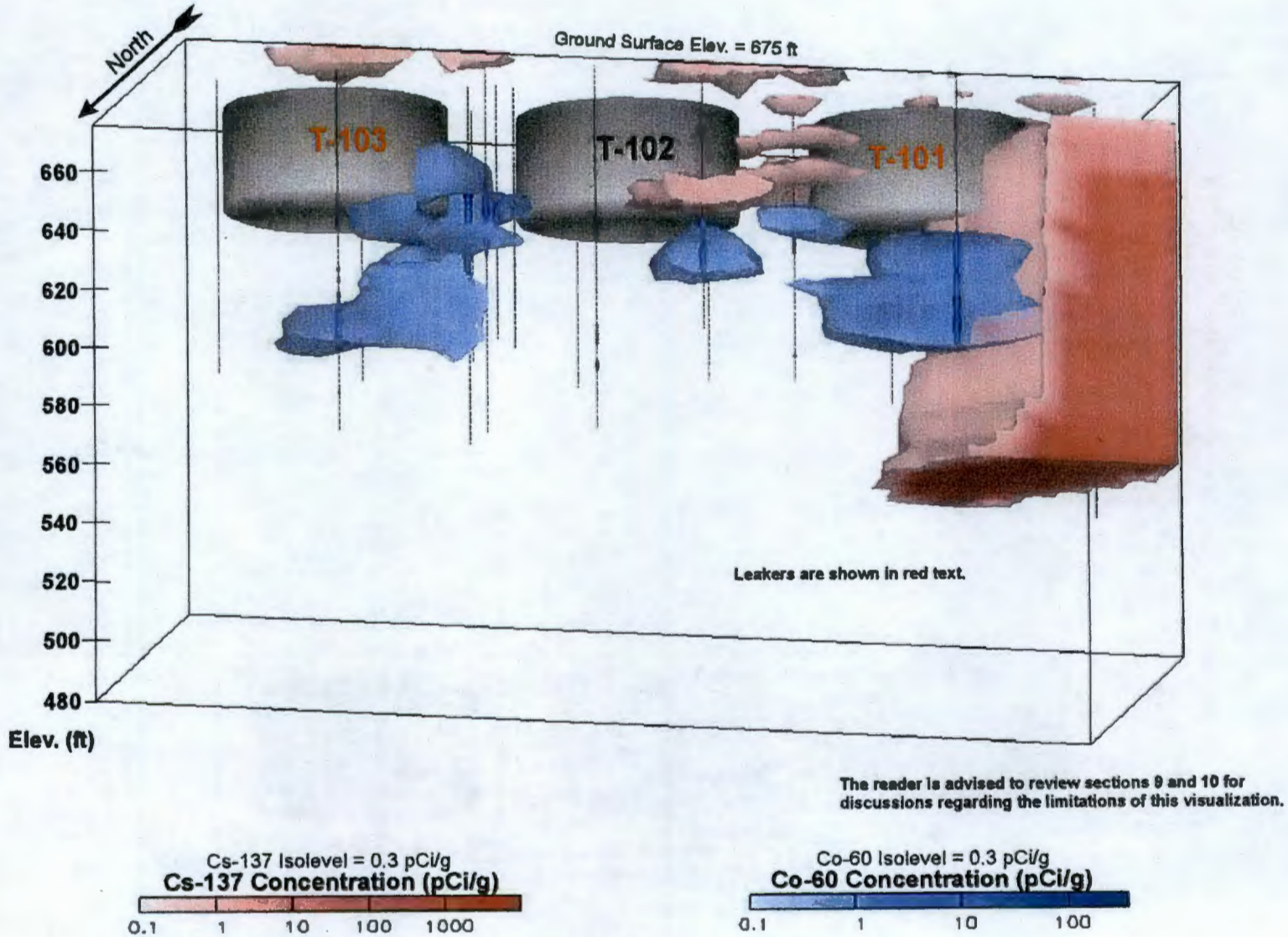

14-50. Visualization of ^{137}Cs and ^{60}Co Contamination in the Vicinity of Tanks T-101, T-102, and T-103, with the ^{60}Co Contamination Superimposed Over the ^{60}Co SGLS Data, Viewed From Below the Tanks From the South-Southwest

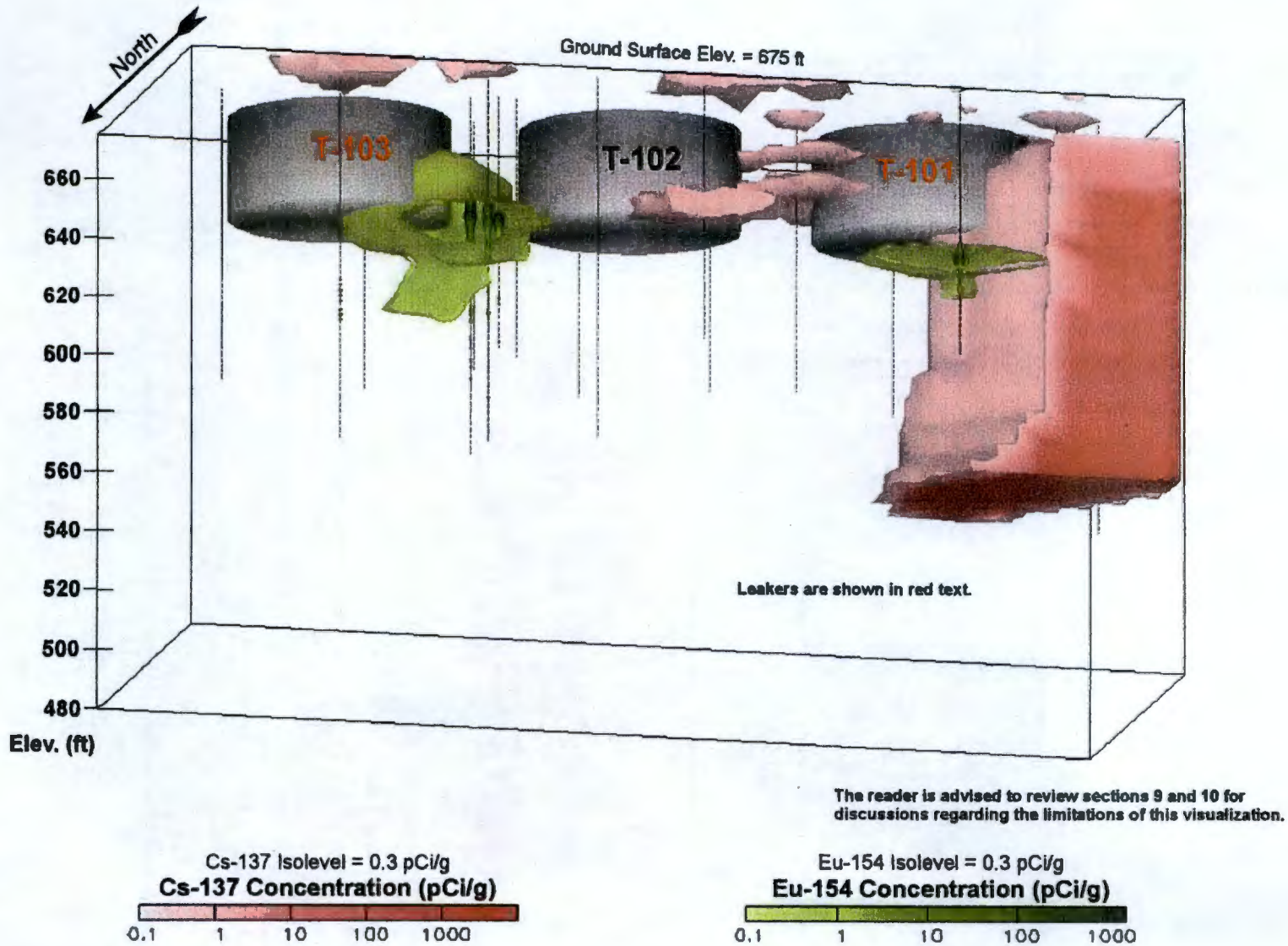

14-51. Visualization of ^{137}Cs and ^{154}Eu Contamination in the Vicinity of Tanks T-101, T-102, and T-103, with the ^{154}Eu Contamination Superimposed Over the ^{154}Eu SGLS Data, Viewed From Below the Tanks From the South-Southwest

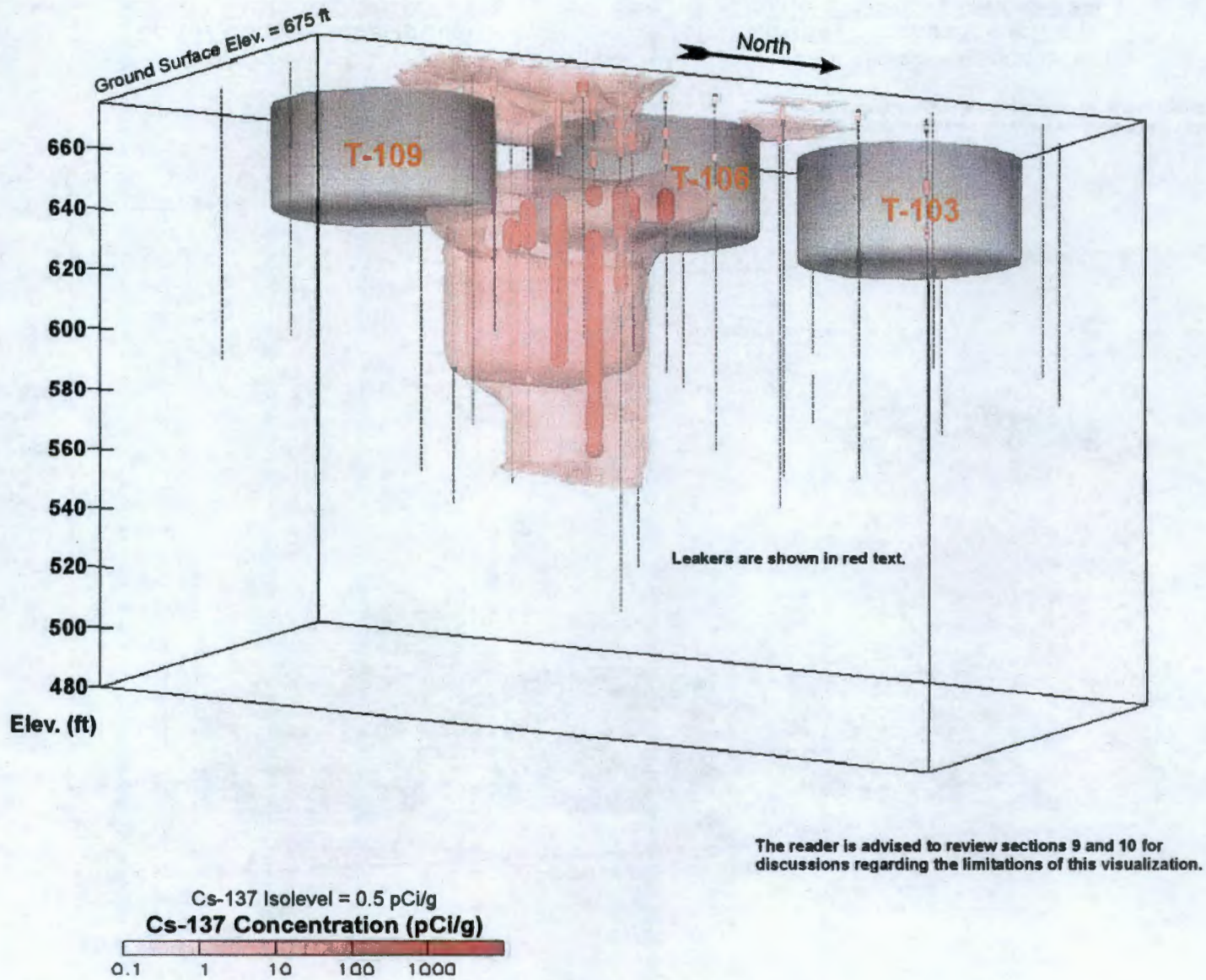

14-52. Visualization of ^{137}Cs Contamination in the Vicinity of Tanks T-103, T-106, and T-109 Superimposed Over the ^{137}Cs SGLS Data, Viewed From Below the Tanks From the Southeast

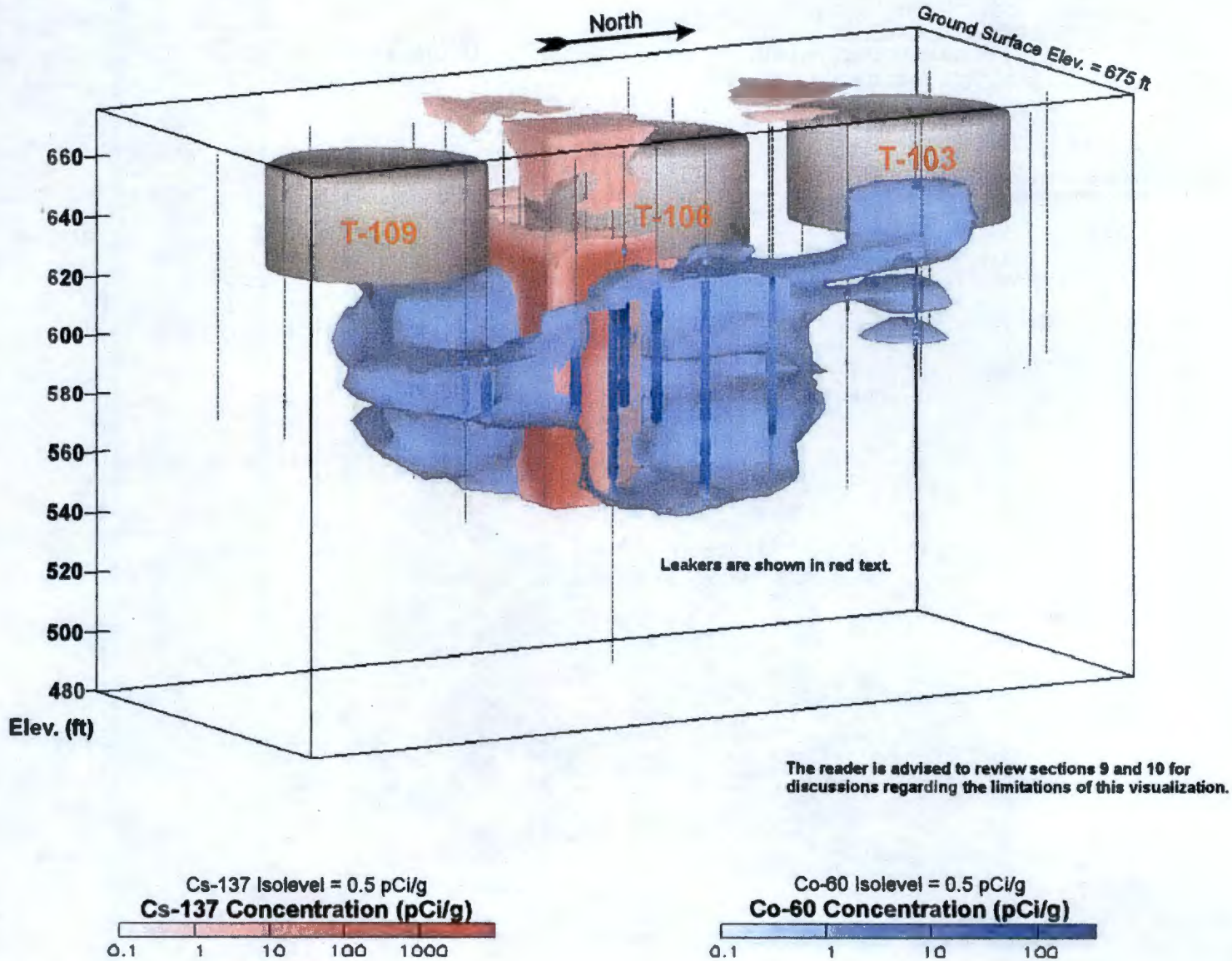

14-53. Visualization of ^{137}Cs and ^{60}Co Contamination in the Vicinity of Tanks T-103, T-106, and T-109, with the ^{60}Co Contamination Superimposed Over the ^{60}Co SGLS Data, Viewed From Above the Tanks From the Southeast

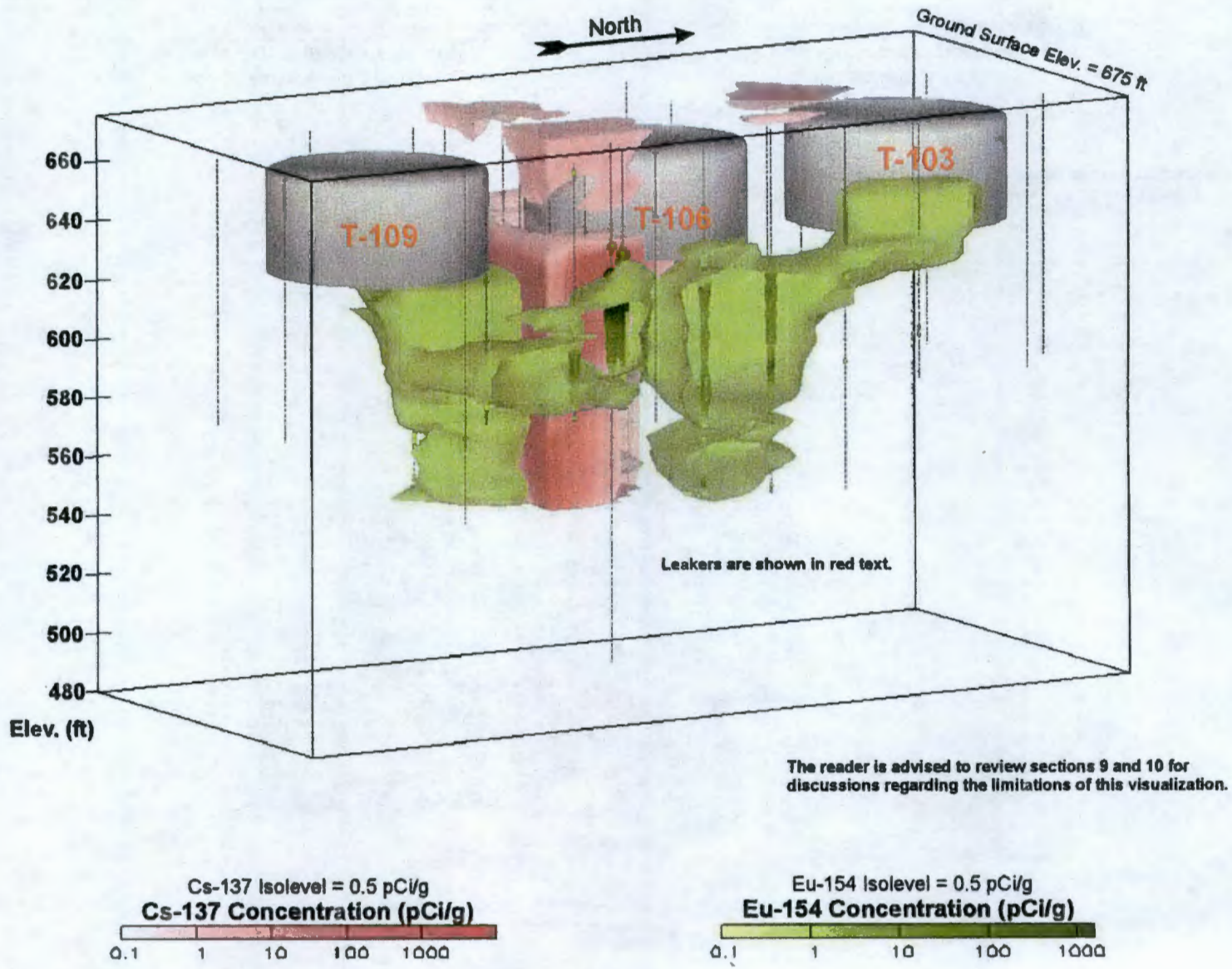

14-54. Visualization of ^{137}Cs and ^{154}Eu Contamination in the Vicinity of Tanks T-103, T-106, and T-109, with the ^{154}Eu Contamination Superimposed Over the ^{154}Eu SGLS Data, Viewed From Above the Tanks From the Southeast

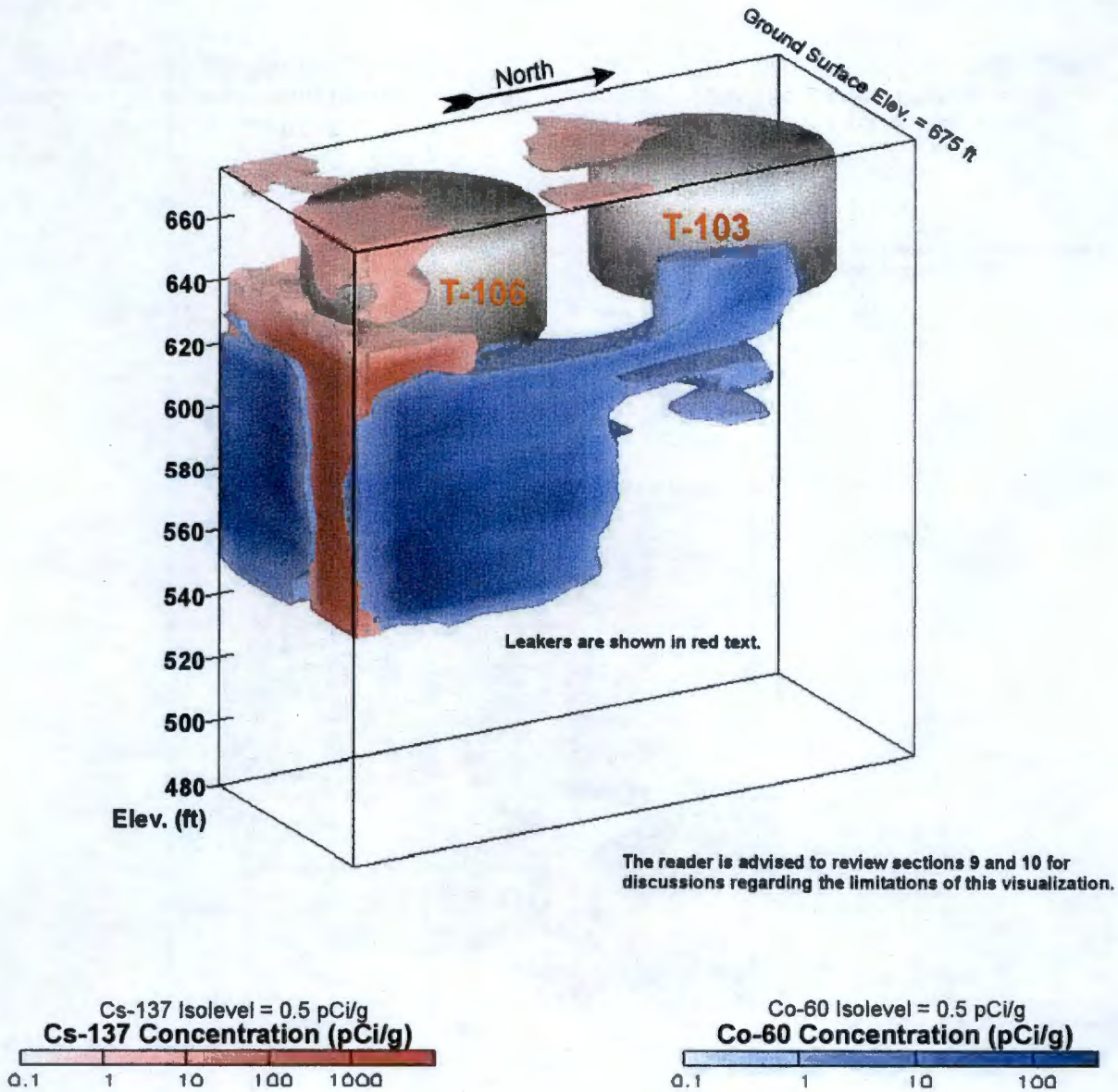

14-55. Visualization of ^{137}Cs and ^{60}Co Contamination in the Vicinity of Tanks T-103 and T-106, Viewed From Above the Tanks From the Southeast

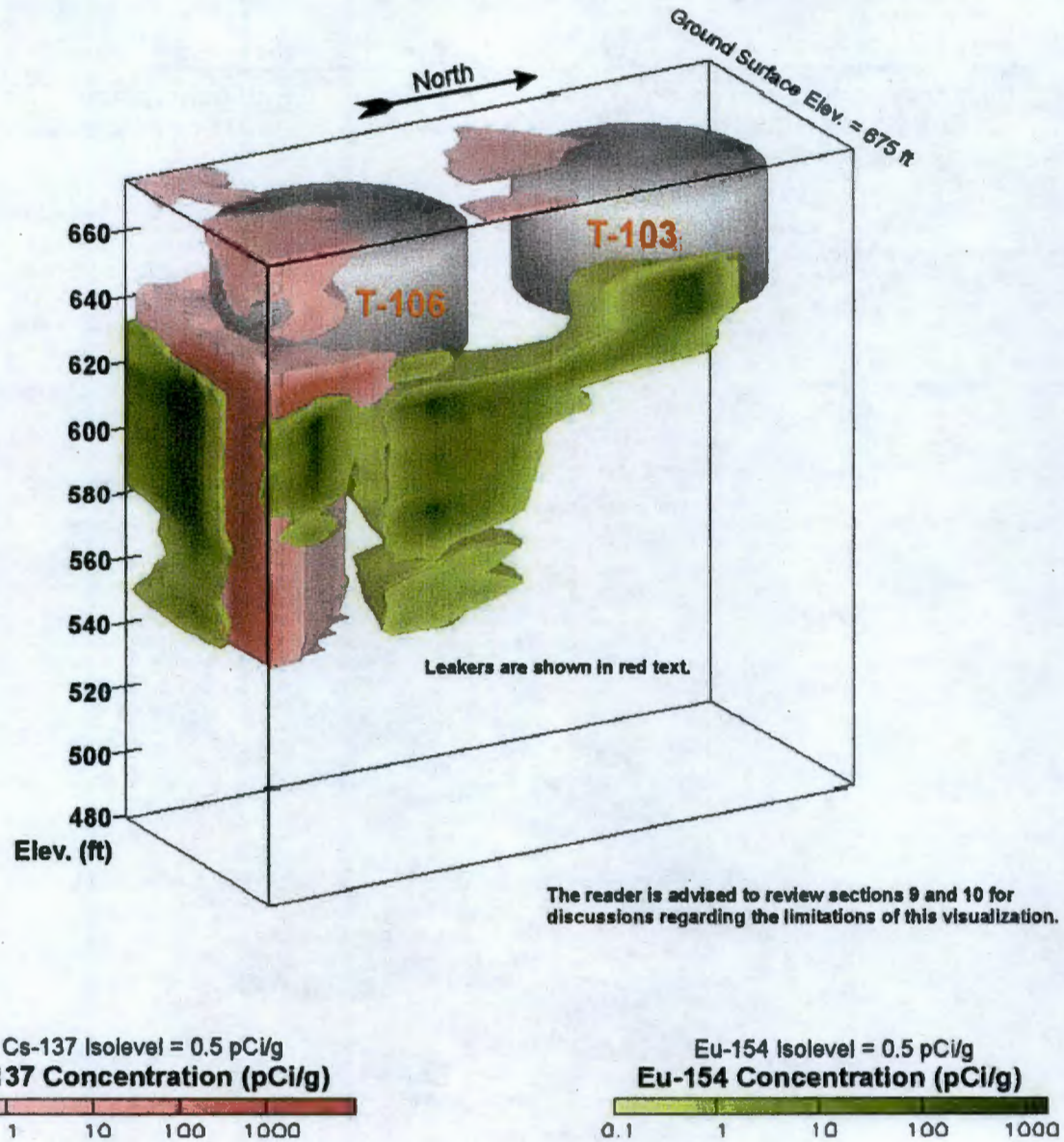

14-56. Visualization of ^{137}Cs and ^{154}Eu Contamination in the Vicinity of Tanks T-103 and T-106, Viewed From Above the Tanks From the Southeast

15.0 References

Adams, J.P., 1995. *National Low-Level Waste Management Program Radionuclide Report Series, Vol. 12, Cobalt-60*, DOE/LLW-128, Idaho National Engineering Laboratory, Idaho Falls, Idaho.

Agnew, S.F., 1997. *Hanford Tank Chemical and Radionuclide Inventories: HDW Model Rev. 4*, LA-UR-96-3860, Los Alamos National Laboratory, Los Alamos, New Mexico.

Agnew, S.F., R.A. Corbin, T.B. Duran, K.A. Jurgensen, T.P. Ortiz, and B.L. Young, 1995. *Waste Status and Transition Record Summary for the Northeast Quadrant of the Hanford 200 Area: WHC-SD-WM-TI-615*, Rev. 1, prepared by Los Alamos National Laboratory for the U.S. Department of Energy, Richland, Washington.

Anderson, J.D., 1990. *A History of the 200 Area Tank Farms*, WHC-MR-0132, Westinghouse Hanford Company, Richland, Washington.

Atlantic Richfield Hanford (ARH), 1973. *241-T-106 Tank Leak Investigation*, ARH-2874, Atlantic Richfield Hanford Company, Richland, Washington.

Baker, U.R., B.N. Bjornstad, A.J. Busacca, K.R. Fecht, E.P. Kiver, U.L. Moody, J.G. Rigby, O.F. Stradling, and A.M. Tallman, 1991. "Quaternary Geology of the Columbia Plateau" in Morrison, R.B. (ed.), *Quaternary Non-Glacial Geology: Conterminous U.S.*, Boulder, Colorado, GSA, the Geology of North America, Vol. K-2.

Bjornstad, B.N., K.R. Fecht, and A.M. Tallman, 1987. *Quaternary Stratigraphy of the Pasco Basin, South Central Washington*, RHO-BW-SA-563A, Rockwell Hanford Operations, Richland, Washington.

Black, R.F., 1980. *Clastic Dikes of the Pasco Basin, Southeastern Washington*, RHO-BWI-C-64, Rockwell Hanford Operations, Richland, Washington.

Boothe, G.F., 1996. *Predominant Radionuclides in Hanford Site Waste Tanks*, WHC-SD-WM-TI-731, Rev. 0, Westinghouse Hanford Company, Richland, Washington.

Brevick, C.H., L.A. Gaddis, and W.W. Pickett, 1995. *Supporting Document for the Historical Tank Content Estimates for T Tank Farm, Vol. 1 and 2*, WHC-SD-WM-ER-320, Westinghouse Hanford Company, Richland, Washington.

Brodeur, J.R., C.J. Koizumi, W.H. Ulbricht, and R.K. Price, 1991. "Calibration of a High-Resolution Passive Gamma-Ray Logging System for Nuclear Waste Assessment" in *Proceedings of the 4th Annual International Symposium on Borehole Geophysics for Minerals, Geotechnical and Groundwater Applications*, sponsored by the Minerals and Geotechnical Logging Society of the Society of Professional Well Log Analysts, Houston, Texas.

Brodeur, J.R., R.K. Price, R.D. Wilson, and C.J. Koizumi, 1993. *Results for Spectral Gamma-Ray Logging of Selected Boreholes for the 200 Aggregate Area Management Study*, WHC-SD-EN-TI-021, Westinghouse Hanford Company, Richland, Washington.

Caggiano, J.A., and C.J. Chou, 1993. *Interim-Status Groundwater Quality Assessment Plan for the Single-Shell Tank Waste Management Areas T and TX-TY*, WHC-SD-EN-AP-132, Westinghouse Hanford Company, Richland, Washington.

Caggiano, J.A., and S.M. Goodwin, 1991. *Interim-Status Groundwater Monitoring Plan for the Single-Shell Tanks*, WHC-SD-EN-AP-012, Westinghouse Hanford Company, Richland, Washington.

Carboneau, M.L., and R.S. Garcia, 1994. *National Low-Level Waste Management Program Radionuclide Report Series,* Vol. 9, *Plutonium-241*, DOE/LLW-125, Idaho National Engineering Laboratory, Idaho Falls, Idaho.

Carboneau, M.L., J.P. Adams, and R.S. Garcia, 1994a. *National Low-Level Waste Management Program Radionuclide Report Series,* Vol. 7, *Strontium-90*, DOE/LLW-123, Idaho National Engineering Laboratory, Idaho Falls, Idaho.

Carboneau, M.L., C.S. Olsen, and R.S. Garcia, 1994b. *National Low-Level Waste Management Program Radionuclide Report Series,* Vol. 6, *Cesium-137*, DOE/LLW-122, Idaho National Engineering Laboratory, Idaho Falls, Idaho.

Catlin, R.J., 1980. *Assessment of the Surveillance Program of the High-Level Waste Storage Tanks at Hanford*, Report to the U.S. Department of Energy Assistant Secretary for Environment, U.S. Department of Energy, Washington D.C.

Conaway, J.G., and P.G. Killeen, 1978. "Quantitative Uranium Determinations from Gamma-Ray Logs by Application of Digital Time Series Analysis," *Geophysics*, Vol. 43, No. 6.

Connelly, M.P., J.V. Borghese, B.H. Ford, 1992. *Hydrogeologic Model for the 200 West Groundwater Aggregate Area*, WHC-SD-EN-TI-014, Westinghouse Hanford Company, Richland, Washington.

David, M., 1977. *Geostatistical Ore Reserve Estimation*, Elsevier, New York.

Deaton, D.E., 1992. Occurrence Report, Subject: "Apparent Decrease in Liquid Level in Single Shell Underground Storage Tank 241-T-101; Leak Suspected; Investigation Continuing," RL-WHC-TANKFARM-1992-0073, Westinghouse Hanford Company, Richland, Washington.

DeFord, D.H., and R.W. Carpenter, 1995. *T Plant Aggregate Area Management Study Technical Baseline Report,* BHI-00177, Rev. 0, Bechtel Hanford Company, Richland, Washington.

Delaney, C.D., K.A. Lindsey, and S.P. Reidel, 1991. *Geology and Hydrology of the Hanford Site: A Standardized Text for Use in Westinghouse Hanford Company Documents and Reports*, WHC-SD-ER-TI-0003, Westinghouse Hanford Company, Richland, Washington.

Dickman, J.F., 1983. Unusual Occurrence Report, Subject: "Tank 241-T-102 Liquid Intrusion," 83-16, Rockwell Hanford Operations, Richland, Washington.

Dresel, P.E., P.D. Thorne, S.P. Lutrell, B.M. Gillespie, W.D. Webber, J.K. Merz, J.T. Rieger, M.A. Chamness, S.K. Wurstner, and B.E. Opitz, 1995. *Hanford Site Ground-Water Monitoring for 1994*, PNL-10698, Pacific Northwest Laboratory, Richland, Washington.

Erdtmann, G., and W. Soyka, 1979. *The Gamma Rays of the Radionuclides: Tables for Applied Gamma Ray Spectrometry*, Verlag Chemie, Weinheim, New York.

Fayer, M.J., and T.B. Walters, 1995. *Estimated Recharge Rates at the Hanford Site*, PNL-10285, Pacific Northwest Laboratory, Richland, Washington.

Fecht, K.R., K.A. Lindsey, B.N. Bjornstad, D.G. Horton, G.V. Last, and S.P. Reidel, 1998. *Clastic Injection Dikes of the Pasco Basin and Vicinity-Geologic Atlas Series*, work in progress, BHI-01103 Draft A, Bechtel Hanford, Inc., Richland, Washington.

Freeman-Pollard, J.R., J.A. Caggiano, S.J. Trent, and EBASCO/Hart Crowser, 1994. *Engineering Evaluation of the GAO/RCED-89-157, Tank 241-T-106 Vadose Zone Investigation*, BHI-00061, Rev. 0, Bechtel Hanford, Inc., Richland, Washington.

General Electric Company (GE), 1989. *Nuclides and Isotopes, Fourteenth Edition, Chart of the Nuclides*, General Electric Company, San Jose, California.

Hanlon, B.M., 1999. *Waste Tank Summary Report for Month Ending March 31, 1999*, HNF-EP-0182-132, Lockheed Martin Hanford Corporation, Richland, Washington.

Hodges, F.N., 1998. *Results of Phase I Groundwater Quality Assessment for Single-Shell Tank Waste Management Areas T and TX-TY at the Hanford Site*, PNNL-11809, prepared by Pacific Northwest National Laboratory for the U.S. Department of Energy, Richland, Washington.

Isaacson, R.E., 1982. *Supporting Information for the Scientific Basis for Establishing Dry-Well Monitoring Frequencies*, RHO-RE-EV-4, Rockwell Hanford Operations, Richland, Washington.

Jensen, H.F., 1975a. Occurrence Report, Subject: "Decreasing Liquid Level In Tank 101-T," 75-17, Atlantic Richfield Hanford Company, Richland, Washington.

Jensen, H.F., 1975b. Occurrence Report, Subject: "Dry Well Radiation Peak Growth," 75-147, Atlantic Richfield Hanford Company, Richland, Washington.

Johnson, V.G., 1993. *Westinghouse Hanford Company Operational Groundwater Status Report, 1990-1992*, WHC-EP-0595, Westinghouse Hanford Company, Richland, Washington.

Journel, A.G., and Ch. J. Huijbregts, 1978. *Mining Geostatistics*, Academic Press, New York.

Koizumi, C.J., 1993. *Calibration Standards for Passive Gamma-Ray Logging at the Hanford Site*, WHC-SD-EN-TI-192, Westinghouse Hanford Company, Richland, Washington.

Koizumi, C.J., J.R. Brodeur, W.H. Ulbricht, and R.K. Price, 1991. *Calibration of the RLS HPGe Spectral Gamma-Ray Logging System*, WHC-EP-0464, Westinghouse Hanford Company, Richland, Washington.

Koizumi, C.J., J.R. Brodeur, R.K. Price, J.E. Meisner, and D.C. Stromswold, 1994. "High-Resolution Gamma-Ray Spectrometry for Contamination Assessment," *Nuclear Geophysics*, Vol. 8, No. 2, pp. 149-164.

Lederer, C.M., and V.S. Shirley (eds.), 1978. *Table of Isotopes 7th Edition*, John Wiley and Sons, Inc., New York, New York.

Lindsay, W.M., 1981. Occurrence Report, Subject: "Liquid Level Increase in Tank 103-T Exceeding the Increase Criterion," 81-25, Rockwell Hanford Operations, Richland, Washington.

Lindsey, K.A., 1993. Memorandum to G.D. Bazinet with attached letter report *Geohydrologic Setting, Flow, and Transport Parameters for the Single Shell Tank Farms,* written by K.A. Lindsey and A. Law, 81231-93-060, Westinghouse Hanford Company, Richland, Washington.

_____, 1995. *Miocene to Pliocene-Aged Suprabasalt Sediments of the Hanford Site, South-Central Washington*, BHI-00184, Rev. 0, Bechtel Hanford, Inc., Richland, Washington.

Lindsey, K.A., and D.G. Horton, 1991. *Geologic Setting of the 200 West Area: An Update*, WHC-SD-EN-TI-008, Westinghouse Hanford Company, Richland, Washington.

Lindsey, K.A., B.N. Bjornstad, J.W. Lindberg, and K.M. Hoffman, 1992. *Geologic Setting of the 200 East Area: An Update*, WHC-SD-EN-TI-012, Rev. 0, Westinghouse Hanford Company, Richland, Washington.

Lindsey, K.A., S.P. Reidel, K.R. Fecht, J.L. Slate, A.G. Law, and A.M. Tallman, 1994. "Geohydrologic Setting of the Hanford Site, South-Central Washington," in *Geologic Field Trips of the Pacific Northwest: 1994 Geological Society of America Annual Meeting*, edited by D.A. Swanson and R.A. Haugerud, Dept. of Geological Sciences, University of Washington, Seattle, Washington, pp. 1C-1 to 1C-16.

MACTEC-ERS, 1996. *General Administrative Procedures Manual*, MAC-1000, Grand Junction Office, Grand Junction Office, Grand Junction, Colorado.

Myers, D.A., D.L. Parker (MACTEC-ERS), G. Gee, V.G. Johnson, V. Last, R.J. Serne (PNNL), and D.J. Moak (Waste Management Northwest), 1998. *Findings of the Extension of Borehole 41-09-39, 241-SX Tank Farm*, HNF-2855, Lockheed Martin Hanford Corporation, Richland, Washington.

Pacific Northwest National Laboratory (PNNL), 1998. *Hanford Site Groundwater Monitoring for Fiscal Year 1997*, PNNL-11793, prepared by Pacific Northwest National Laboratory for the U.S. Department of Energy, Richland, Washington.

Price, W.H., and K.R. Fecht, 1976. *Geology of the 241-T Tank Farm,* ARH-LD-135, Atlantic Richfield Hanford Company, Richland, Washington.

Raymond, R., 1991. White Paper, Subject: "Potential Leak in Tank 241-T-107," Westinghouse Hanford Co., Richland, Washington.

Routson, R.C., W.H. Price, D.J. Brown, and K.R. Fecht, 1979. *High-Level Waste Leakage from the 241-T-106 Tank at Hanford*, RHO-ST-14, prepared for the U.S. Department of Energy by Rockwell Hanford Operations, Richland, Washington.

Rudin, M.J., and R.S. Garcia, 1992a. *National Low-Level Waste Management Program Radionuclide Report Series,* Vol. 1, *Introduction*, DOE/LLW-117, Idaho National Engineering Laboratory, Idaho Falls, Idaho.

_____, 1992b. *National Low-Level Waste Management Program Radionuclide Report Series,* Vol. 4, *Iodine-129*, DOE/LLW-120, Idaho National Engineering Laboratory, Idaho Falls, Idaho.

Rudin, M.J., C. Stanton, R.G. Patterson, and R.S. Garcia, 1992. *National Low-Level Waste Management Program Radionuclide Report Series,* Vol. 2, *Technitium-99*, DOE/LLW-118, Idaho National Engineering Laboratory, Idaho Falls, Idaho.

Scott, K.V., 1993. *Engineering Assessment of Hanford Single-Shell High-Level Waste Tank Leak Detection*, WHC-SD-WM-EX-264, Rev. 0, Westinghouse Hanford Company, Richland, Washington.

Smith, D.L., 1996. *216-T-4 Interim Stabilization Final Report,* BHI-00616, Rev. 0, Bechtel Hanford Incorporated, Richland, Washington.

Tallman, A.M., K.R. Fecht, M.C. Marratt, and G.V. Last, 1979. *Geology of the Separations Areas, Hanford Site, South-Central Washington,* RHO-ST-23, Rockwell Hanford Operations, Richland, Washington.

Tolan, T.L., and S.P. Reidel, 1989. "Structure Map of a Portion of the Columbia River Flood Basalt Province," in *Volcanism and Tectonism in the Columbia River Flood Basalt Province,* Special Paper 239, edited by S.P. Reidel and P.R. Hooper, Geologic Society of America, Boulder, Colorado, Plate 1.

Tucker, R.P., 1994. Occurrence Report, Subject: "Apparent Liquid Level Decrease in Single Shell Underground Storage Tank 241-T-111; Declared an Assumed Re-Leaker," WHC-TANKFARM-1994-0009, Westinghouse Hanford Company, Richland, Washington.

U.S. Department of Energy (DOE), 1944. *Specifications for Construction of Composite Storage Tanks Bldg. No. 241,* Hanford Engineer works Project 9536, issued January 11, 1944.

_____, 1988. *Consultation Draft Characterization Plan,* DOE/RW-0164, Vol. 1-9, Office of Civilian Radioactive Waste Management, U.S. Department of Energy, Washington, D.C.

_____, 1992. *T Plant Source Aggregate Area Management Study Report,* DOE/RL-91-61, Rev. 0, Prepared by Westinghouse Hanford Company, Richland, Washington, November.

_____, 1993. *200 West Groundwater Aggregate Area Management Study Report,* DOE/RL-92-16, Rev. 0, Richland Operations Office, Richland, Washington.

_____, 1995a. *Vadose Zone Characterization Project at the Hanford Tank Farms, Calibration of Two Spectral Gamma-Ray Logging Systems for Baseline Characterization Measurements in the Hanford Tank Farms*, GJPO-HAN-1, prepared by Rust Geotech for the Grand Junction Projects Office, Grand Junction, Colorado.

_____, 1995b. *Vadose Zone Characterization Project at the Hanford Tank Farms, Evaluation of In-Tank Leak Detection Methods and Recommendations for a Tank Leak-Verification and Monitoring System*, DOE/ID/12584-227, prepared by Rust Geotech for the Grand Junction Projects Office, Grand Junction, Colorado.

_____, 1995c. *Vadose Zone Characterization Project at the Hanford Tank Farms, Spectral Gamma-Ray Borehole Geophysical Logging Characterization and Baseline Monitoring Plan for the Hanford Single-Shell Tanks*, P-GJPO-1786, prepared by Rust Geotech for the Grand Junction Projects Office, Grand Junction, Colorado.

U.S. Department of Energy (DOE), 1995d. *Hanford Tank Farms Vadose Zone, Tank Summary Data Report for Tank T-107*, GJ-HAN-2, prepared by MACTEC-ERS for the Grand Junction Office, Grand Junction, Colorado, August.

_____, 1995e. *Hanford Tank Farms Vadose Zone, Tank Summary Data Report for Tank T-110*, GJ-HAN-1, prepared by MACTEC-ERS for the Grand Junction Office, Grand Junction, Colorado, August.

_____, 1996a. *Hanford Site Groundwater Monitoring for Fiscal Year 1995*, PNNL-114-41, prepared by Pacific Northwest National Laboratory for the U.S. Department of Energy, Richland, Washington.

_____, 1996b. *Single-Shell Tank Closure Work Plan*, DOE/RL-89-16, Rev. 1, Richland Operations Office, Richland, Washington.

_____, 1996c. *Vadose Zone Characterization Project at the Hanford Tank Farms, Biannual Calibration of Two Spectral Gamma-Ray Logging Systems Used for Baseline Characterization Measurements in the Hanford Tank Farms*, GJPO-HAN-3, prepared by Rust Geotech for the Grand Junction Projects Office, Grand Junction, Colorado.

_____, 1996d. *Vadose Zone Characterization Project at the Hanford Tank Farms, Second Biannual Recalibration of Two Spectral Gamma-Ray Logging Systems Used for Baseline Characterization Measurements at the Hanford Tank Farms*, GJPO-HAN-5, prepared by Rust Geotech for the Grand Junction Projects Office, Grand Junction, Colorado.

_____, 1997a. *Hanford Tank Farms Vadose Zone, Calibration Plan for Spectral Gamma-Ray Logging Systems*, MAC-VZCP 1.7.3, Rev. 1, prepared by MACTEC-ERS for the Grand Junction Office, Grand Junction, Colorado.

_____, 1997b. *Hanford Tank Farms Vadose Zone, Data Analysis Manual*, MAC-VZCP 1.7.9, Rev. 1, prepared by MACTEC-ERS for the Grand Junction Office, Grand Junction, Colorado.

_____, 1997c. *Hanford Tank Farms Vadose Zone, Health and Safety Plan*, MAC-VZCP 1.7.4, Rev. 1, prepared by MACTEC-ERS for the Grand Junction Office, Grand Junction, Colorado.

_____, 1997d. *Hanford Tank Farms Vadose Zone, High-Resolution Passive Spectral Gamma-Ray Logging Procedures*, MAC-VZCP 1.7.10-1, Rev. 2, prepared by MACTEC-ERS for the Grand Junction Office, Grand Junction, Colorado.

_____, 1997e. *Hanford Tank Farms Vadose Zone, Preventive Maintenance Procedures for the Spectral Gamma Logging System*, MAC-VZCP 1.7.10-2, Rev. 1, prepared by MACTEC-ERS for the Grand Junction Office, Grand Junction, Colorado.

U.S. Department of Energy (DOE), 1997f. *Hanford Tank Farms Vadose Zone, Project Management Plan*, MAC-VZCP 1.7.2, Rev. 1, prepared by MACTEC-ERS for the Grand Junction Office, Grand Junction, Colorado.

_____, 1997g. *Hanford Tank Farms Vadose Zone, Third Biannual Recalibration of Two Spectral Gamma-Ray Logging Systems Used for Baseline Characterization Measurements in the Hanford Tank Farms,* GJO-HAN-13, prepared by MACTEC-ERS for the Grand Junction Office, Grand Junction, Colorado.

_____, 1997h. *TWRS Vadose Zone Contamination Issue Expert Panel Status Report*, DOE/RL-97-49, Rev. 0, Fluor Daniel Hanford, Inc., Richland, Washington.

_____, 1997i. *Vadose Zone Characterization Project at the Hanford Tank Farms, TX Tank Farm Report*, GJO-HAN-11, prepared by MACTEC-ERS for the Grand Junction Office, Grand Junction, Colorado, September.

_____, 1998a. *Hanford Tank Farms Vadose Zone, Fourth Biannual Recalibration of Spectral Gamma-Ray Logging Systems Used for Baseline Characterization Measurements in the Hanford Tank Farms*, GJO-HAN-14, prepared by MACTEC-ERS for the Grand Junction Office, Grand Junction, Colorado.

_____, 1998b. *Hanford Tank Farms Vadose Zone, Fifth Biannual Recalibration of Spectral Gamma-Ray Logging Systems Used for Baseline Characterization Measurements in the Hanford Tank Farms*, GJO-HAN-20, prepared by MACTEC-ERS for the Grand Junction Office, Grand Junction, Colorado.

_____, 1998c. *Hanford Tank Farms Vadose Zone, Tank Summary Data Report for Tank T-108*, GJ-HAN-121, prepared by MACTEC-ERS for the Grand Junction Office, Grand Junction, Colorado, December.

_____, 1998d. *Hanford Tank Farms Vadose Zone, Tank Summary Data Report for Tank T-109*, GJ-HAN-122, prepared by MACTEC-ERS for the Grand Junction Office, Grand Junction, Colorado, November.

_____, 1998e. *Hanford Tank Farms Vadose Zone, Tank Summary Data Report for Tank T-111*, GJ-HAN-123, prepared by MACTEC-ERS for the Grand Junction Office, Grand Junction, Colorado, December.

_____, 1998f. *Hanford Tank Farms Vadose Zone, Tank Summary Data Report for Tank T-112*, GJ-HAN-124, prepared by MACTEC-ERS for the Grand Junction Office, Grand Junction, Colorado, November.

U.S. Department of Energy (DOE), 1998g. *Vadose Zone Characterization Project at the Hanford Tank Farms, TY Tank Farm Report*, GJO-HAN-16, prepared by MACTEC-ERS for the Grand Junction Office, Grand Junction, Colorado, January.

_____, 1999a. *Hanford Tank Farms Vadose Zone, A Tank Farm Report*, GJO-HAN-23, prepared by MACTEC-ERS for the Grand Junction Office, Grand Junction, Colorado, March.

_____, 1999b. *Hanford Tank Farms Vadose Zone, Tank Summary Data Report for Tank T-101*, GJ-HAN-115, prepared by MACTEC-ERS for the Grand Junction Office, Grand Junction, Colorado, March.

_____, 1999c. *Hanford Tank Farms Vadose Zone, Tank Summary Data Report for Tank T-102*, GJ-HAN-116, prepared by MACTEC-ERS for the Grand Junction Office, Grand Junction, Colorado, February.

_____, 1999d. *Hanford Tank Farms Vadose Zone, Tank Summary Data Report for Tank T-103*, GJ-HAN-117, prepared by MACTEC-ERS for the Grand Junction Office, Grand Junction, Colorado, March.

_____, 1999e. *Hanford Tank Farms Vadose Zone, Tank Summary Data Report for Tank T-104*, GJ-HAN-118, prepared by MACTEC-ERS for the Grand Junction Office, Grand Junction, Colorado, March.

_____, 1999f. *Hanford Tank Farms Vadose Zone, Tank Summary Data Report for Tank T-105*, GJ-HAN-119, prepared by MACTEC-ERS for the Grand Junction Office, Grand Junction, Colorado, July.

_____, 1999g. *Hanford Tank Farms Vadose Zone, Tank Summary Data Report for Tank T-106*, GJ-HAN-120, prepared by MACTEC-ERS for the Grand Junction Office, Grand Junction, Colorado, June.

U.S. General Accounting Office (GAO), 1989. *Nuclear Waste: DOE's Management of Single-Shell Tanks at Hanford Washington*, U.S. General Accounting Office, Department of Energy, Washington D.C.

Vermeulen, N.J., 1991. Occurrence Report, Subject: "Surface Level Measurement Decrease in Tank 241-T-107," A-6000-576, Westinghouse Hanford Co., Richland, Washington.

Walker, C.M., 1988. Internal Memo, Subject: "Summary of Leaker or Questionable Integrity Tanks," 13331-88-460, Westinghouse Hanford Company, Richland, Washington.

Walker, C.M., and S. Stalos, 1987. *Waste Storage Tank Status and Leak Detection Criteria*, RHO-CD-213, Rockwell Hanford Operations, Richland, Washington.

Washington State Department of Ecology (Ecology), 1994. *Dangerous Waste Portion of the Resource Conservation and Recovery Act Permit for the Treatment, Storage, and Disposal of Dangerous Waste,* Permit Number WA7890008967.

Washington State Department of Ecology (Ecology), U.S. Environmental Protection Agency, and U.S. Department of Energy, 1996. *Hanford Federal Facility Agreement and Consent Order,* 89-10, Amendments 4, 5, and 6, Rev. 4.

Welty, R.K., 1988. *Waste Storage Tank Status and Leak Detection Criteria,* SD-WM-TI-356, Westinghouse Hanford Company, Richland, Washington.

Welty, R.K., and N.J. Vermeulen, 1989. *Waste Storage tank And Leak Detection Criteria,* WHC-SD-WM-TI-357, Westinghouse Hanford Company, Richland, Washington.

Westinghouse Hanford Company (WHC), 1994. *Operating Specifications for Tank Farm Leak Detection,* WHC-OSD0151-00031, Westinghouse Hanford Company, Richland, Washington.

Wilson, R.D., 1997. *Hanford Tank Farms Vadose Zone, Spectrum Shape-Analysis Techniques Applied to the Hanford Tank Farms Spectral Gamma Logs,* GJO-HAN-7, prepared by MACTEC-ERS for the U.S. Department of Energy Grand Junction Office, Grand Junction, Colorado.

_____, 1998. *Hanford Tank Farms Vadose Zone, Enhancements, Validations, and Applications of Spectrum Shape-Analysis Techniques Applied to Hanford Tank Farms Spectral Gamma Logs,* GJO-HAN-15, prepared by MACTEC-ERS for the Grand Junction Office, Grand Junction, Colorado.

Winberg, M.R., and R.S. Garcia, 1995. *National Low-Level Waste Management Program Radionuclide Report Series,* Vol. 14, *Americium-241,* DOE/LLW-130, Idaho National Engineering Laboratory, Idaho Falls, Idaho.

Appendix A
Groundwater Monitoring Data

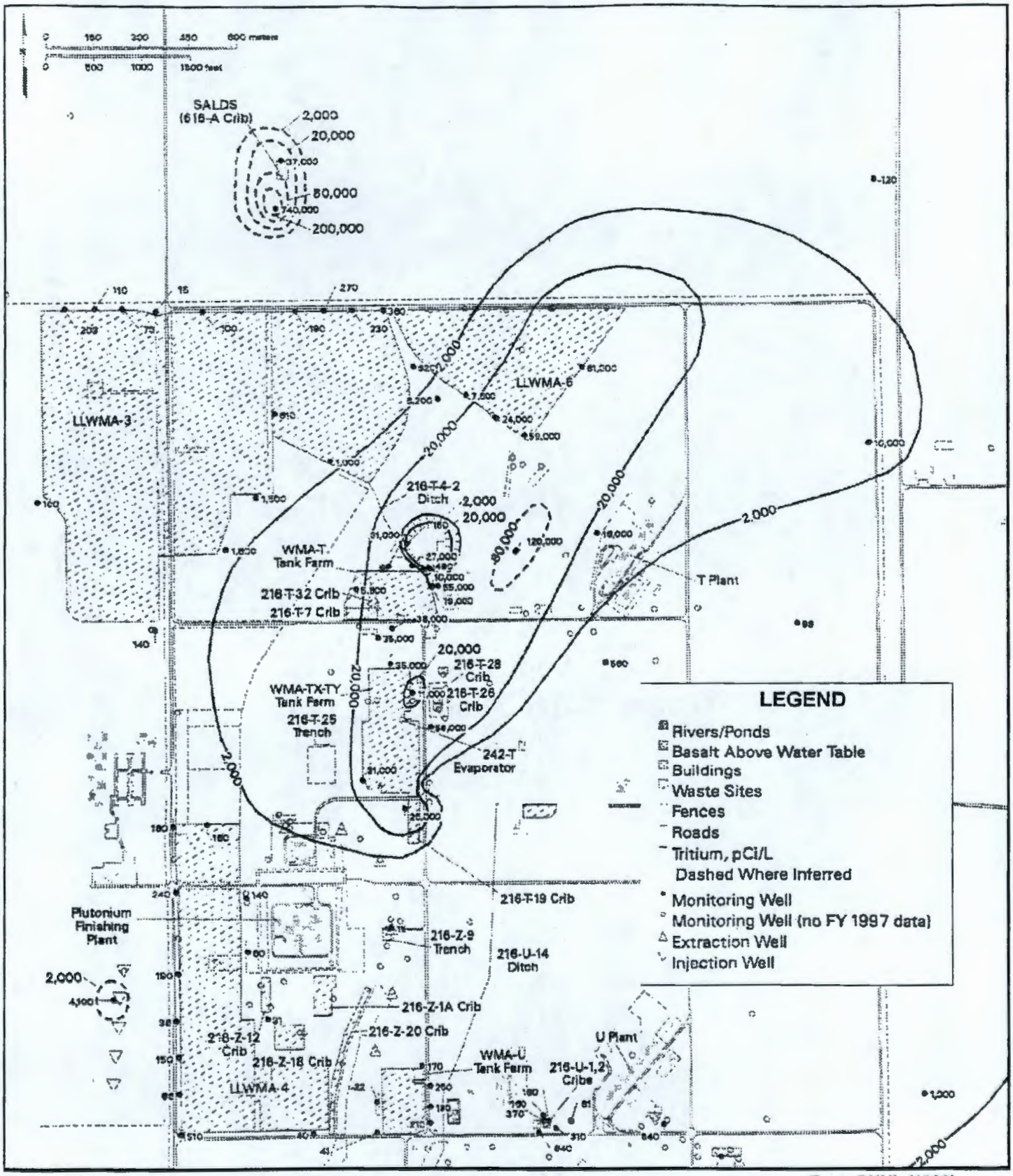

From PNNL (1998)

Figure A-1. FY 1997 Average Tritium Concentrations

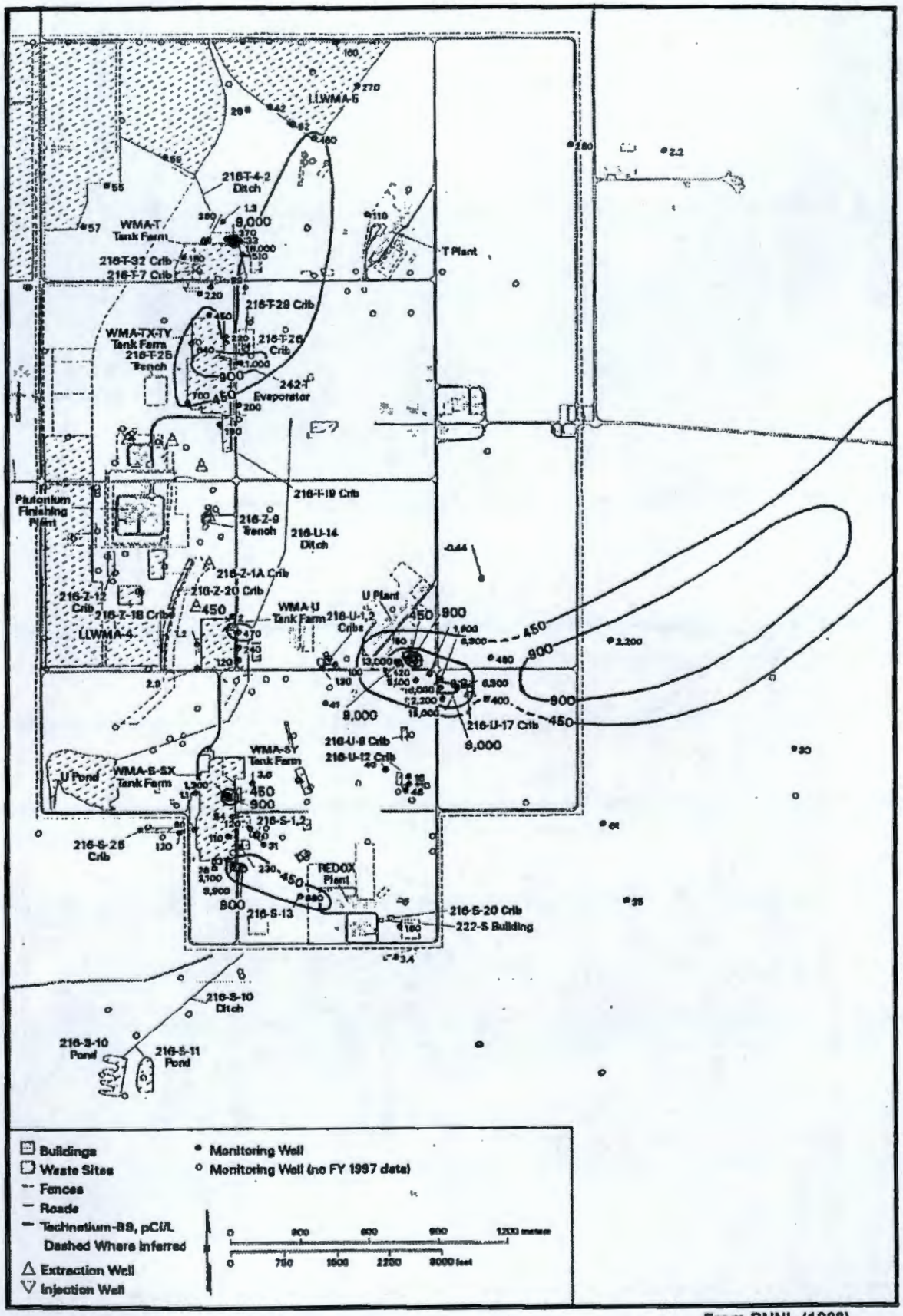

From PNNL (1998)

Figure A-2. FY 1997 Average Technetium-99 Concentrations

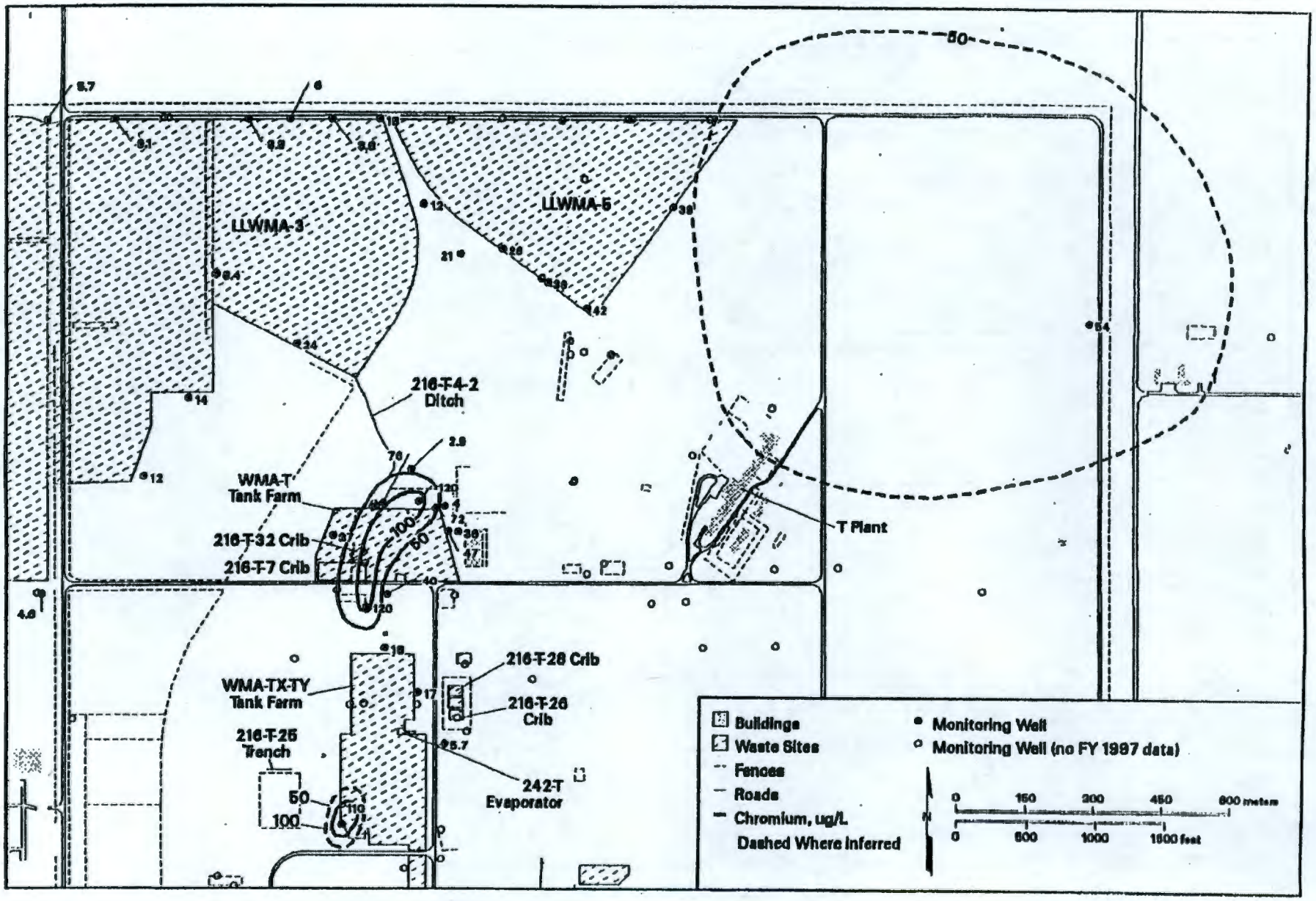

From PNNL (1998)

Figure A-3. FY 1997 Average Chromium Concentrations

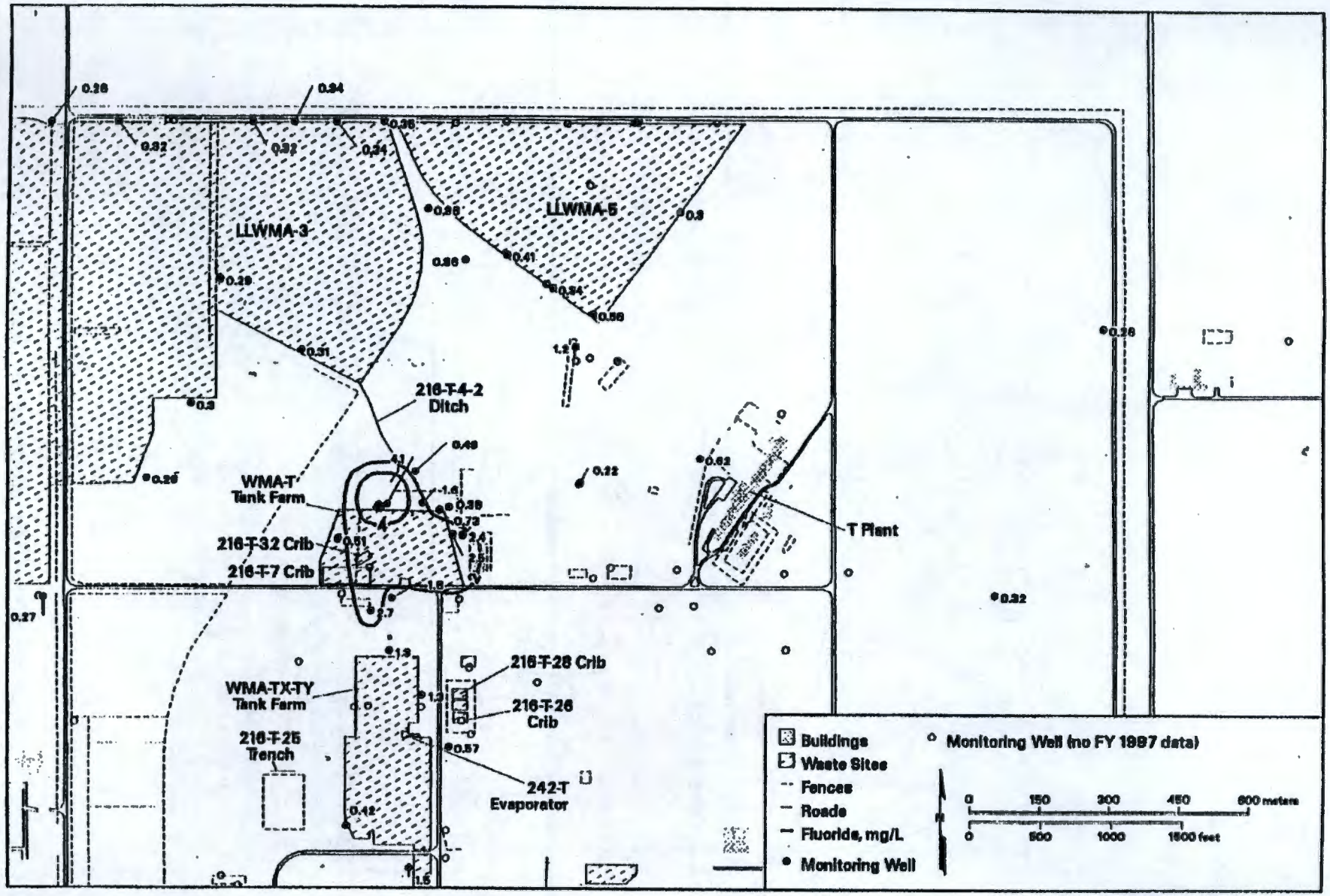

From PNNL (1998)

Figure A-4. FY 1997 Average Fluoride Concentrations

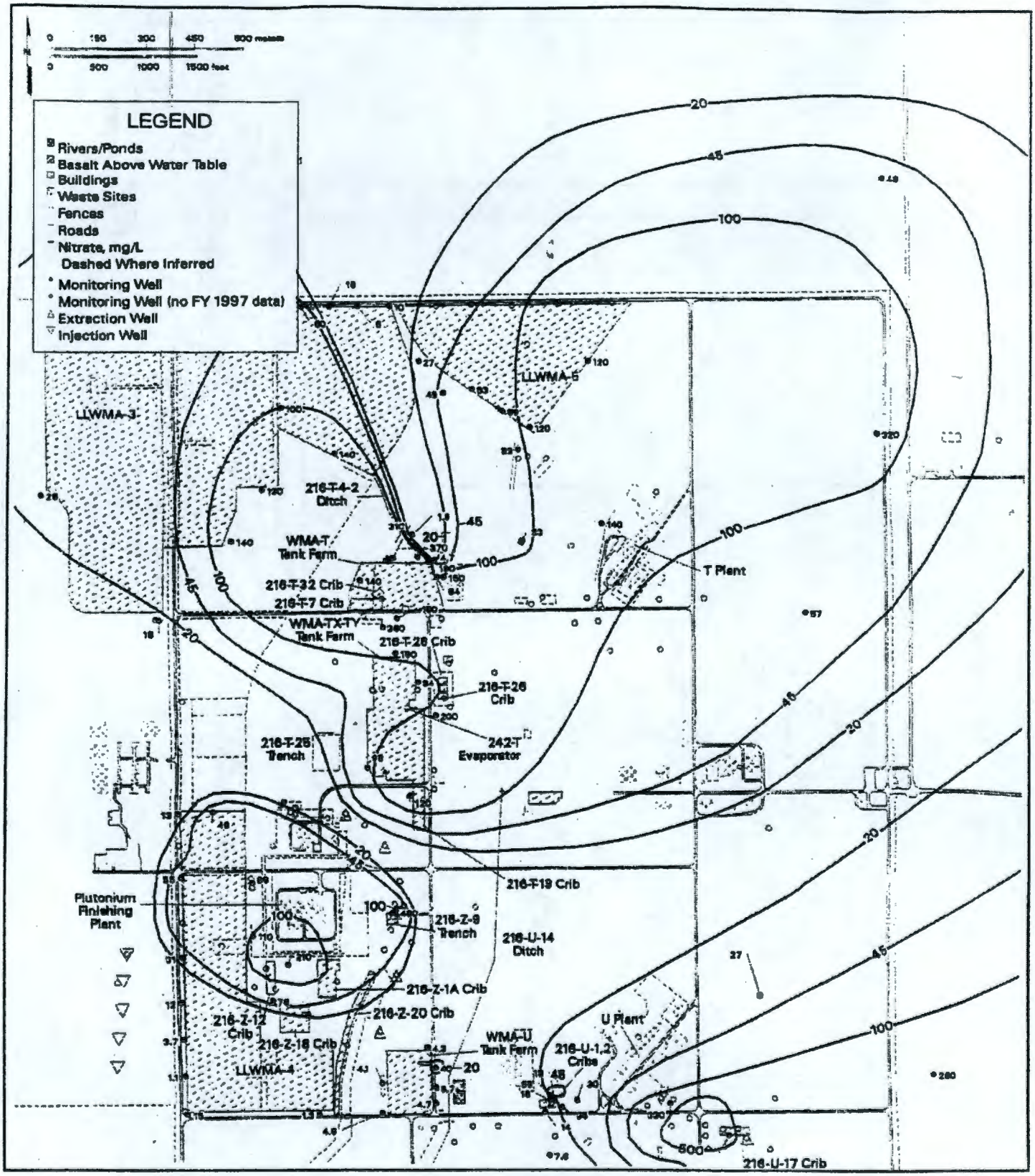

From PNNL (1998)

Figure A-5. FY 1997 Average Nitrate Concentrations

Appendix B
T Tank Farm Correlation Plots

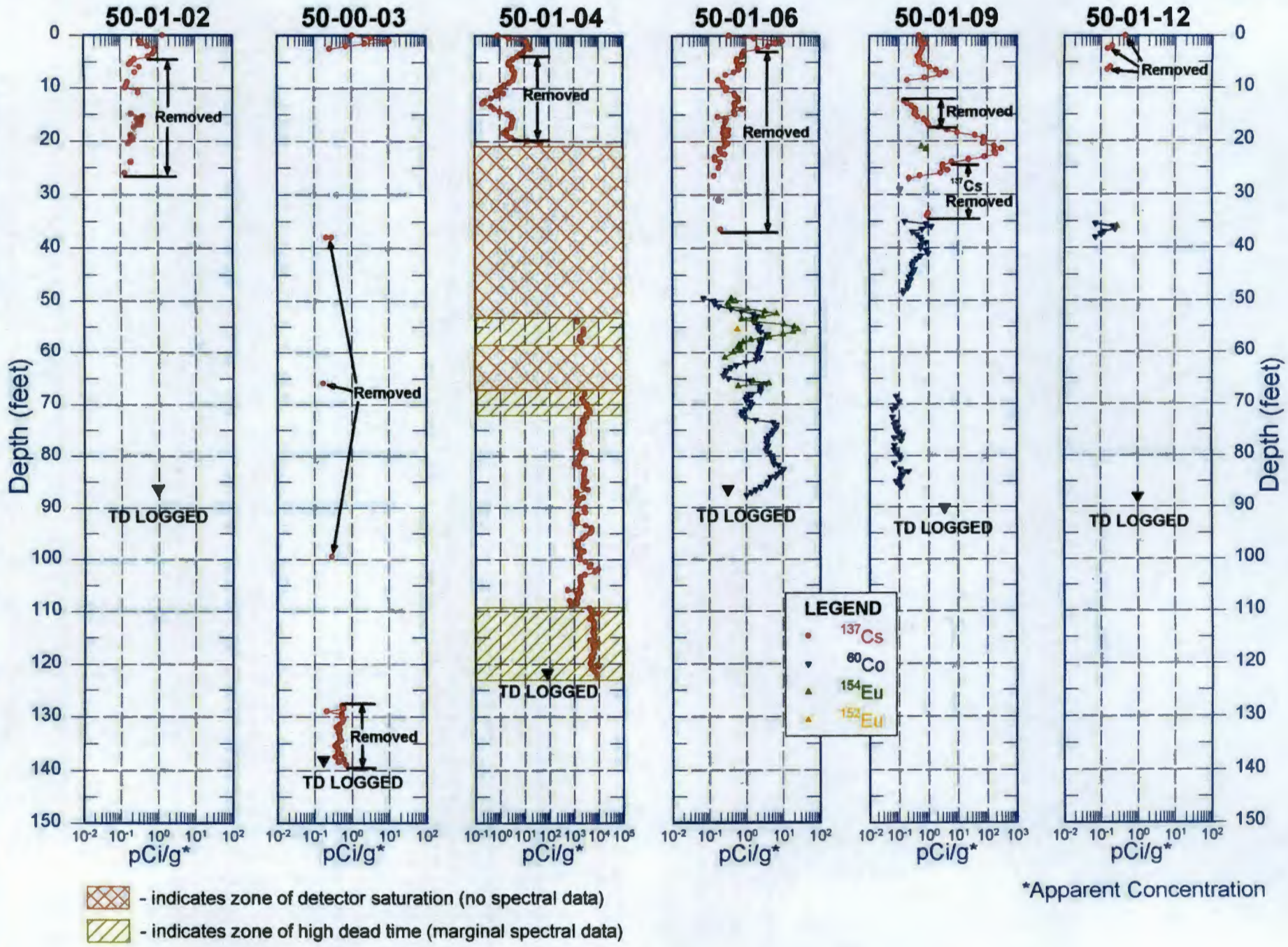

Figure B-1. Correlation Plot of ^{137}Cs, ^{60}Co, ^{152}Eu, and ^{154}Eu Concentrations in Boreholes Surrounding T-101

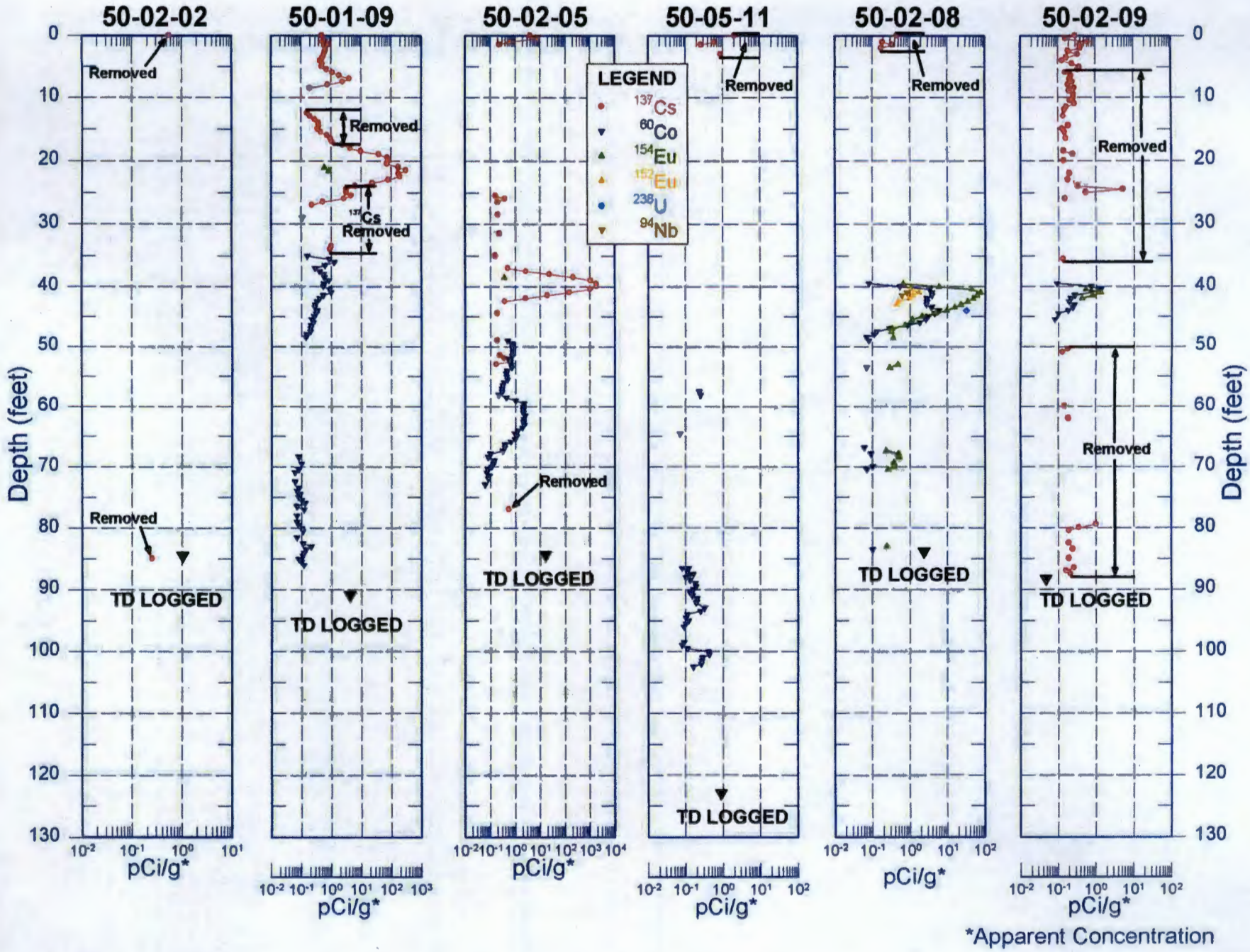

Figure B-2. Correlation Plot of ^{137}Cs, ^{60}Co, ^{152}Eu, ^{154}Eu, ^{238}U, and ^{94}Nb Concentrations in Boreholes Surrounding T-102

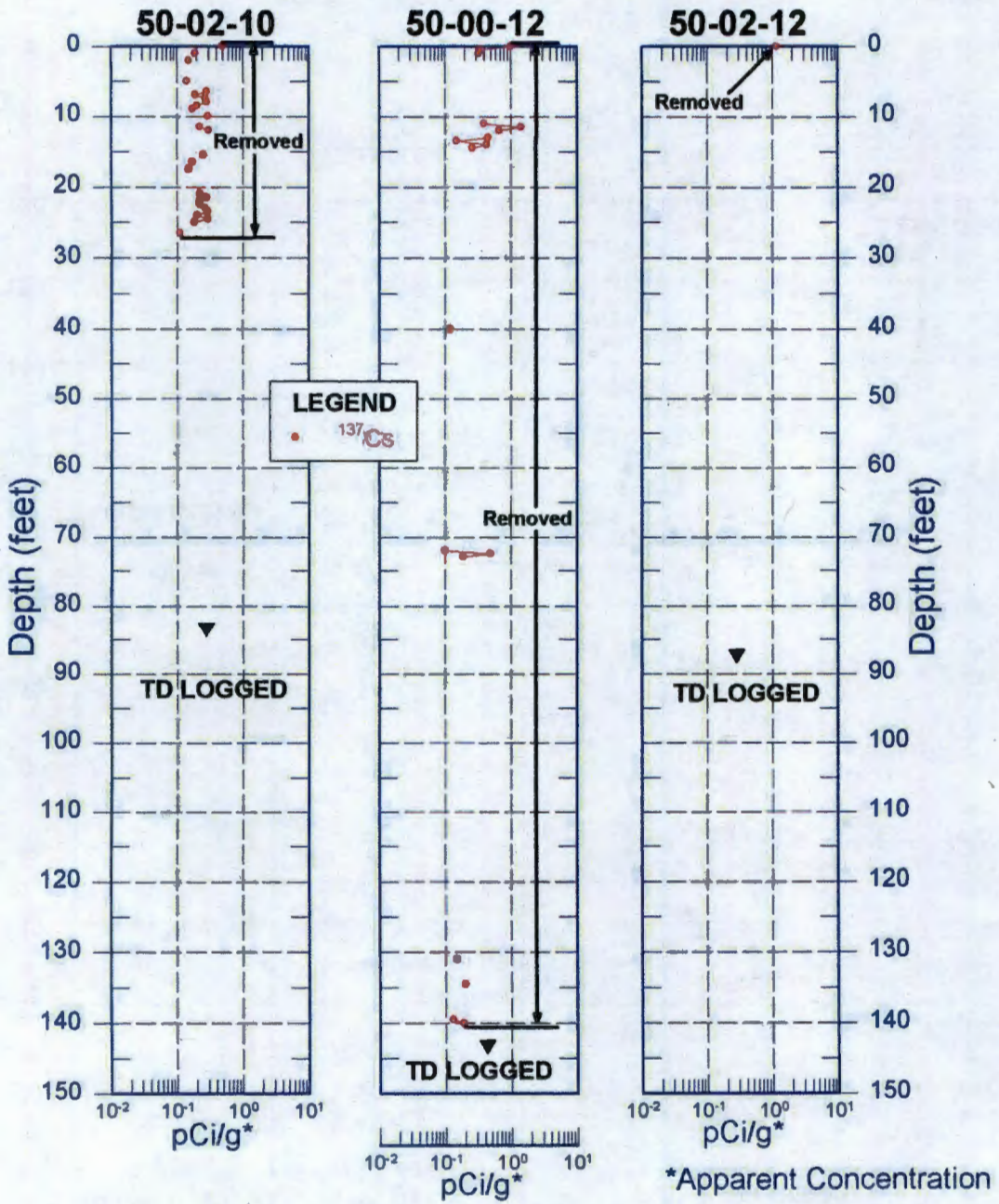

Figure B-2 (continued). Correlation Plot of ^{137}Cs, ^{60}Co, ^{152}Eu, ^{154}Eu, ^{238}U, and ^{94}Nb Concentrations in Boreholes Surrounding T-102

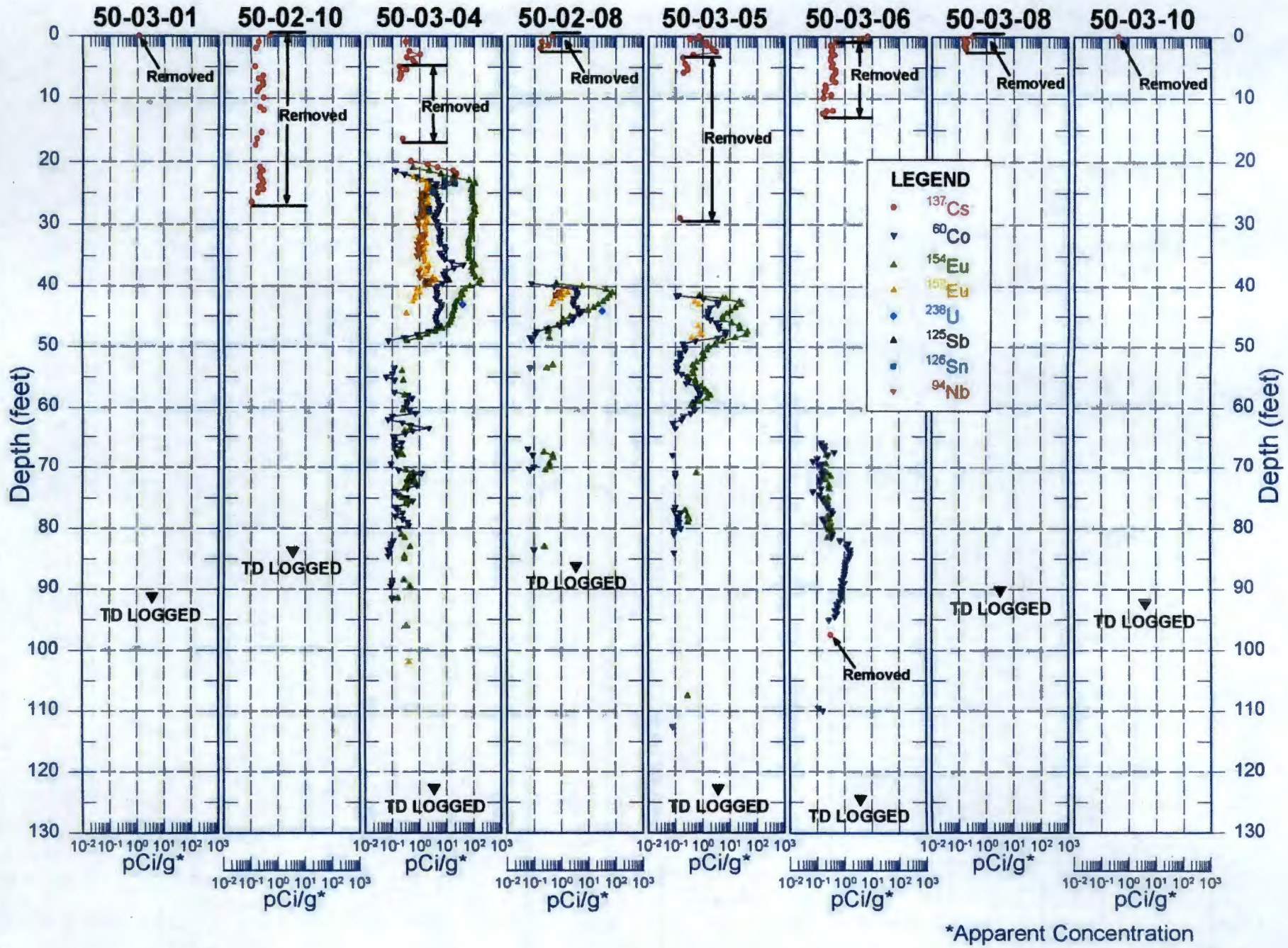

Figure B-3. Correlation Plot of ^{137}Cs, ^{60}Co, ^{152}Eu, ^{154}Eu, ^{238}U, ^{125}Sb, ^{126}Sn, and ^{94}Nb Concentrations in Boreholes Surrounding T-103

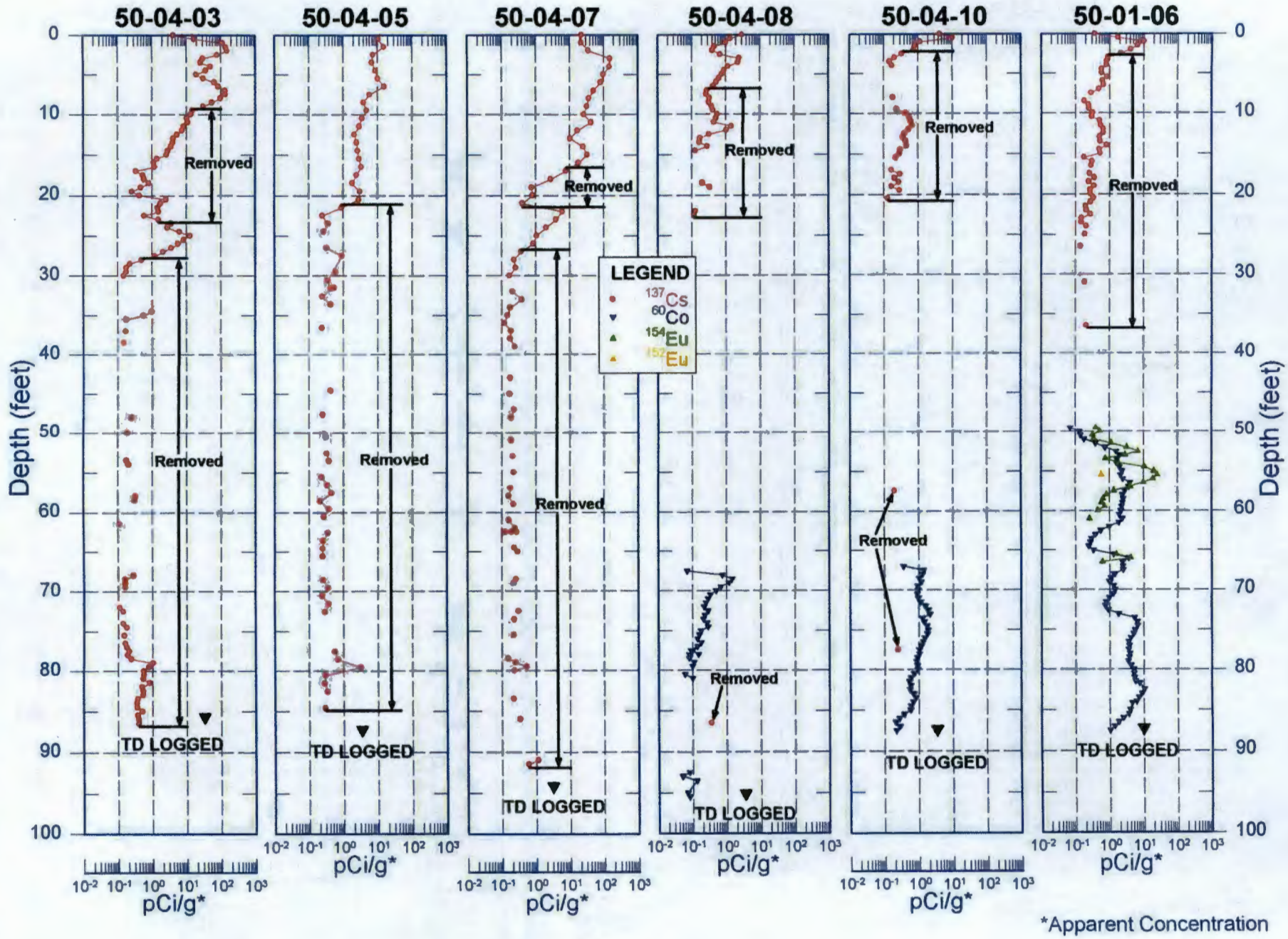

Figure B-4. Correlation Plot of ^{137}Cs, ^{60}Co, ^{152}Eu, and ^{154}Eu Concentrations in Boreholes Surrounding T-104

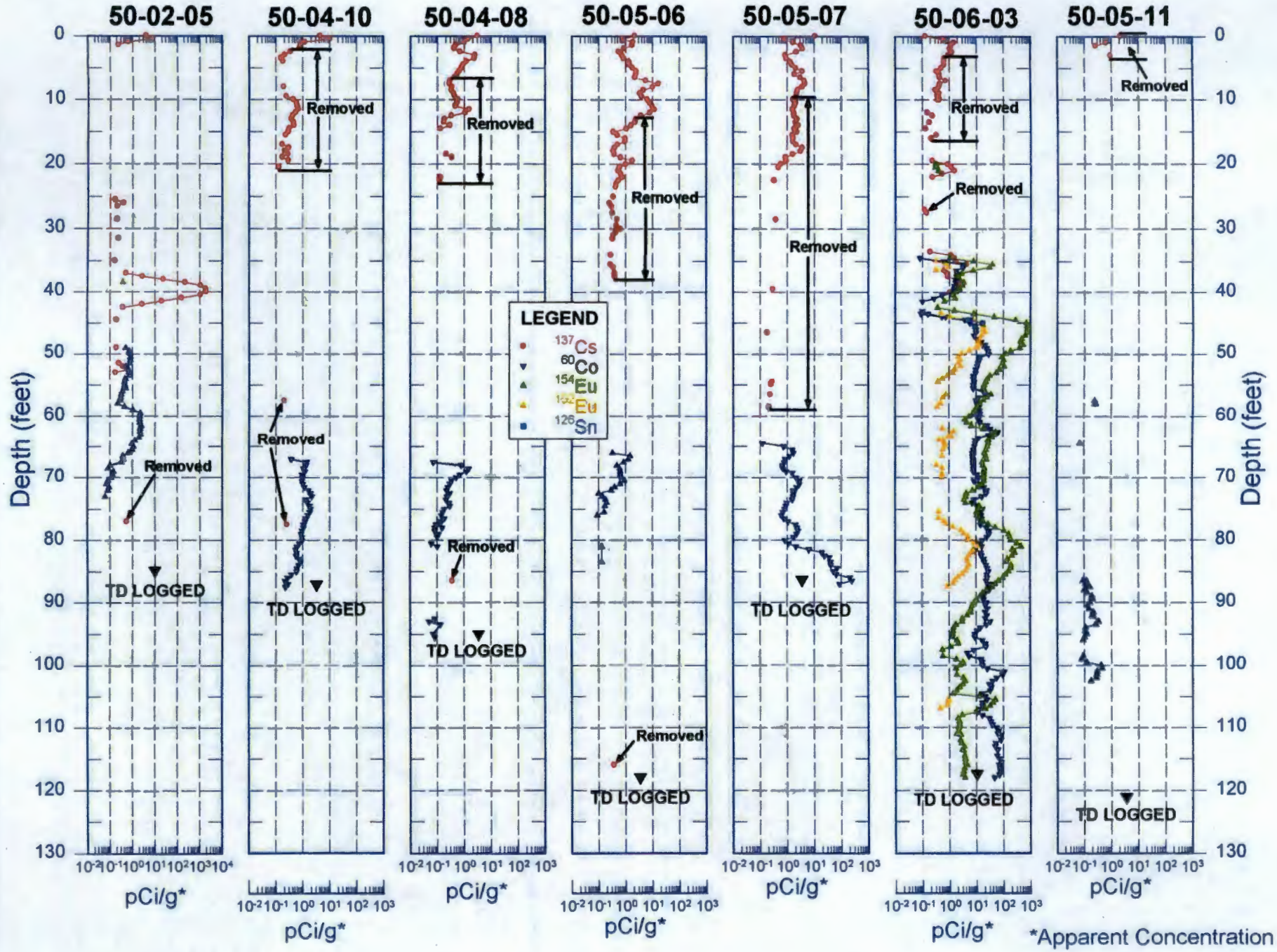

Figure B-5. Correlation Plot of ^{137}Cs, ^{60}Co, ^{152}Eu, ^{154}Eu, and ^{126}Sn Concentrations in Boreholes Surrounding T-105

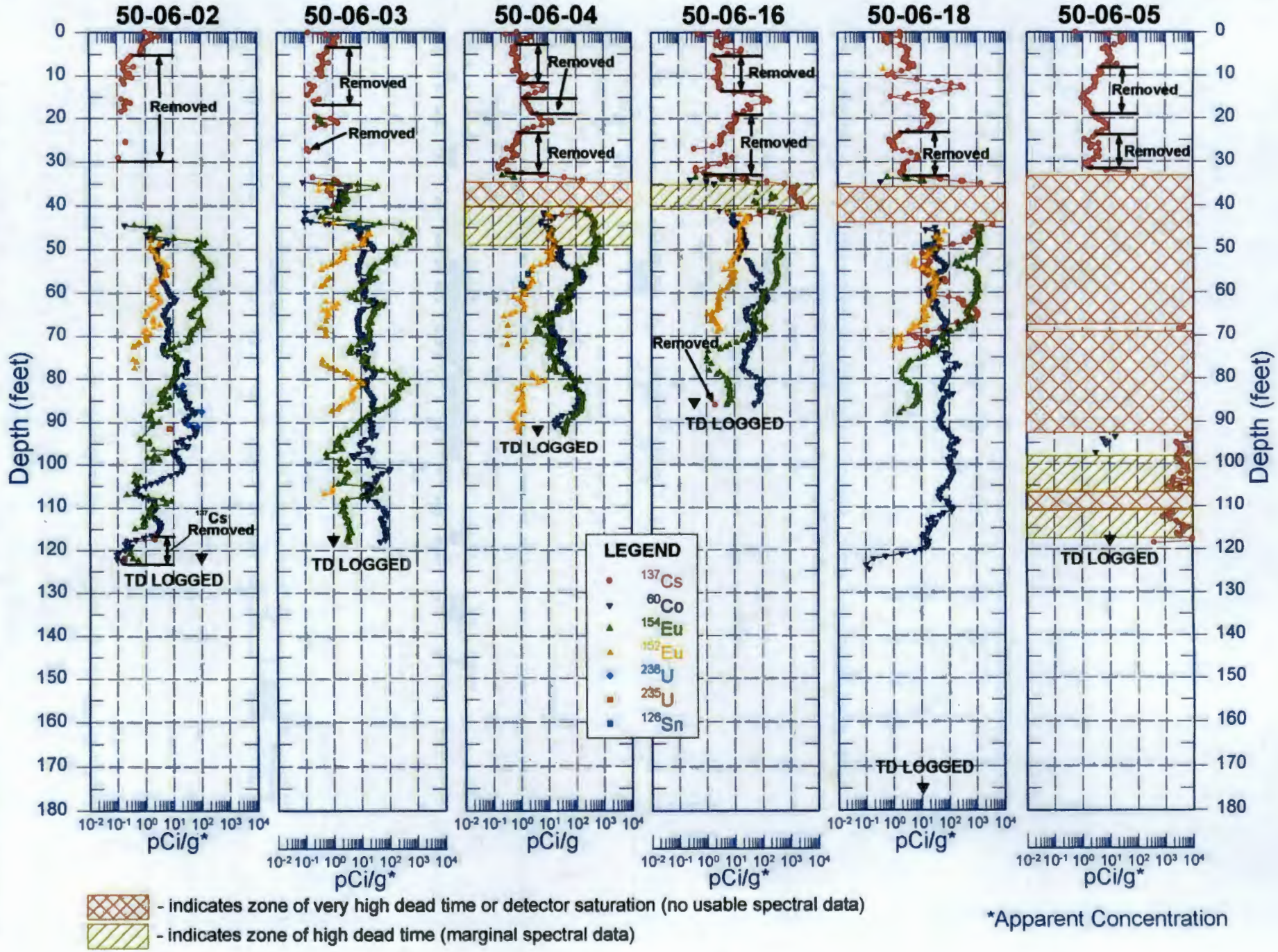

Figure B-6. Correlation Plot of ^{137}Cs, ^{60}Co, ^{152}Eu, ^{154}Eu, ^{238}U, ^{235}U, ^{125}Sb, and ^{126}Sn Concentrations in Boreholes Surrounding T-106

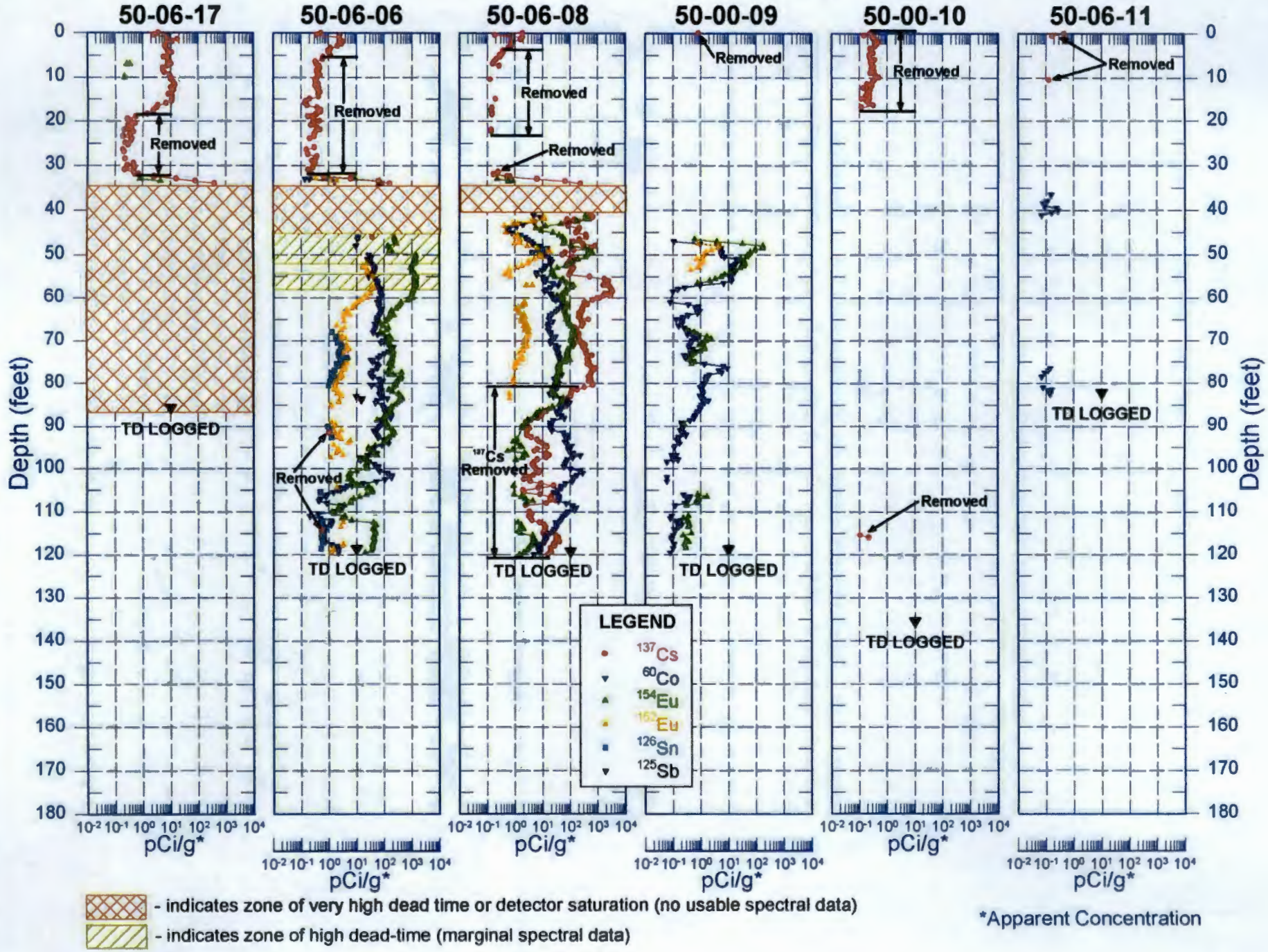

Figure B-6 (continued). Correlation Plot of ^{137}Cs, ^{60}Co, ^{152}Eu, ^{154}Eu, ^{238}U, ^{235}U, ^{125}Sb, and ^{126}Sn Concentrations in Boreholes Surrounding T-106

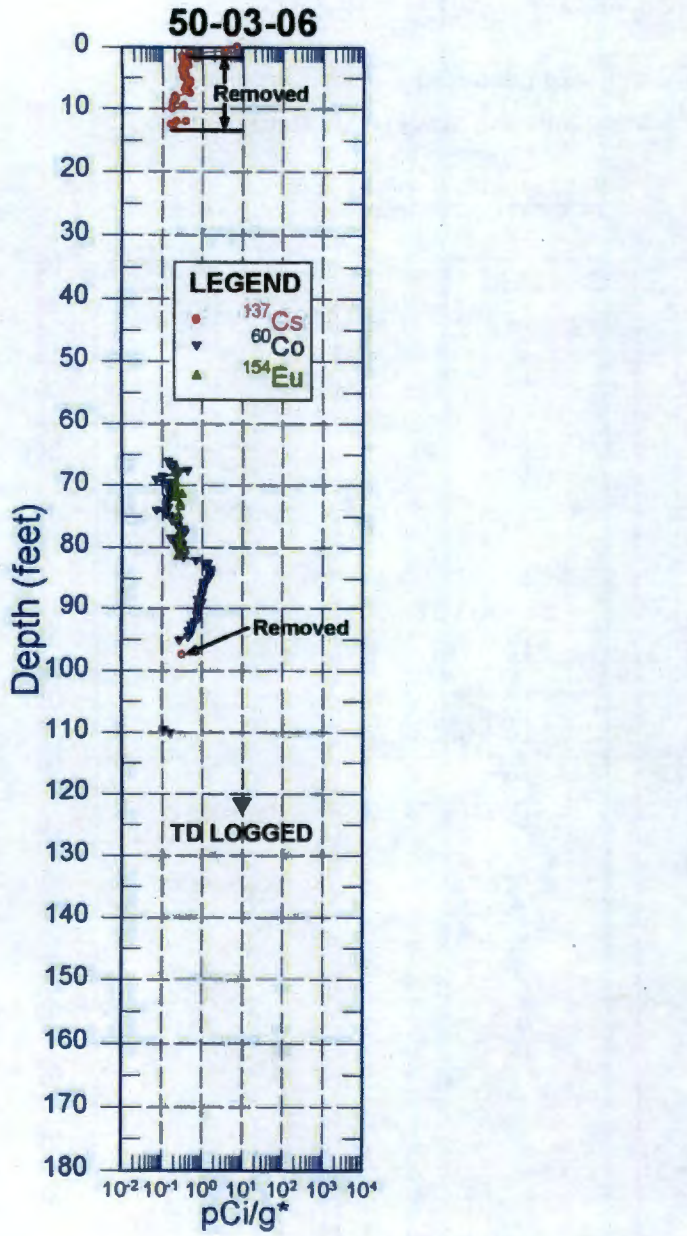

*Apparent Concentration

Figure B-6 (continued). Correlation Plot of ^{137}Cs, ^{60}Co, ^{152}Eu, ^{154}Eu, ^{238}U, ^{235}U, ^{125}Sb, and ^{126}Sn Concentrations in Boreholes Surrounding T-106

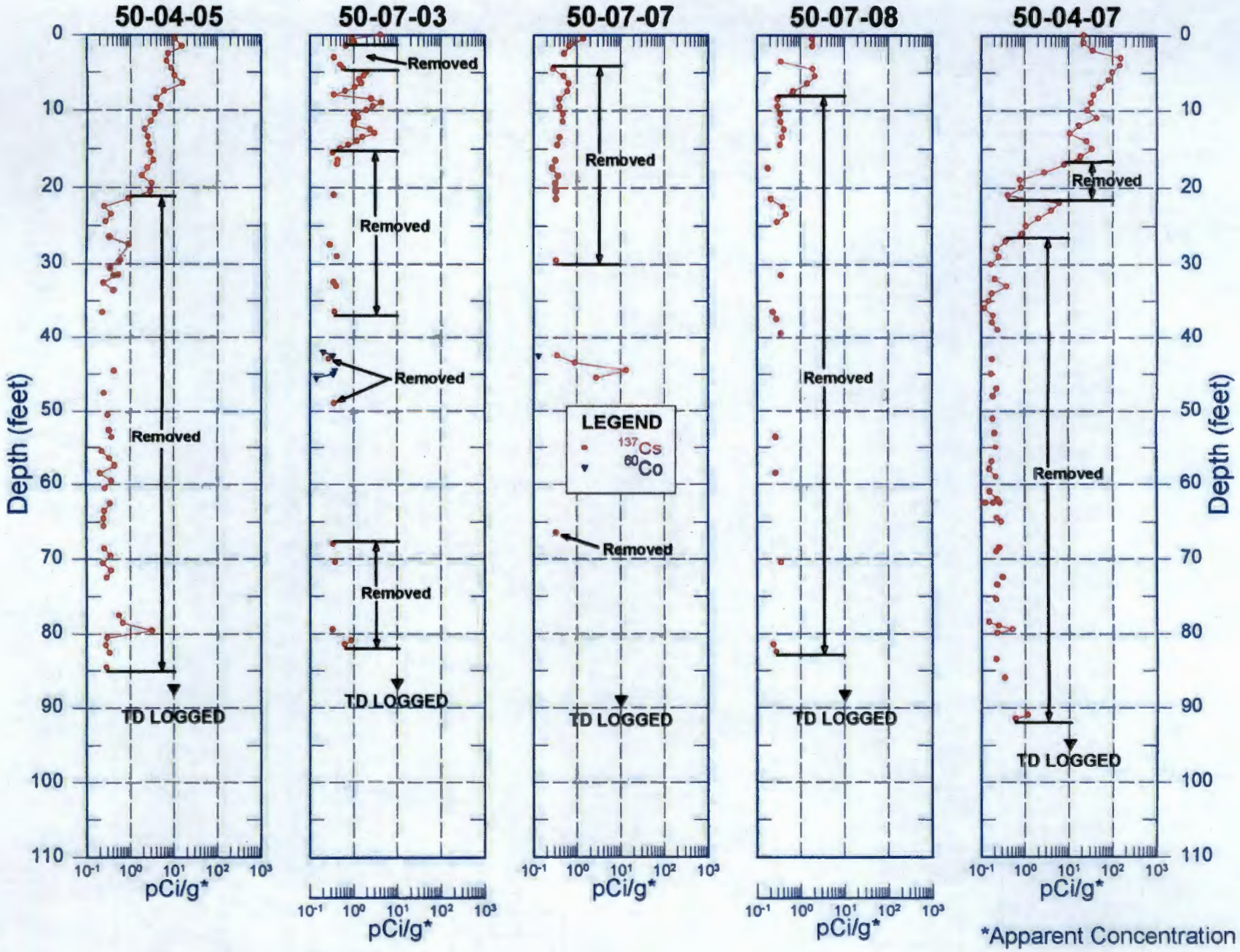

Figure B-7. Correlation Plot of ^{137}Cs and ^{60}Co Concentrations in Boreholes Surrounding T-107

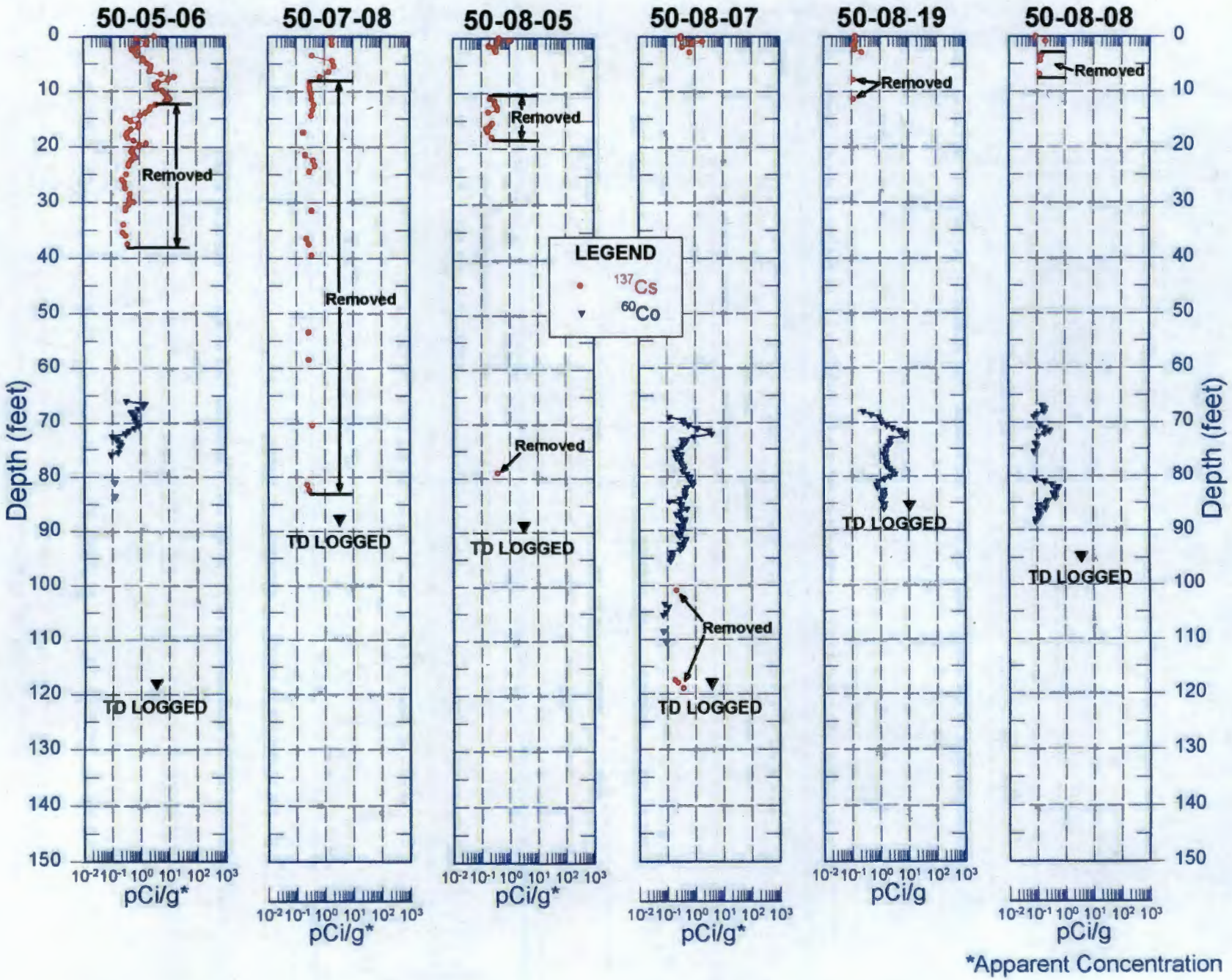

Figure B-8. Correlation Plot of ^{137}Cs, ^{60}Co, ^{152}Eu, and ^{154}Eu Concentrations in Boreholes Surrounding T-108

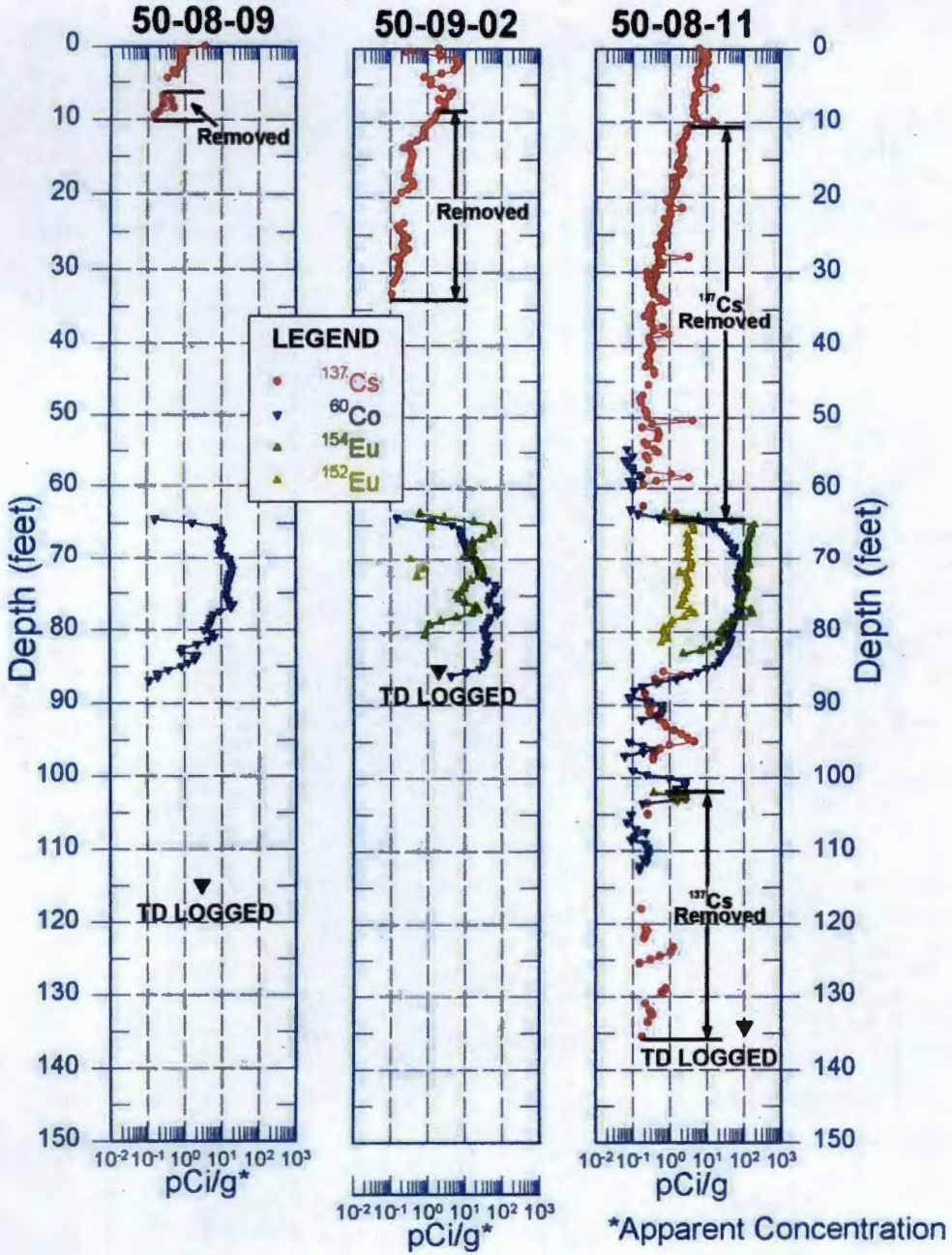

Figure B-8 (continued). Correlation Plot of ^{137}Cs, ^{60}Co, ^{152}Eu, and ^{154}Eu Concentrations in Boreholes Surrounding T-108

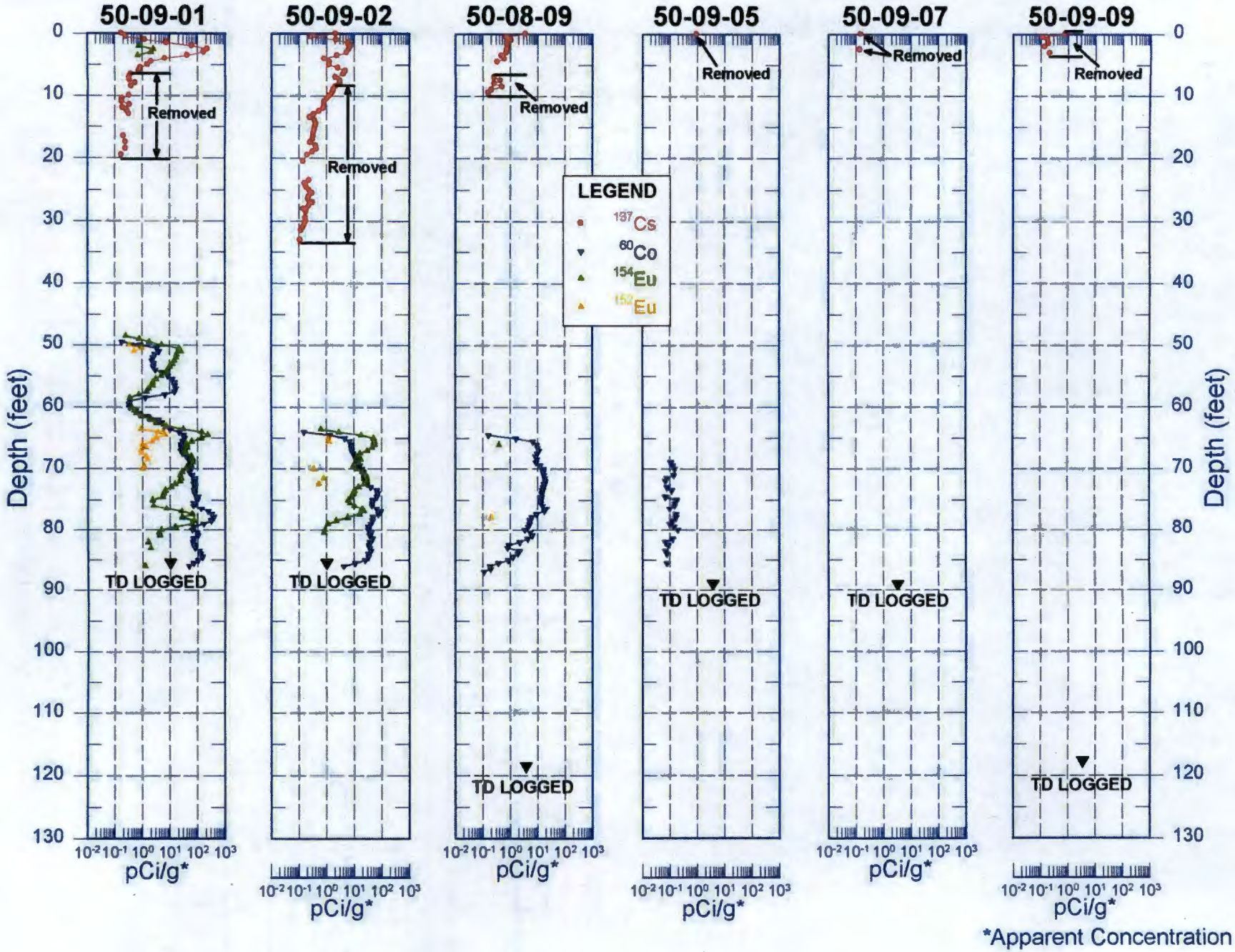

Figure B-9. Correlation Plot of ^{137}Cs, ^{60}Co, ^{152}Eu, ^{154}Eu, ^{125}Sb, and ^{126}Sn Concentrations in Boreholes Surrounding T-109

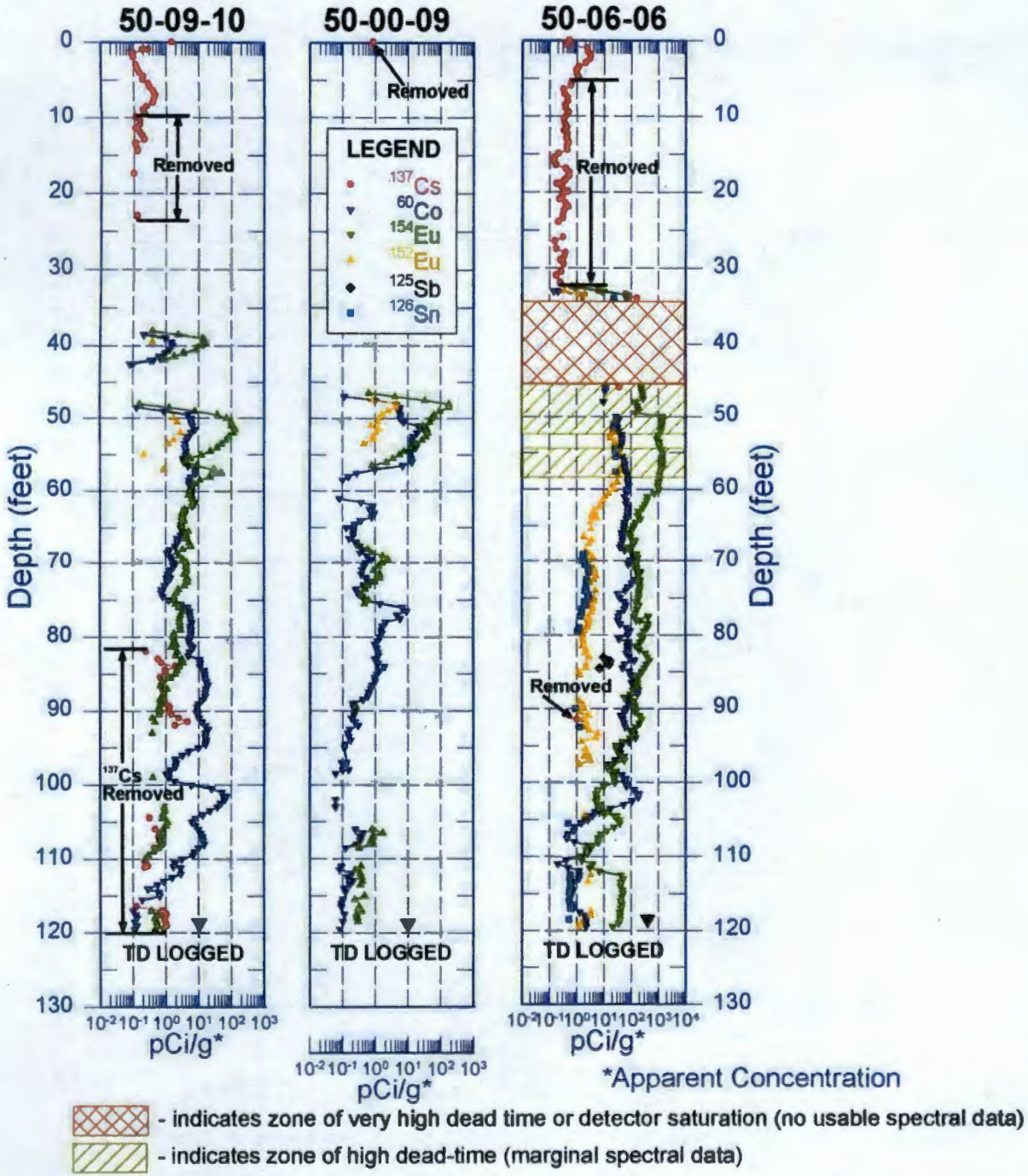

Figure B-9 (continued). Correlation Plot of ^{137}Cs, ^{60}Co, ^{152}Eu, ^{154}Eu, ^{125}Sb, and ^{126}Sn Concentrations in Boreholes Surrounding T-109

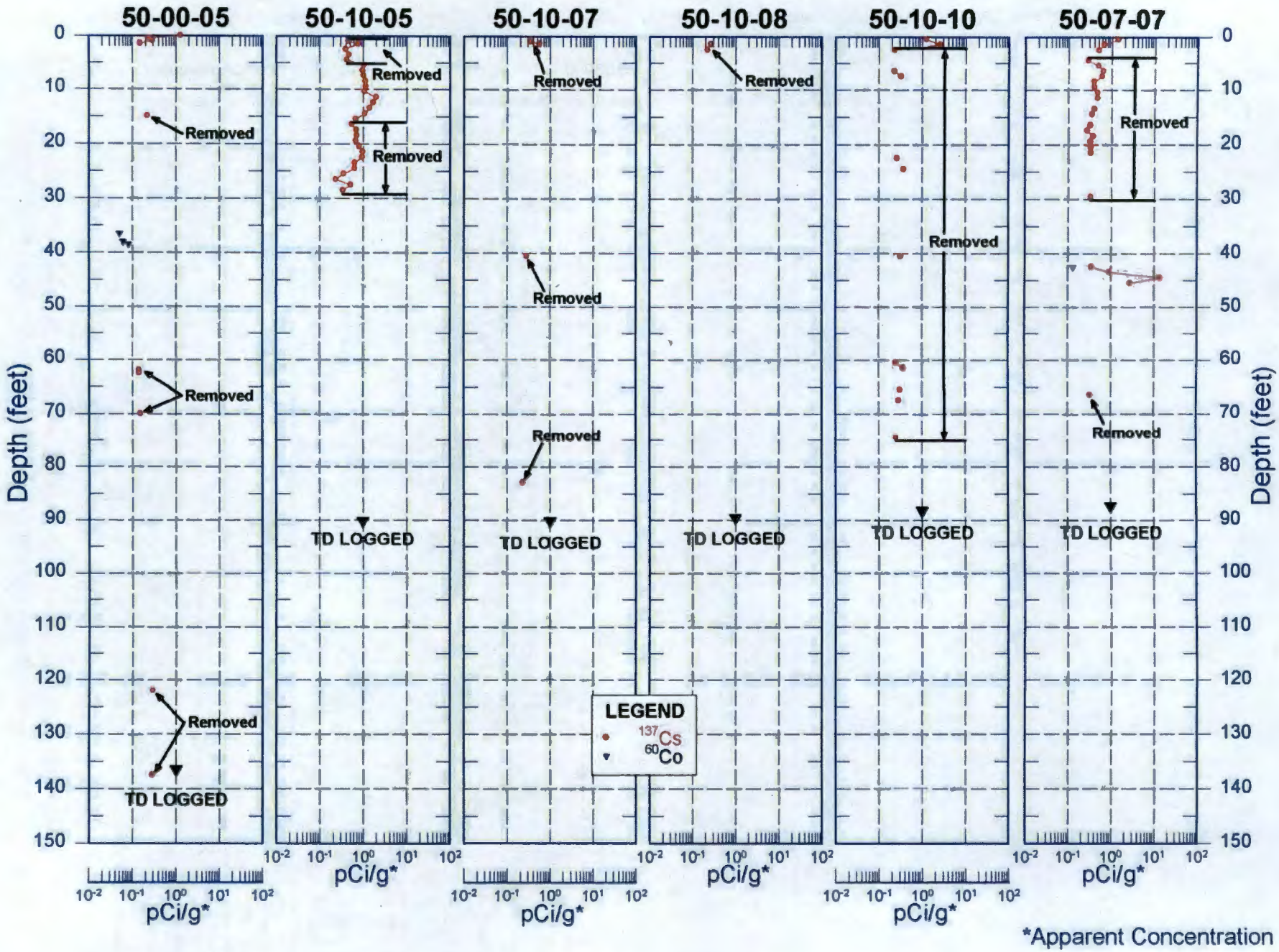

Figure B-10. Correlation Plot of ^{137}Cs and ^{60}Co Concentrations in Boreholes Surrounding T-110

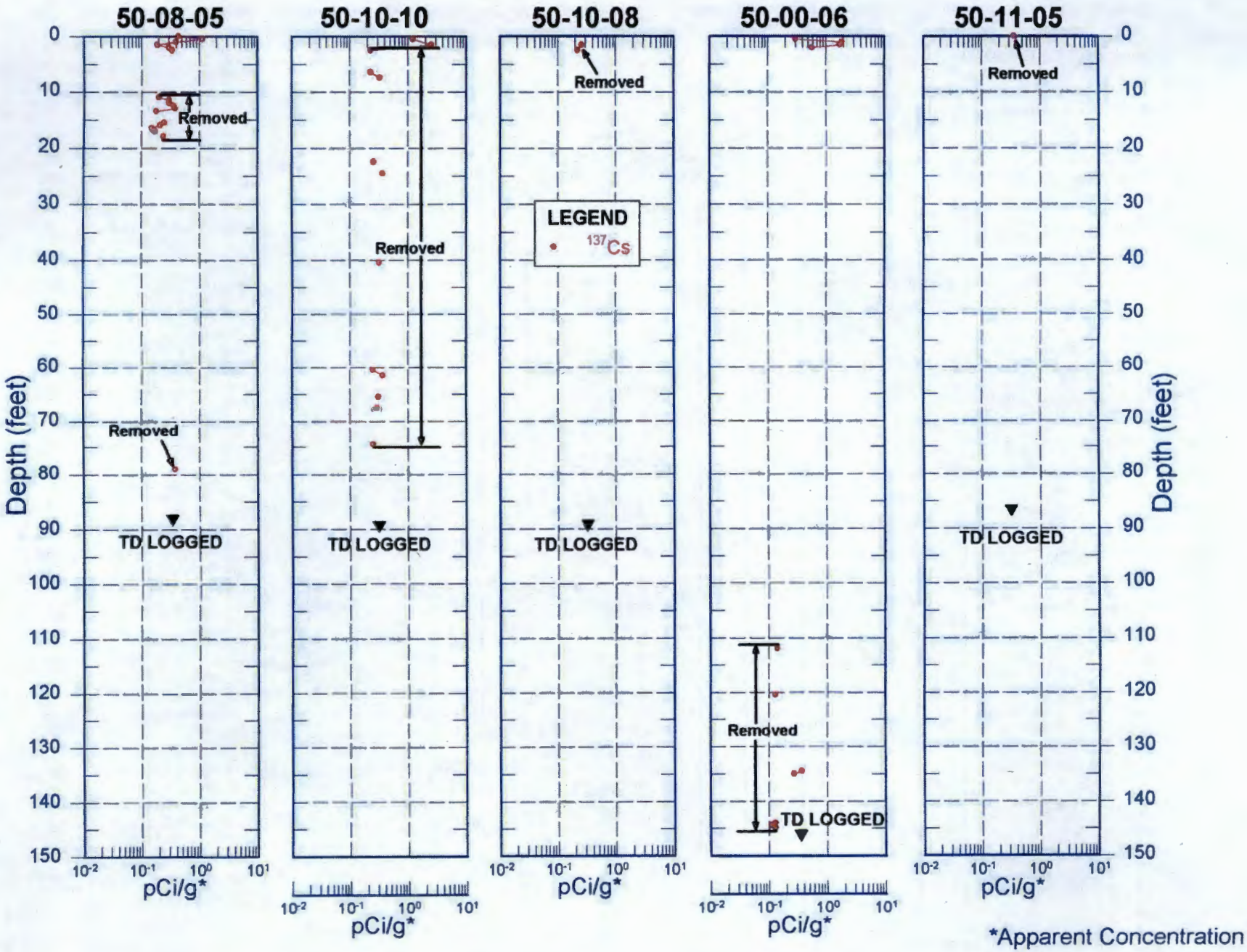

Figure B-11. Correlation Plot of ^{137}Cs and ^{60}Co Concentrations in Boreholes Surrounding T-111

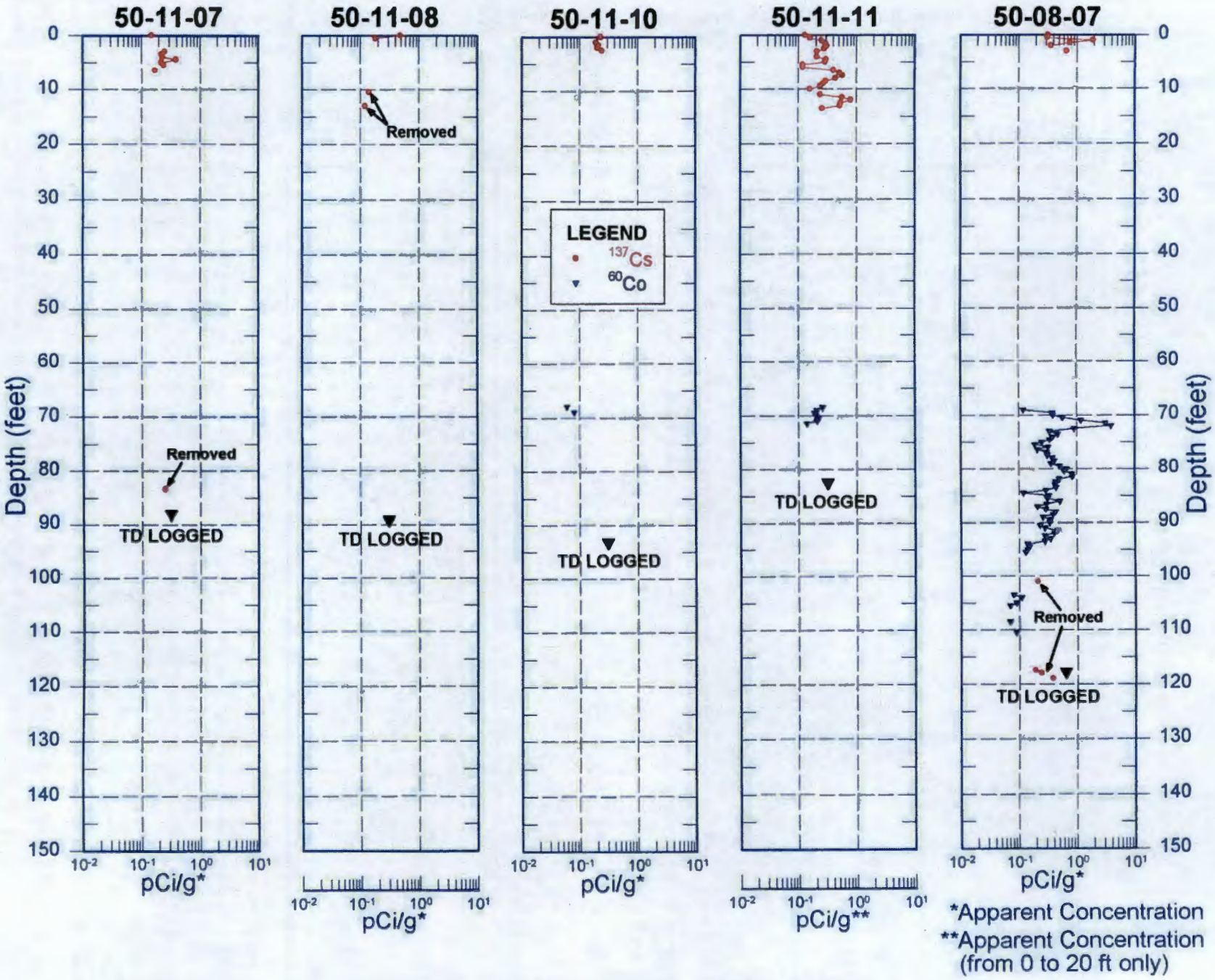

Figure B-11 (continued). Correlation Plot of ^{137}Cs and ^{60}Co Concentrations in Boreholes Surrounding T-111

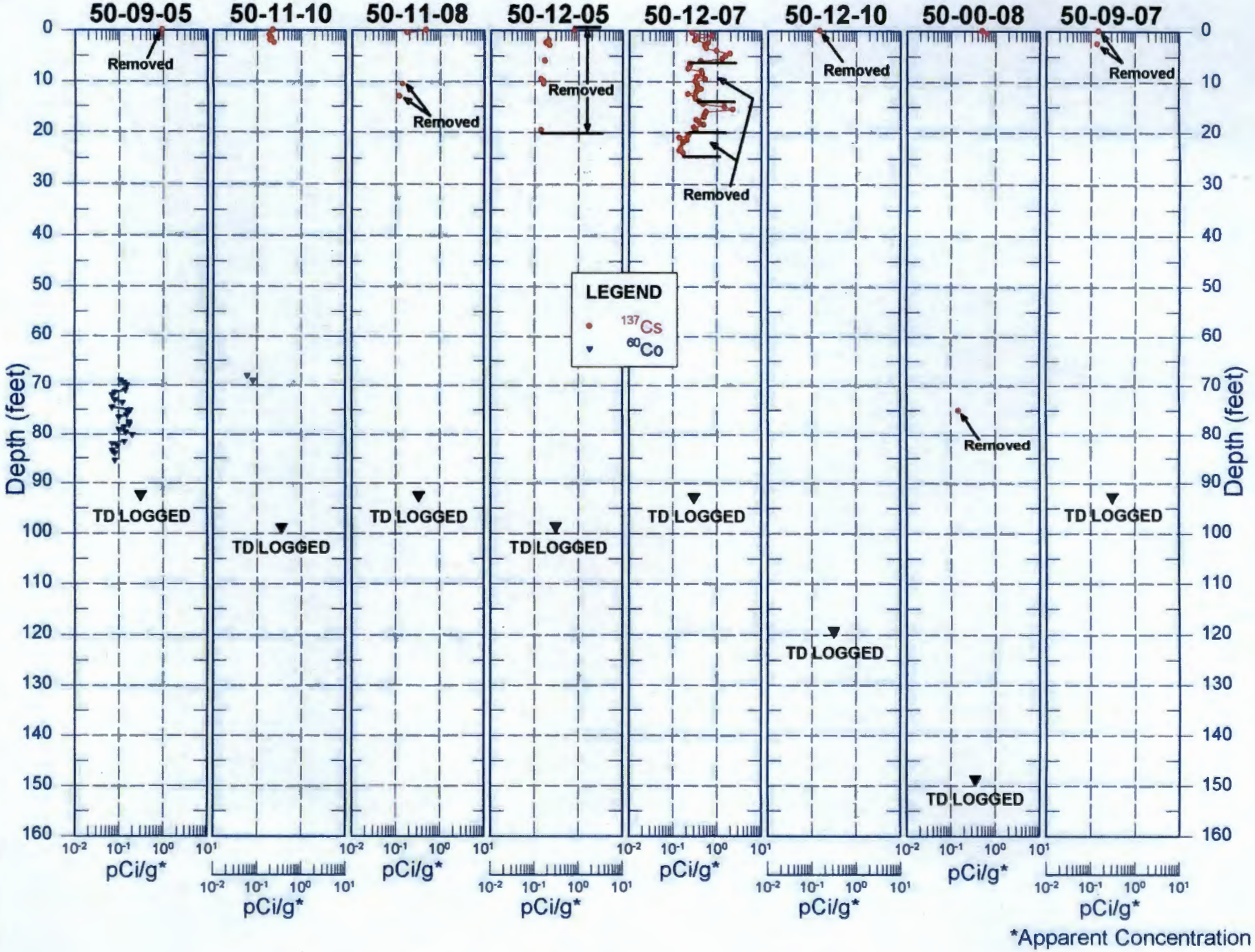

Figure B-12. Correlation Plot of ^{137}Cs and ^{60}Co Concentrations in Boreholes Surrounding T-112